Physics of iron-based high temperature superconductors (I)

Yuji Matsuda

Department of Physics
Kyoto University
Kyoto, Japan

Superconducting Elements

In Bulk at Ambient Pressure

At High Pressure

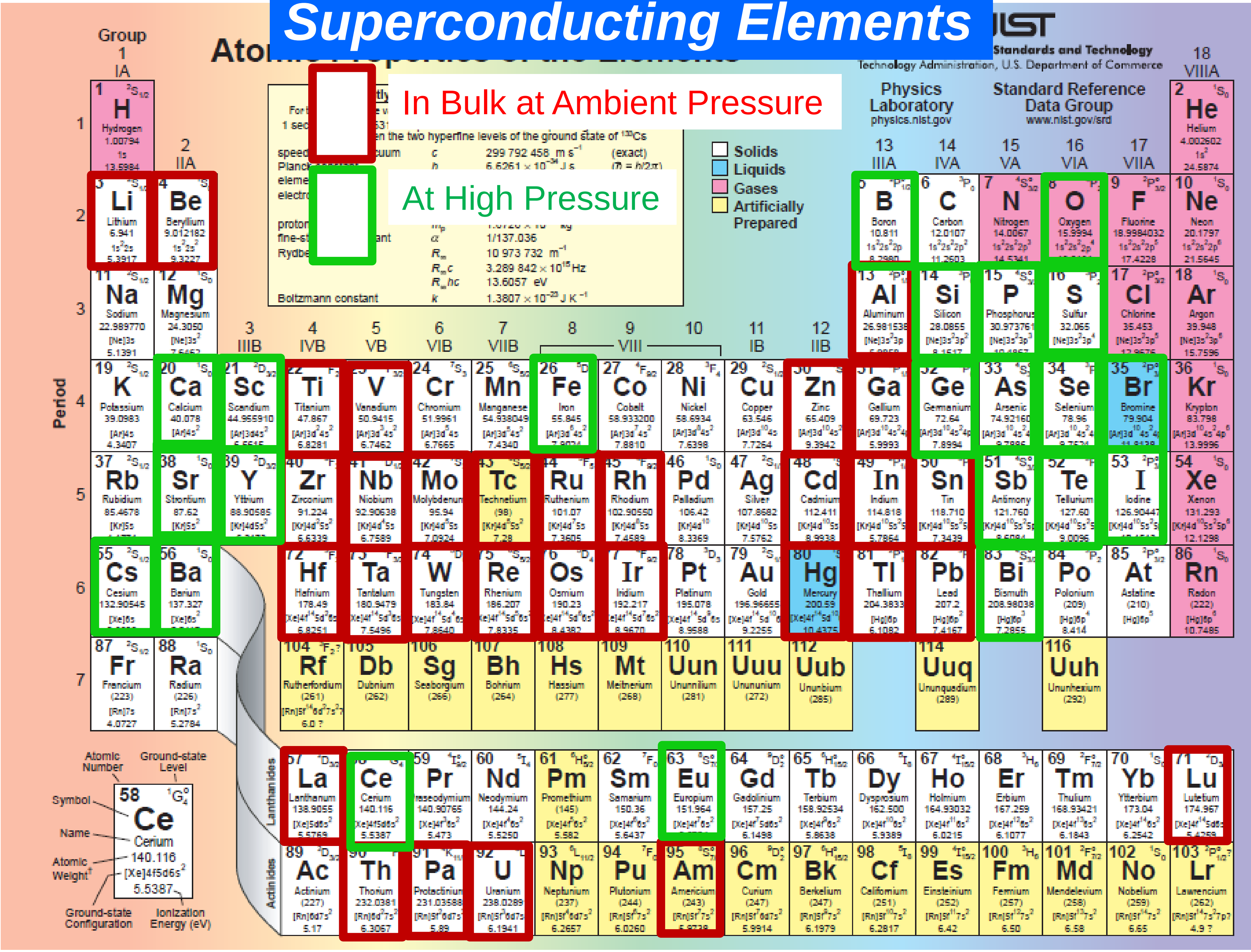

At pressures of around 100 GPa, solid oxygen becomes superconducting, with T_c of 0.6 K.

40GPa

60GPa

120GPa

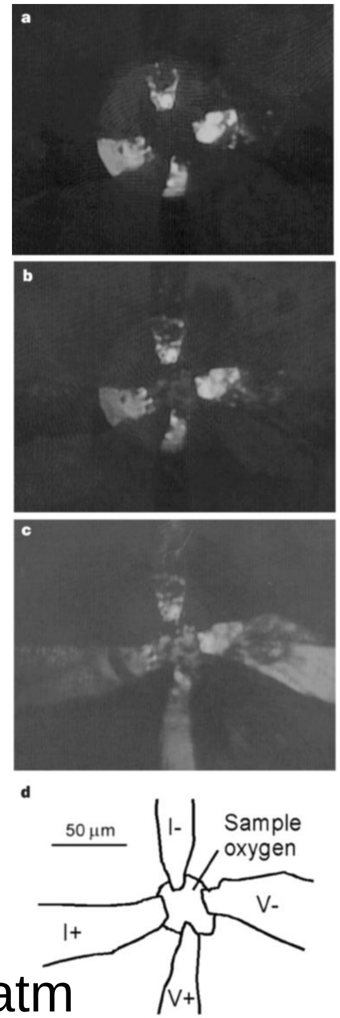

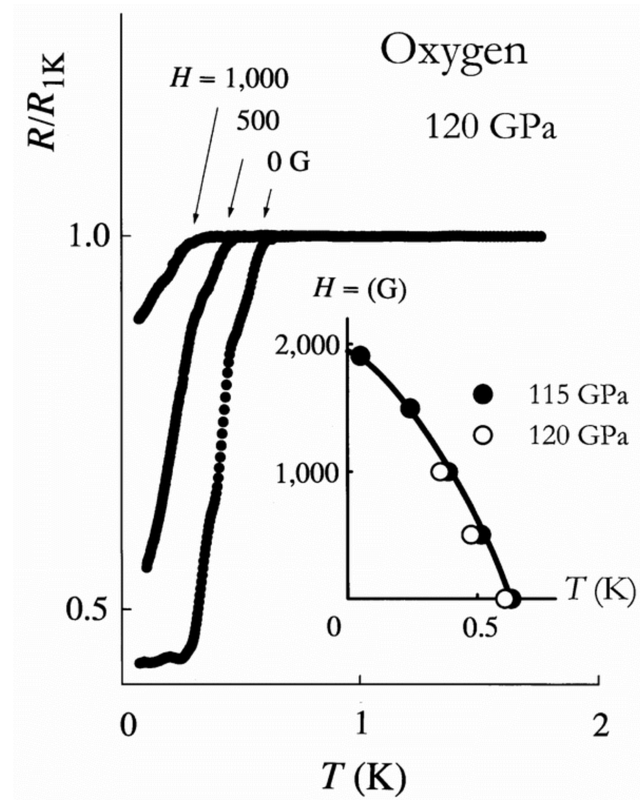

Solid Oxygen becomes shiny at high pressure (metallic color)

1GPa＝10kbar=10,000 atm
cf. 1 atm~10m water depth
10,000 atm~100 km water depth

K. Shimizu et al. Nature (1998)

Conventional Superconductor

Bardeen-Cooper-Schrieffer theory

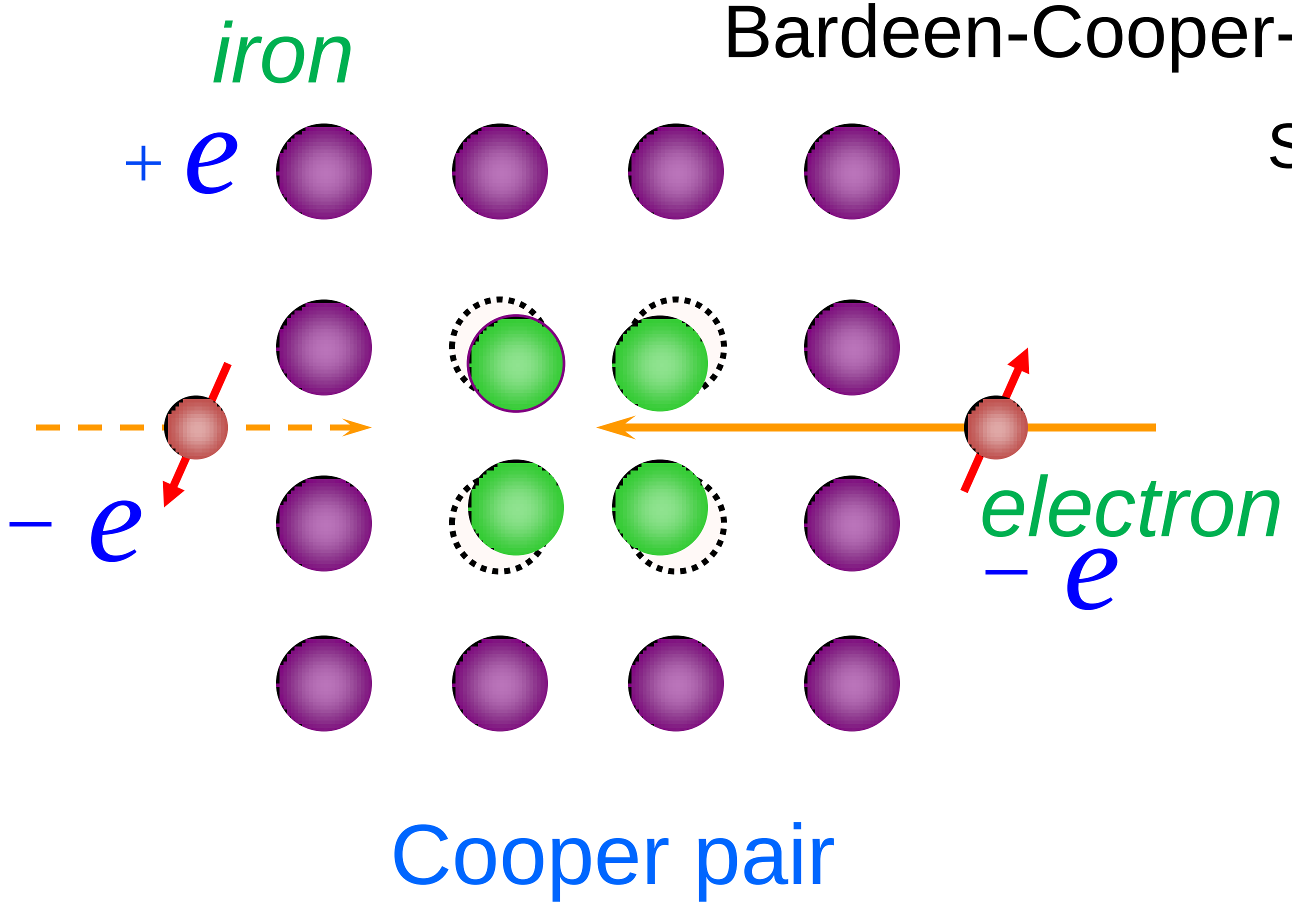

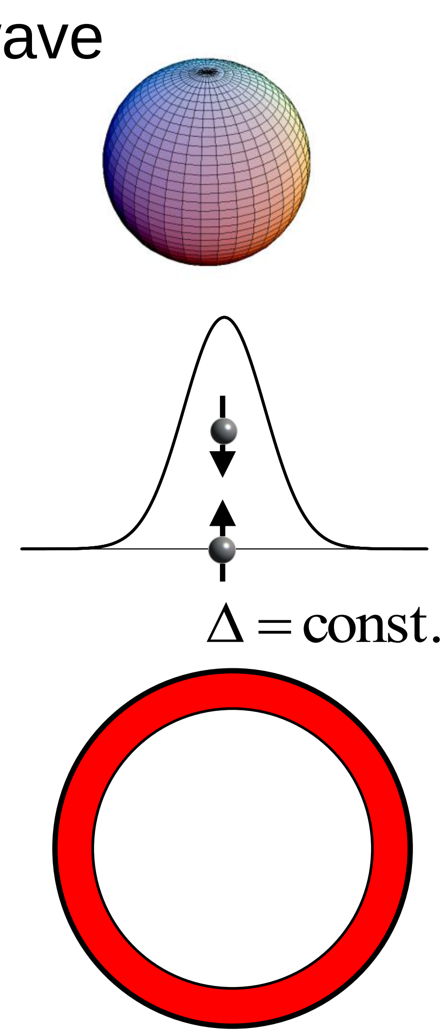

Attractive electron-phonon interactions

MgB_2 (T_c =39 K)

J. Nagamatsu *et al*., Nature (2001)

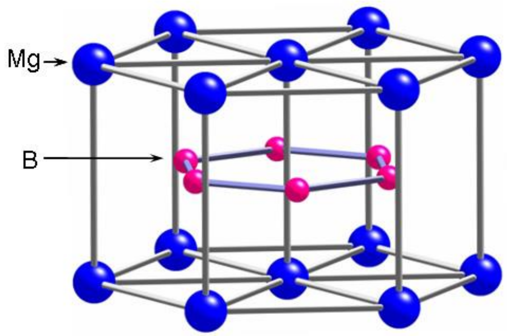

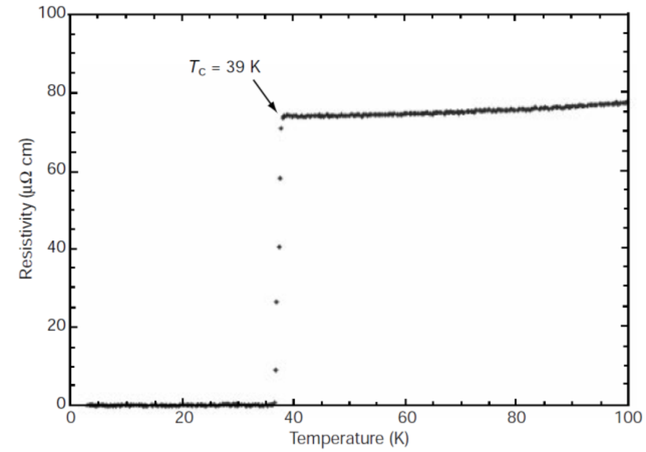

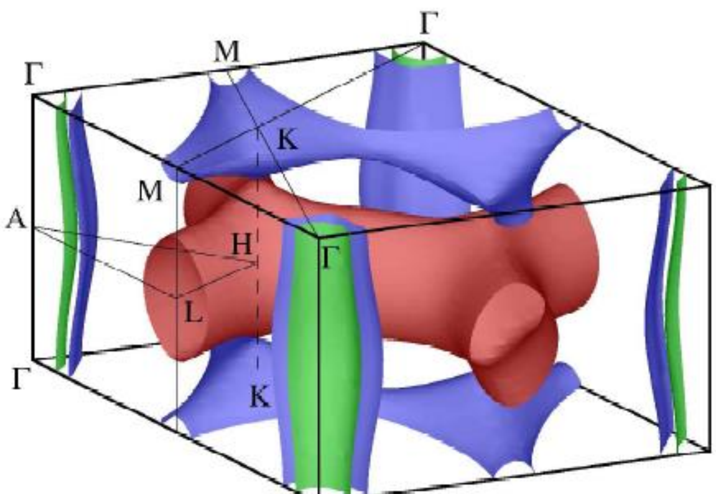

FIG. 1. Fermi surface of MgB_2. The figure is taken from Ref. [5]. Holes in the σ-band form cylinders around the ΓA-line. The π-band has electron and hole pockets located near the H- and K-points, respectively.

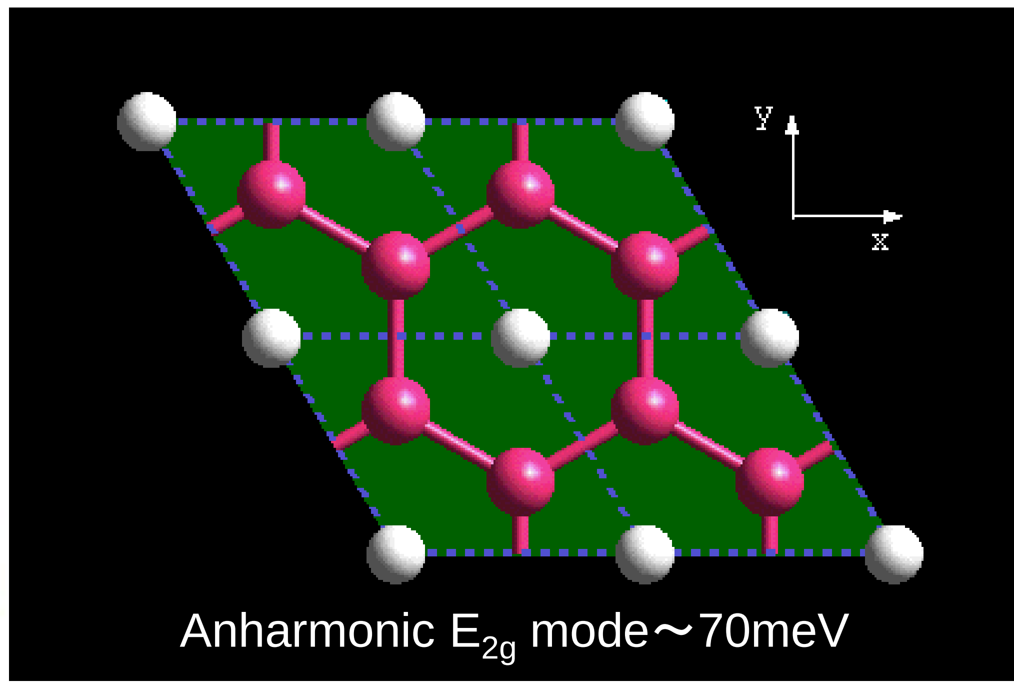

High-T_c cuprates

Possible High T_c Superconductivity in the Ba – La – Cu – O System

J.G. Bednorz and K.A. Müller
IBM Zürich Research Laboratory, Rüschlikon, Switzerland

Received April 17, 1986

Metallic, oxygen-deficient compounds in the Ba – La – Cu – O system, with the composition $Ba_xLa_{5-x}Cu_5O_{5(3-y)}$ have been prepared in polycrystalline form. Samples with $x=1$ and 0.75, $y>0$, annealed below 900 °C under reducing conditions, consist of three phases, one of them a perovskite-like mixed-valent copper compound. Upon cooling, the samples show a linear decrease in resistivity, then an approximately logarithmic increase, interpreted as a beginning of localization. Finally an abrupt decrease by up to three orders of magnitude occurs, reminiscent of the onset of percolative superconductivity. The highest onset temperature is observed in the 30 K range. It is markedly reduced by high current densities. Thus, it results partially from the percolative nature, bute possibly also from $2D$ superconducting fluctuations of double perovskite layers of one of the phases present.

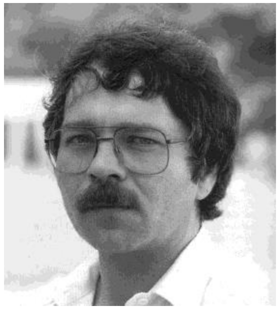

Superconductivity in CuO_2 planes

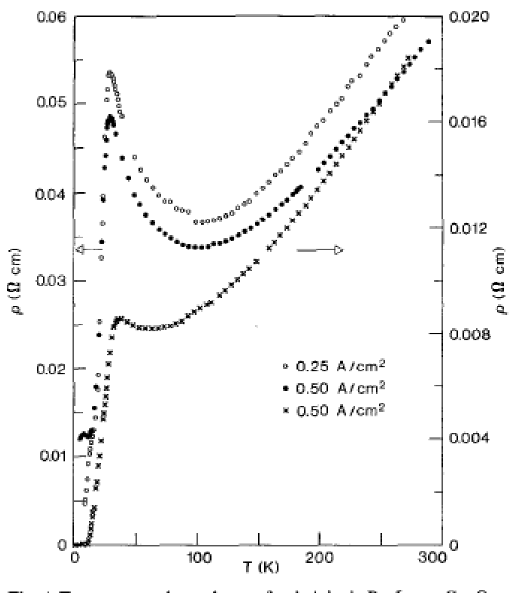

$La_{2-x}Sr_xCuO_4$

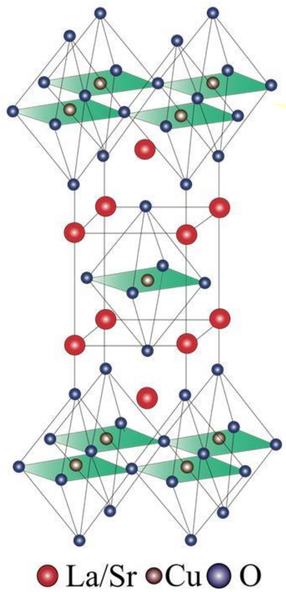

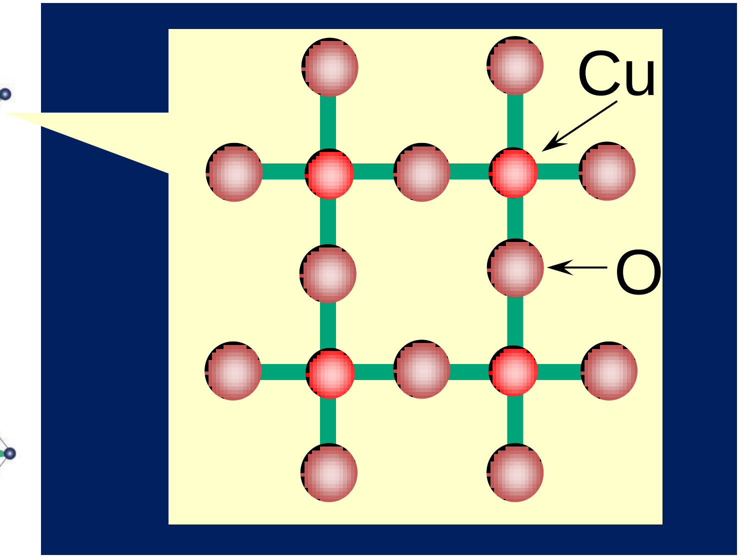

J. G. Bednorz and K.A. Müller, Zeitschrift für Physik B **64**, 189 (1986).

Fe-based high-T_c superconductors

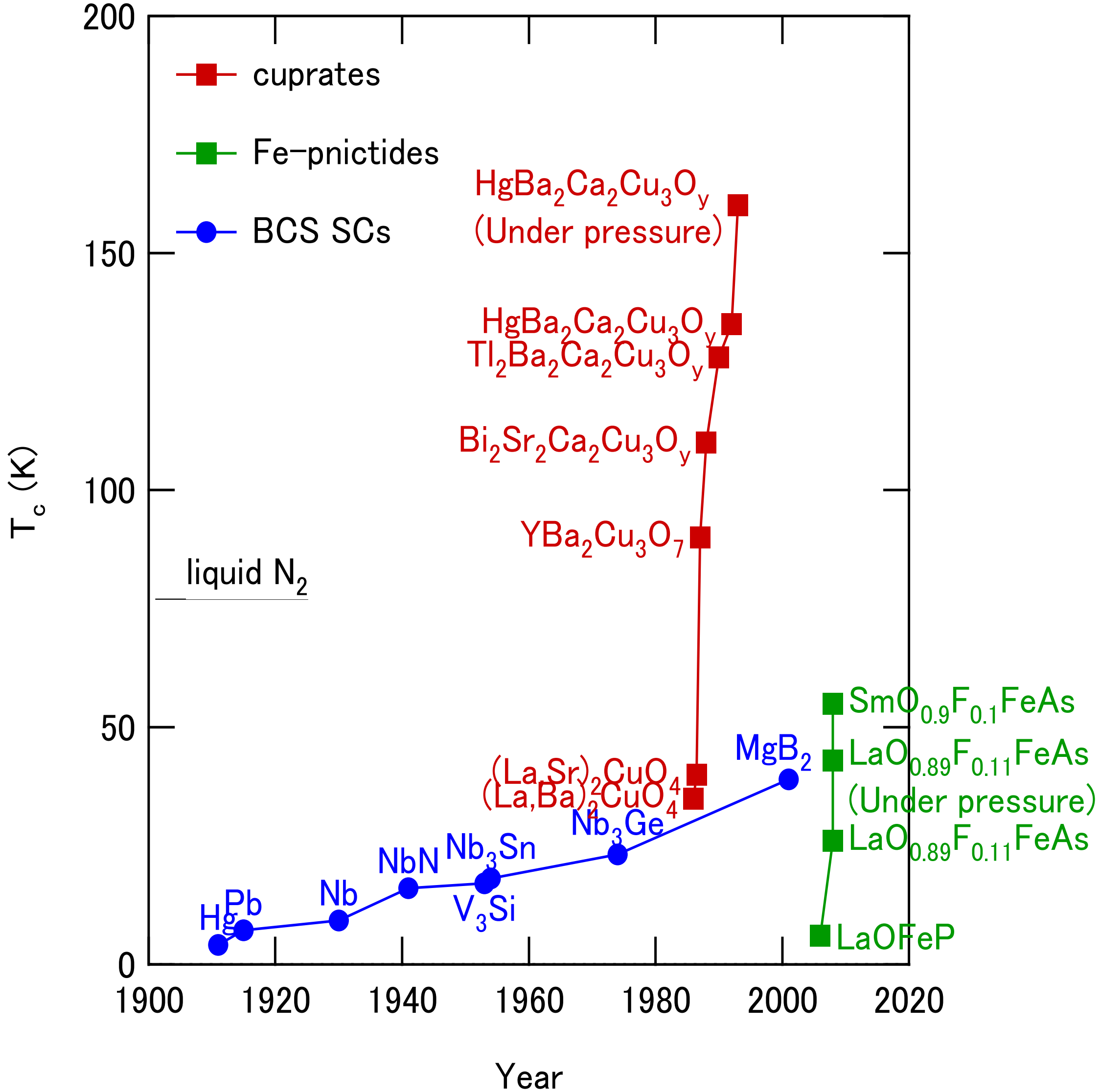

Superconductivity in Fe-Pnictides — Discovery

J|A|C|S
COMMUNICATIONS

Published on Web 02/23/2008

Iron-Based Layered Superconductor La[$O_{1-x}F_x$]FeAs (x = 0.05–0.12) with T_c = 26 K

Yoichi Kamihara,*,† Takumi Watanabe,‡ Masahiro Hirano,†,§ and Hideo Hosono†,‡,§

ERATO-SORST, JST, Frontier Research Center, Tokyo Institute of Technology, Mail Box S2-13, Materials and Structures Laboratory, Tokyo Institute of Technology, Mail Box R3-1, and Frontier Research Center, Tokyo Institute of Technology, Mail Box S2-13, 4259 Nagatsuta, Midori-ku, Yokohama 226-8503, Japan

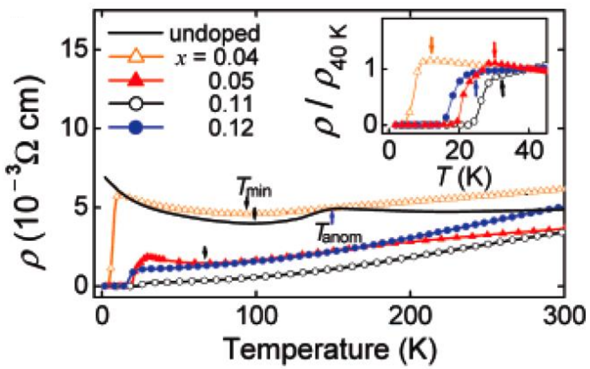

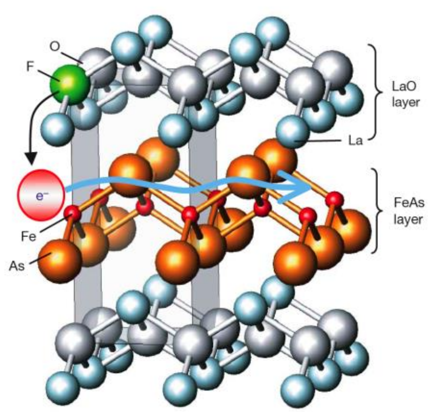

LaFeAs($O_{1-x}F_x$)

Y. Kamihara *et al.*, JACS, **130**, 3296 (2008).

Superconductivity in Fe-Pnictides — Discovery

Hosono's group was not looking for superconductor, but trying to create new kind of transparent semiconductors for flat-panel display.

LaFePO	T_c=4 K
LaFeP(O,F)	T_c=7 K
LaFeAs(O,F)	T_c=26 K
SmFeAs(O,F)	T_c=56 K

Only two months!

Fe-based high-T_c superconductors

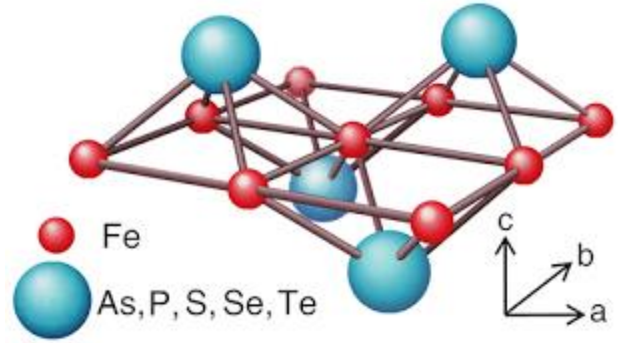

2D square lattice of Fe

42622
(32522)

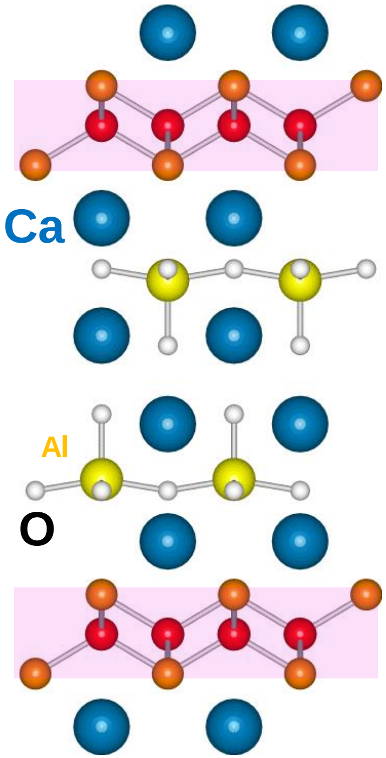

$(A_4M_2O_6)\ Fe_2As_2$

T_c(max)=47K

Zhu et al.(2009)
Ogino et al. (2009)

1111

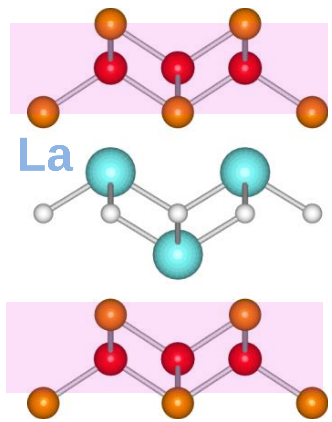

Ln FeAsO

T_c(max)=55K

Y. Kamihara et al.(2008)

122

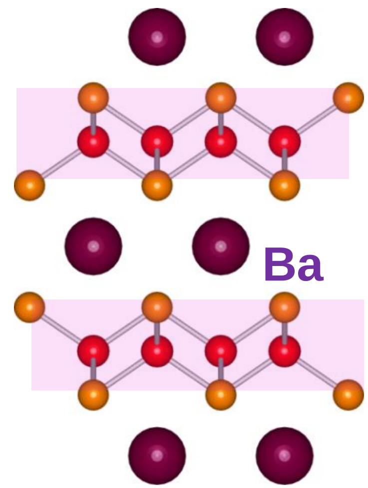

$BaFe_2As_2$

T_c(max)=38K

M. Rotter et al.(2008)

111

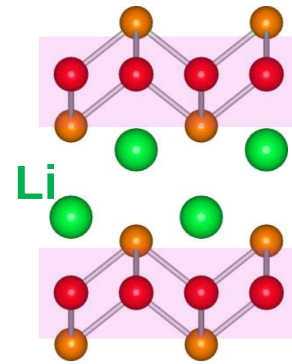

LiFeAs

T_c= 18 K

X.C.Wang et al.(2008)

11

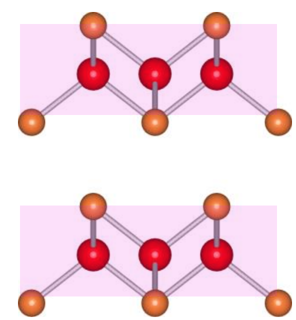

FeSe

T_c= 8 K

F.C.Hsu et al.(2008)

Fe-based high-T_c superconductors

Are iron-pnictides an Electron-Phonon Superconductor?

$$T_c \sim \omega_D e^{-\frac{1}{\lambda}}$$

$$\omega_D \sim 200\ \mathrm{K}$$

ω_D Debye frequency

$$\lambda \sim 0.2$$

λ Electron-phonon coupling

Comparable to the conventional metals

$$\Rightarrow \quad T_c \sim 1\ \mathrm{K}$$

Electron-phonon coupling is not sufficient to explain superconductivity in the whole family of Fe-As based superconductors

L. Boeri, O.V. Dolgov, and A.A. Golubov, PRL **101**, 026403 (2008).

Why are Fe-based HTSC important?

1. A new class of high temperature superconductors

They knocked the cuprates off their pedestal as a unique class of high temperature superconductors.

2. A new family of unconventional superconductors

A possible new mechanism of high-T_c superconductivity

3. They would be easier to work into technological applications than the cuprates.

Physics of iron-based high temperature superconductors

1) Introduction

2) Simiilarities and differences between cuprates and Fe-pnictides

3) Normal state properties

Electronic structure and magnetism

4) Superconducting properties

Superconducting gap structure

5) Some recent topics

QCP, BCS-BEC crossover,
A novel high field SC state, Nematicity・・・・

Superconductivity

Macroscopic wave function with a well defined amplitude and phase

$$\psi(r) = \sqrt{n_s} e^{i\theta(r)}$$

2nd order phase transition

Symmetry breaking

Gauge transformation

$$\psi \to e^{i\theta}\psi \qquad \psi^\dagger \to e^{-i\theta}\psi^\dagger$$

Order parameter

$$\Delta \sim <\psi\psi> \to \Delta e^{2i\theta}$$

U(1) Gauge symmetry breaking

Unconventional superconductivity

Conventional definition of unconventional superconductivity

Full symmetry group ***G***

$$\boldsymbol{G} = \boldsymbol{U(1)} \times \boldsymbol{G} \times \boldsymbol{SU(2)} \times \boldsymbol{T}$$

U(1) gauge symmetry

G symmetry group of ***crystal lattice***

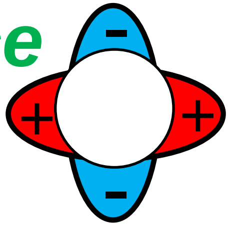

e.g. *d*-wave in tetragonal lattice

SU(2) symmetry group of ***spin*** rotation

Spin triplet

T ***time*** reversal symmetry operation

$$\Psi \rightarrow \Psi_1 + i\Psi_2$$

One or more symmetries in addition to ***U(1)*** are broken at T_c

A more general definition

Superconductivity not mediated by phonon

e.g. Nodal superconductors

Three families of unconventional superconductor

Iron pnictide (Fe)	Cuprate (Cu)	Heavy fermion compound (Ce, U)
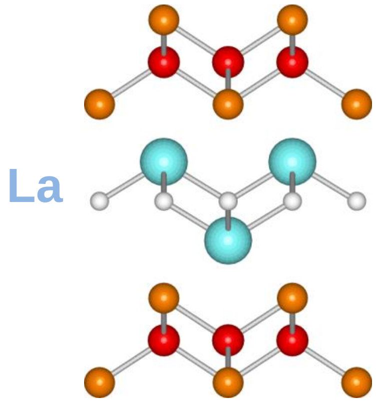	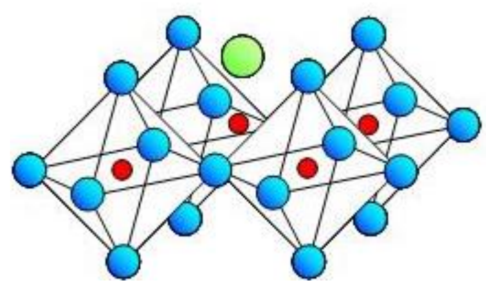	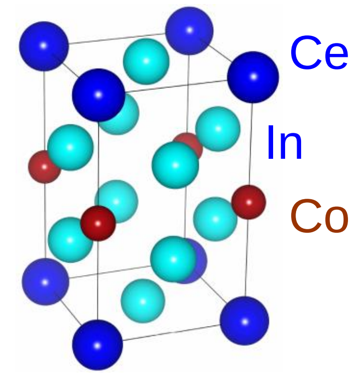
Weakly localized 3*d*-electrons	Strongly localized 3*d*-electrons	Very strongly localized 4*f*, 5*f* electrons

Weak correlation

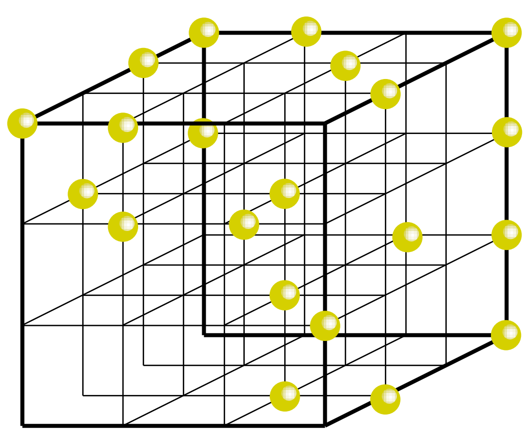

Strong correlation

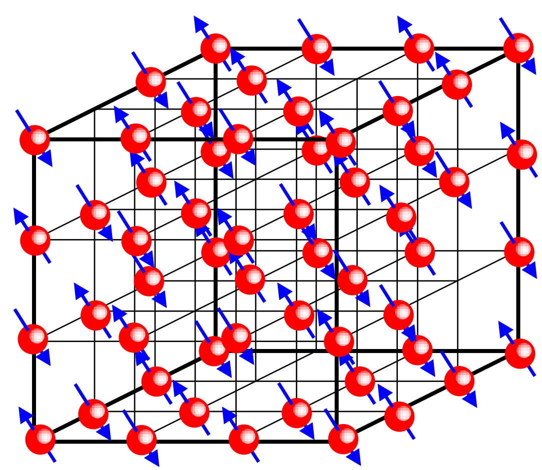

Three classes of unconventional superconductor

Iron pnictide (Fe)

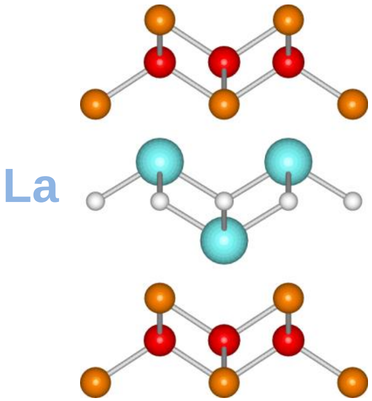

Cuprate (Cu)

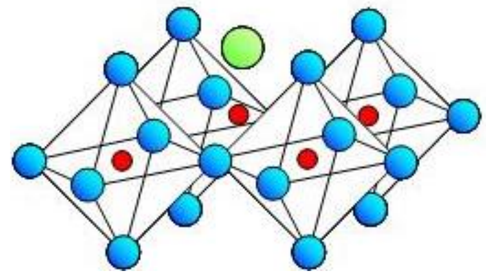

Heavy fermion compound (Ce, U)

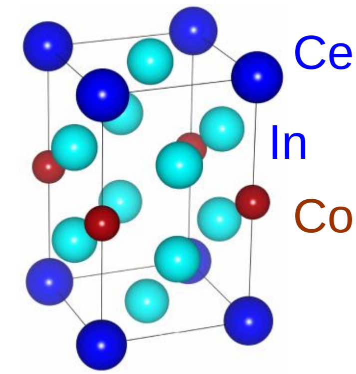

La_2CuO_4

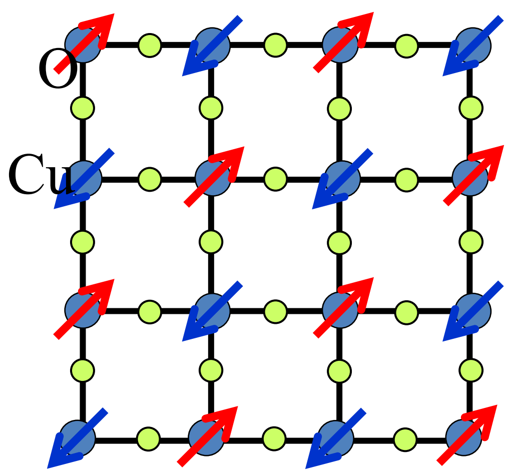

Mott insulator

$(La_{1-x}Sr_x)_2CuO_4$ $La^{3+} \rightarrow Ba^{2+}$

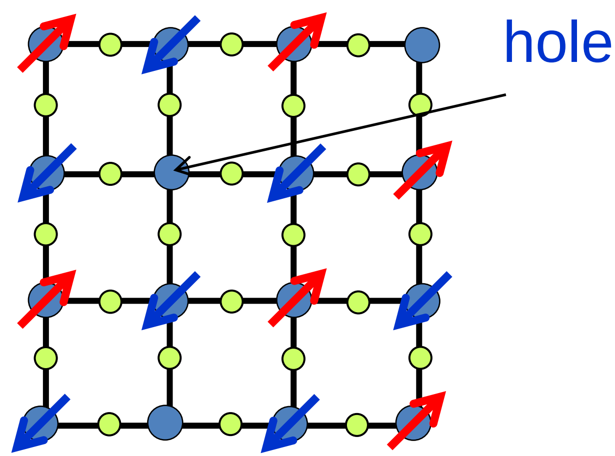

High-T_c superconductor

Carrier doping

Three families of unconventional superconductor

Iron pnictide (Fe)

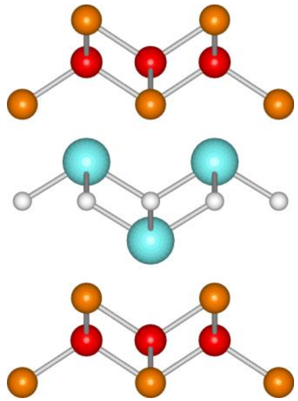

Cuprate (Cu)

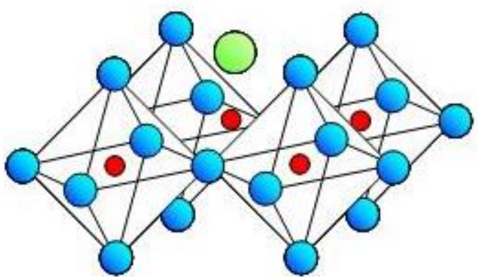

Heavy fermion compound (Ce, U)

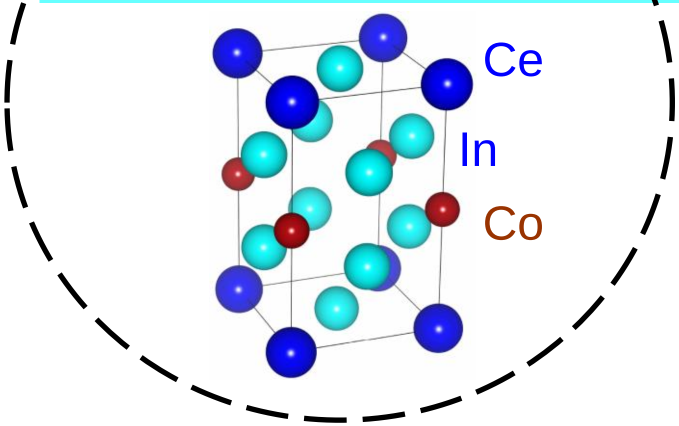

Up to ~1000 times the free electron mass “Heavy Fermions”

Hybridization with conduction electrons

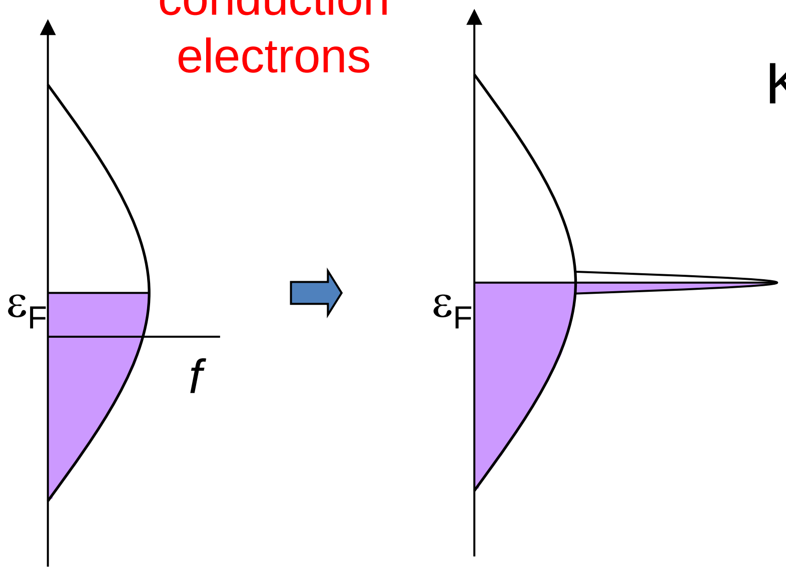

High temperature

Low temperature

Kondo effect

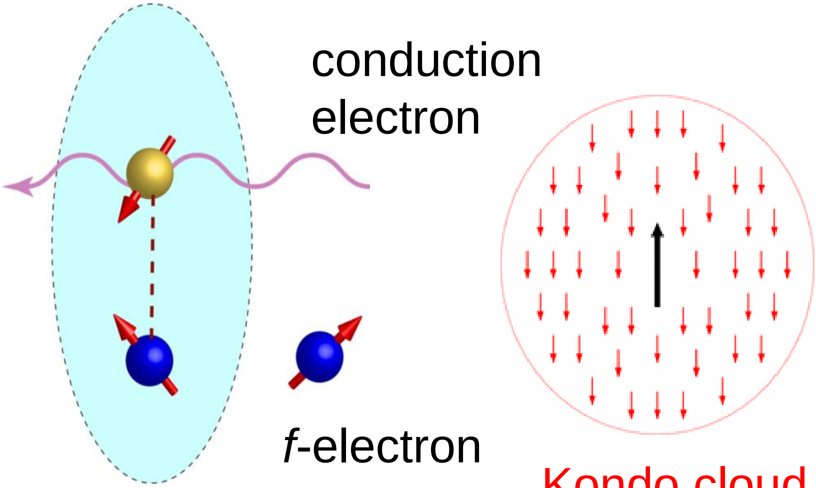

Kondo cloud

Three families of unconventional superconductor

Iron pnictide (Fe)

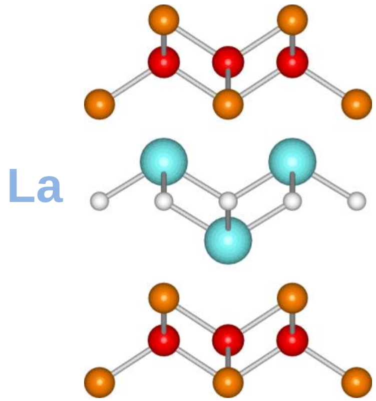

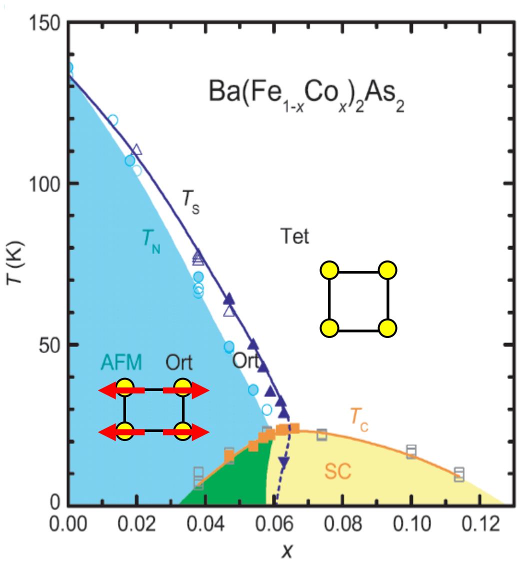

Cuprate (Cu)

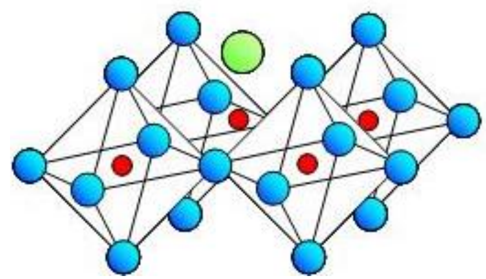

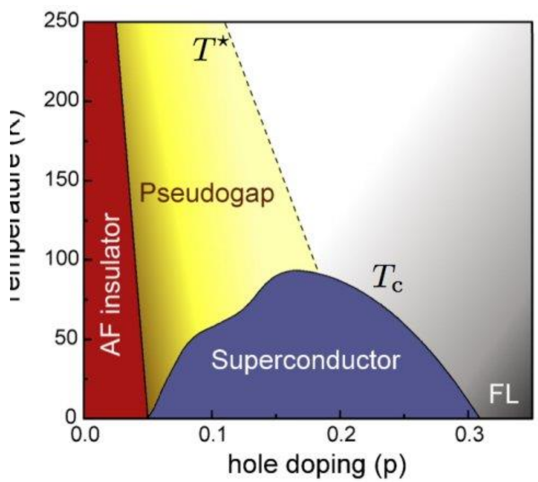

Heavy fermion compound (Ce, U)

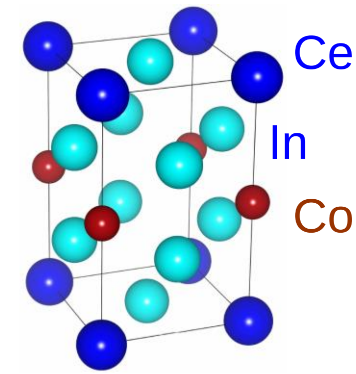

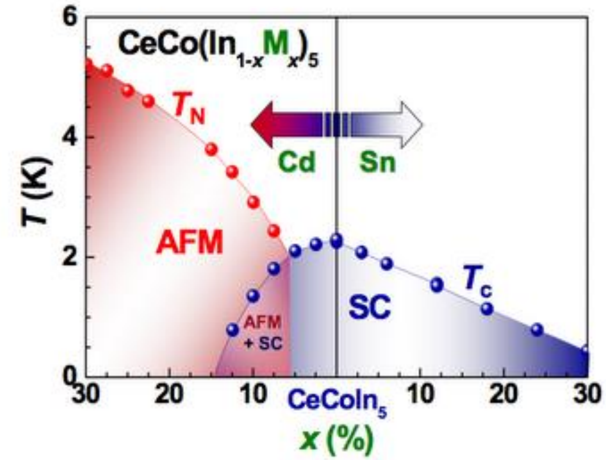

Superconductivity is induced by suppressing a magnetically ordered phase

Magnetic fluctuations may bind the Cooper pairs

Three families of unconventional superconductor

Iron pnictide (Fe)	Cuprate (Cu)	Heavy fermion compound (Ce, U)

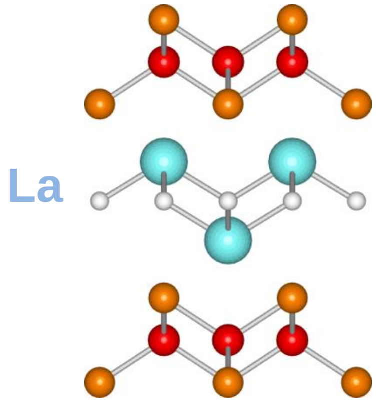

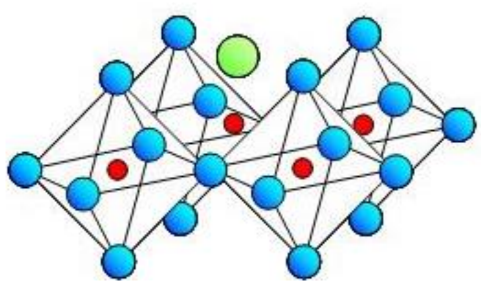

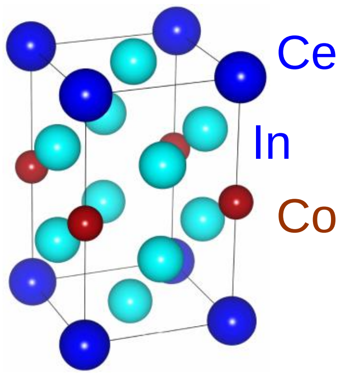

	Pnictide		Cuprate		Heavy Fermion
Electron correlation	strong	<	strong	<	very strong
Fermi surface	simple 2D		Very simple 2D		Complicated 3D
Magnetic structure	simple		simple		complicated
Physics	Multi-orbital		Mott		Kondo

Physics of iron-based high temperature superconductors

1) Introduction

2) Simiilarities and differences between cuprates and Fe-pnictides

3) Normal state properties

Electronic structure and magnetism

4) Superconducting properties

Superconducting gap structure

5) Some recent topics

QCP, BCS-BEC crossover,
A novel high field SC state, Nematicity・・・・

Similarities and differences between cuprates and pnictides

Cuprates

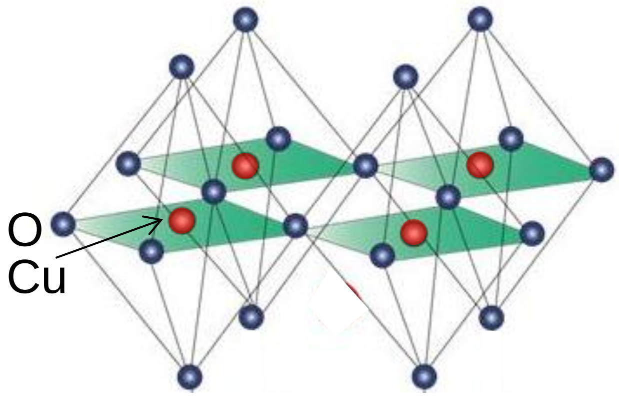

Fe-pnictides

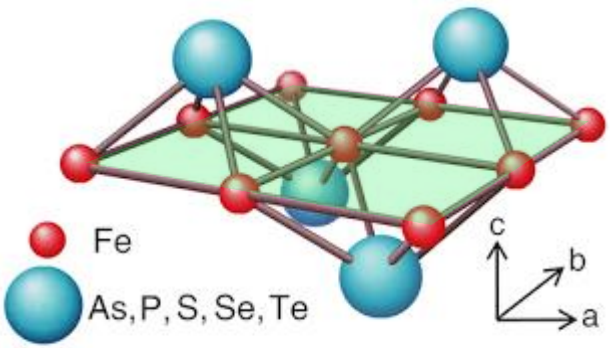

Superconductivity in 2D planes

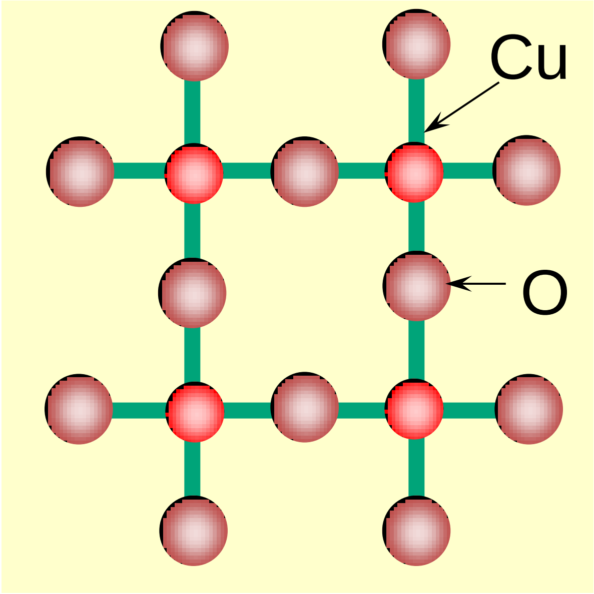

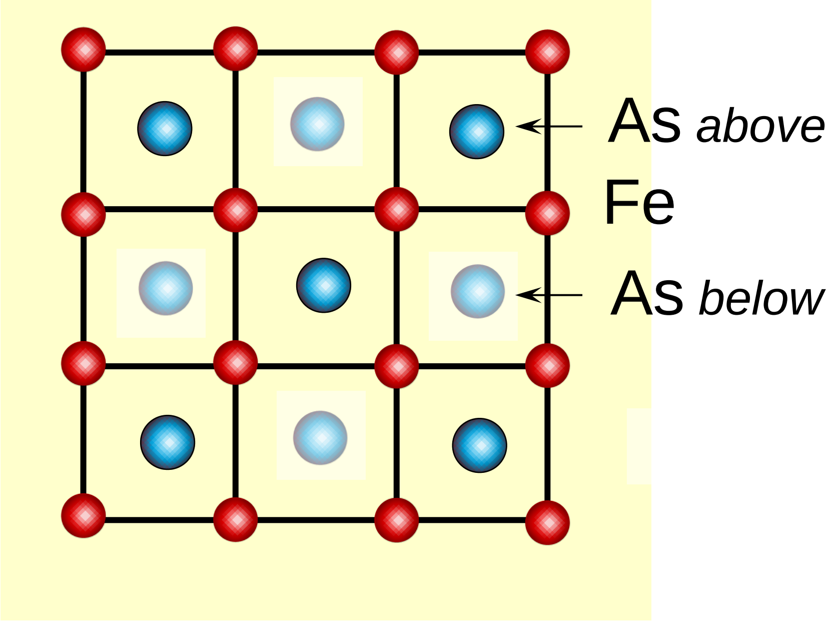

Enhanced fluctuations → suppression of magnetic order

Similarities and differences between cuprates and pnictides

Cuprates

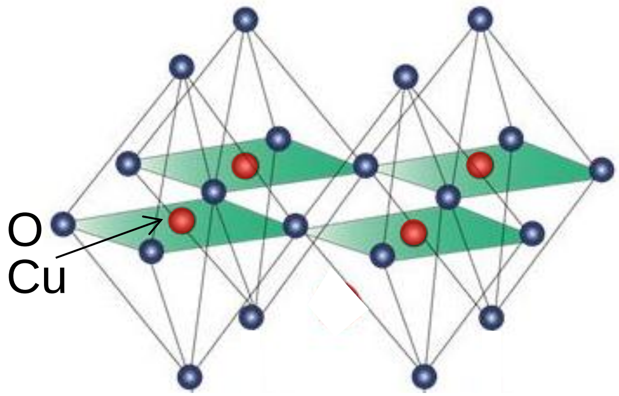

Fe-pnictides

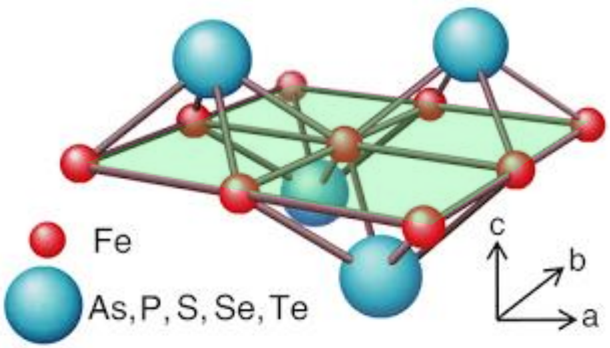

Parent compound

AFM insulator

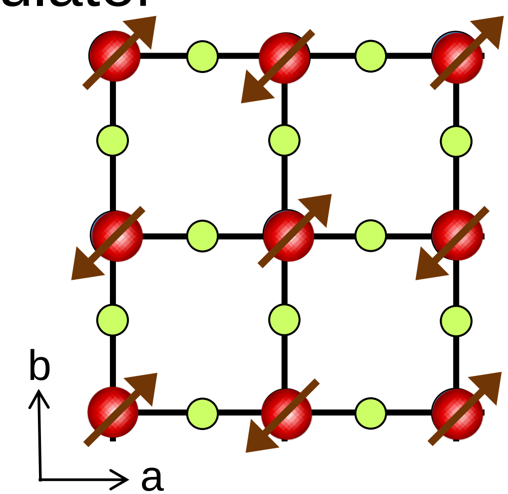

Cu

S=1/2 $1\ \mu_B$

$\sim 0.6\ \mu_B$

2D quantum fluctuation

SDW metal

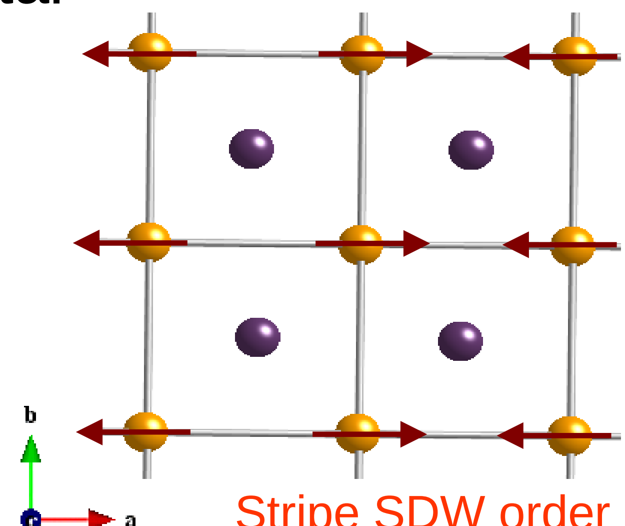

Stripe SDW order

$BaFe_2As_2$ $0.8\text{-}1\ \mu_B$

Similarities and differences between cuprates and pnictides

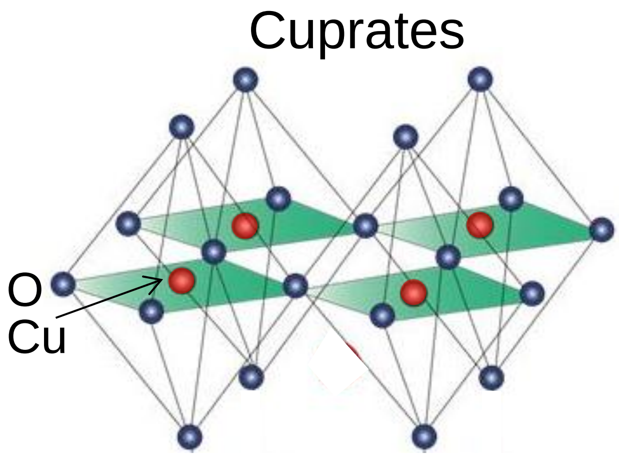

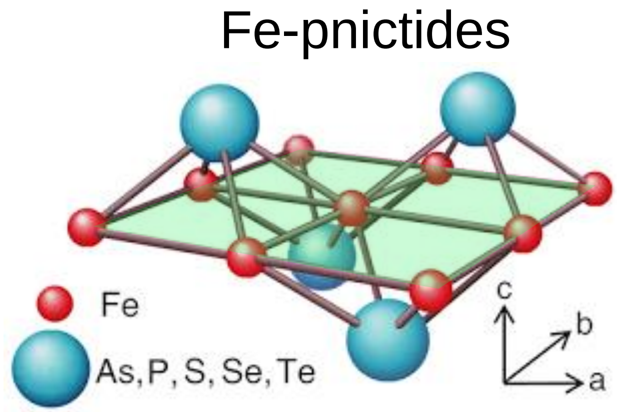

Parent compound

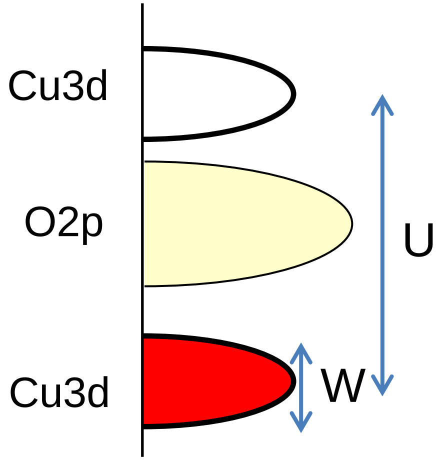

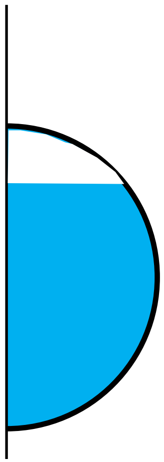

U : Coulomb ~ 8eV

W : Band width ~ 3eV

Strong electron-electron correlation

Mott insulator

U~W~2-3 eV

Intermediate correlation

Spin density wave (SDW) metal

Similarities and differences between cuprates and pnictides

Cuprates

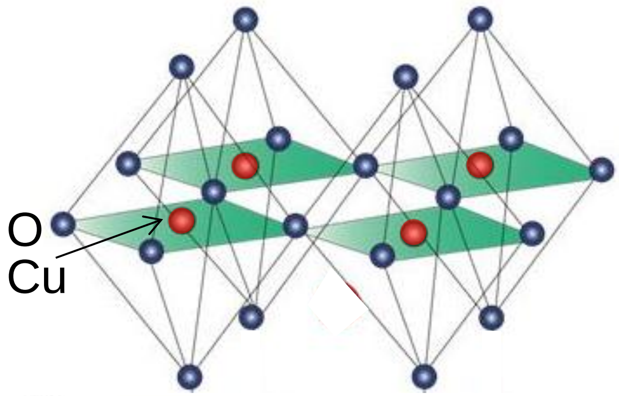

Fe-pnictides

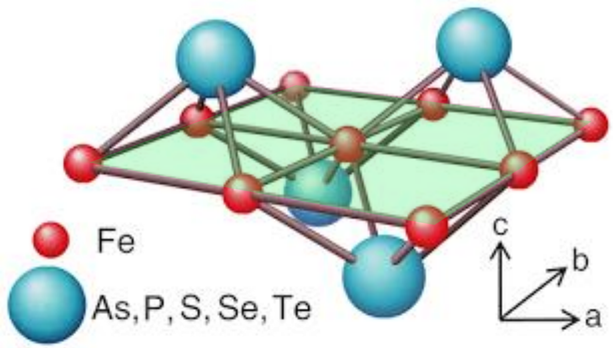

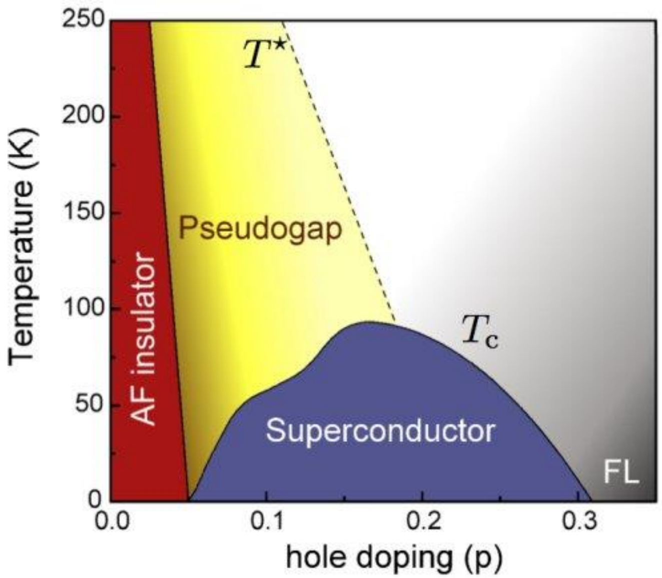

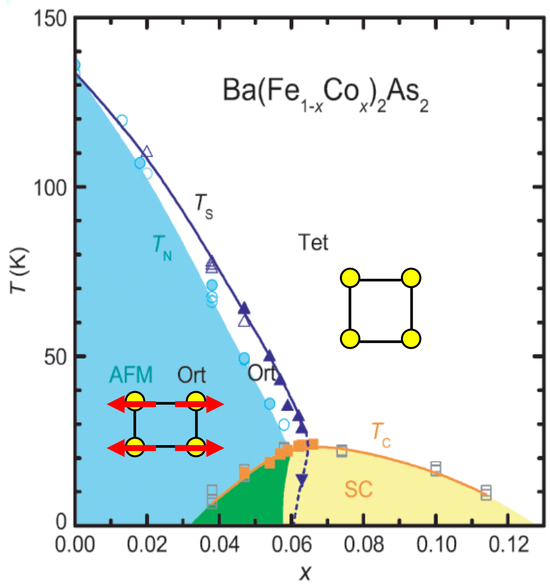

Superconductivity occurs in the vicinity of magnetic order

In Fe-pnictides, structural (T_S) and AFM transition (T_N) lines follow closely each other

Similarities and differences between cuprates and pnictides

Cuprates

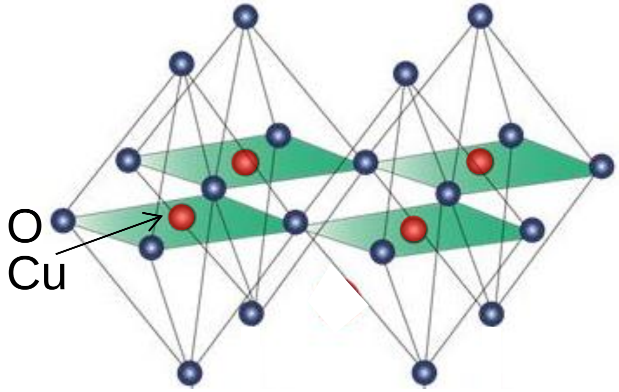

Fe-pnictides

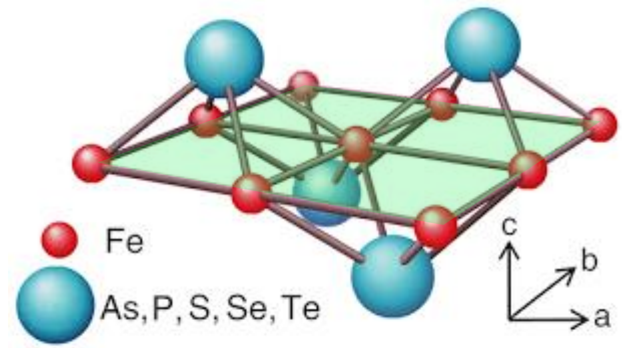

Superconductivity induced by doping holes or electrons

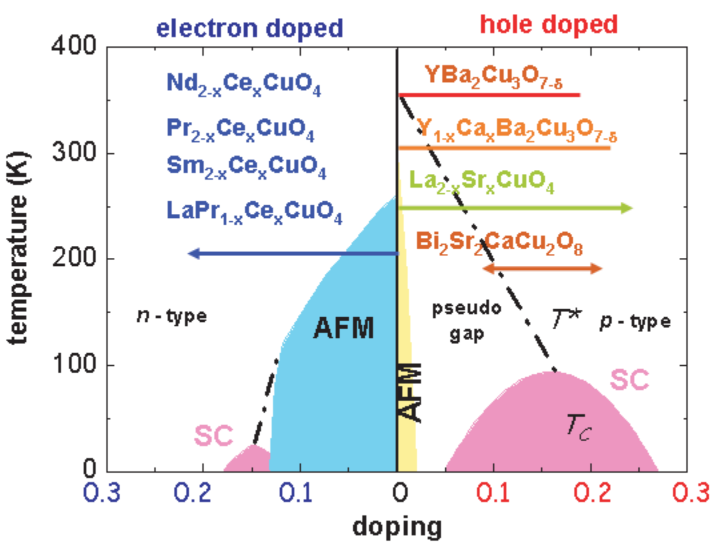

Ground state can be tuned without doping carriers

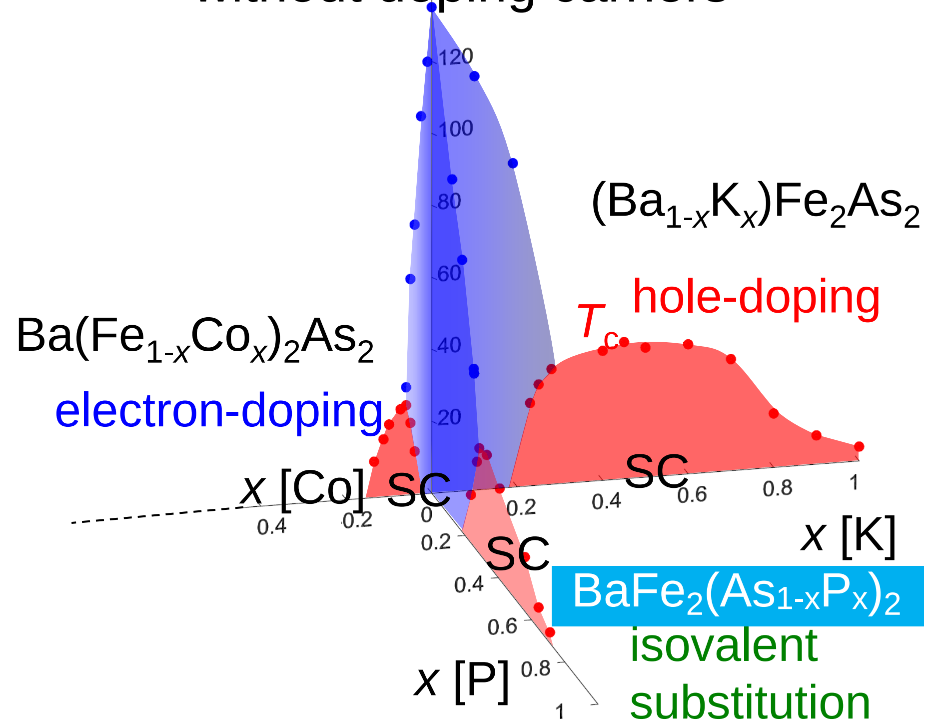

Similarities and differences between cuprates and pnictides

Cuprates

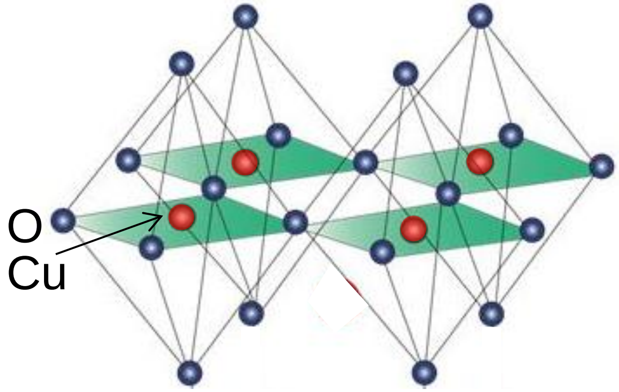

Fe-pnictides

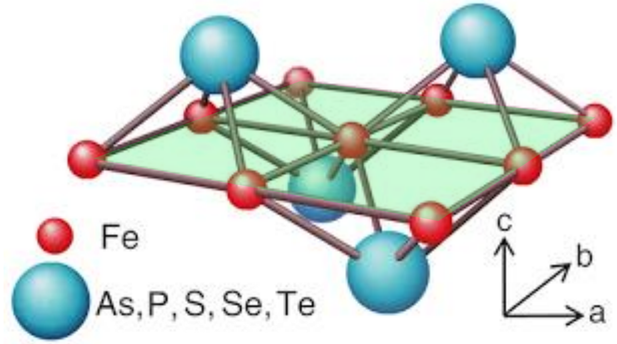

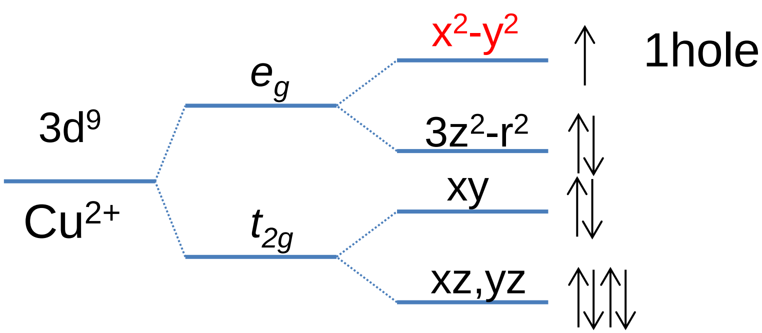

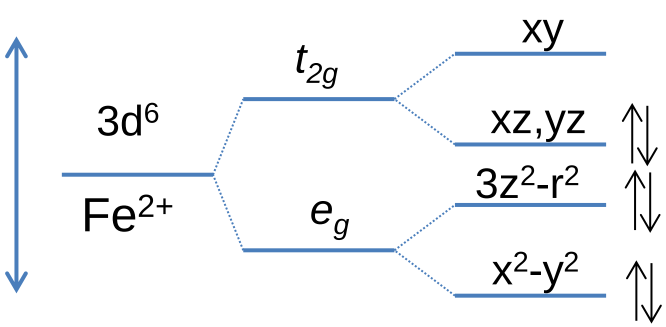

Large crystal field ~2-3 eV

Small crystal field (~500meV)

Similarities and differences between cuprates and pnictides

Cuprates

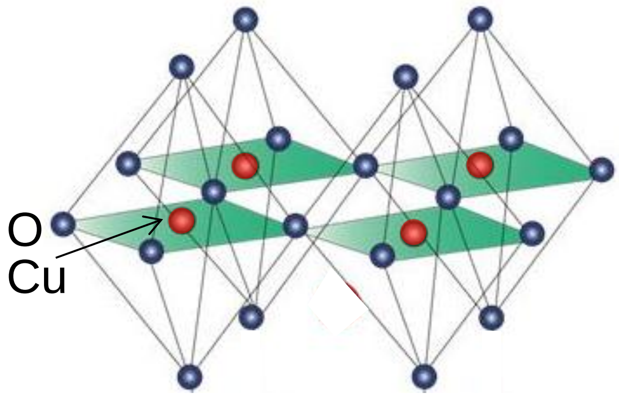

Fe-pnictides

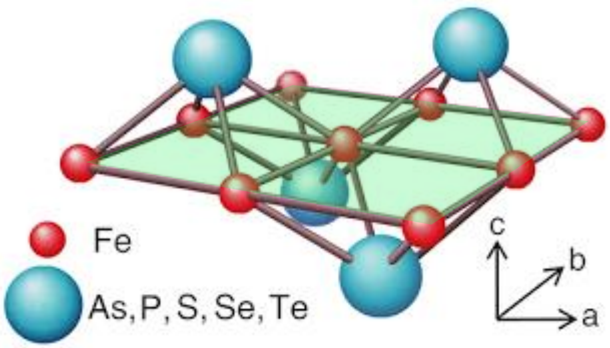

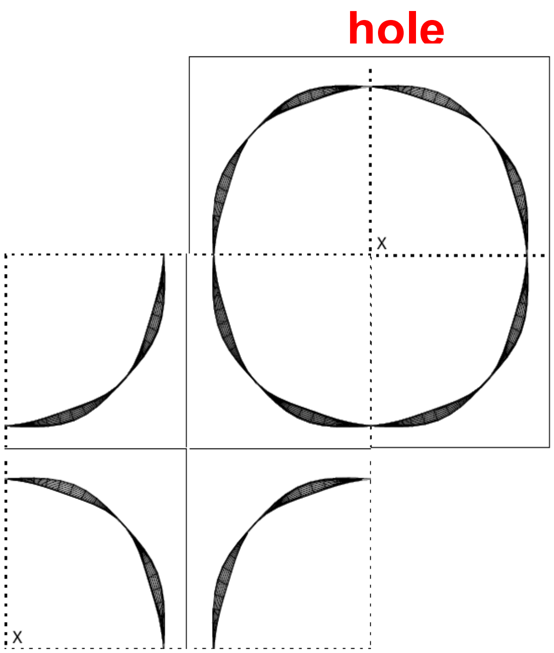

Only hole band

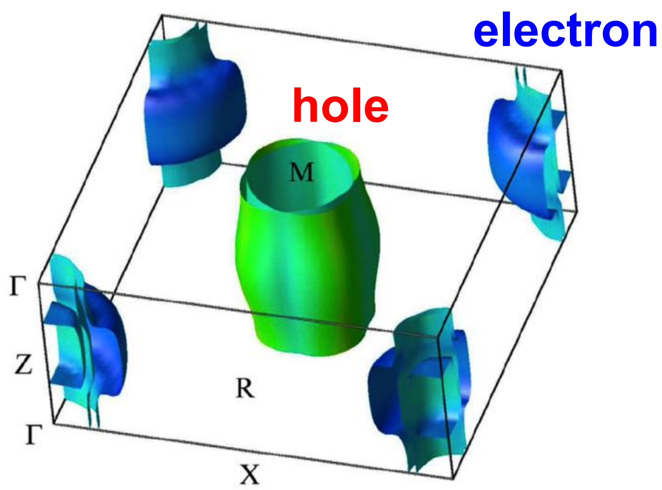

Well separated hole and electron bands

Similarities and differences between cuprates and pnictides

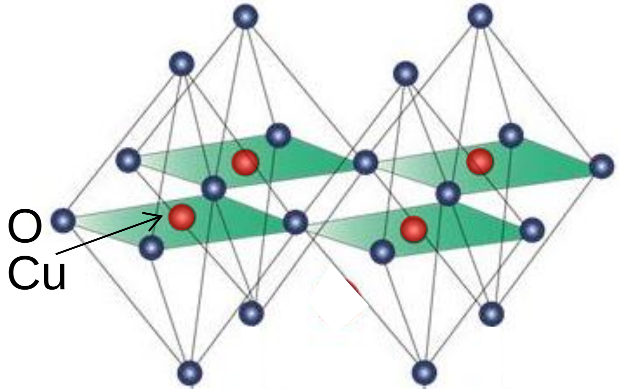

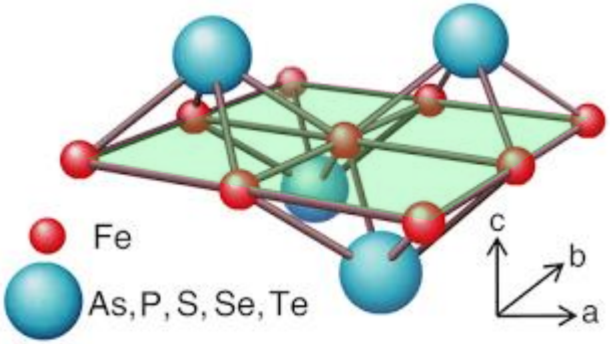

One orbital

x^2-y^2

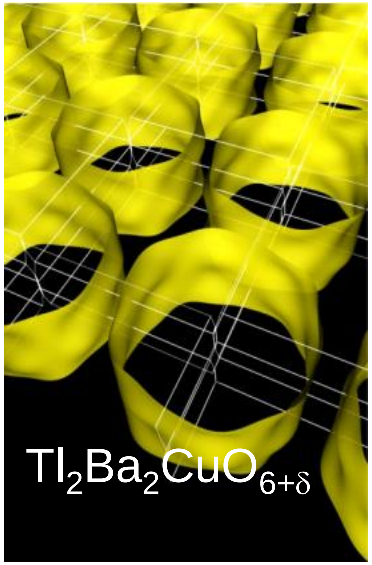

N. E. Hussey *et al.*, Nature (2003).

Mainly three orbitals

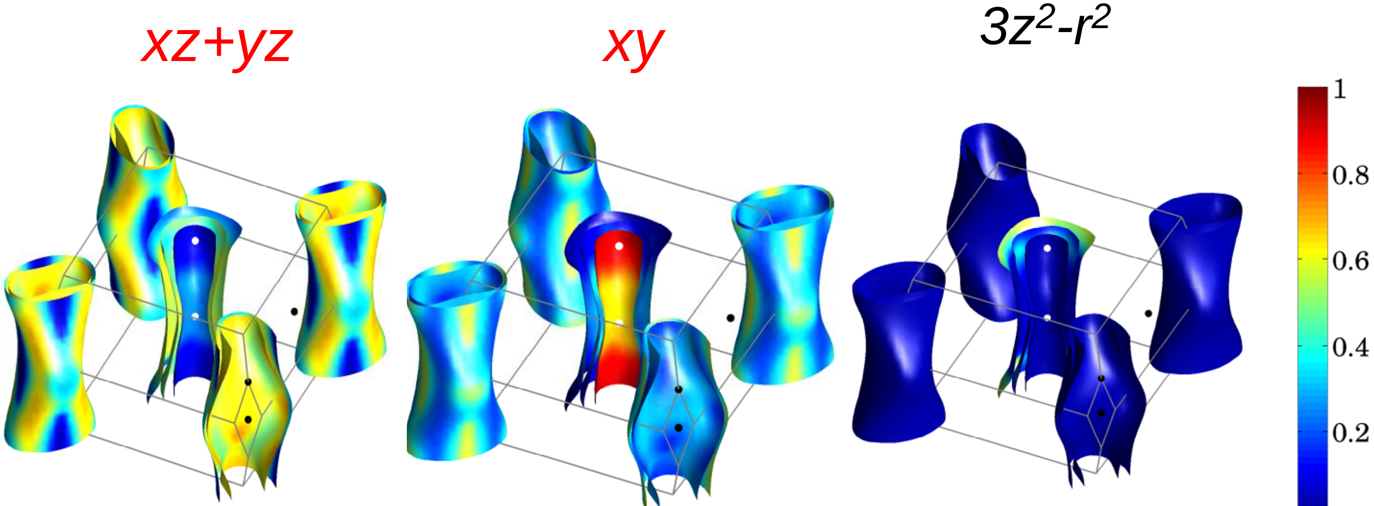

$BaFe_2As_2$

Brillouin Zone of Fe pnictides

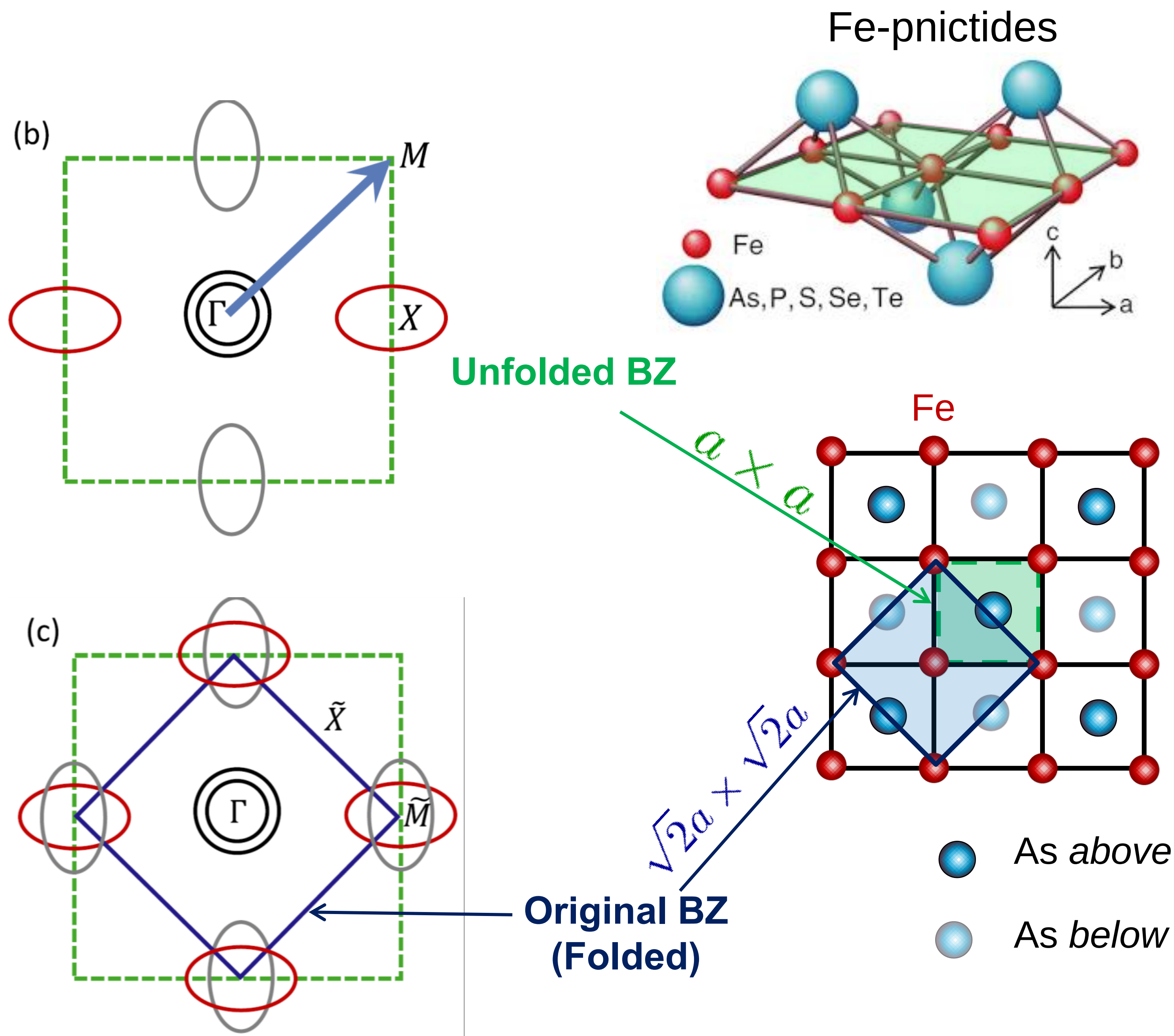

Similarities and differences between cuprates and pnictides

Cuprates

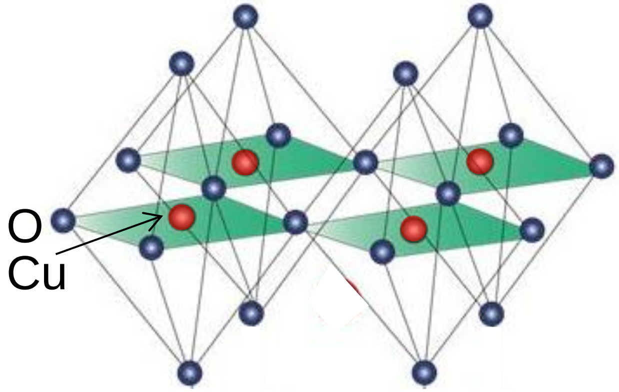

Fe-pnictides

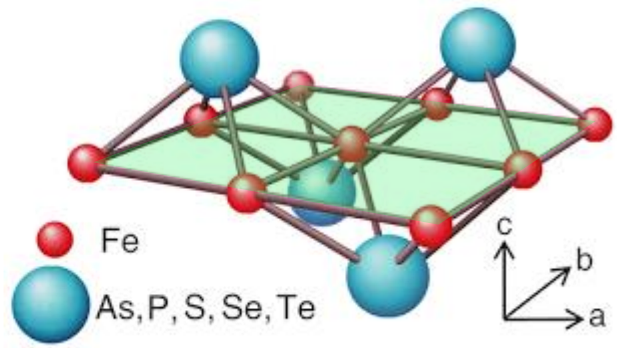

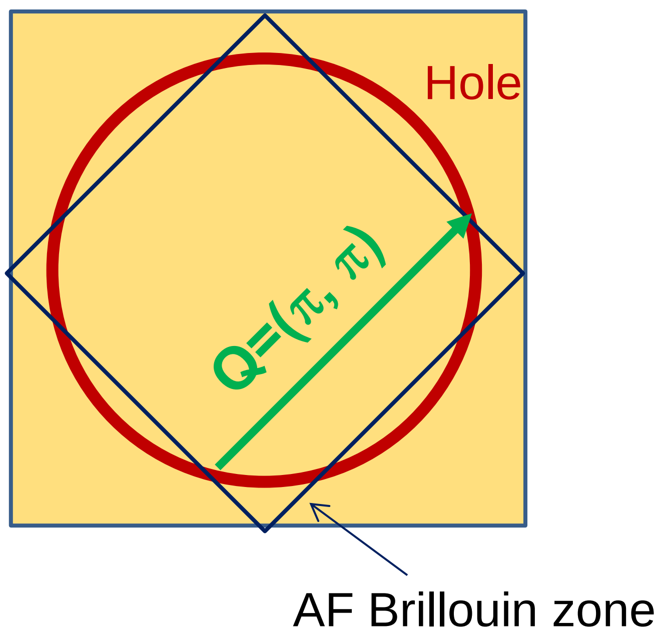

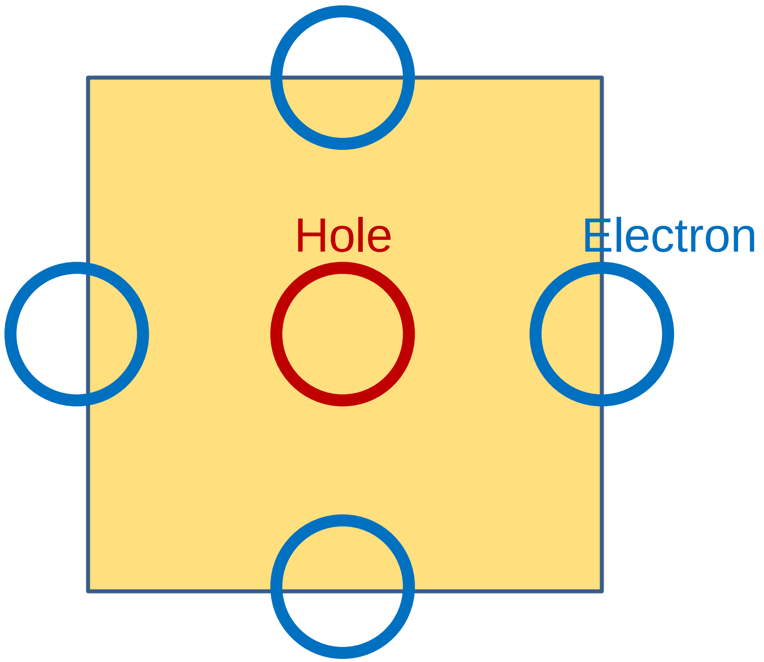

Similarities and differences between cuprates and pnictides

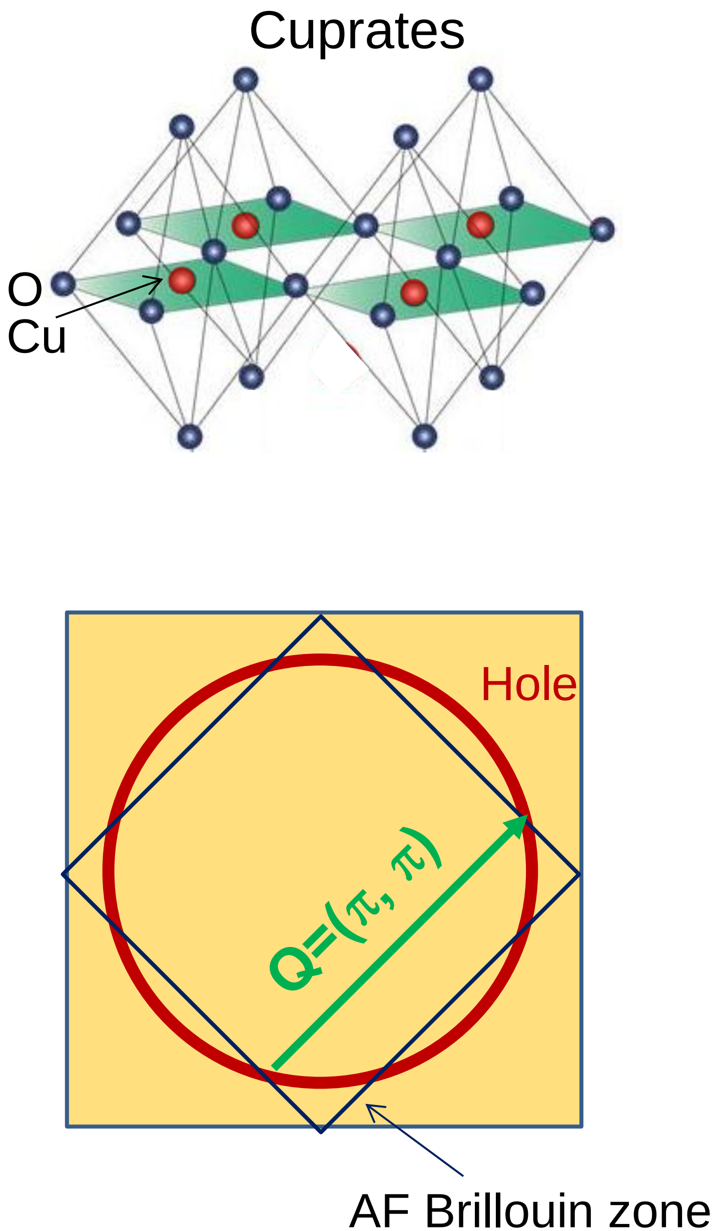

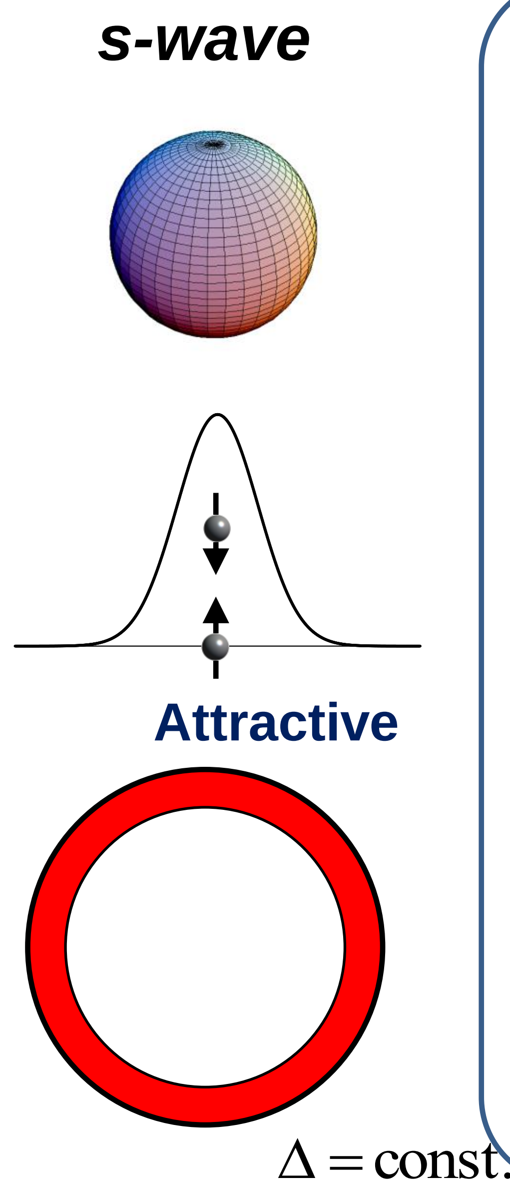

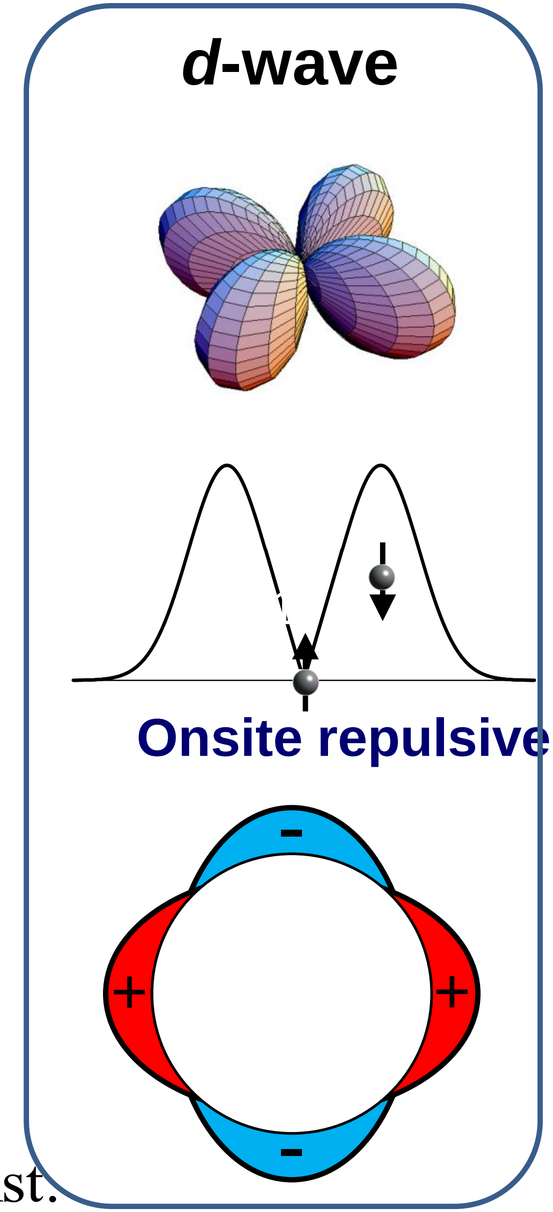

d-wave superconductivity in cuprates

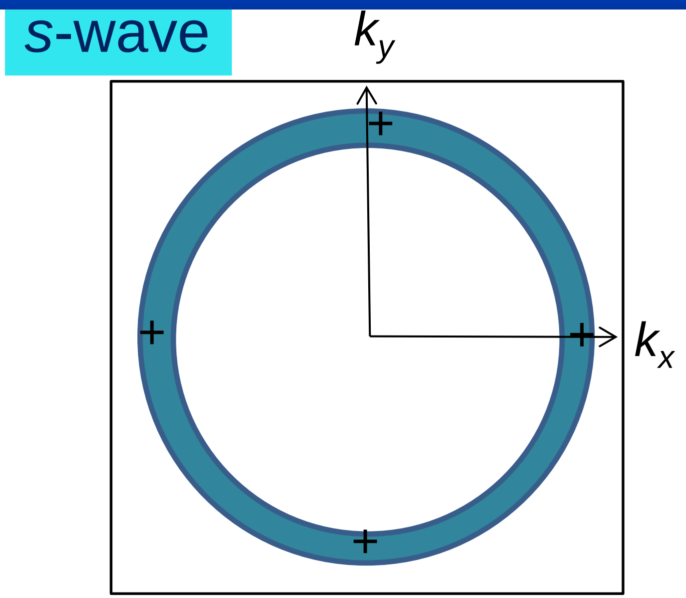

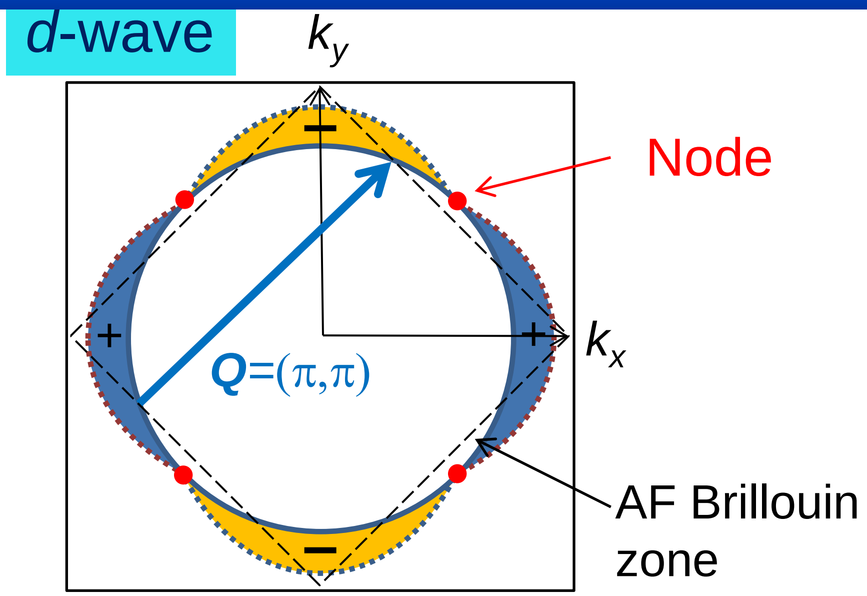

V(***q***): pairing interaction

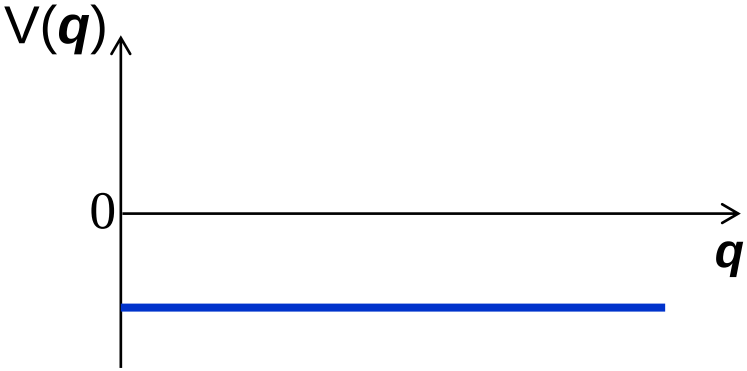

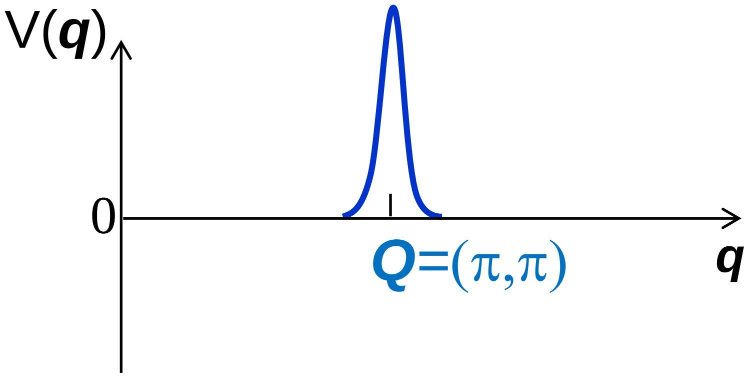

V(***q***) is negative and constant

V(***q***) is positive and peaks at ***q***=***Q***

$$V_{kp} \simeq \frac{3}{2}U^2\chi(k-p) \quad \chi(q) \sim \delta(q-Q)$$

d-wave superconductivity in cuprates

s-wave

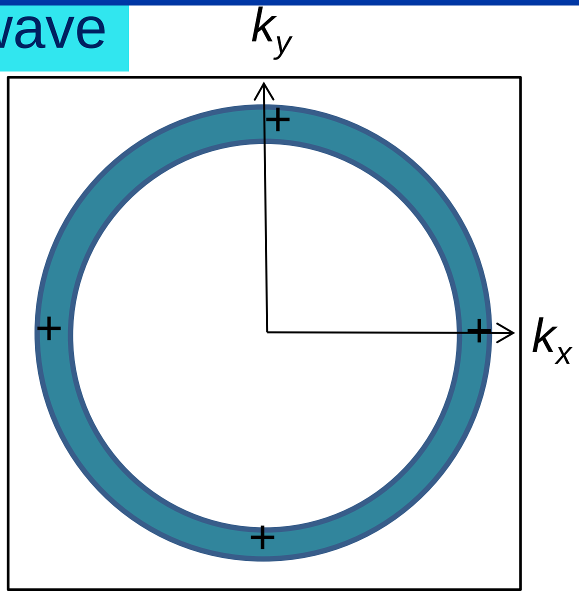

d-wave

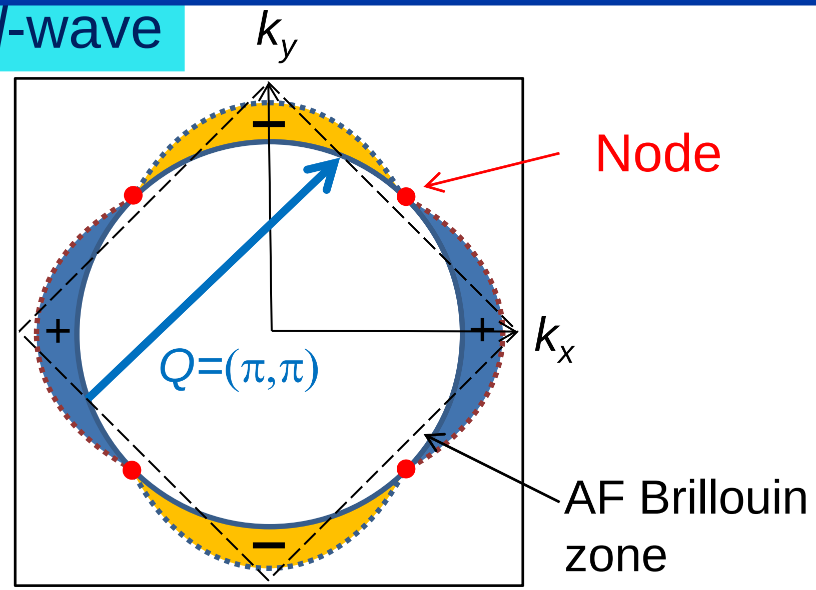

Gap equation

$$\Delta(k) = -\sum_p V_{kp} \frac{\tanh(\varepsilon_p/2T)}{2\varepsilon_p} \Delta(p) \qquad \varepsilon_p = \sqrt{\Delta_p^2 + \xi_p^2}$$

$$\Delta(k) = \Delta$$

$$\Delta = -\sum_p V_{kp} \underbrace{\frac{\tanh(\varepsilon_p/2T)}{\varepsilon_p}}_{>0} \Delta$$

$$V_{kp} = V < 0$$

$$V(r) \sim -\delta(r)$$

$$V_{kp} \simeq \underbrace{\frac{3}{2}U^2}_{\text{Coulomb}} \underbrace{\chi(k-p)}_{\text{Magnetic fluctuation}} \qquad \chi(q) \sim \delta(q-Q) \qquad Q=(\pi,\pi)$$

$$\Delta(k) \sim -\sum_p U^2 \delta(k-p+Q) \frac{\tanh(\varepsilon_p/2T)}{2\varepsilon_p} \Delta(p)$$

$$= -U^2 \frac{\tanh(\varepsilon_{k+Q}/2T)}{2\varepsilon_{k+Q}} \Delta(k+Q)$$

$\Delta(k+Q)\Delta(k) < 0$ sign change

$$V(x,y) \sim \cos\pi(x+y) + \cos\pi(x-y)$$

d-wave superconductivity in cuprates

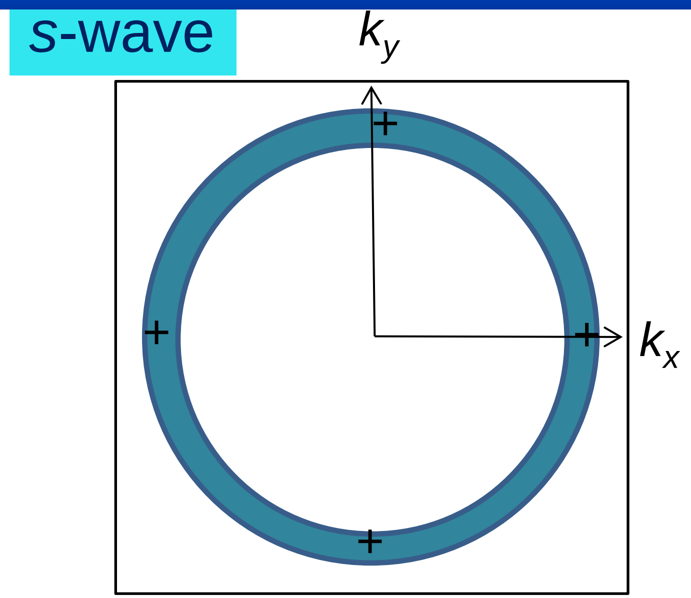

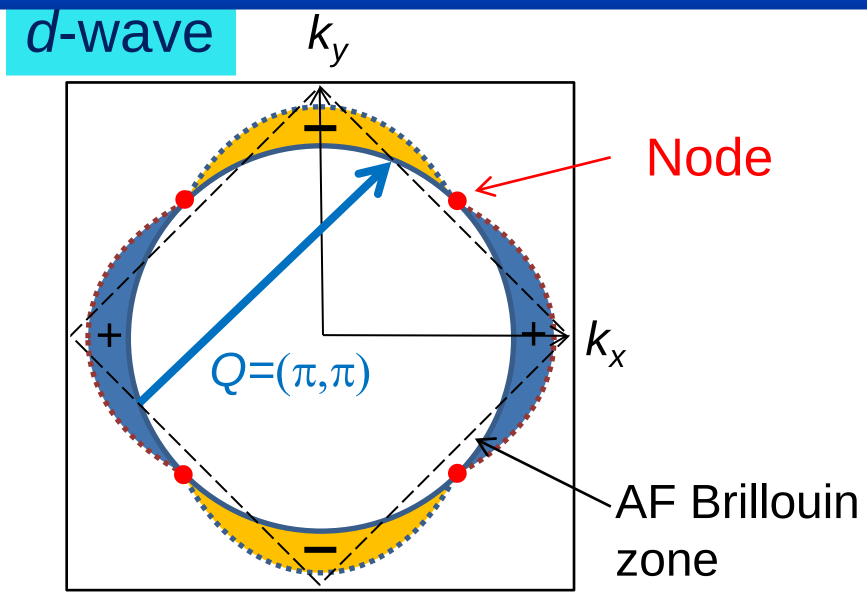

$$V(x,y) \sim \cos\pi(x+y) + \cos\pi(x-y)$$

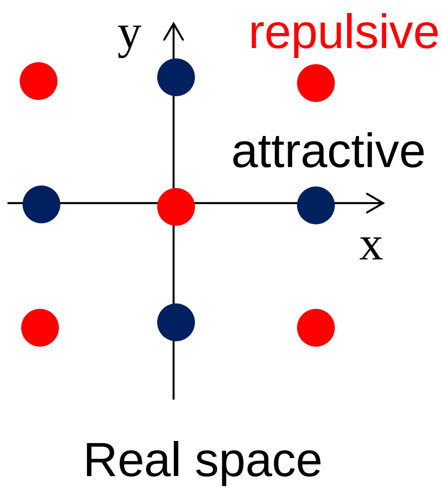

d-wave superconductivity in cuprates

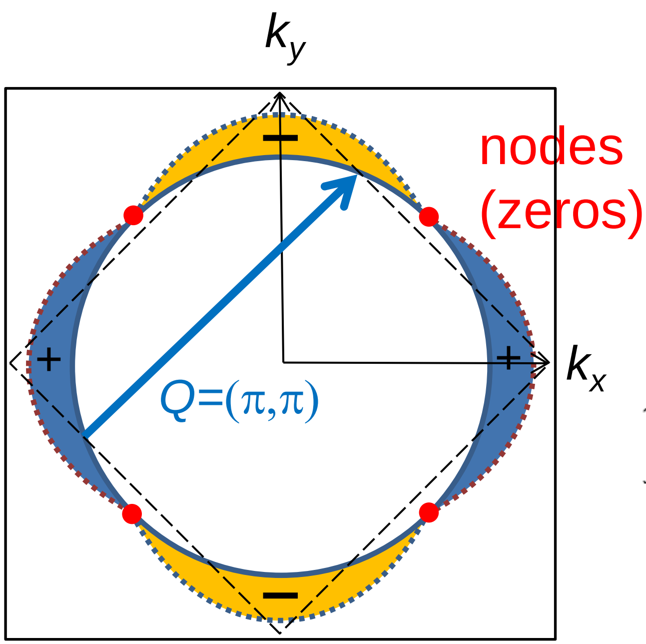

$d_{x^2-y^2}$ $(k_x^2-k_y^2)$

zeros at $k_x=+k_y$, $-k_y$

V(q) broadly peaks at (π, π)

Repulsive V(q)>0

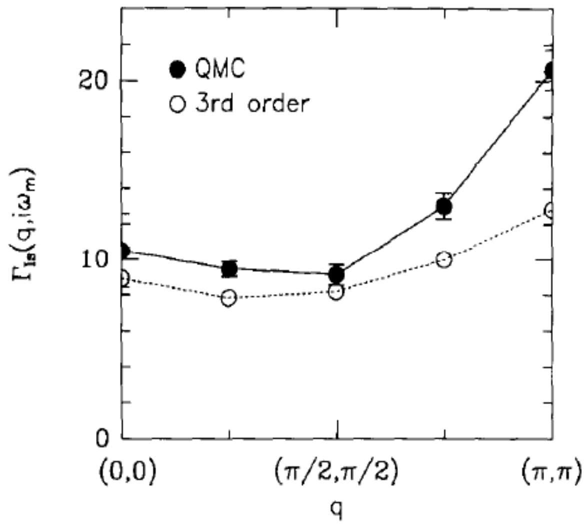

q-space

Repulsive on-site and
attractive off-site interaction

+0.01	−0.12	+0.12	−0.12	+0.01
−0.12	+0.43	−0.50	+0.43	−0.12
+0.12	−0.50	+9.6	−0.50	+0.12
−0.12	+0.43	−0.50	+0.43	−0.12
+0.01	−0.12	+0.12	−0.12	+0.01

r-space

D. J. Scalapino, Phys. Rep. (1995).

d-wave superconductivity in cuprates

YBCO tricrystal
superconducting ring
(1994)

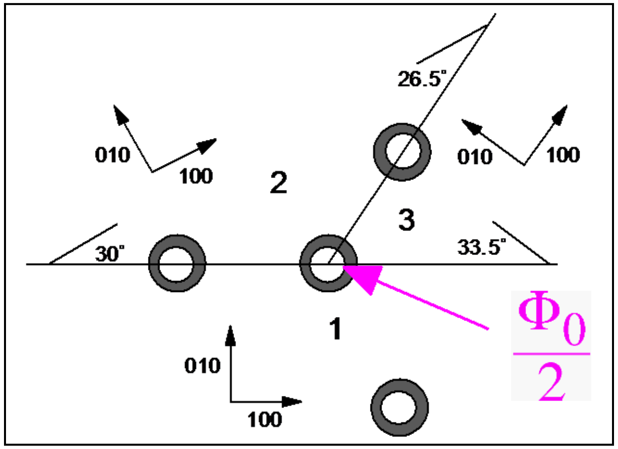

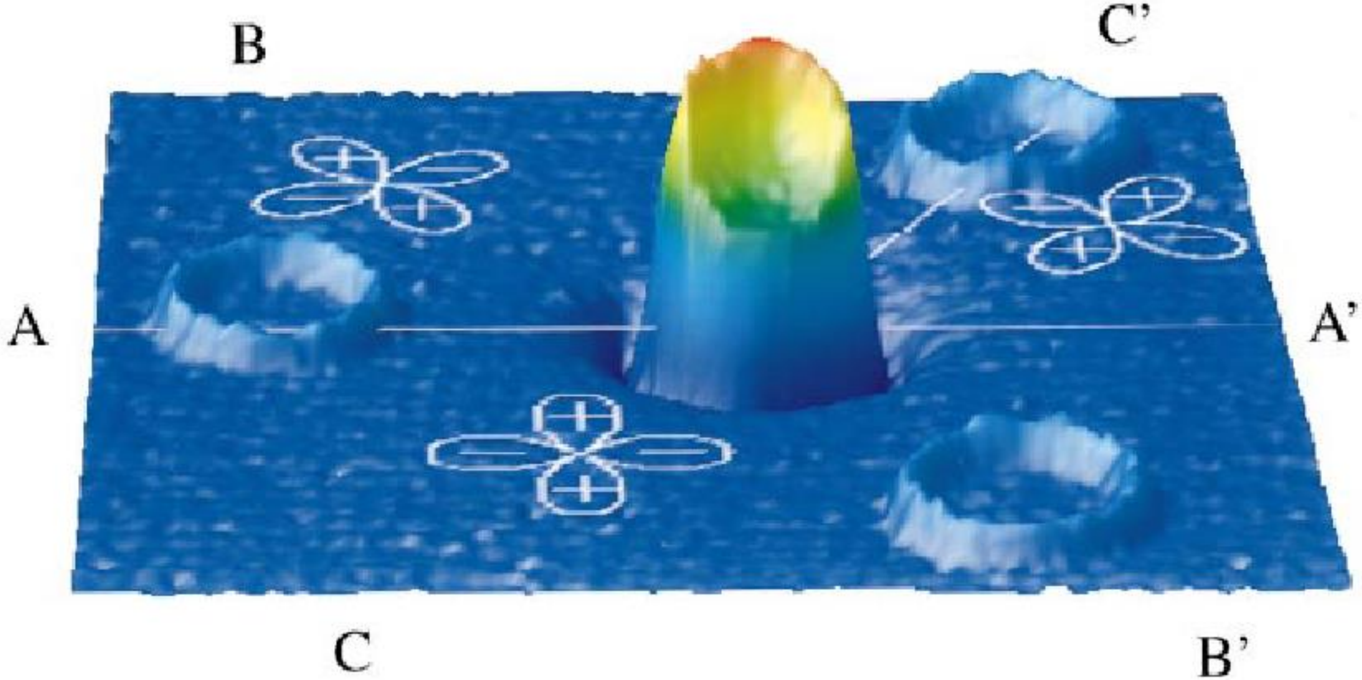

C.C. Tsuei *et al*. PRL (94)

Similarities and differences between cuprates and pnictides

Cuprates

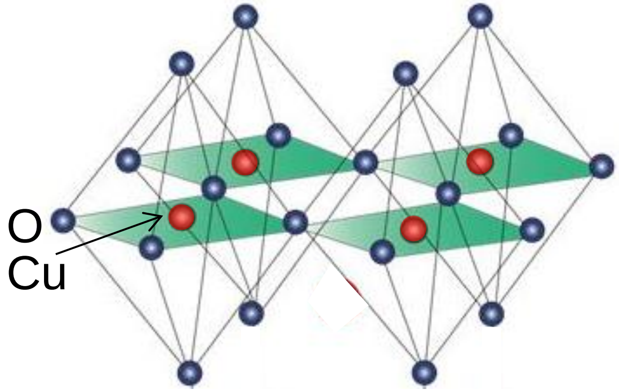

Fe-pnictides

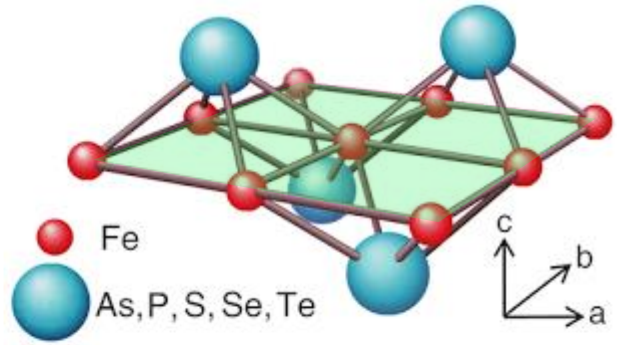

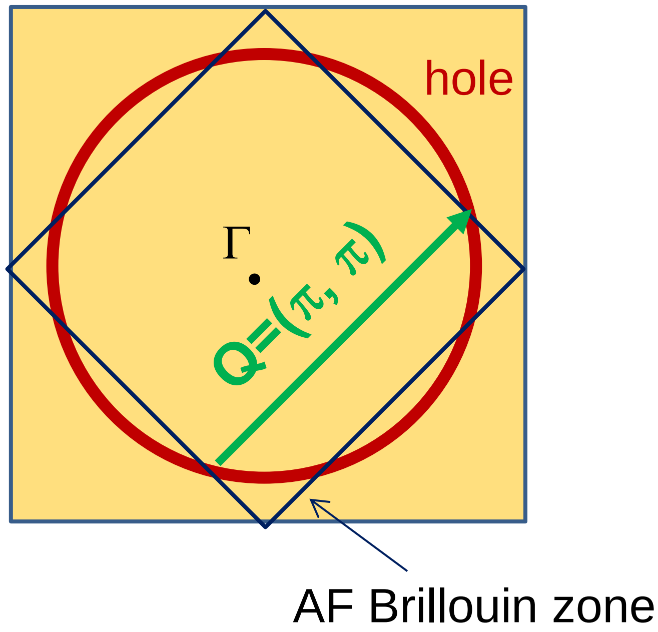

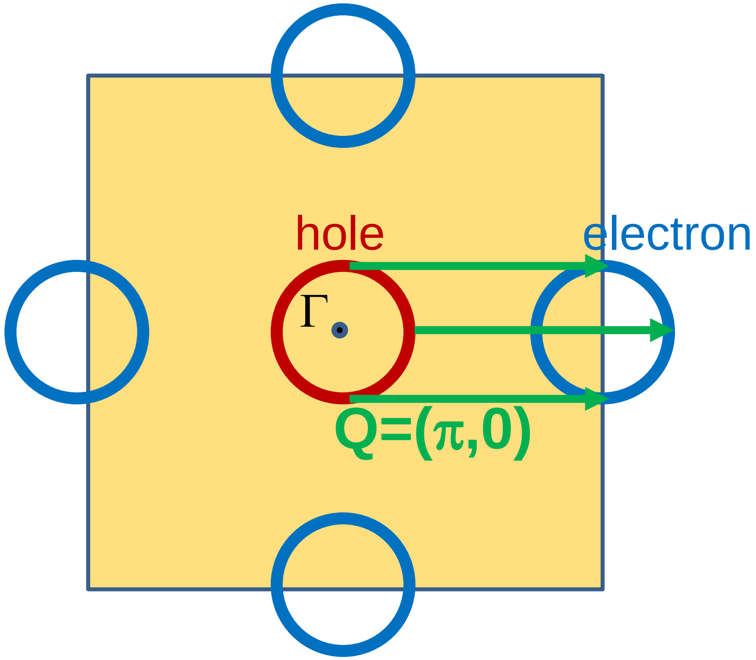

Iron pnictides: candidate for the SC state

Two band superconductor

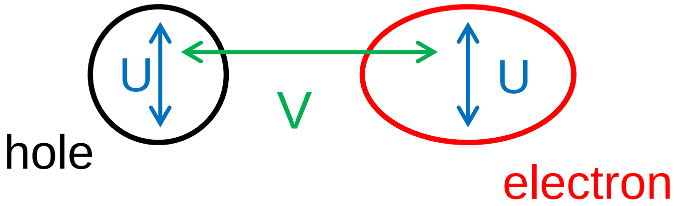

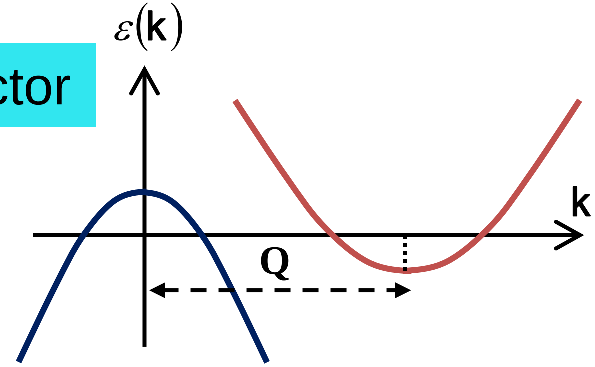

disconnected Fermi surfaces

Gap equation

$$\Delta_e = -V\Delta_h \sum_q \frac{\tanh \frac{\varepsilon_q}{2T_c}}{\varepsilon_q} - U\Delta_e \sum_q \frac{\tanh \frac{\varepsilon_q}{2T_c}}{\varepsilon_q}$$

$$\Delta_h = -V\Delta_e \sum_q \frac{\tanh \frac{\varepsilon_q}{2T_c}}{\varepsilon_q} - U\Delta_h \sum_q \frac{\tanh \frac{\varepsilon_q}{2T_c}}{\varepsilon_q}$$

$$U = 0$$

$$|V|N(0)\ln \frac{W}{T_c} = 1$$

W: band width

At T_c:

$$\begin{pmatrix} \Delta_e \\ \Delta_h \end{pmatrix} = A \begin{pmatrix} 0 & -1 \\ -1 & 0 \end{pmatrix} \begin{pmatrix} \Delta_e \\ \Delta_h \end{pmatrix} \qquad A = \pm 1$$

$V > 0$ repulsive $\quad A = +1 \quad \Delta_e = -\Delta_h$ Sign change $S_\pm$

$V < 0$ attractive $\quad A = -1 \quad \Delta_e = \Delta_h$ No sign change S_{++}

Iron pnictides: candidate for the SC state

S_{+-}

Fe-pnictides

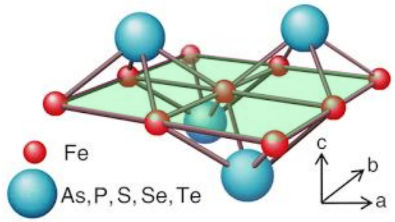

k-space (repulsive)

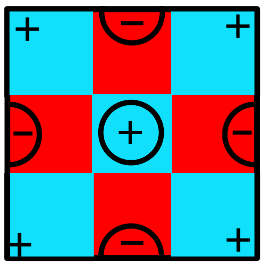

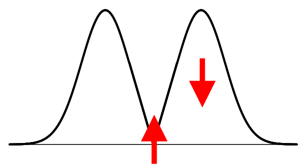

r-space

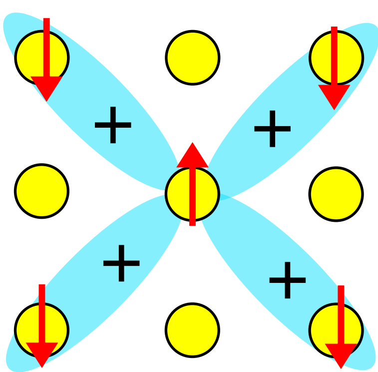

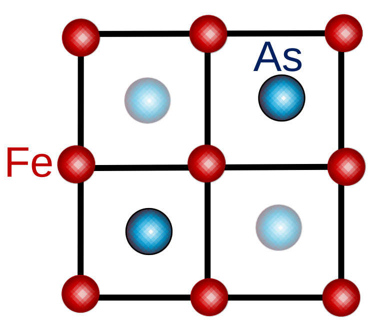

$$\Delta(\cos k_x \cos k_y)$$

$d_{x^2-y^2}$

Cuprates

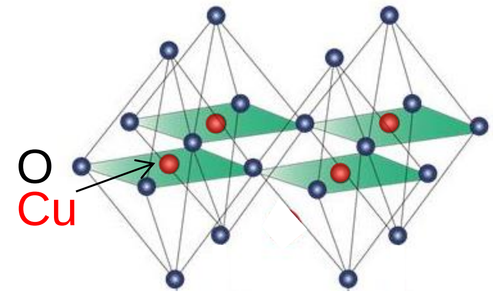

k-space (repulsive)

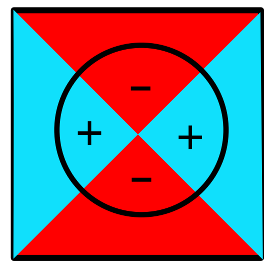

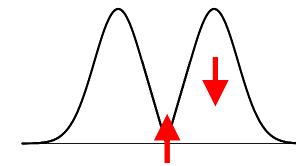

r-space

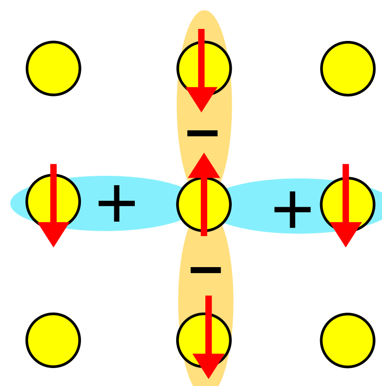

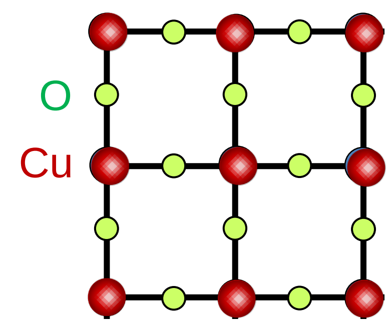

$$\Delta(\cos k_x - \cos k_y)$$

Iron pnictides: candidate for the SC state

S_{+-}

Fe-pnictides

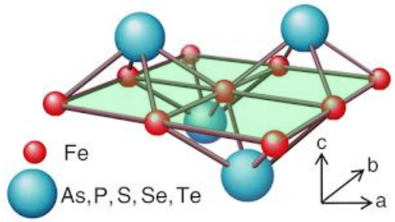

k-space (repulsive)

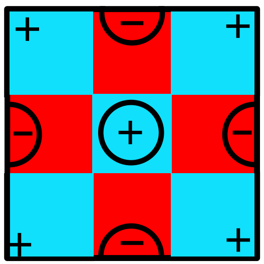

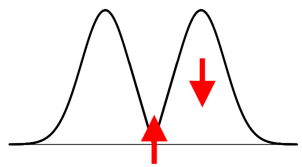

r-space

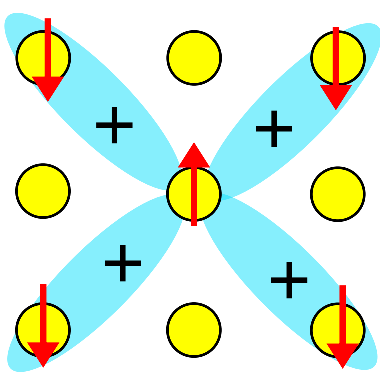

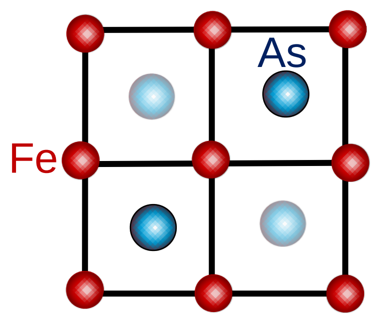

$$\Delta(\cos k_x \cos k_y)$$

S_{++}

k-space (attractive)

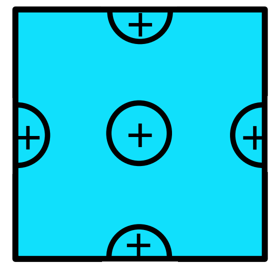

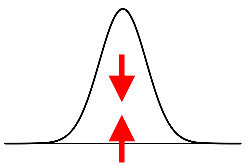

r-space

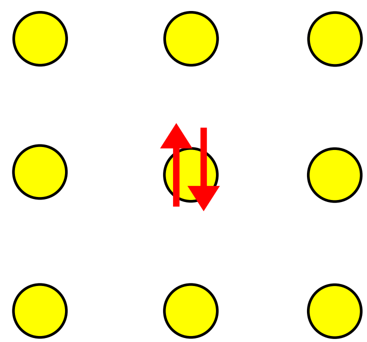

$$\Delta$$

Iron pnictides: candidate for the SC state

- Pairing due to purely repulsive interaction

$$V > 0$$

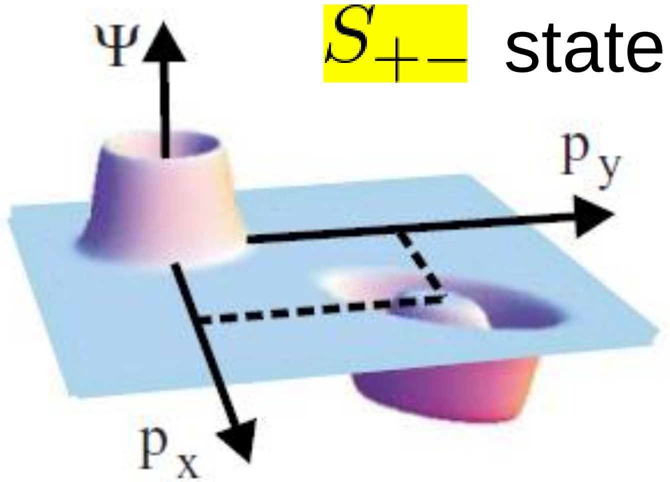

I. I. Mazin *et al*., PRL **101**, 057003 (2008).
K. Kuroki *et al*., PRL **101**, 087004 (2008).
& PRB **79**, 224511 (2009).
A. V. Chubkov *et al*., PRB **80**, 140515(R) (2009).
S. Graser *et al*., NJP **11**, 025016 (2009).
H. Ikeda, PRB **81**, 054502 (2010).
K. Seo *et al*., PRL **101**, 206404 (2008).
F. Wang *et al*., PRL **102**, 047005 (2009).
⋮

- Pairing due to attractive interaction

$$V < 0$$

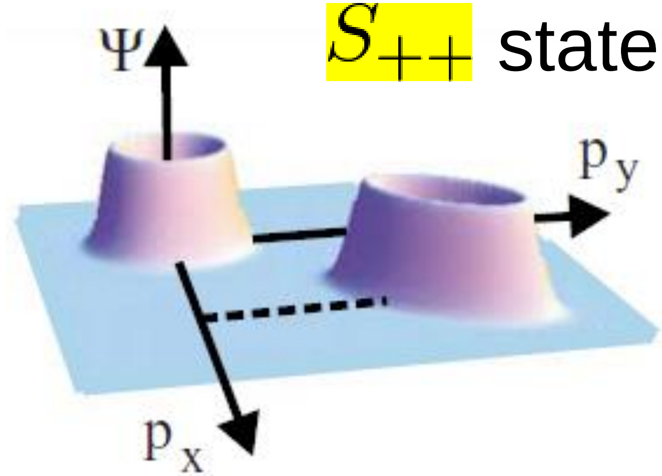

H. Kontani & S. Onari, PRL **104**, 157001 (2010).
F. Kruger *et al*., PRB **79**, 054504 (2009).
Y. Yanagi *et al*., PRB **81**, 054518 (2010).
⋮

Physics of iron-based high temperature superconductors

1) Introduction

2) Similarities and differences between cuprates and Fe-pnictides

3) Normal state properties

Electronic structure and magnetism

4) Superconducting properties

Superconducting gap structure

5) Some recent topics

QCP, BCS-BEC crossover,
A novel high field SC state, Nematicity・・・・

Electron correlations

Electron correlations change the band structure

Band narrowing

Mass enhancement

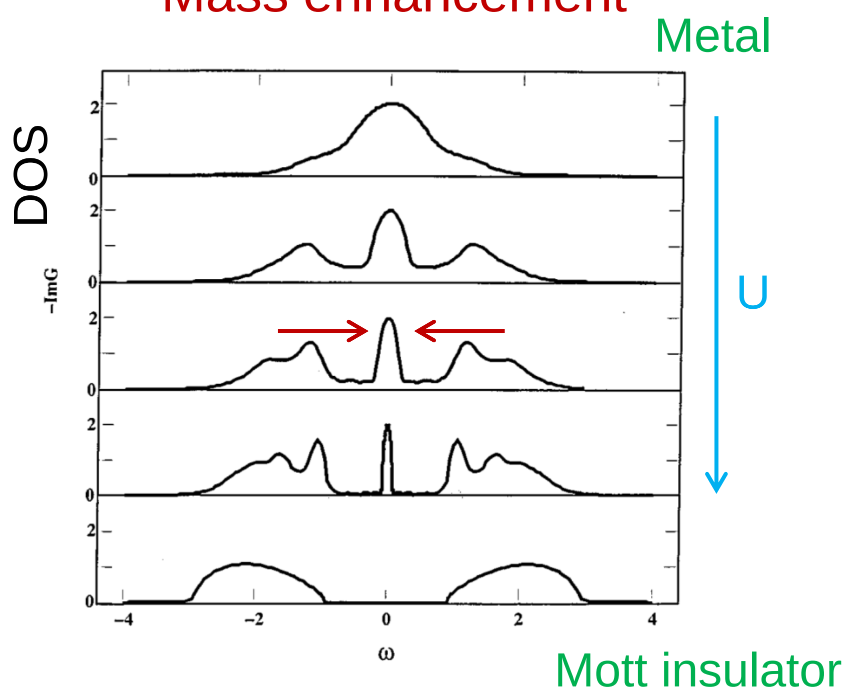

Band shift

Particularly important for multiband system

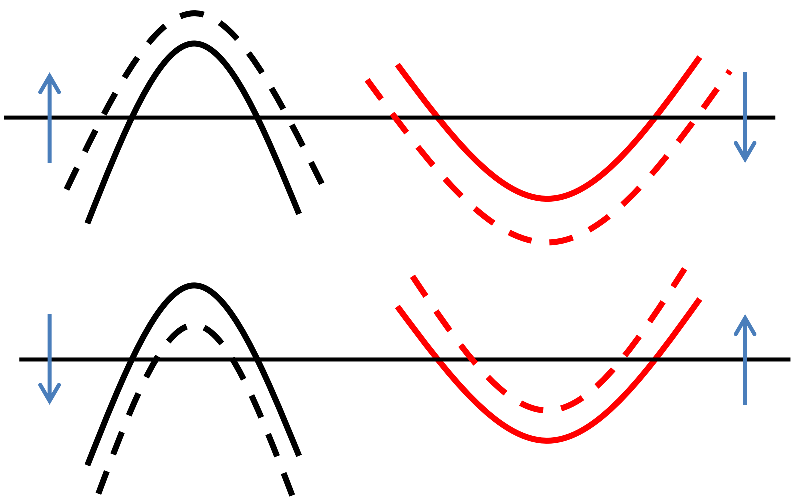

A. Georges, G. Kotoliar, W. Krauth and M.J. Rozenberg, Rev. Mod. Phys. 68, 13 (1996)

LDA calculation (major part of electron correlation is dropped.)

LDA: local density approximation

Difference between LDA and measured Fermi surface is a measure of the influence of the electron correlation.

Determination of Fermi surface

Quantum oscillations

Landau quantization

Quantization of the orbital motion of electrons in magnetic field

$$E = (n + 1/2)\hbar\omega_c \qquad \omega_c = \frac{eB}{m^*c}$$

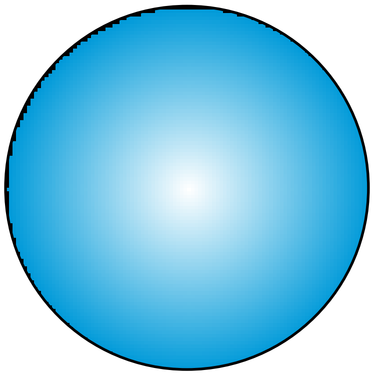

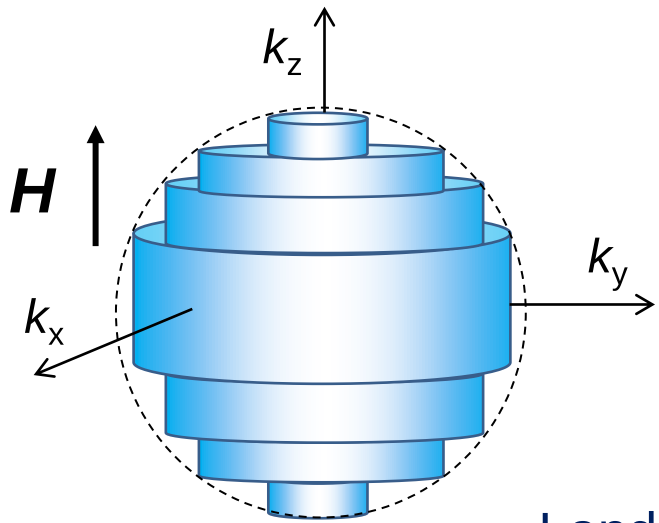

Allowed orbits are in the plane perpendicular to the magnetic field direction on a series space of constant energy surfaces in *k*-space.

Landau tubes

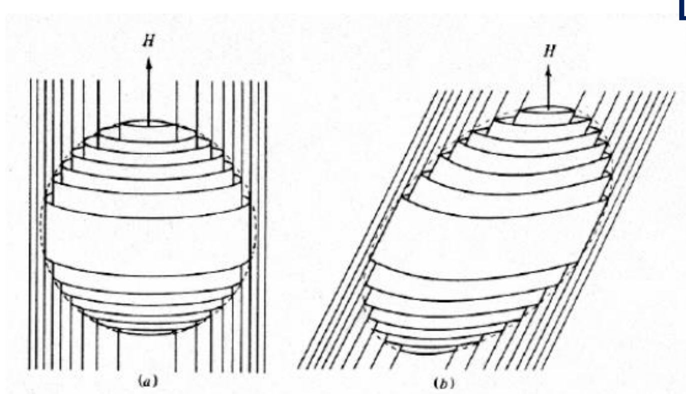

De Haas–van Alphen effect
Magnetization

Shubnikov–de Haas effect
Resistivity

Determination of Fermi surface

Lifshits-Kosevich formula (1954)

$$\Delta\left(\frac{1}{B}\right) = \frac{2\pi e}{\hbar c S}$$

$$M_{osc} = A \sin\left(\frac{2\pi F}{H} + \Phi\right)$$

$$A \propto J_2(x) T H^{-1/2} \left|\frac{\partial^2 S}{\partial k_{\mathrm{H}}^2}\right|^{-1/2} R_{\mathrm{T}} R_{\mathrm{D}} R_{\mathrm{S}}$$

$$F = \frac{\hbar c}{2\pi e} S_F$$ Oscillatory (dHvA) frequency

S_F Fermi surface extremal cross section

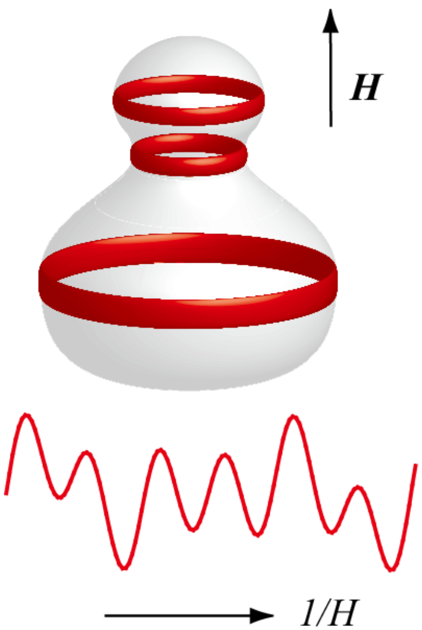

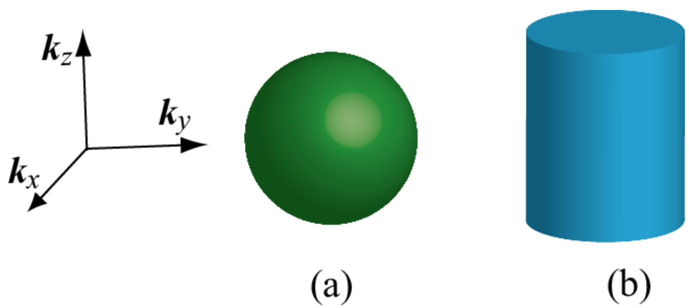

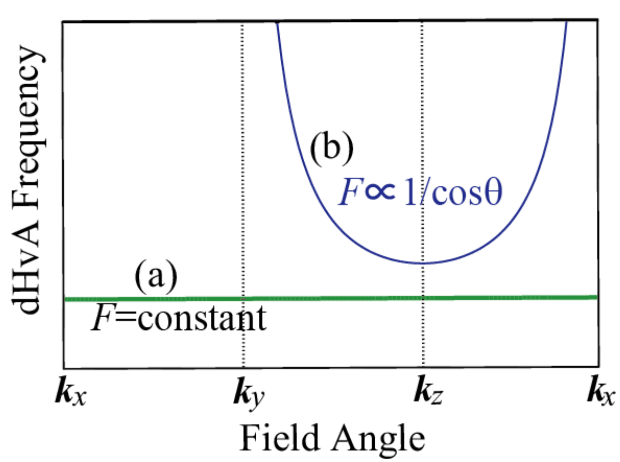

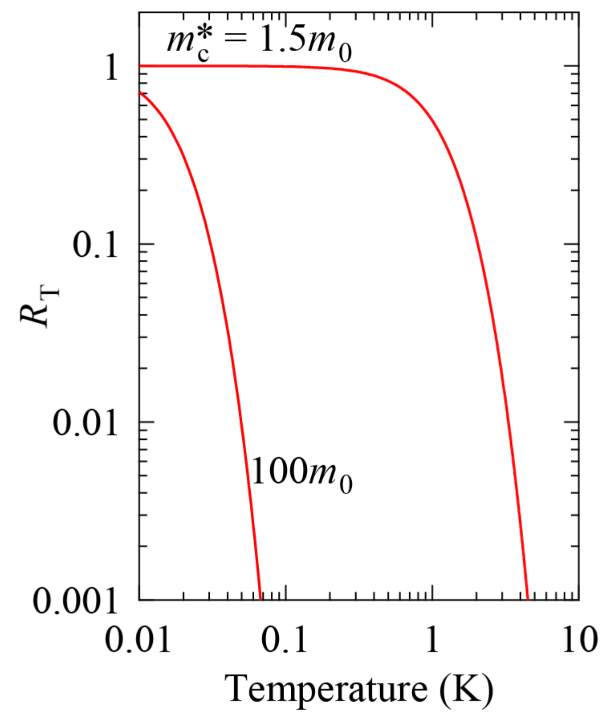

$$R_T = \frac{\alpha m_c^* T}{H} \times \frac{1}{\sinh\left(\alpha m_c^* \frac{T}{H}\right)}$$

Determination of Fermi surface

Angle resolved photoemission spectroscopy

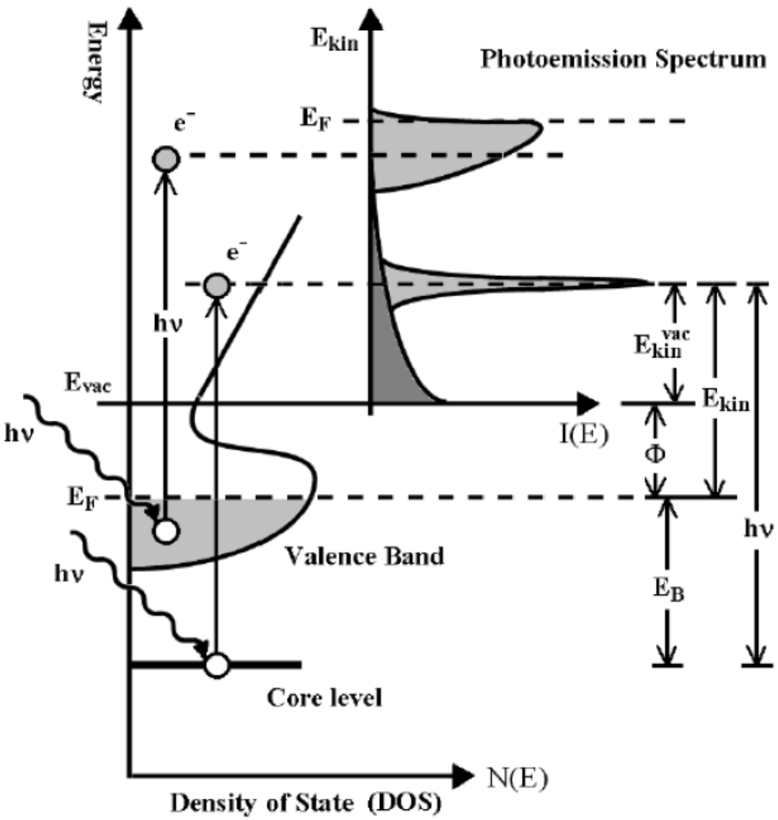

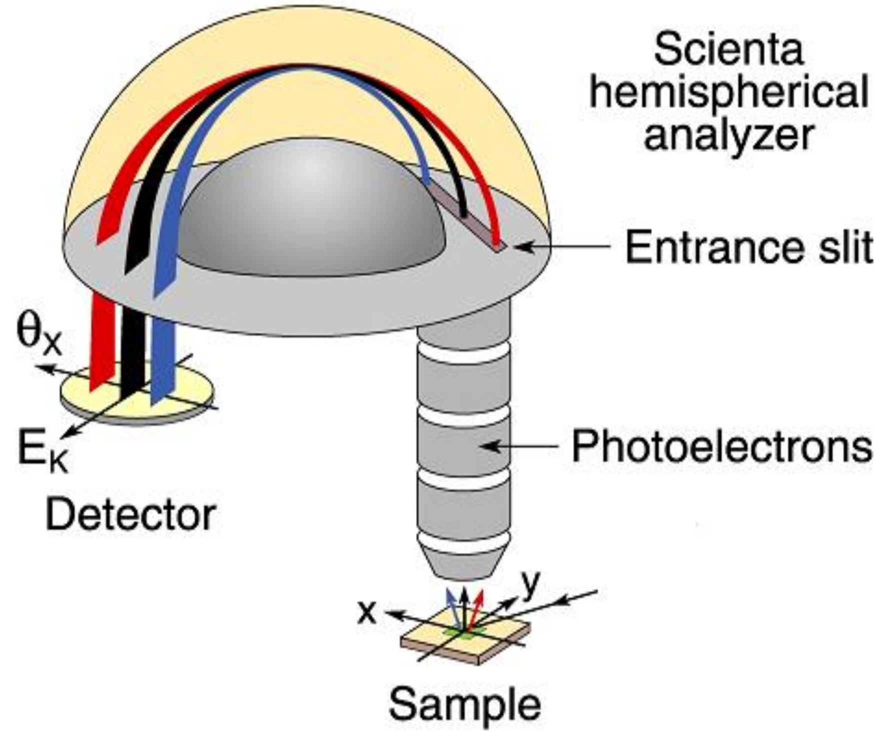

Fe-based high-T_c superconductors

1111

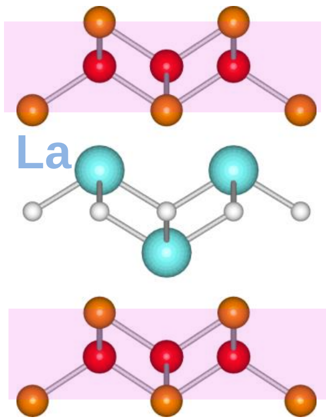

Ln FeAsO
T_c(max)=55K

122

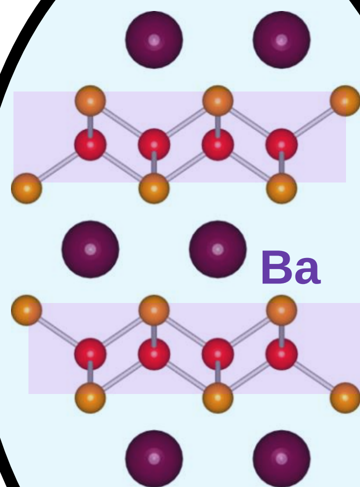

$BaFe_2As_2$
T_c(max)=38K

111

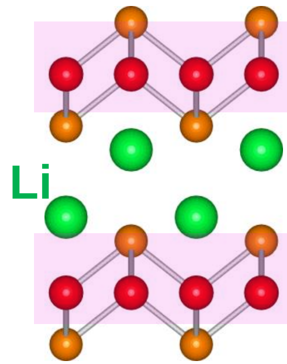

LiFeAs
T_c= 18 K

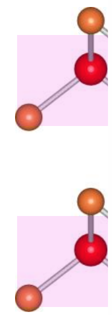

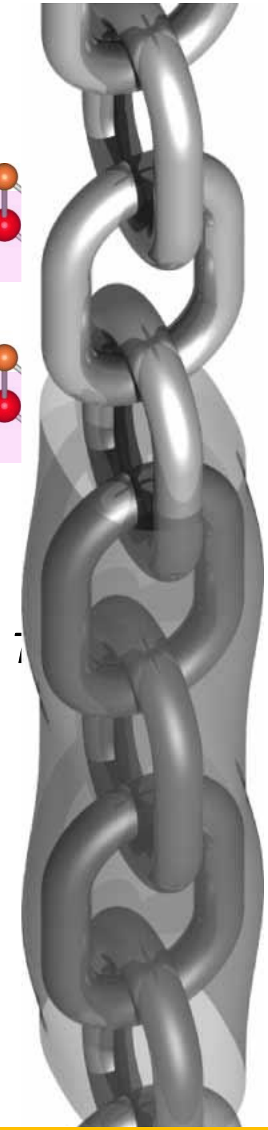

Parent compound
$BaFe_2As_2$
(AF Metal)

Correlated metal

Similar to overdoped cuprates

D.N.Basov *et al.*
Nature Phys. (09)

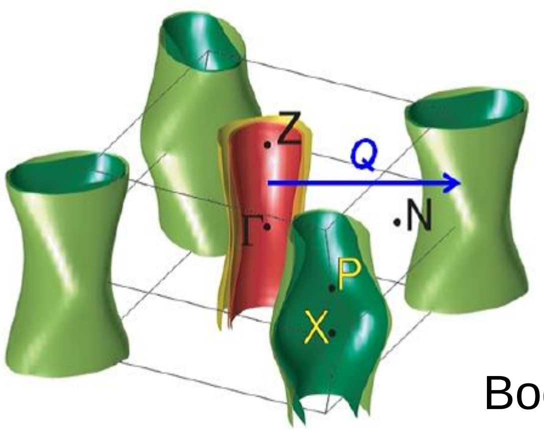

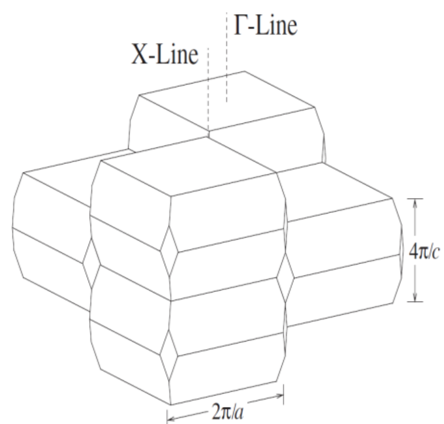

Body-centered tetragonal

The `snake that swallowed a chain'

Superconductivity in $BaFe_2As_2$ systems

Parent compound

$BaFe_2As_2$

(AF Metal)

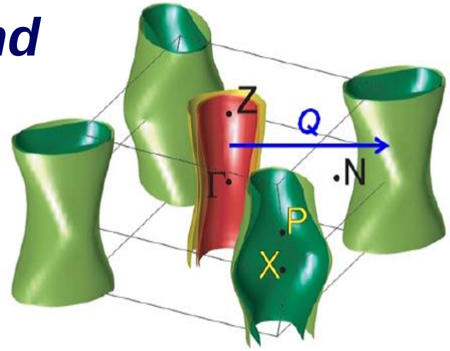

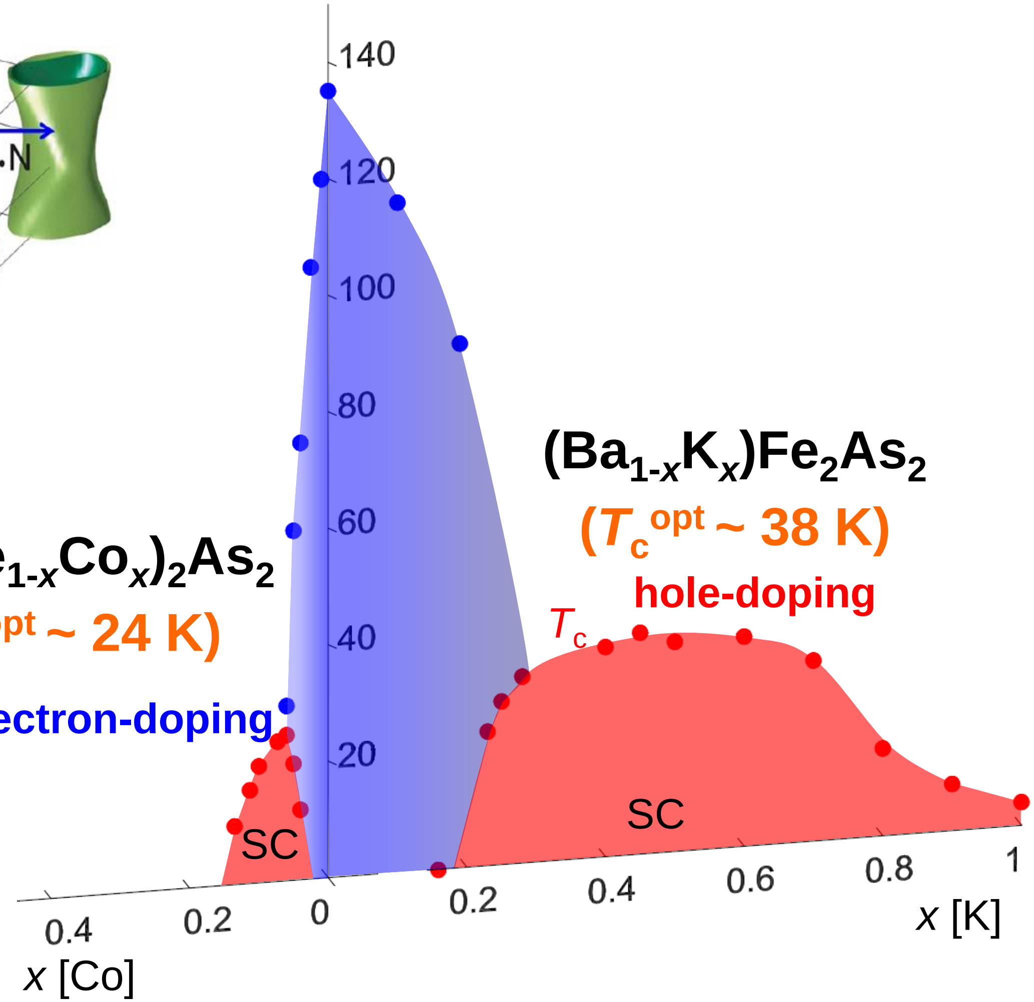

Superconductivity in $BaFe_2As_2$ systems

Parent compound
$BaFe_2As_2$
(AF Metal)

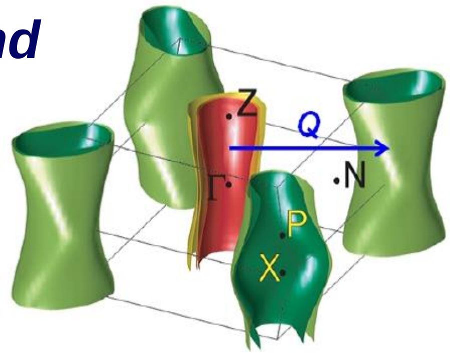

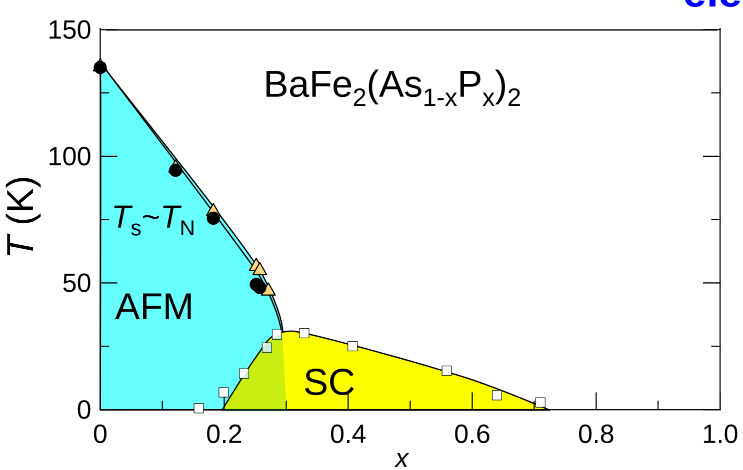

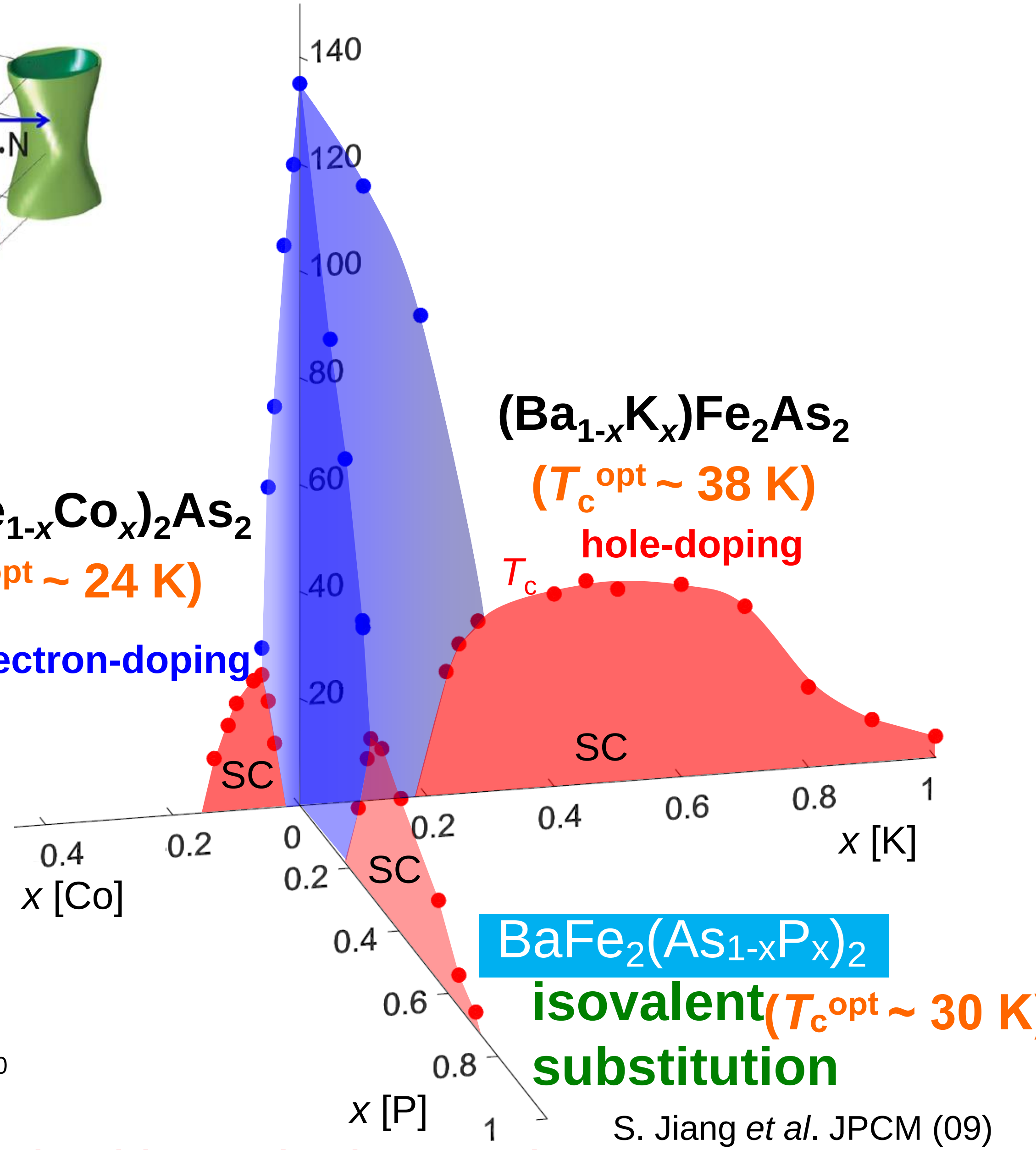

S. Jiang *et al*. JPCM (09)

Ground state can be tuned without doping carriers

$BaFe_2(As_{1-x}P_x)_2$

LDA A. Carrington

x=0.0

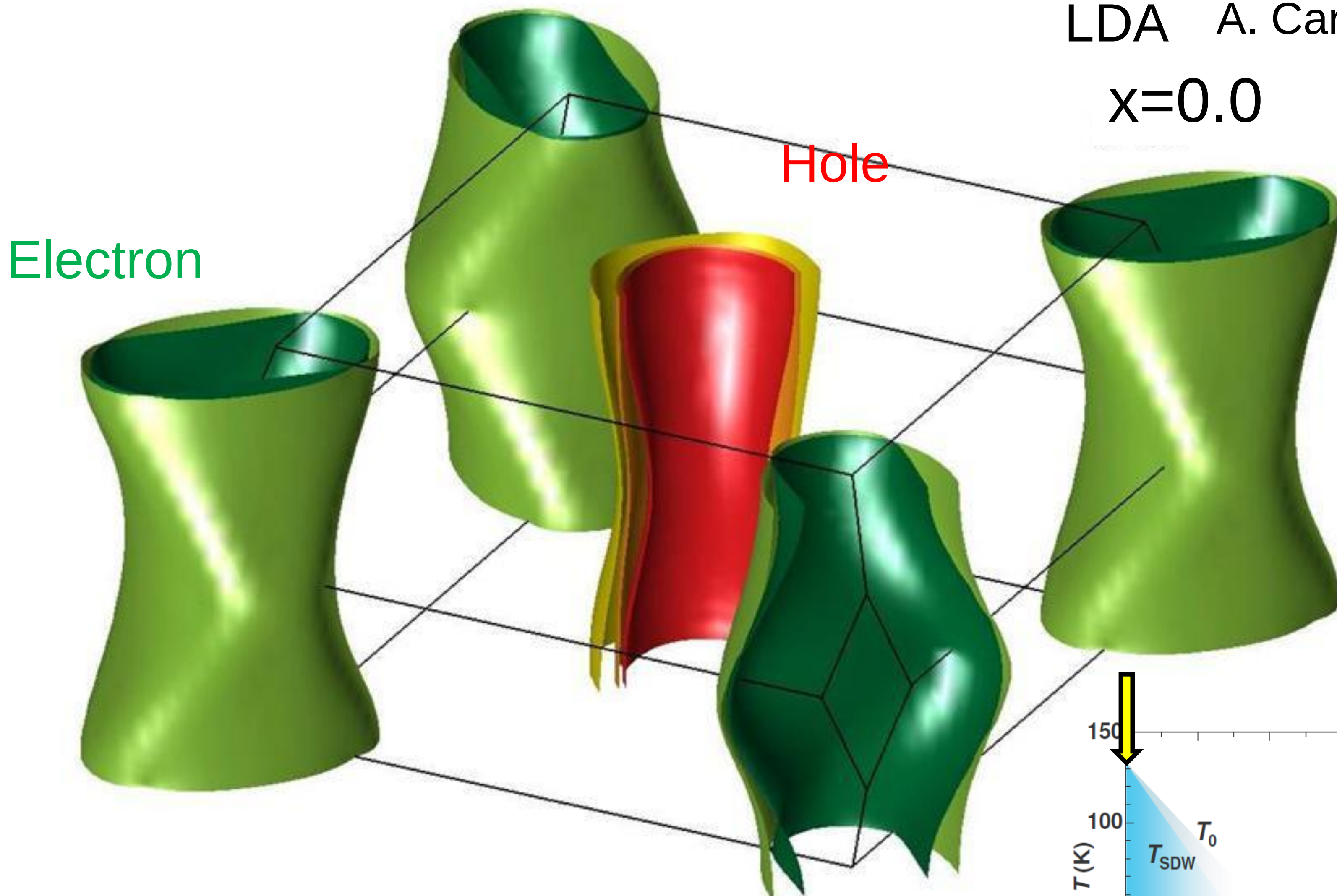

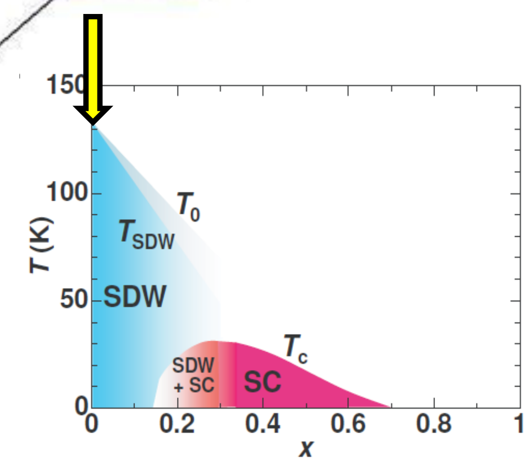

$BaFe_2(As_{1-x}P_x)_2$

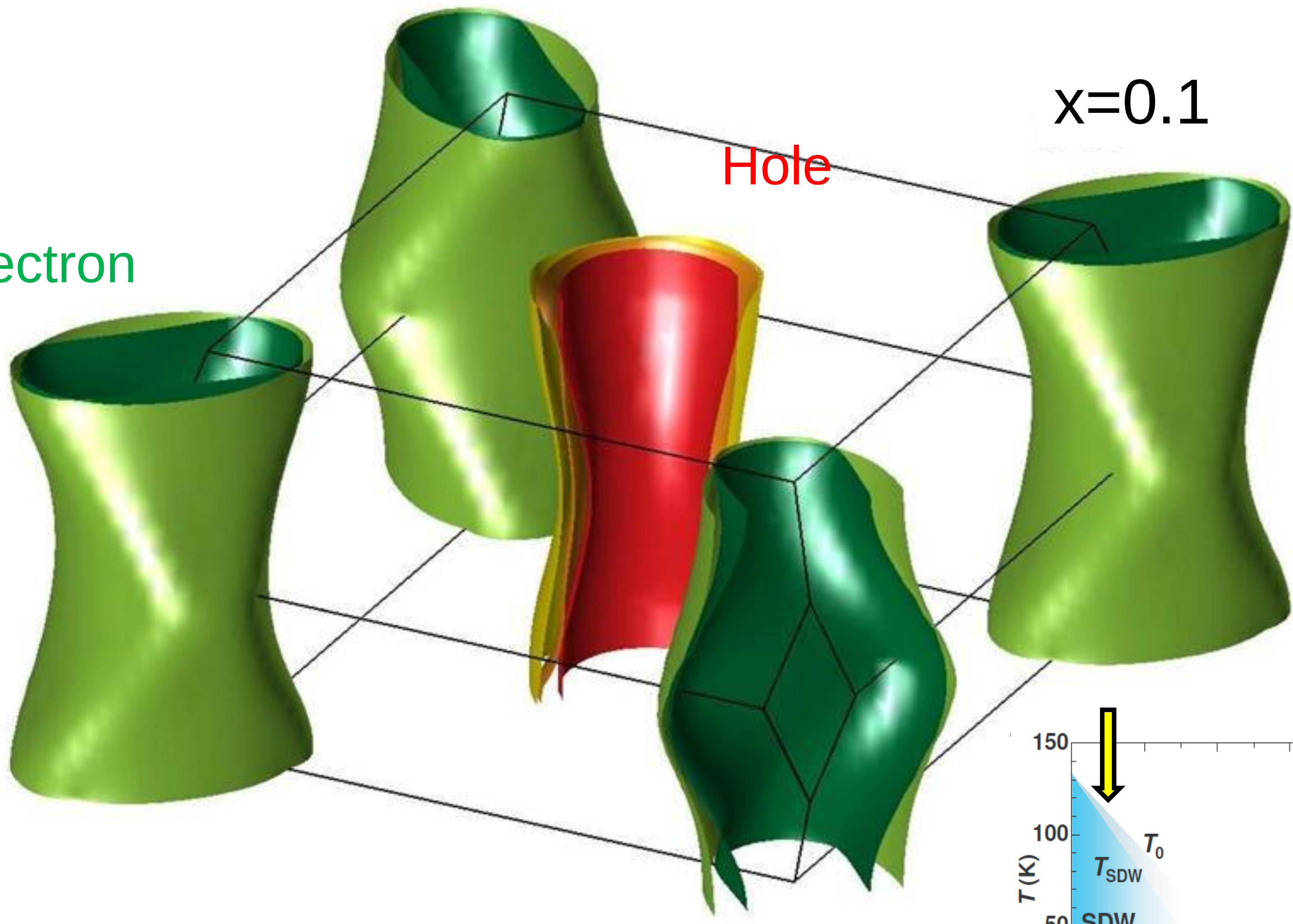

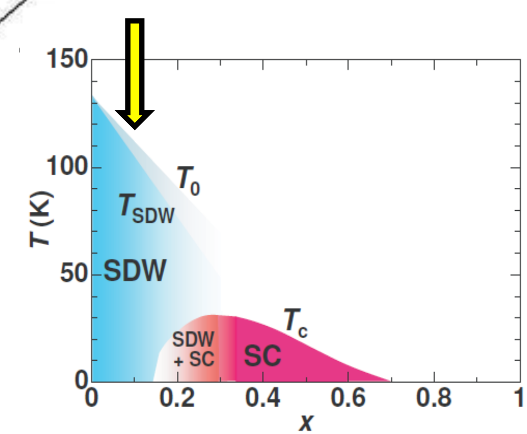

$BaFe_2(As_{1-x}P_x)_2$

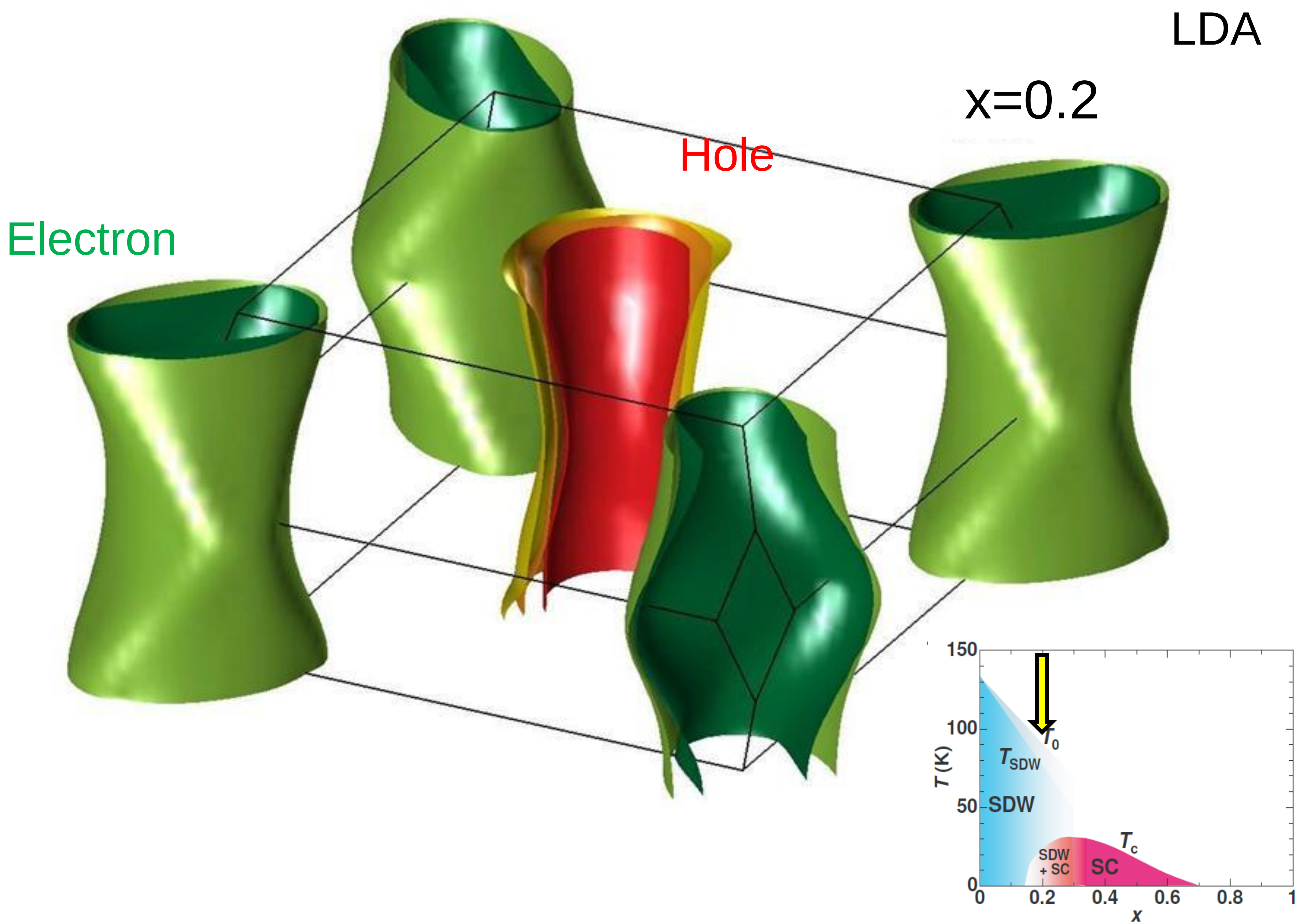

$BaFe_2(As_{1-x}P_x)_2$

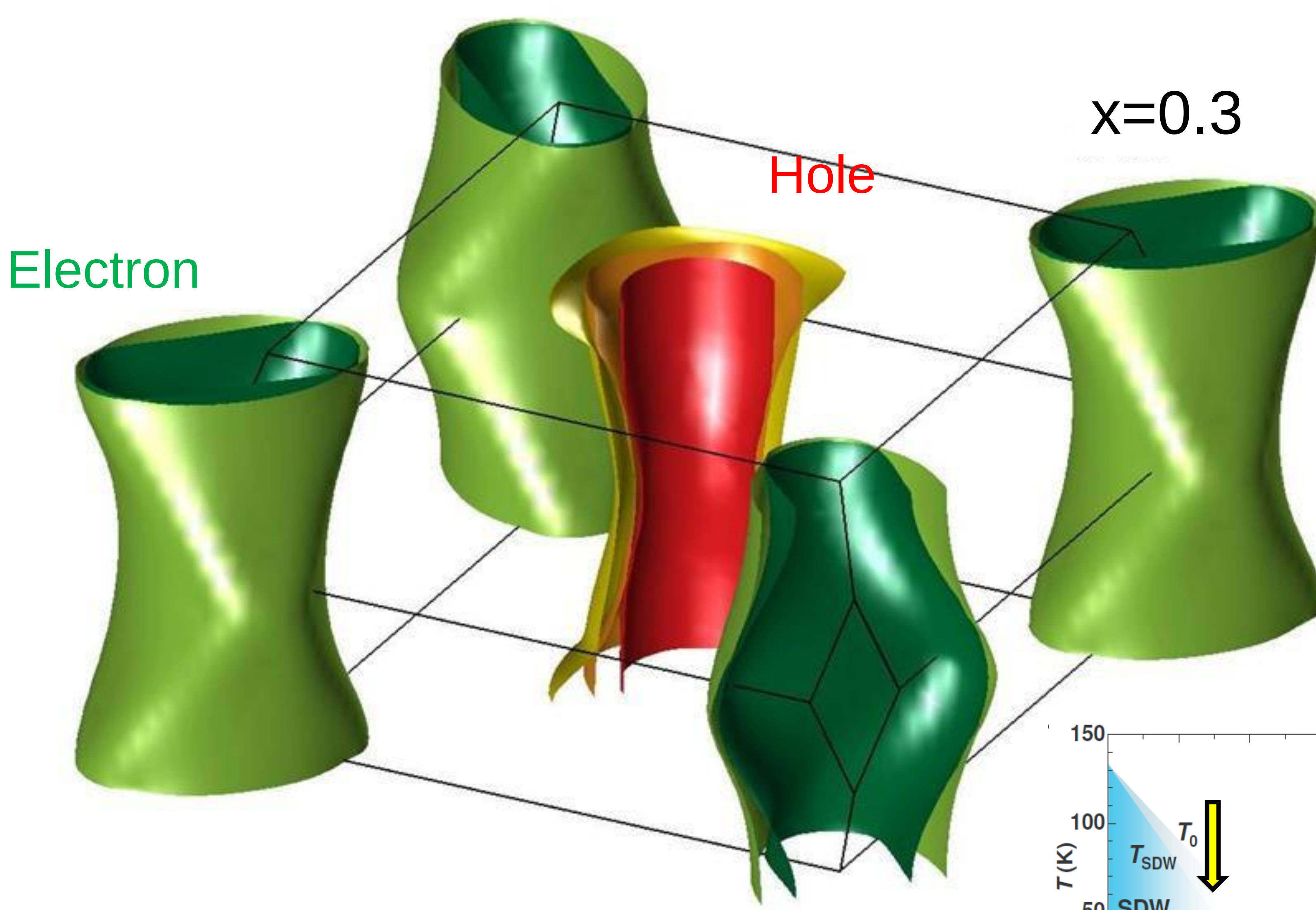

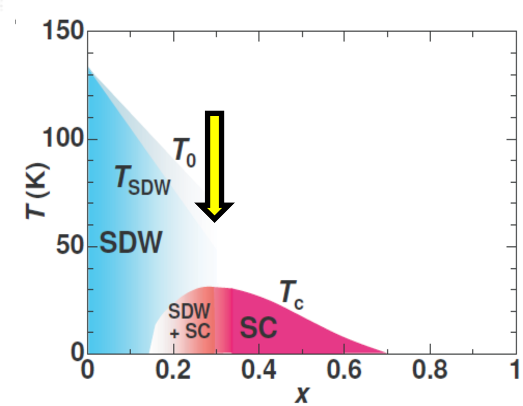

$BaFe_2(As_{1-x}P_x)_2$

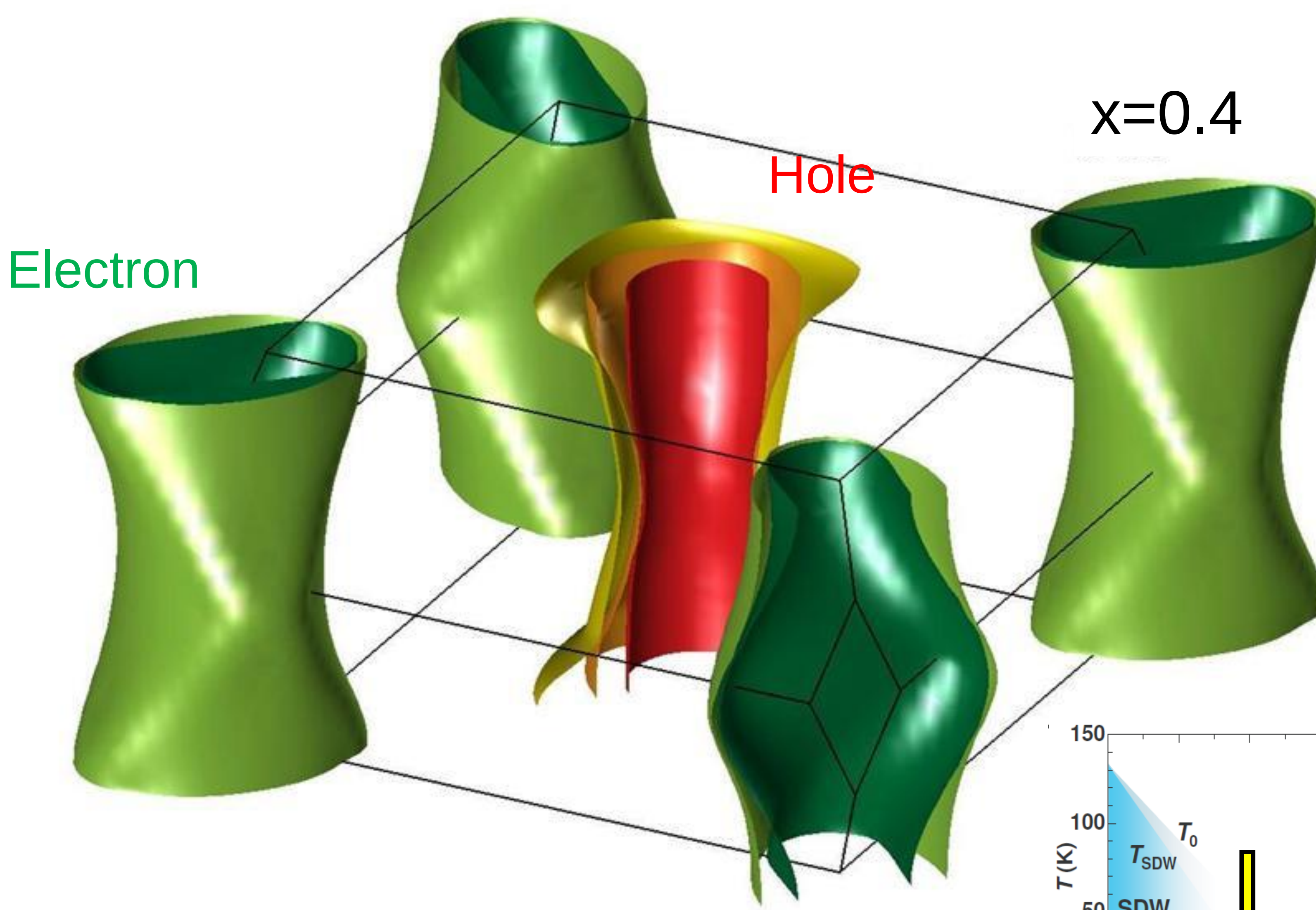

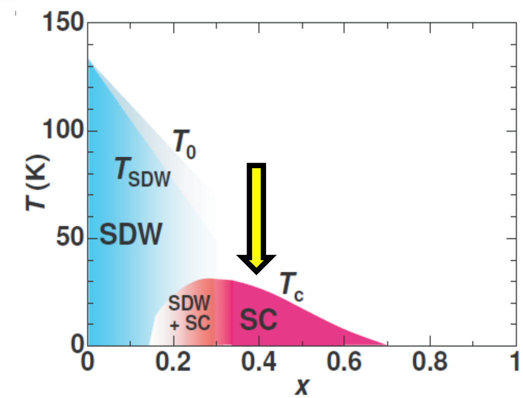

$BaFe_2(As_{1-x}P_x)_2$

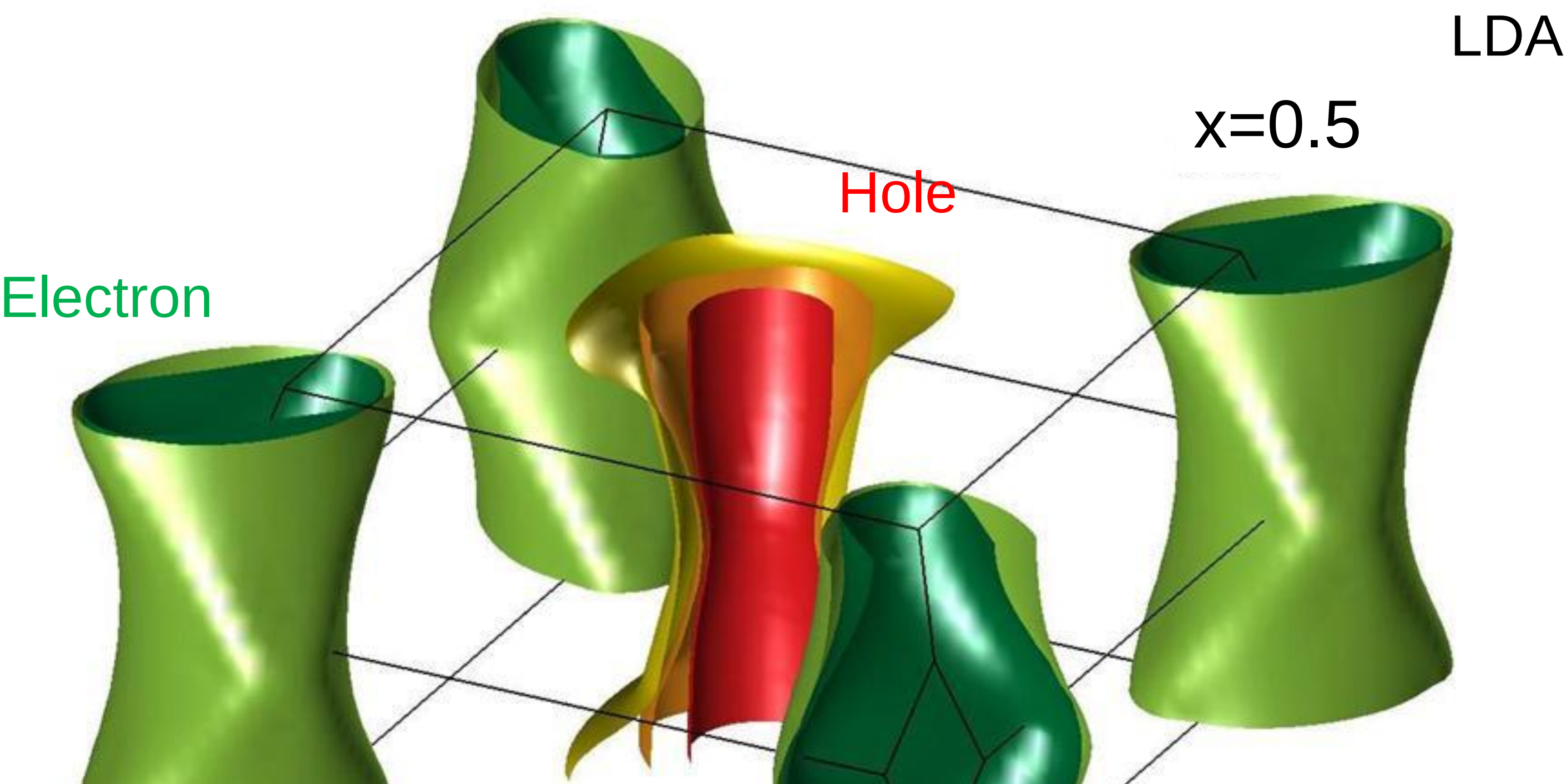

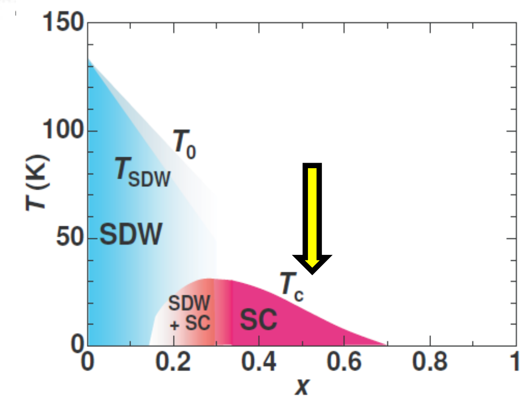

$BaFe_2 (As_{1-x}P_x)_2$

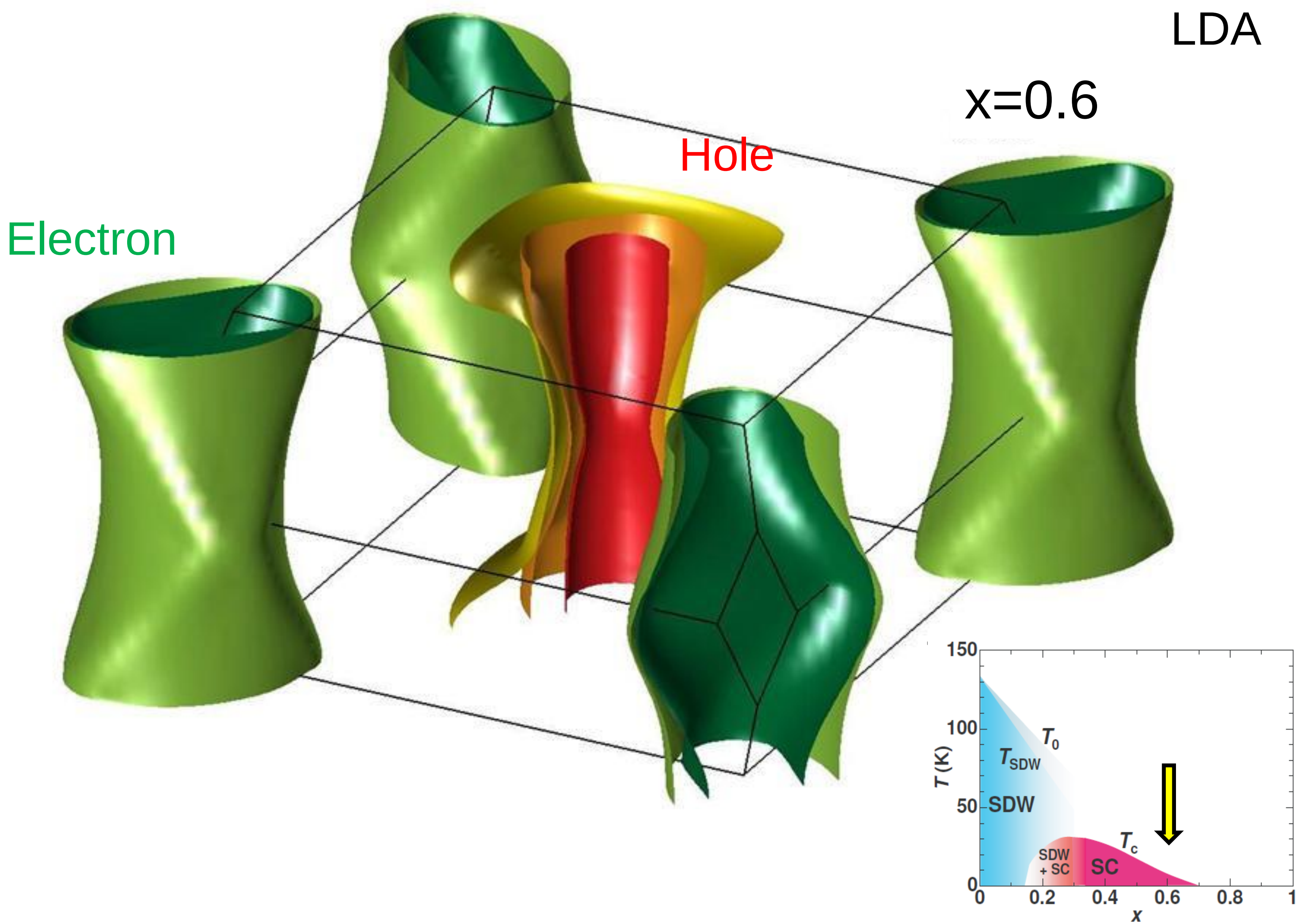

$BaFe_2(As_{1-x}P_x)_2$

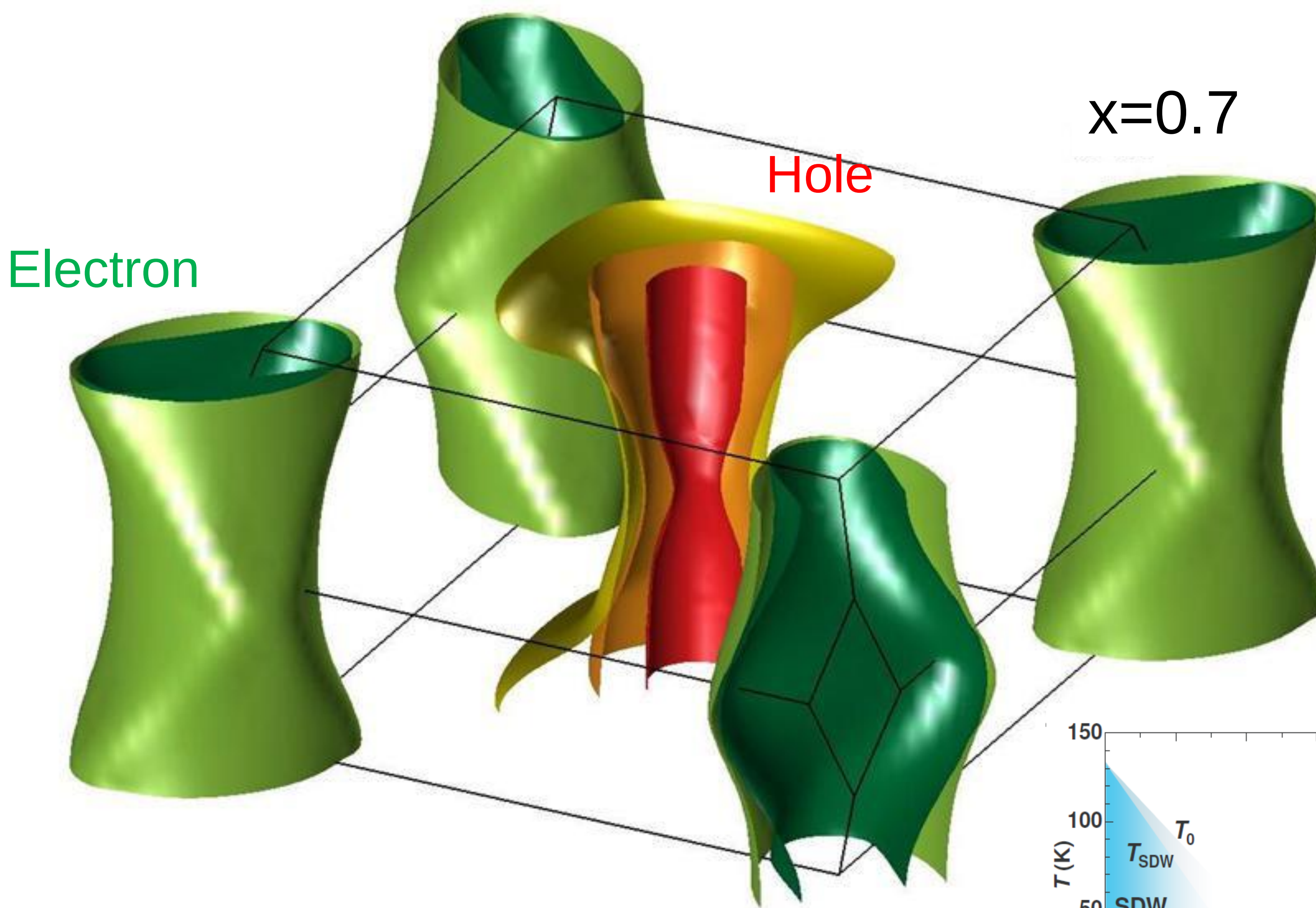

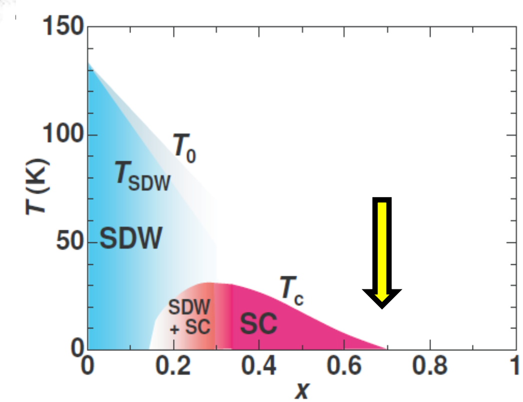

$BaFe_2(As_{1-x}P_x)_2$

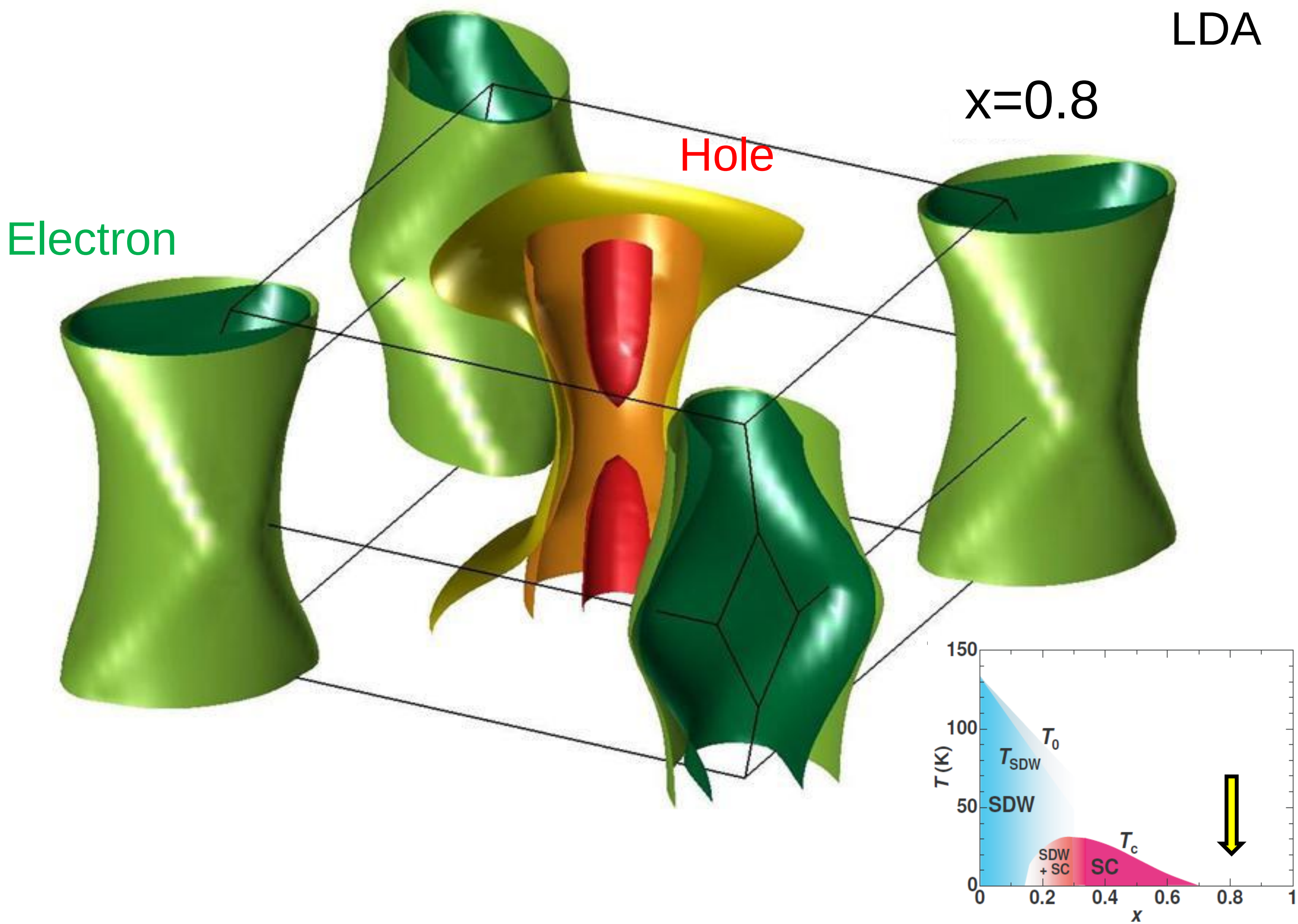

$BaFe_2(As_{1-x}P_x)_2$

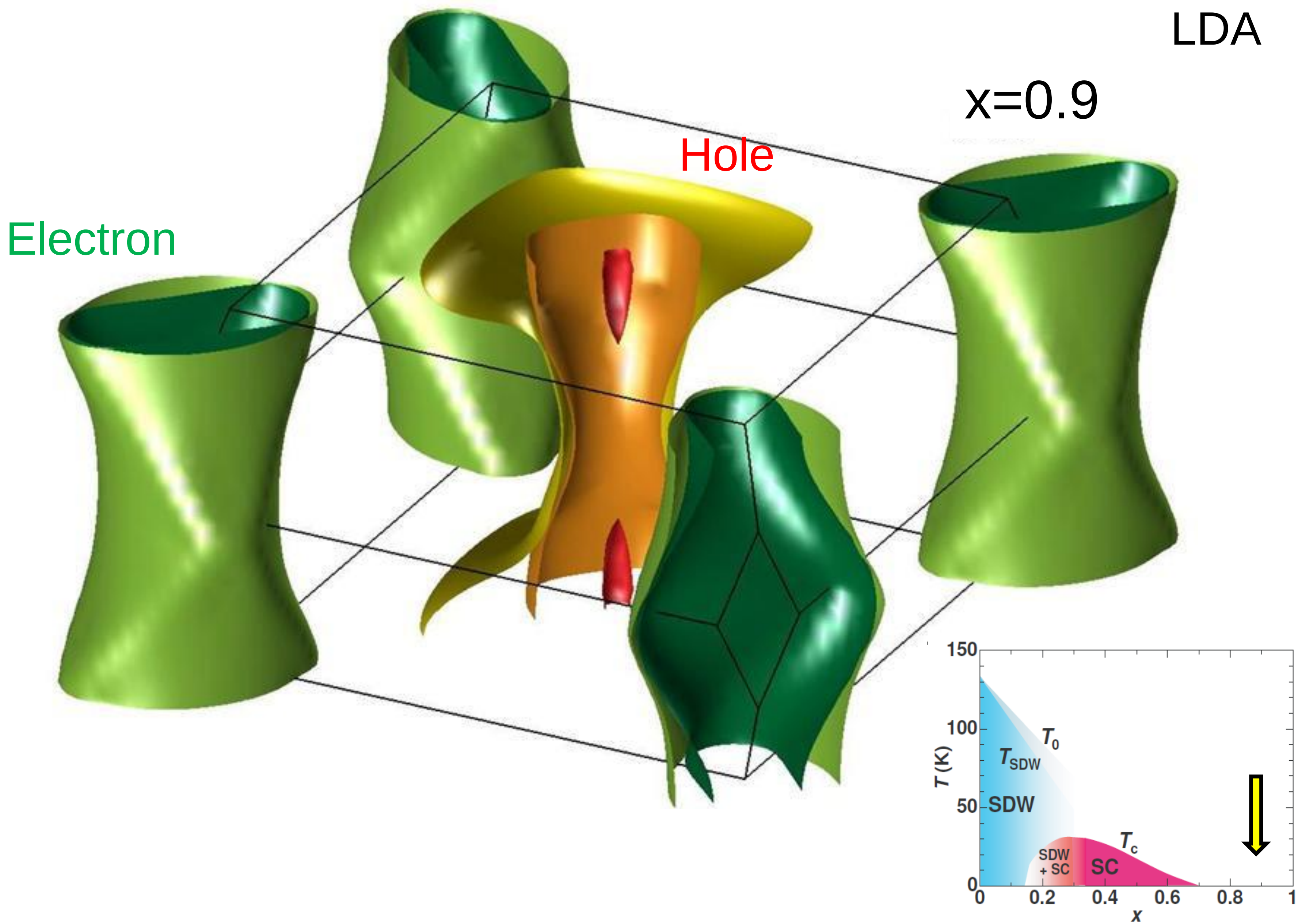

$BaFe_2(As_{1-x}P_x)_2$

LDA A. Carrington

x=1.0

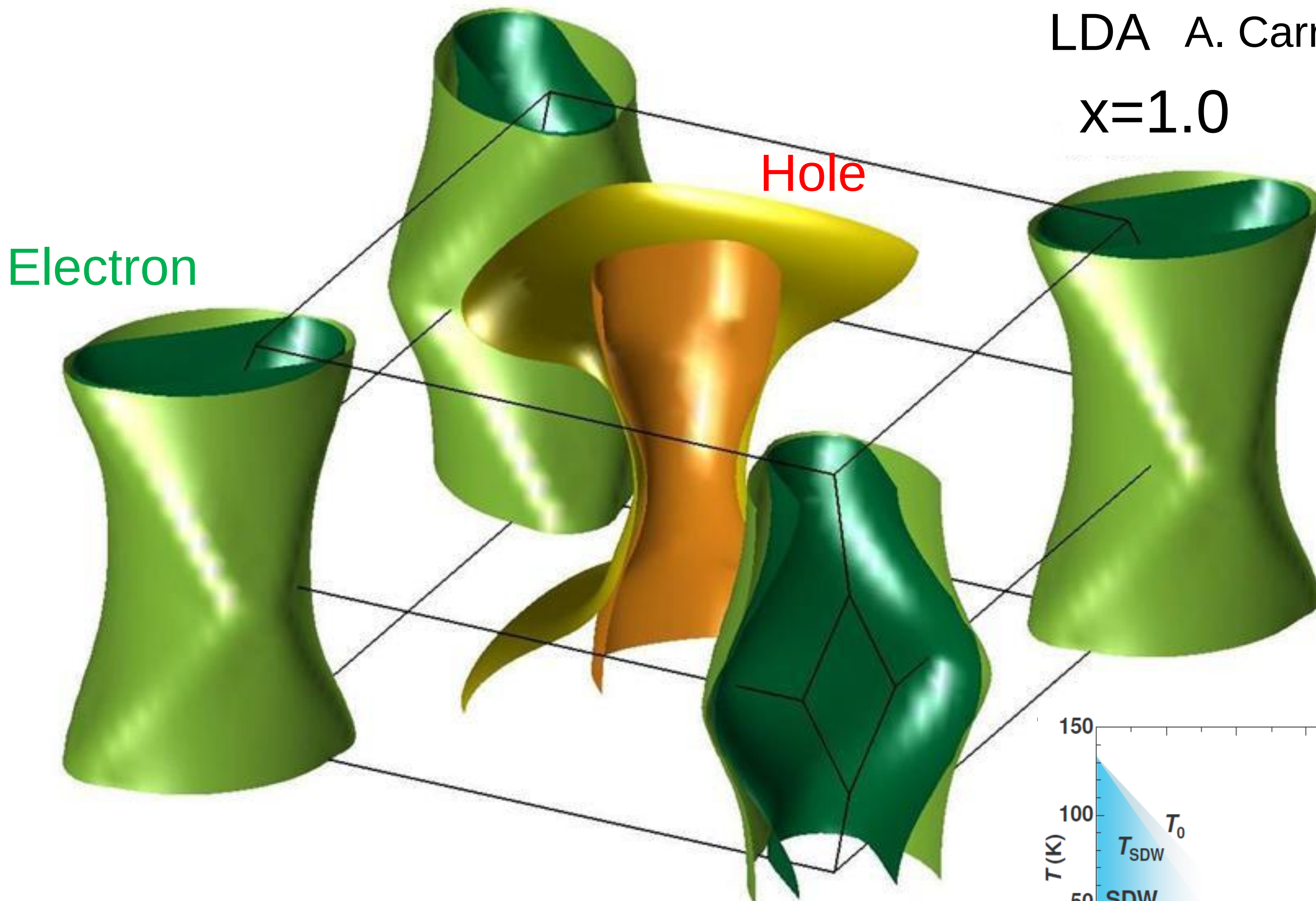

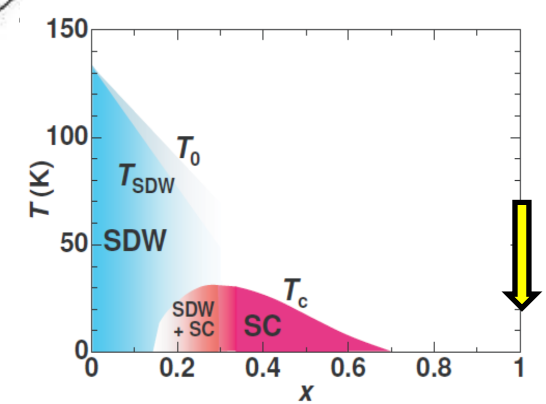

Electron correlations

Electron correlations change the band structure

Band narrowing

Band shift

Mass enhancement

Difference between LDA and measured Fermi surface

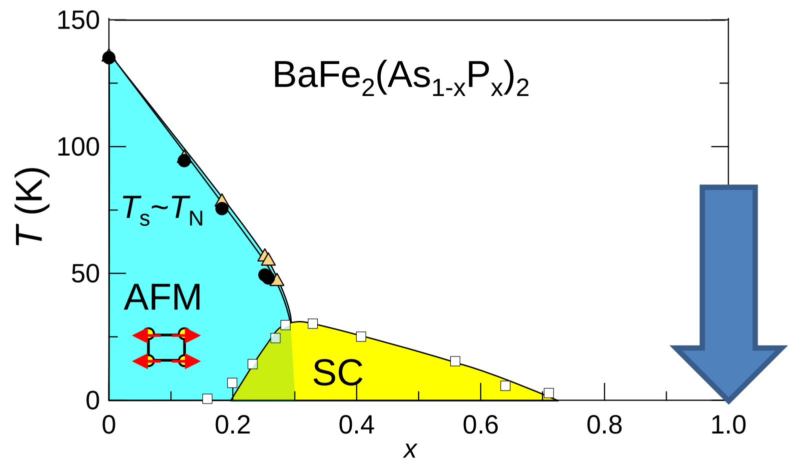

$BaFe_2P_2$

Weak electron correlation

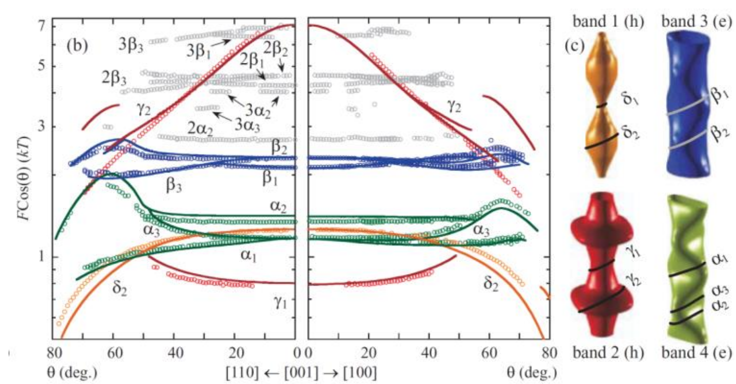

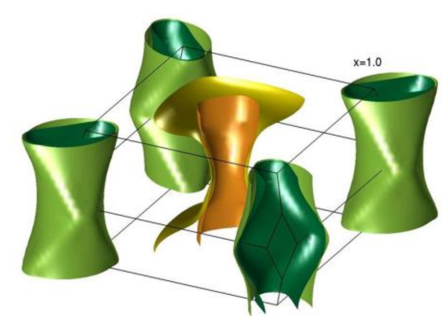

FS is well reproduced by LDA

m^*/m_b~1.5-1.8

Electron correlations

Electron correlations change the band structure

Band narrowing

Mass enhancement

Band shift

Difference between LDA and measured Fermi surface

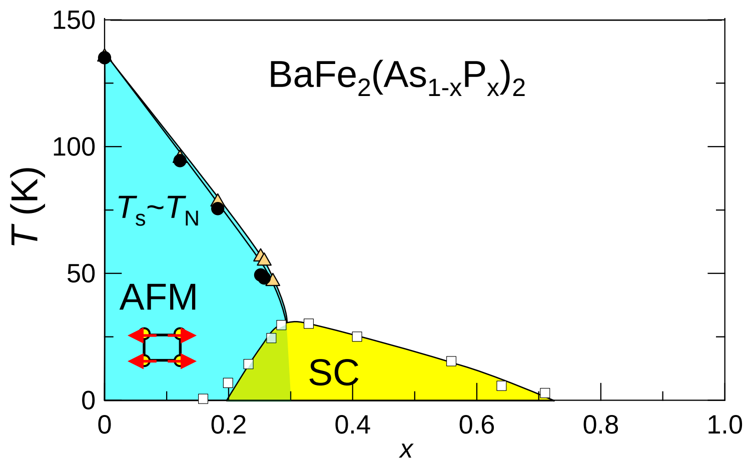

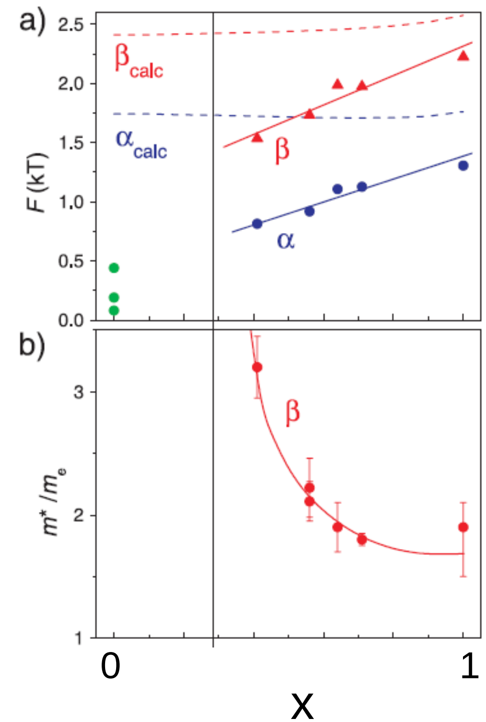

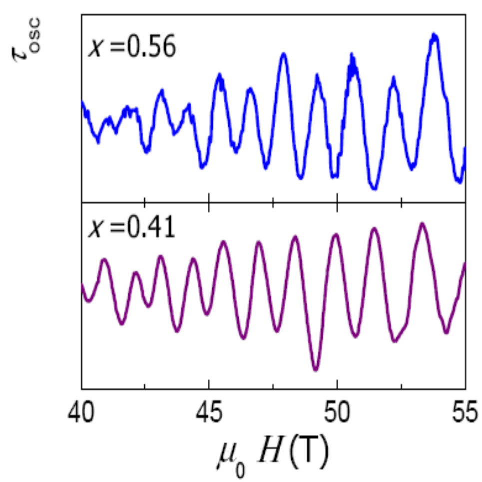

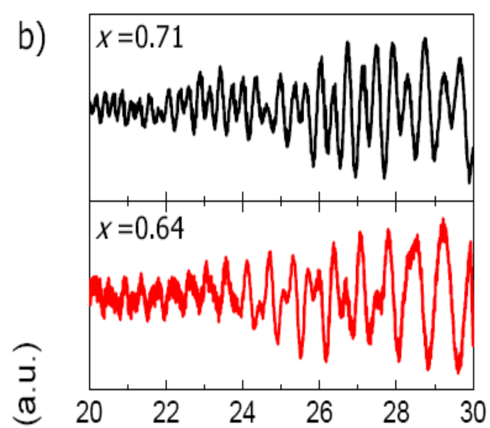

F decreases: shrinkage of the FS

Correlation induced band shift

Electron correlations

Cuprates

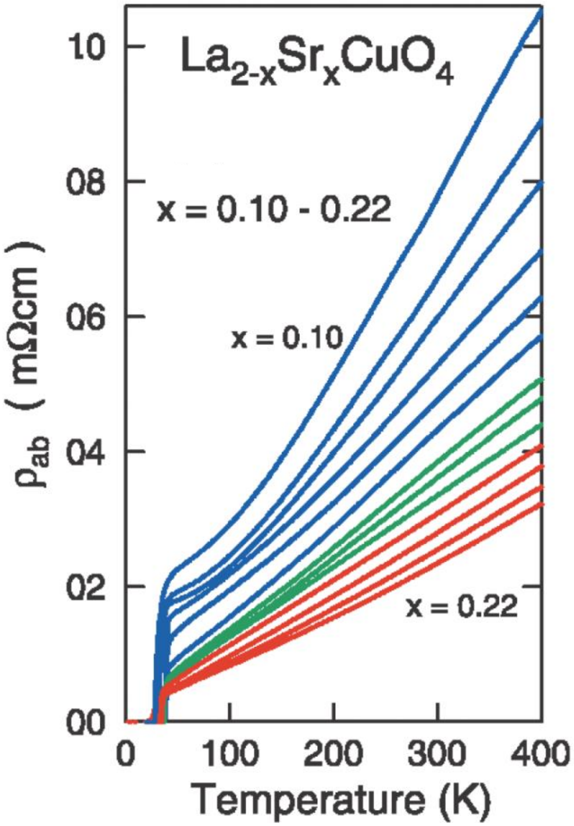

Y. Ando *et al*. PRL (04).

Fe-pnictides

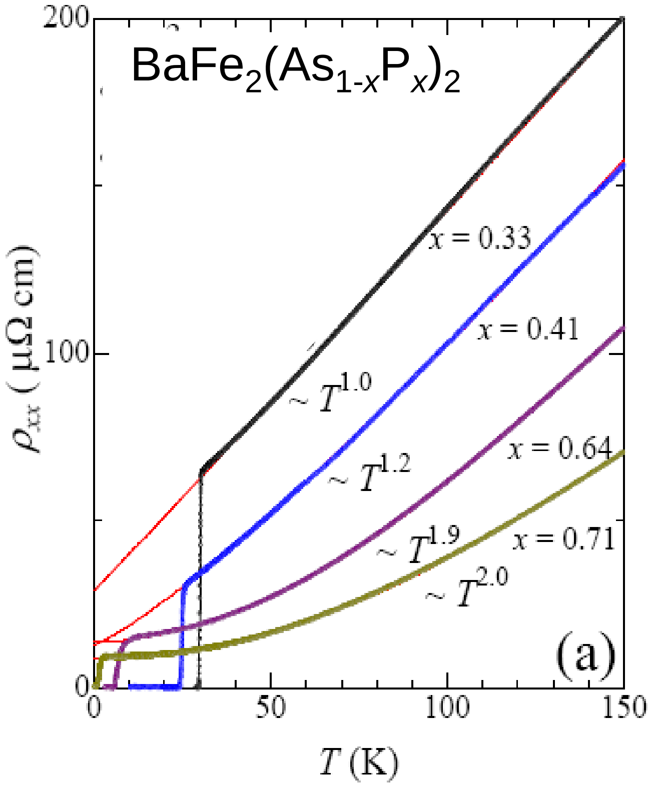

S. Kasahara *et al*., PRB (10)

T-linear resistivity ⇨ Importance of electron correlation

Electron correlations

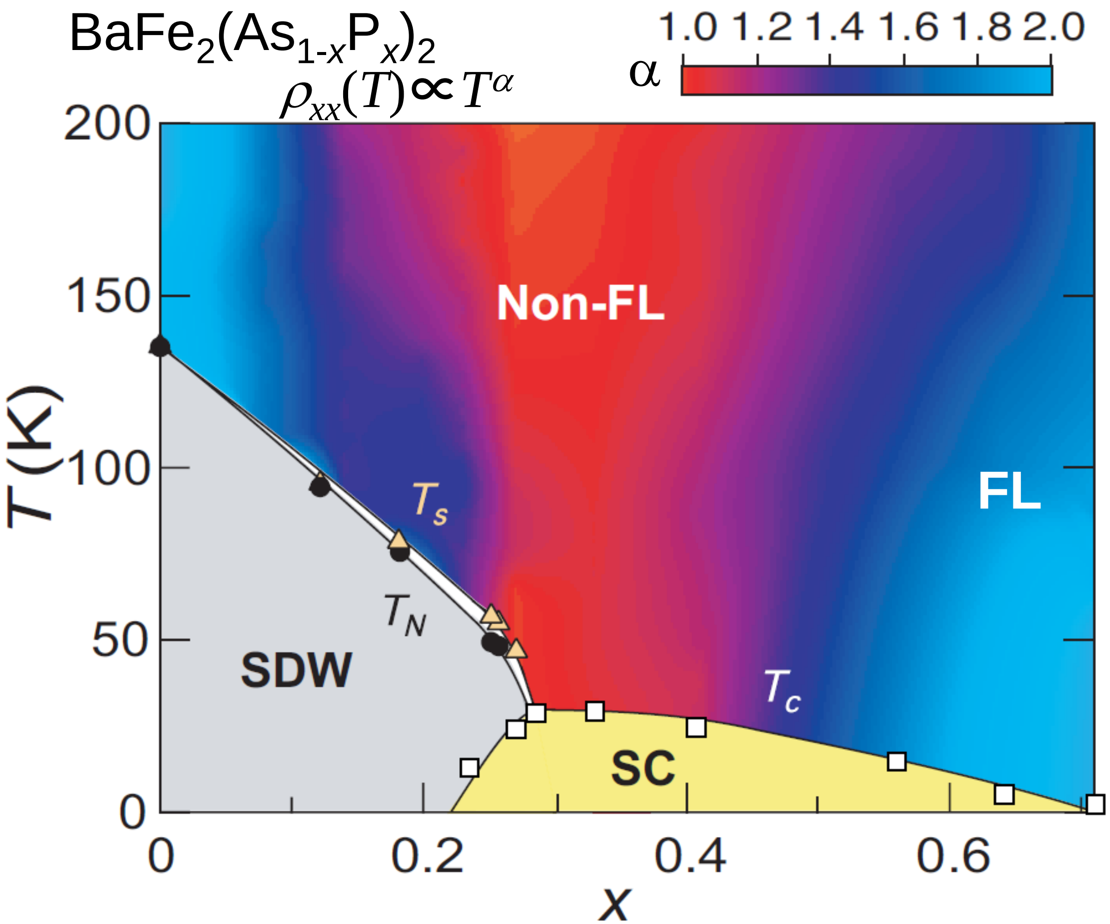

S. Kasahara *et al*., PRB **81**, 184519 (10)

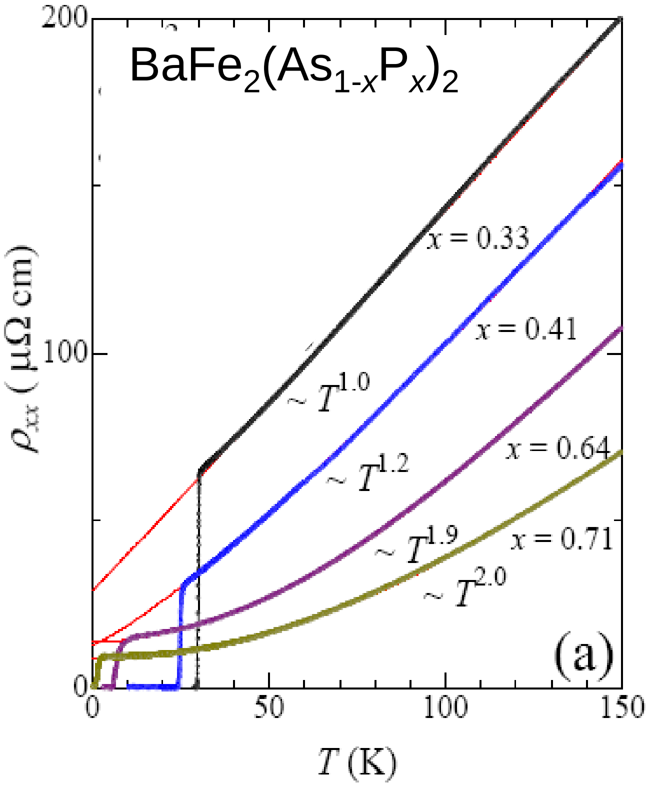

T-linear resistivity at *x*=0.33 just beyond SDW end point (x_c=0.3)

Hallmark of non-Fermi liquid

T^2-dependence at *x*=0.71

Fermi-liquid behavior

Electron correlations

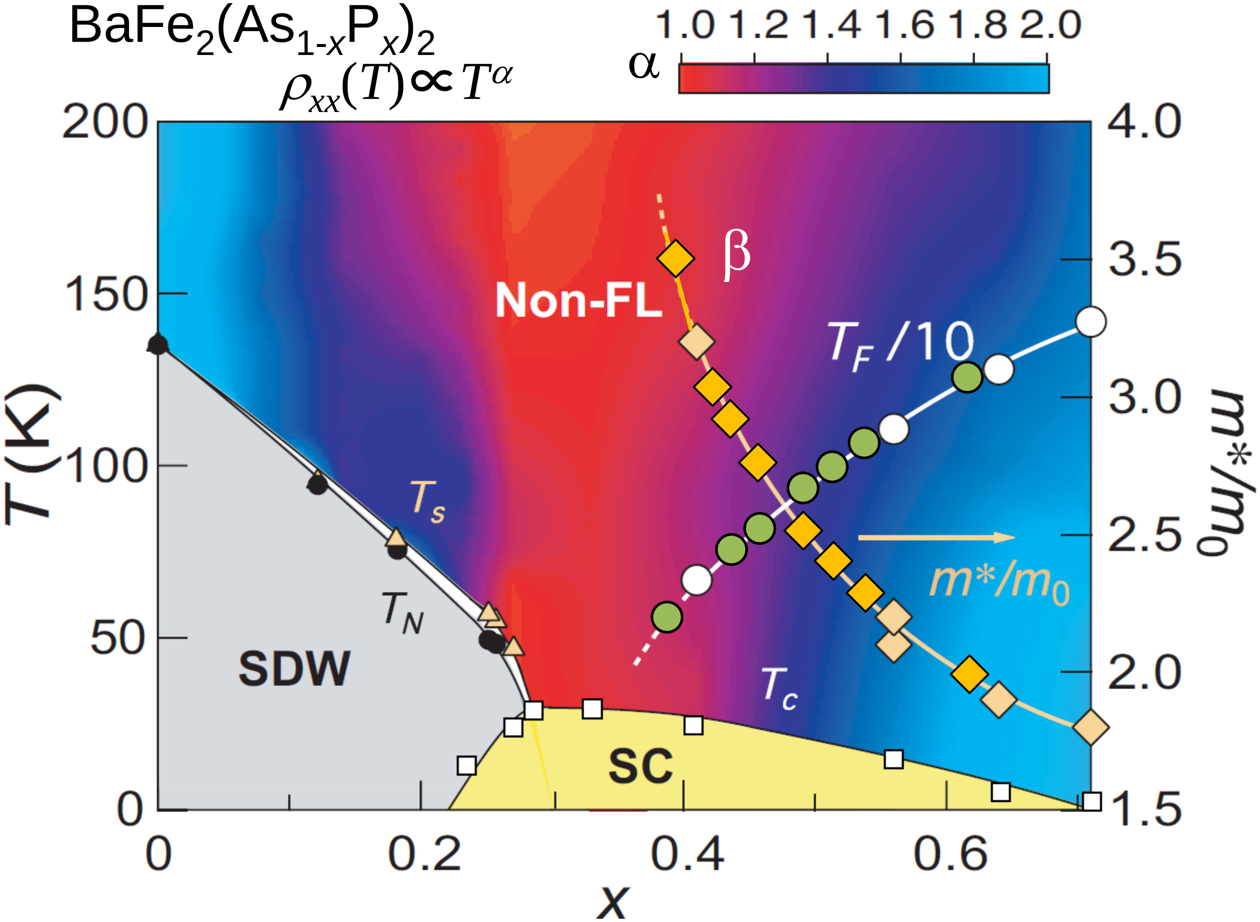

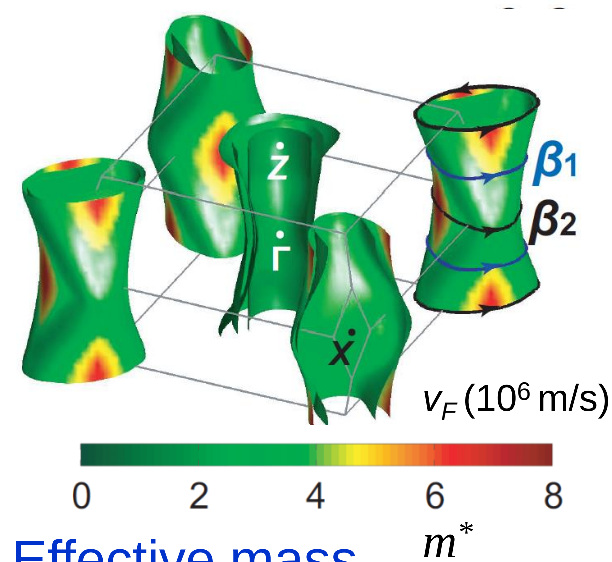

Effective mass m^*

Fermi temperature

$$T_F = \hbar e F / m^* k_B$$

dHvA

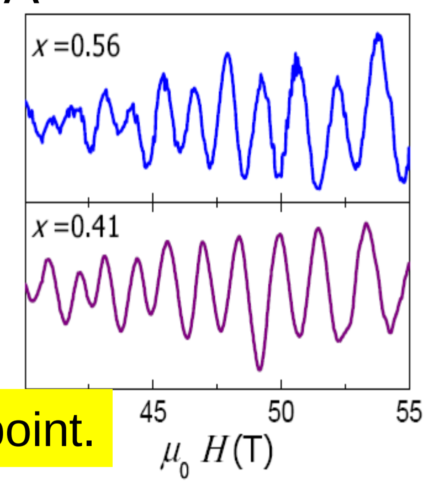

As x is tuned towards the maximum T_c,

Effective mass m^* is strongly enhanced

Measured FS strikingly deviates from LDA calculation

Electron correlations are particularly important at the SDW end point.

H.Shishido *et al*. PRL (09) B. J. Arnold *et al*. PRB (R)(11), P. Walmsley *et al*. PRL(13)

Electron correlations

Electron correlations change the band structure

Band narrowing

Mass enhancement

Band shift

Difference between LDA and measured Fermi surface

Hole dope

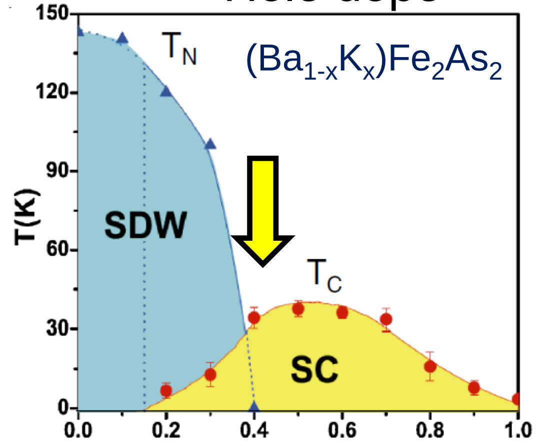

$Ba_{0.6}K_{0.4}Fe_2As_2$

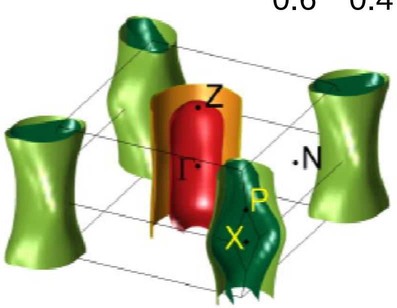

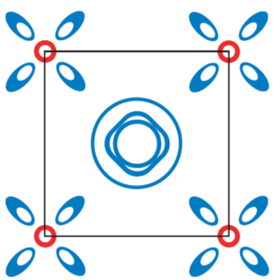

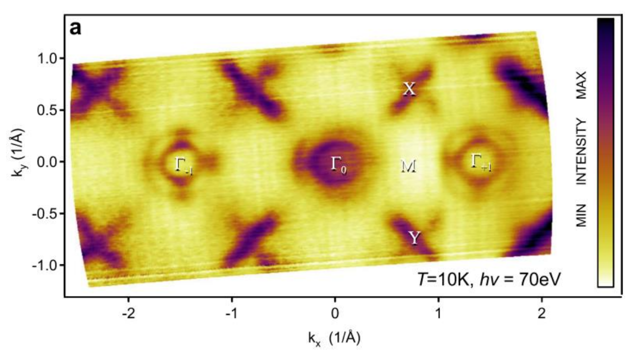

Propeller-like

Fermi surface topologically different from LDA.

Large band shift

Electron correlations

Electron correlations change the band structure

Band narrowing

Mass enhancement

Band shift

Difference between LDA and measured Fermi surface

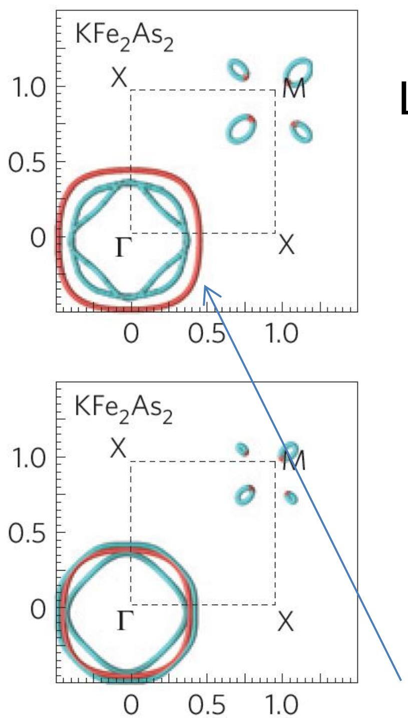

LDA +DMFT

LDA

No correlation

Hole dope

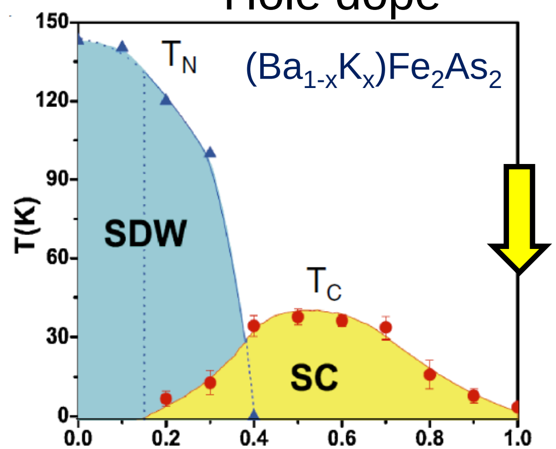

ARPES xy-character

T. Yoshida *et al*. Frontiers in Phys.(`14)

γ~100 mJ/K^{2}mol

Heavy fermion!

Mass enhancement m^*/m_{LDA}~10

Z.P.Yin, K. Haule and G. Kotoliar, Nature Mat. 10, 932 (2011)

Strong electron correlation

Physics of iron-based high temperature superconductors

1) Introduction

2) Simiilarities and differences between cuprates and Fe-pnictides

3) Normal state properties

Electronic structure and magnetism

4) Superconducting properties

Superconducting gap structure

5) Some recent topics

QCP, BCS-BEC crossover,
A novel high field SC state, Nematicity・・・・

Magnetic structure

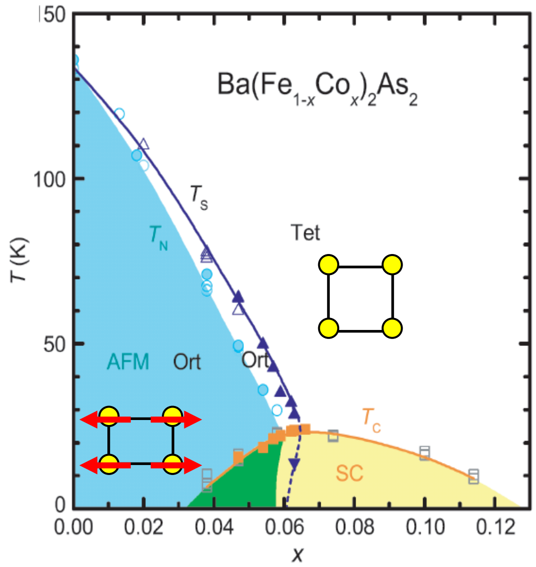

Stripe type AFM

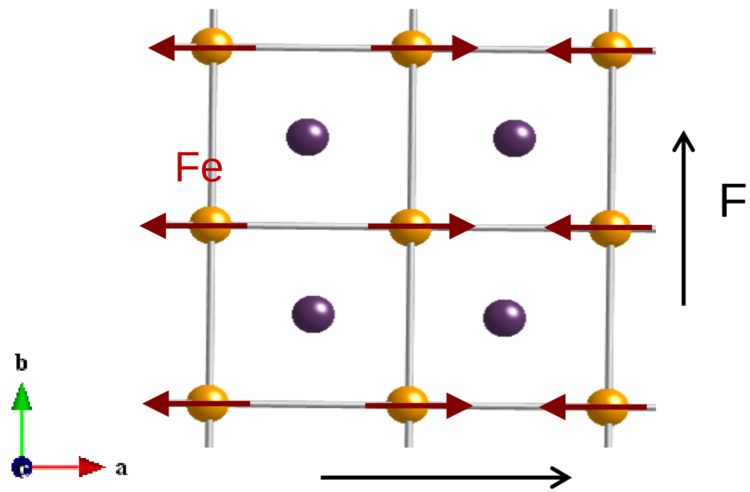

High-*T*

Low-*T*

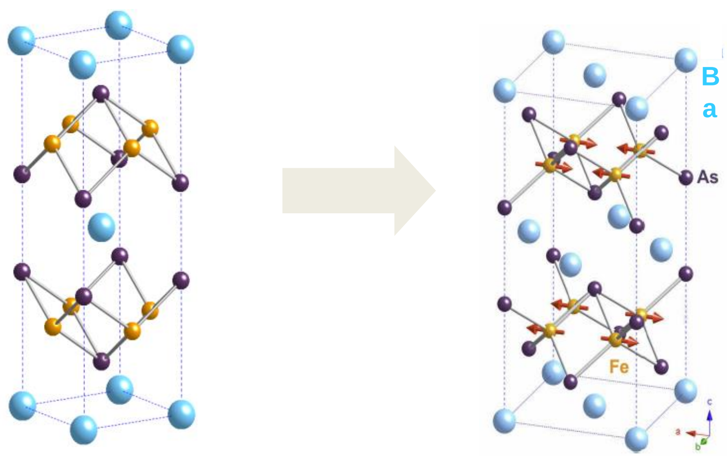

Tetragonal
Paramagnetic

Orthorhombic.
Antiferromagnetic

What is the origin of stripe type AFM?

1) Orbital ordering

   i) Localized picture
   ii) Itinerant picture

2) Spin nematic ordering

Magnetic structure (orbital ordering, localized spin)

Approach using localized spins: J_1-J_2 model

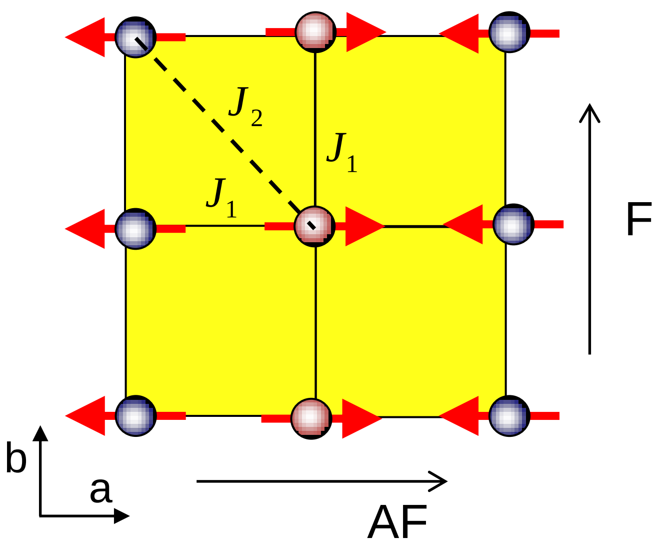

Strong frustration

$$J_2 > J_1/2$$

P. Chandra, P. Coleman and A.I. Larkin, PRL 64, 88 (1990)

Magnetic structure (orbital ordering, localized spin)

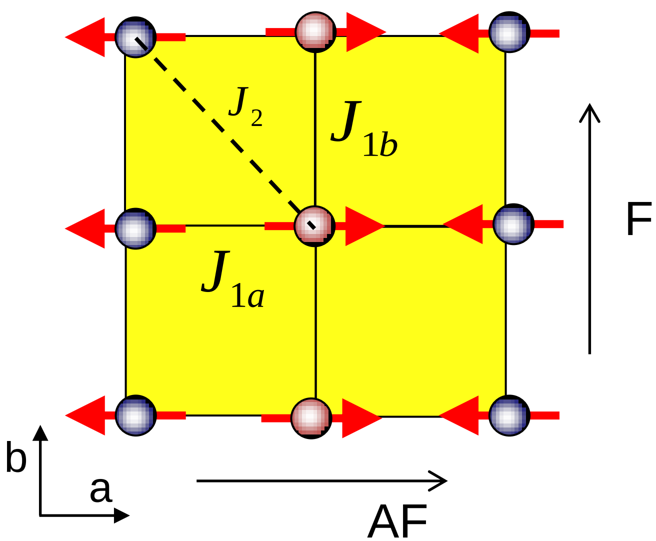

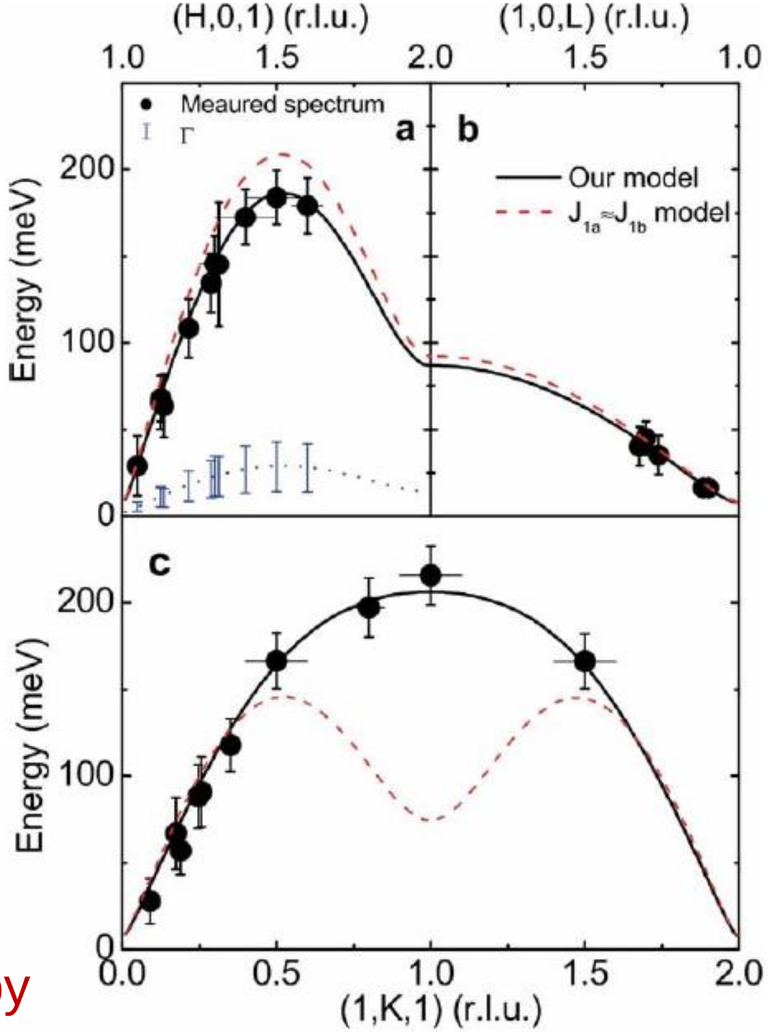

J_{1a} = 49 J_{1b} = -5.7 J_2 = 19 meV

Large in-plane exchange coupling anisotropy

Localized model in tetragonal lattice (J_{1a}=J_{1b}) cannot explain the magnetic excitations

Jun Zhao *et al.*, Nature Phys. (2009)

What is the origin of the in-plane anisotropy?

Magnetic structure (orbital ordering, localized spin)

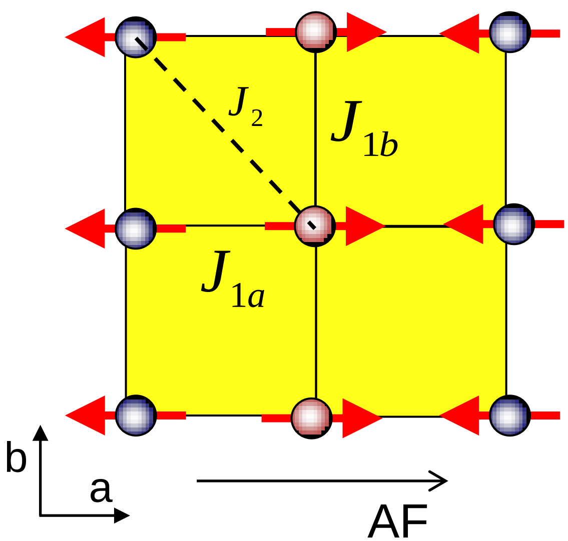

Orbital ordering

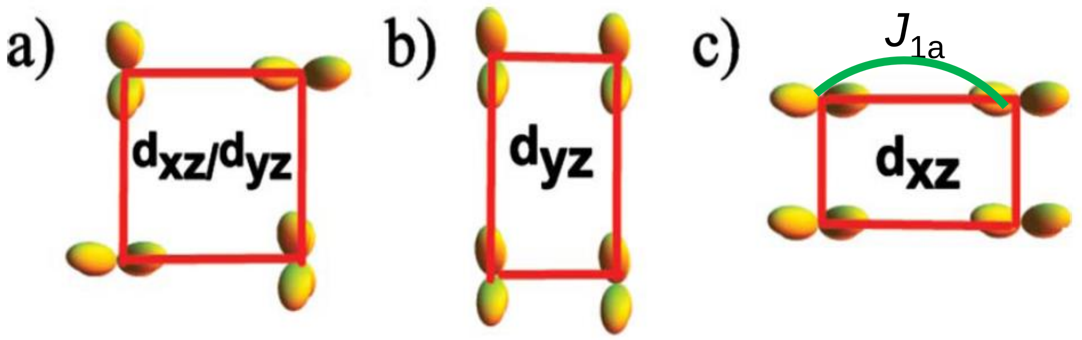

$J_{1a} = J_{1b}$ $J_{1a} < J_{1b}$ $J_{1a} > J_{1b}$

xz↓ yz↑

ARPES in $BaFe_2As_2$

Kruger et al., PRB (09)
Lv et al., PRB (09)

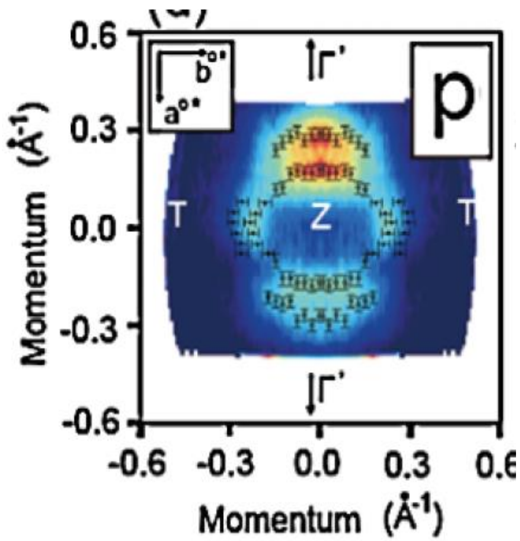

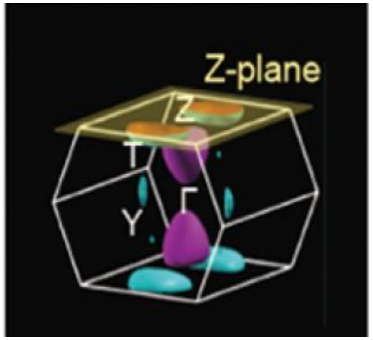

T. Shimojima *et al.*, PRL (2010).

Magnetic structure (orbital ordering, itinerant)

Fermi Surface

Multiband electronic structure with well-separated **hole** and **electron** sheets

Good nesting condition

➔ **Antiferromagnetic SDW ordering**

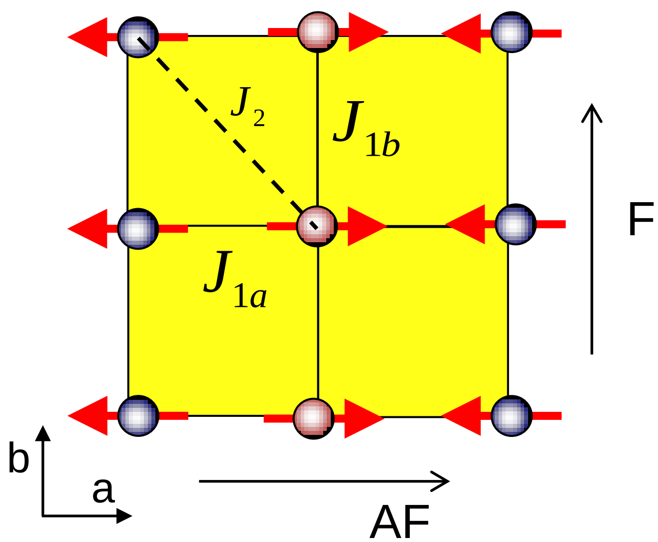

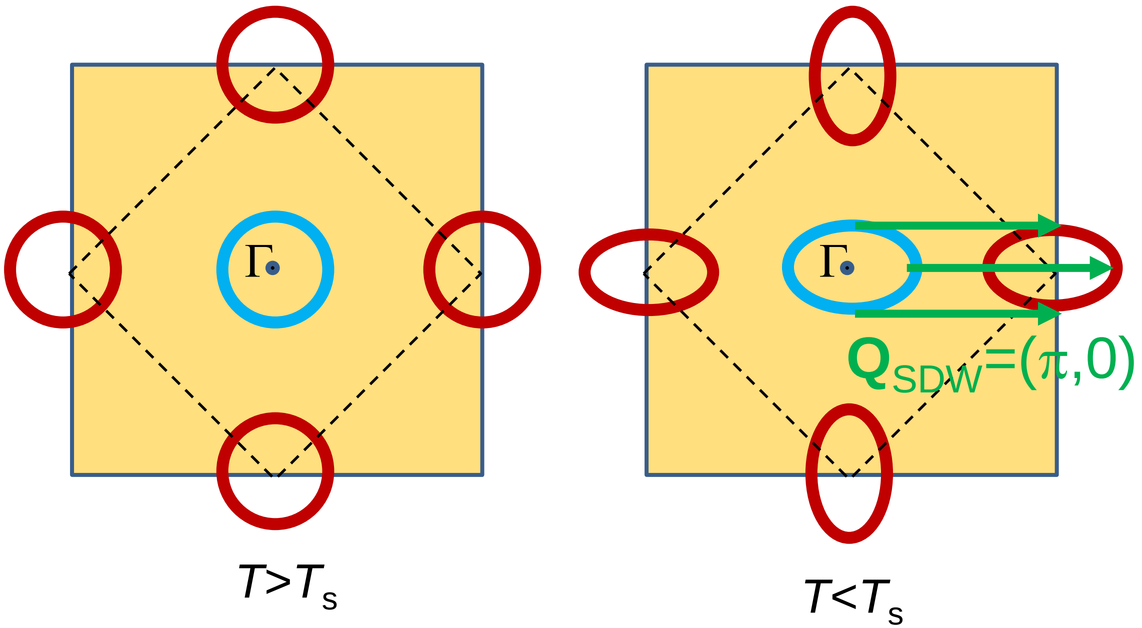

Because of orbital ordering, $(\pi,0)$ nesting becomes better than $(0,\pi)$.

Magnetic structure (orbital ordering, itinerant)

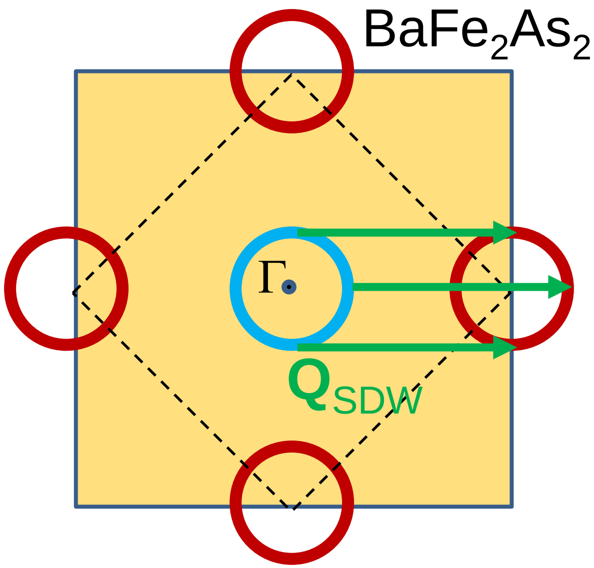

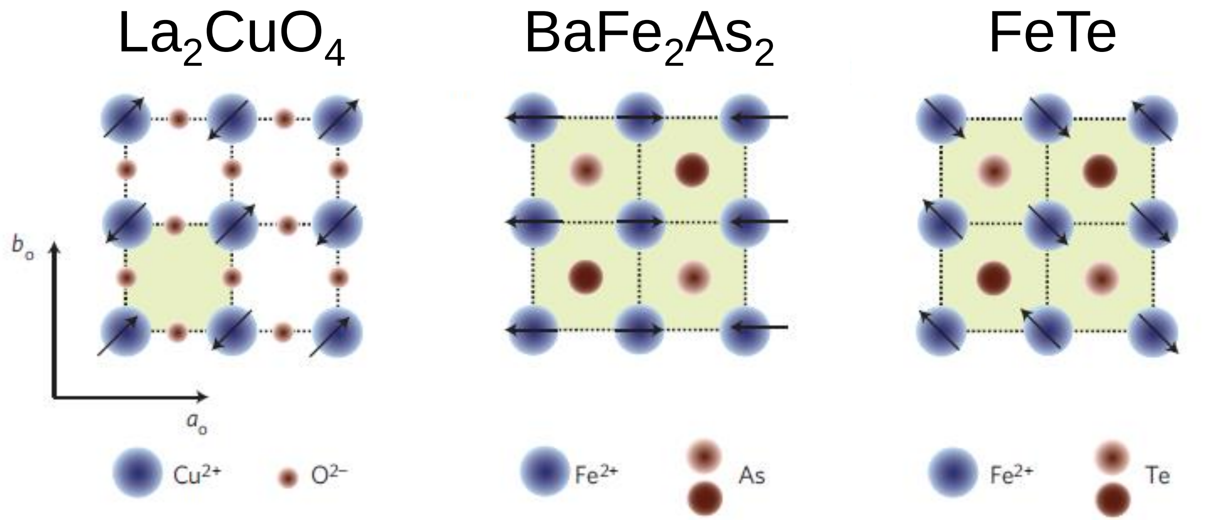

P. Dai, J. Hu, and E. Dagotto, Nat. Phys (12)

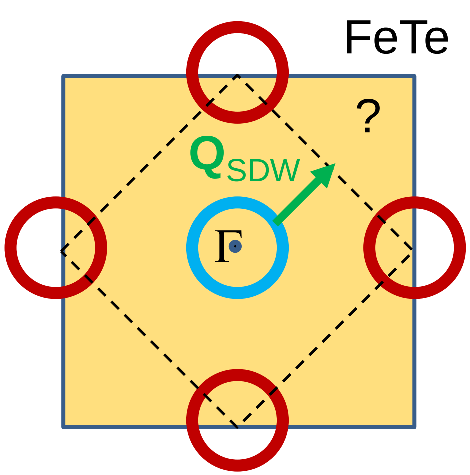

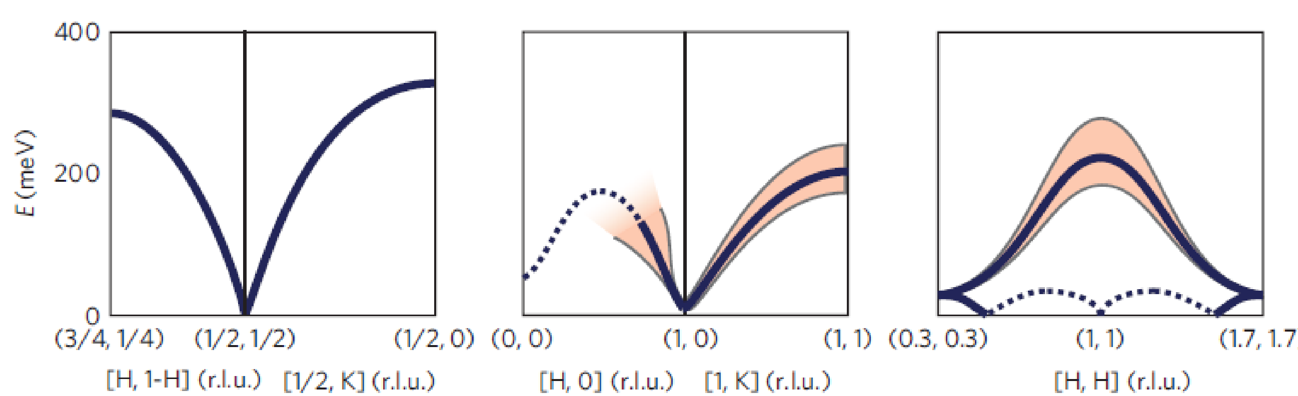

・Well defined spin wave at the BZ boundary

No observation of Landau damping

・ Cannot explain bi-collinear structure of FeTe with similar FS

Magnetic structure (orbital ordering)

1111

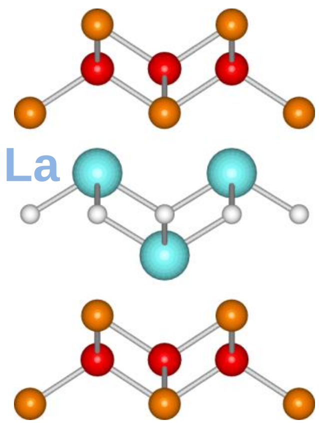

$0.3\text{-}0.5\ \mu_B$

122

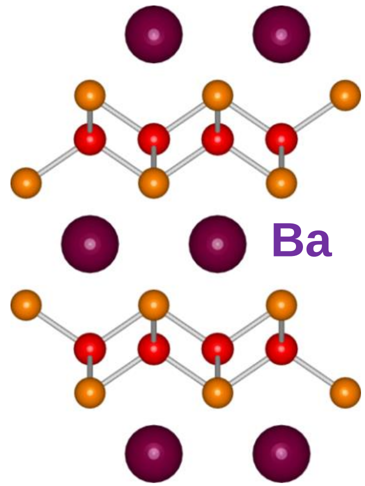

$0.8\text{-}1\ \mu_B$

11

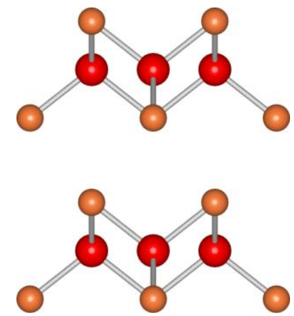

$\sim 2\ \mu_B$

itinerant ⟷ localized

Spin nematic order

R.M. Fernandes, A.V. Chubkov and J. Schmalian, Nature Phys. (14)

a state that breaks Z_2 (Ising) symmetry, but remains paramagnetic

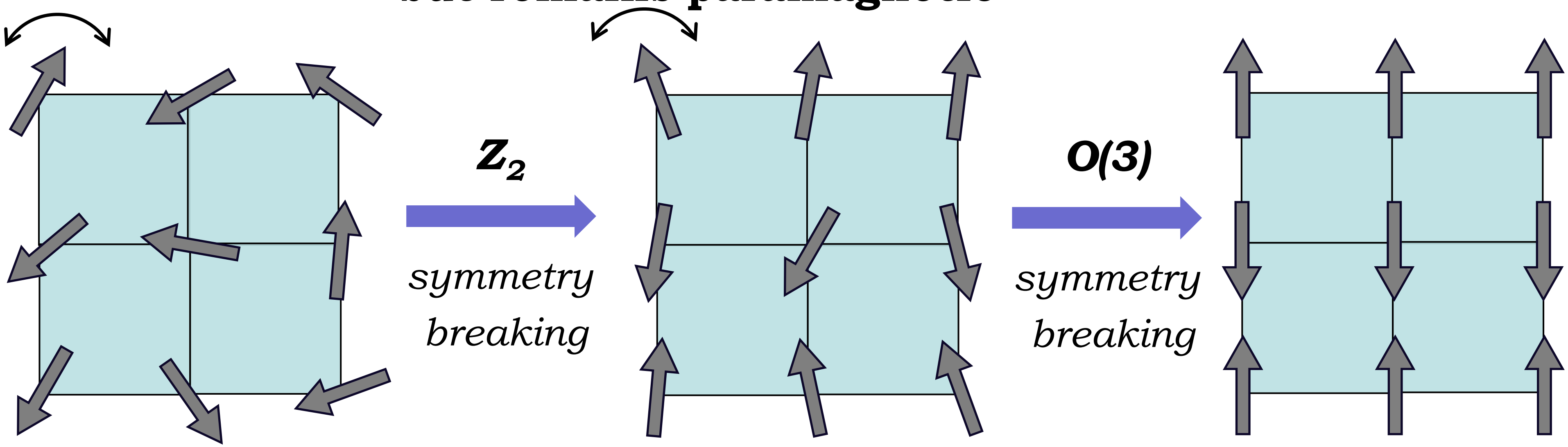

disordered state	nematic state	magnetic state
$\langle \mathbf{m}_i \rangle = 0 \quad \langle \mathbf{m}_j \rangle = 0$	$\langle \mathbf{m}_i \rangle = 0 \quad \langle \mathbf{m}_j \rangle = 0$	$\langle \mathbf{m}_i \rangle \neq 0 \; \langle \mathbf{m}_j \rangle \neq 0$
$\langle \mathbf{m}_i \cdot \mathbf{m}_j \rangle = 0$	$\langle \mathbf{m}_i \cdot \mathbf{m}_j \rangle \neq 0$	

Spin nematic induces orbital order through the spin-lattice coupling

Relationship between magnetic order and structural transition

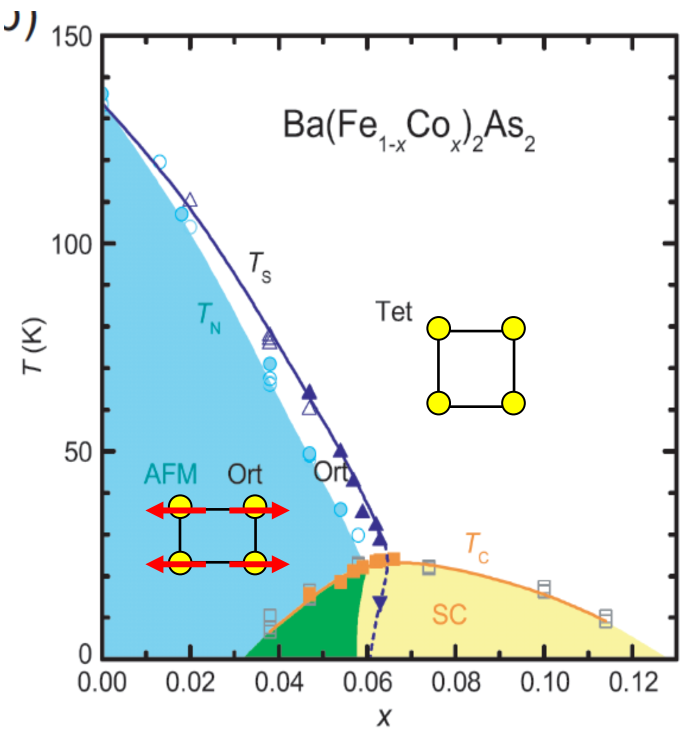

Two scenarios

1) Orbital ordering triggers stripe SDW order.

2) Magnetic interaction (spin nematic) induces orbital order through the spin-lattice coupling.

Structural (T_S) and AFM transition (T_N) lines follow closely each other

T_s: orbital order

T_N: SDW order


Who is the driver?

Summary

Iron pnictide

A new family of unconventional superconductors

Normal state properties

Electron correlation effects are definitely important.

Importance of orbital degrees of freedom.

Relationship between orbital order and stripe SDW order is controversial.

Physics of iron-based high temperature superconductors (II)

Yuji Matsuda

Department of Physics
Kyoto University
Kyoto, Japan

Physics of iron-based high temperature superconductors

1) Introduction

2) Simiilarities and differences between cuprates and Fe-pnictides

3) Normal state properties

Electronic structure and magnetism

4) Superconducting properties

Superconducting gap structure

5) Some recent topics

QCP, BCS-BEC crossover, Nematicity・・・・

Superconductivity in $BaFe_2As_2$ systems

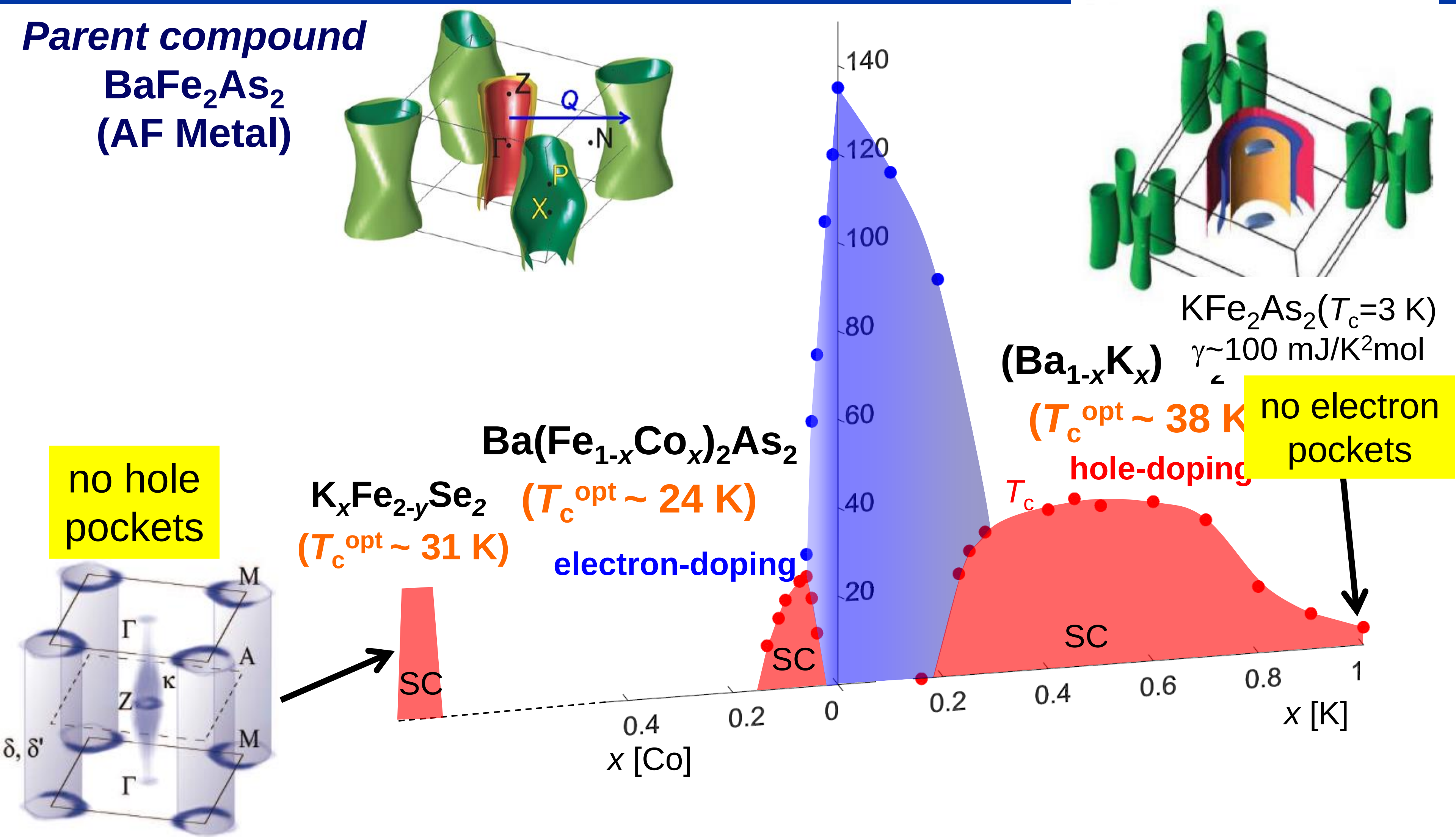

Superconductivity in $BaFe_2As_2$ systems

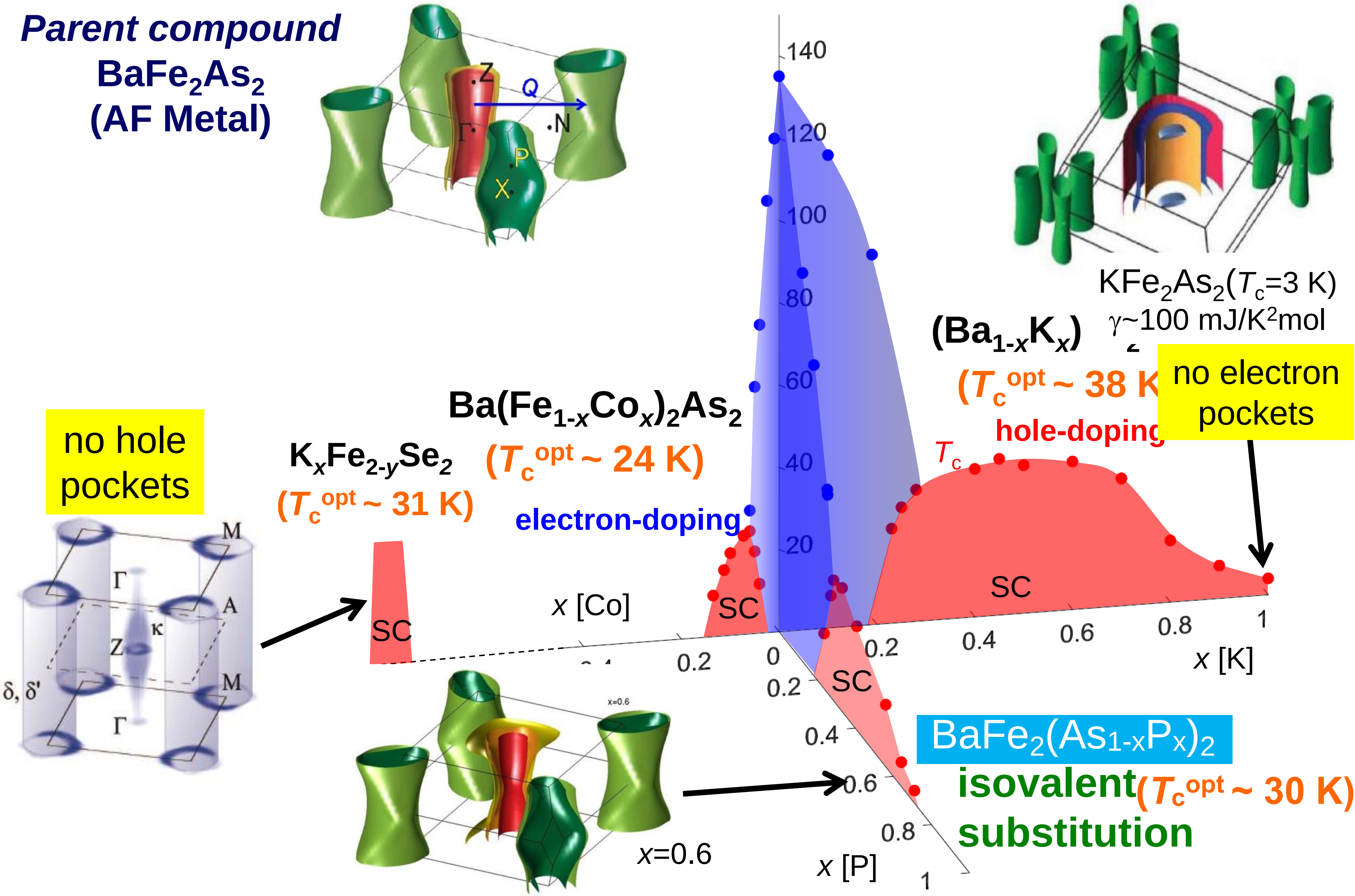

Ground state can be tuned without doping carriers

Superconducting gap structure of iron pnictides

Gap structure is closely related to the pairing interaction

Full gap or nodal?

Full gap

Does the gap change sign between the hole and electron pockets?

Is the major pairing interaction repulsive or attractive?

Nodal

⇨ Presence of repulsive interaction.

Is the node accidental or symmetry protected?

Accidental : presence of two (or more) competing pairing interactions

Iron pnictides: candidate for the SC state

- Pairing due to purely repulsive electronic interaction (enhanced by spin fluctuations)

$$V > 0$$

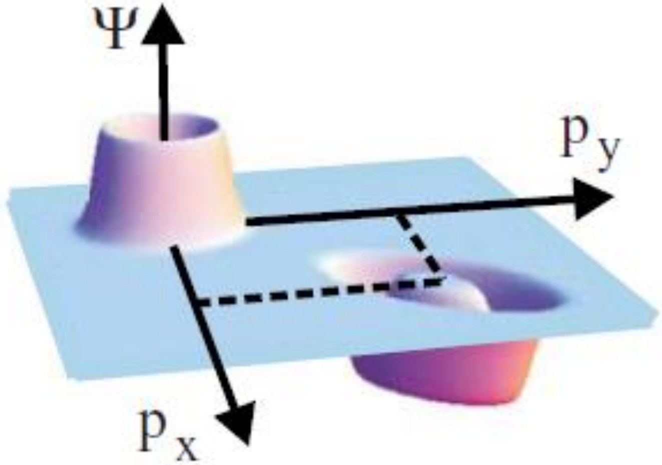

S_{+-}

cf. *d*-wave cuprate

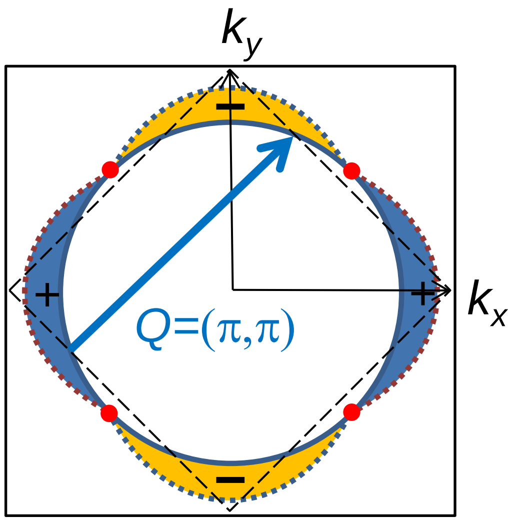

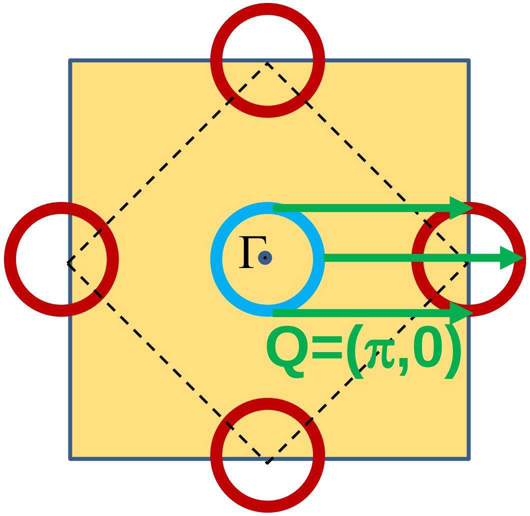

I. I. Mazin *et al*., PRL **101**, 057003 (2008).
K. Kuroki *et al*., PRL **101**, 087004 (2008).
& PRB **79**, 224511 (2009).
A. V. Chubkov *et al*., PRB **80**, 140515(R) (2009).
S. Graser *et al*., NJP **11**, 025016 (2009).
H. Ikeda, PRB **81**, 054502 (2010).
K. Seo *et al*., PRL **101**, 206404 (2008).
F. Wang *et al*., PRL **102**, 047005 (2009).
⋮

Iron pnictides: candidate for the SC state

- Pairing due to attractive interaction caused by charge/orbital fluctuations.

s_{++} $V < 0$

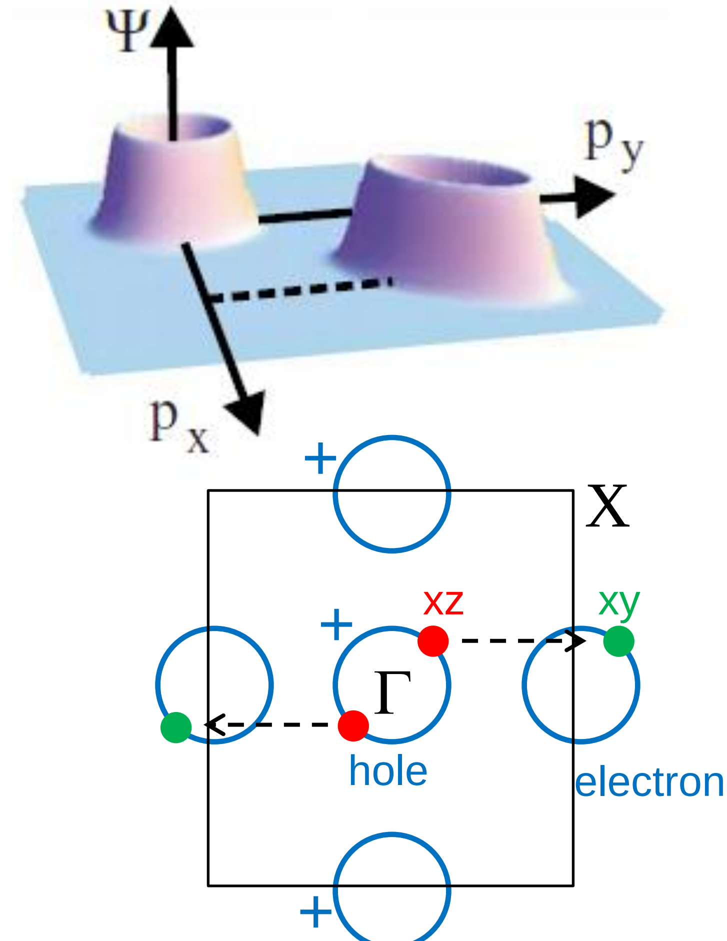

Orbital fluctuations
(Quadrupole fluctuation)

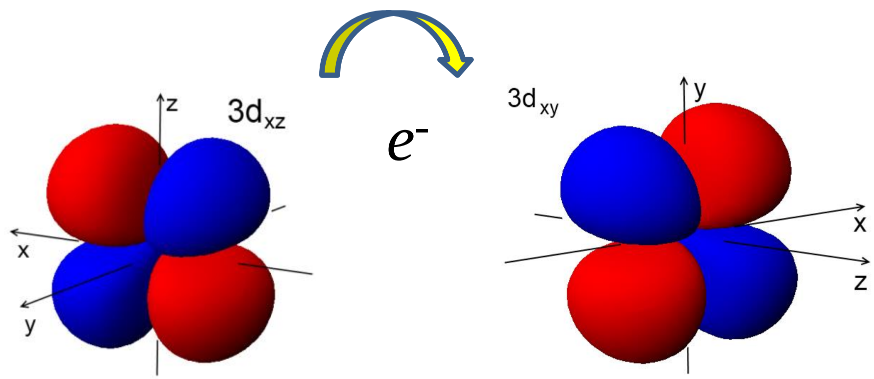

Charge up

Charge down

Occupation number of each orbit at each Fe site fluctuates

H. Kontani & S. Onari, PRL **104**, 157001 (2010).
F. Kruger *et al*., PRB **79**, 054504 (2009).
Y. Yanagi *et al*., PRB **81**, 054518 (2010).

Iron pnictides: candidate for the SC state

S_{+-}

S_{++}

Spin fluctuations

_k_-space (repulsive)

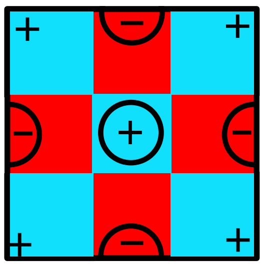

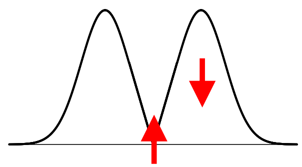

_r_-space

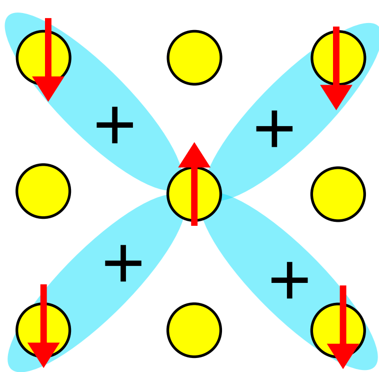

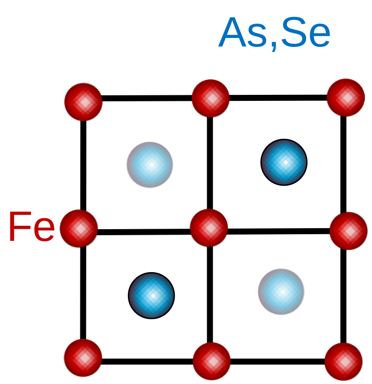

$$\Delta(\cos k_x \cos k_y)$$

Orbital fluctuations

_k_-space (attractive)

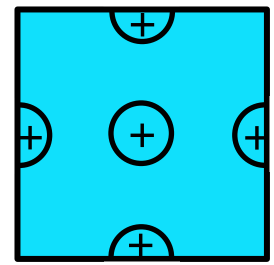

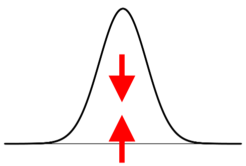

_r_-space

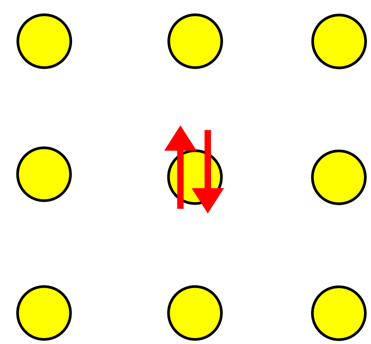

$$\Delta$$

Iron pnictides: candidate for the SC state

AF

ng

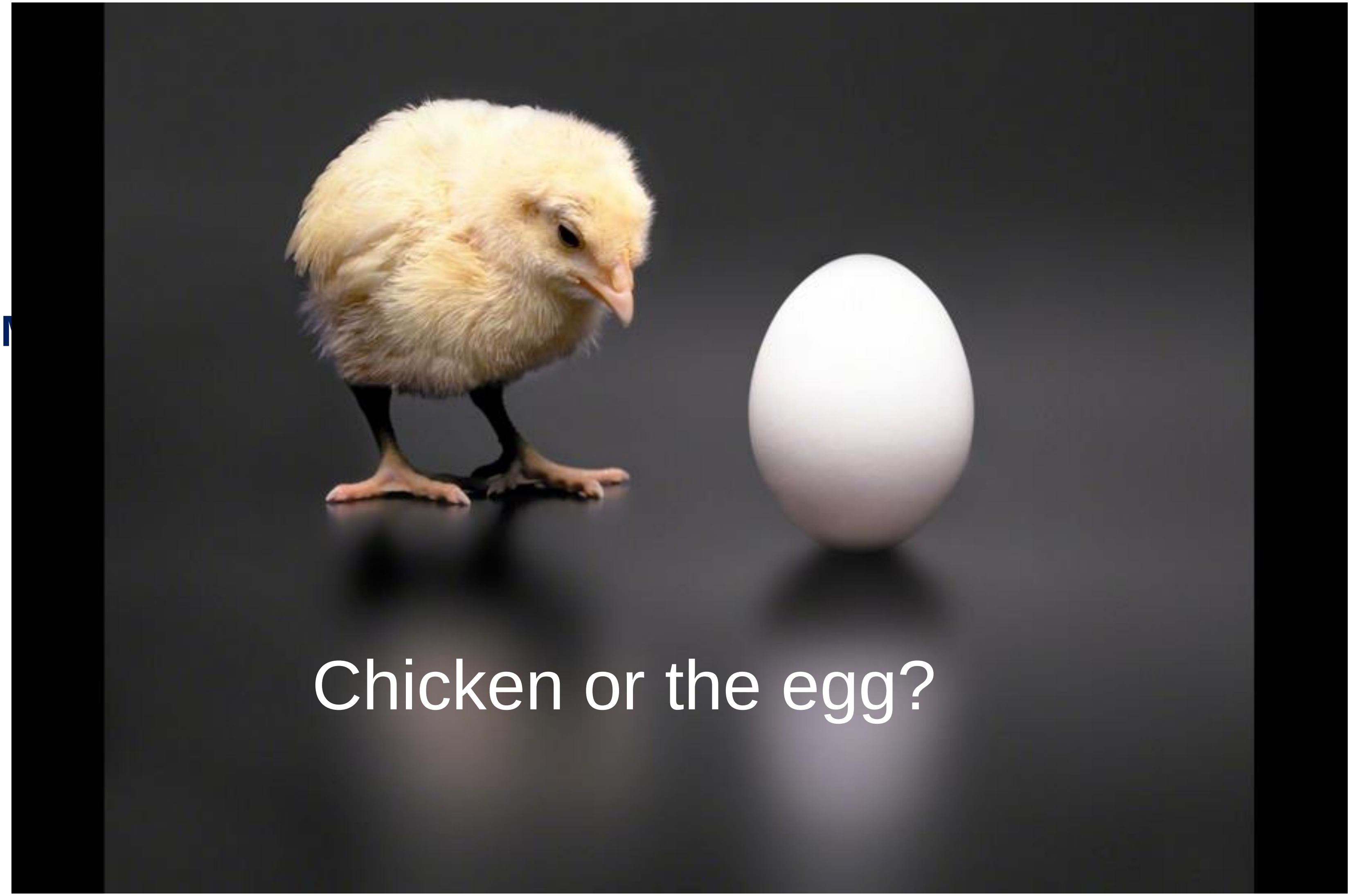

Spin fluctuations or orbital fluctuations?

Possible gap functions of iron-based superconductors

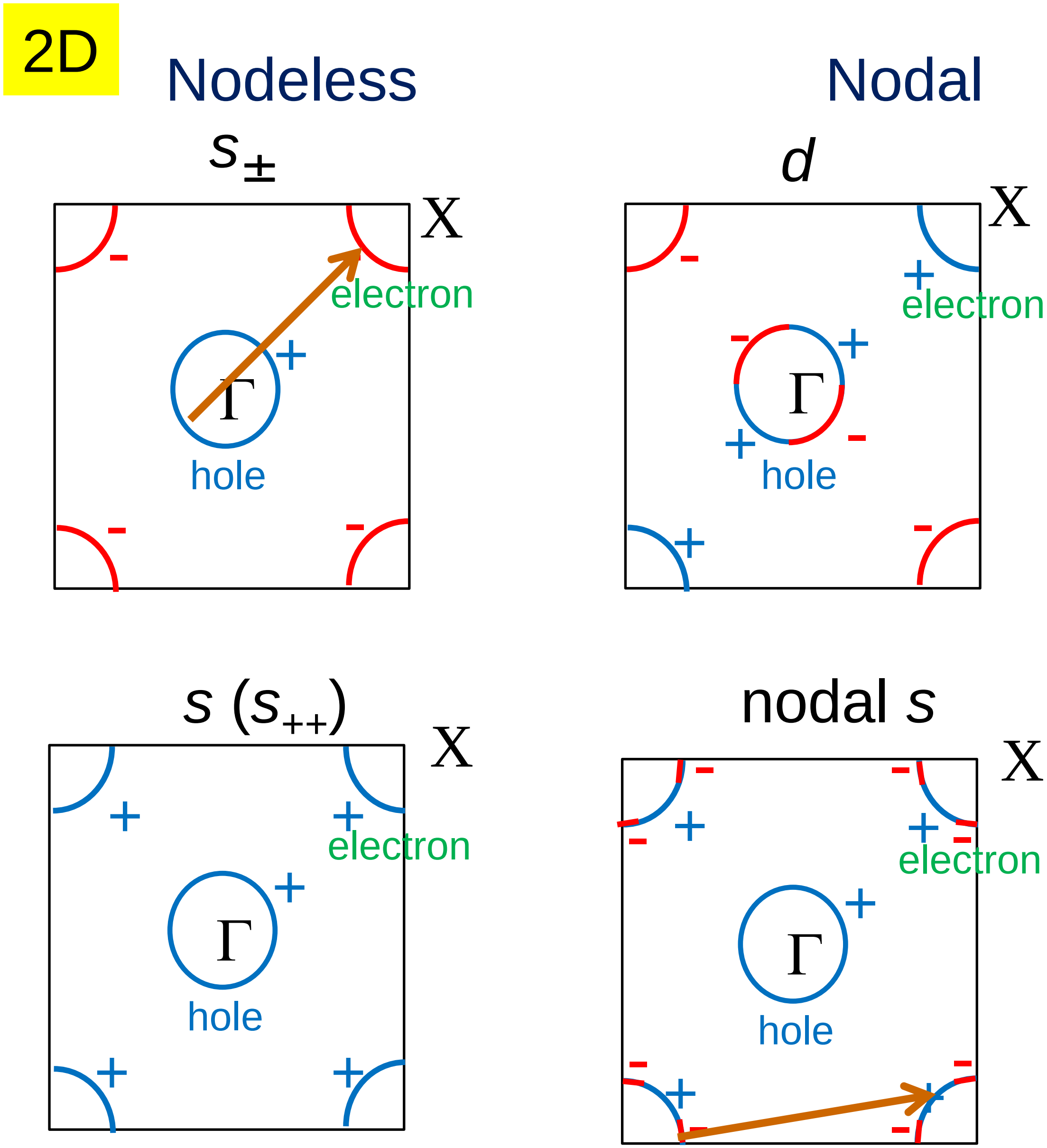

Large $\chi(\boldsymbol{q})$

$\downarrow$

$\Delta(\boldsymbol{k}+\boldsymbol{q})\Delta(\boldsymbol{k}) < 0$

Sign change

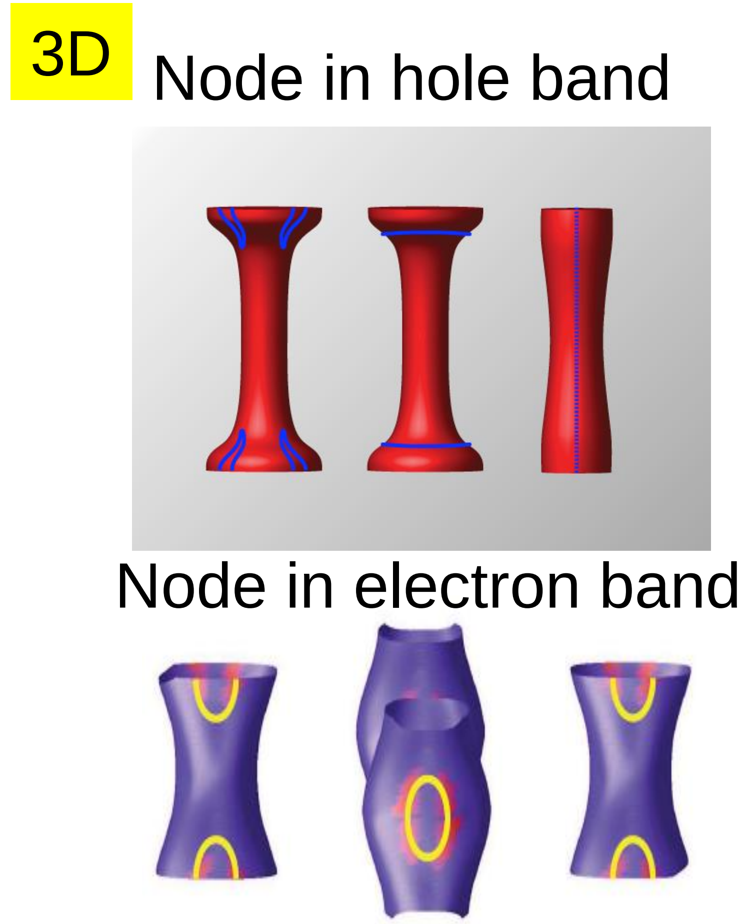

P.J. Hirshfeld, M.M. Korshunov and I.I. Mazin, Rep. Prog. Phys. (11) see references therein

Knight shift

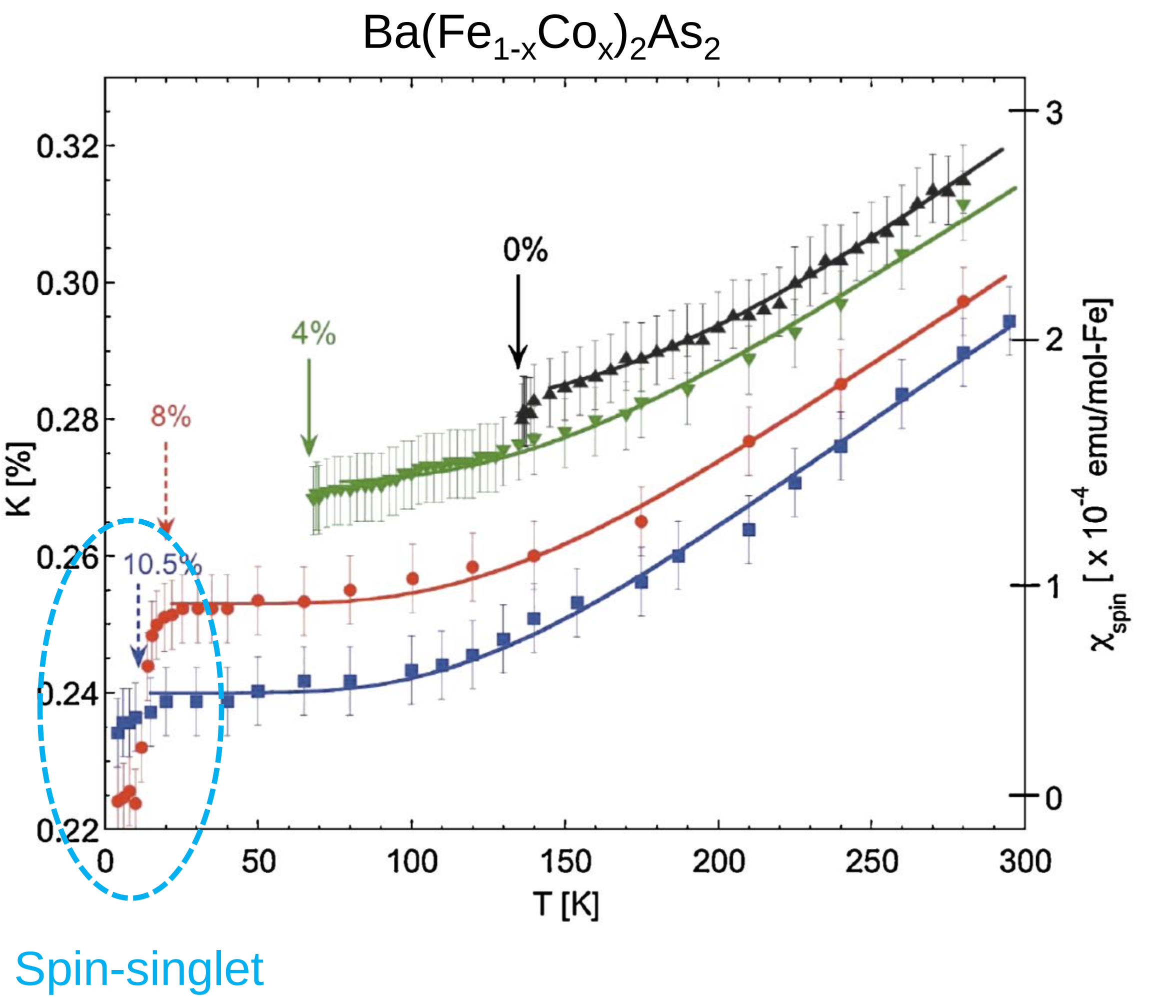

F.L. Ning *et al*. JPSJ 78, 013711 (2009).

Gap structure of iron pnictides

Full gap or nodal?

Thermally excited QPs

Full gap

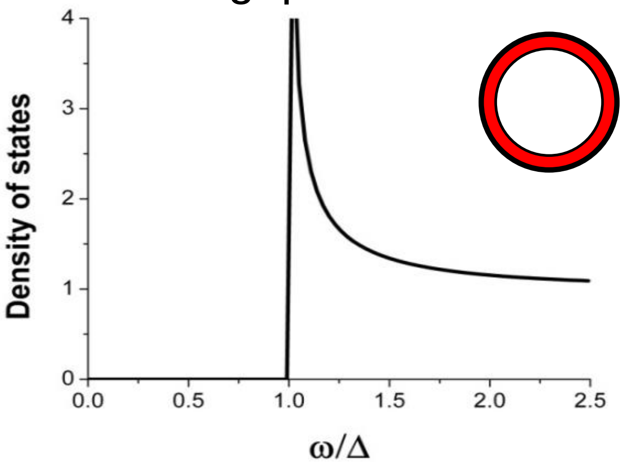

Line node

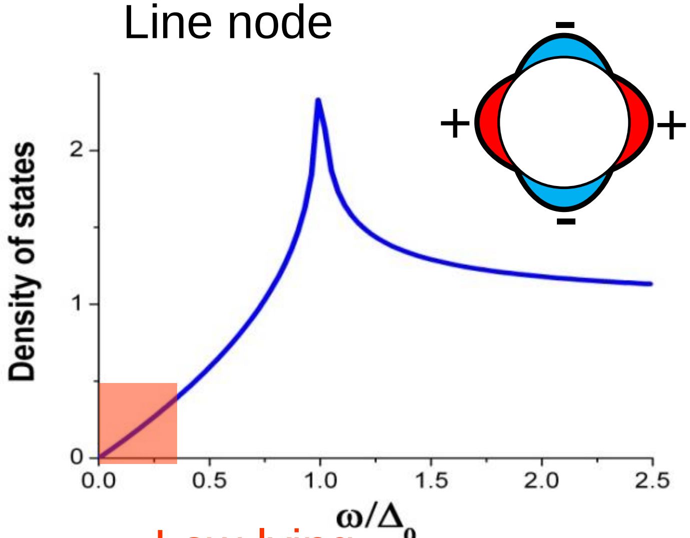

Low-lying excitations

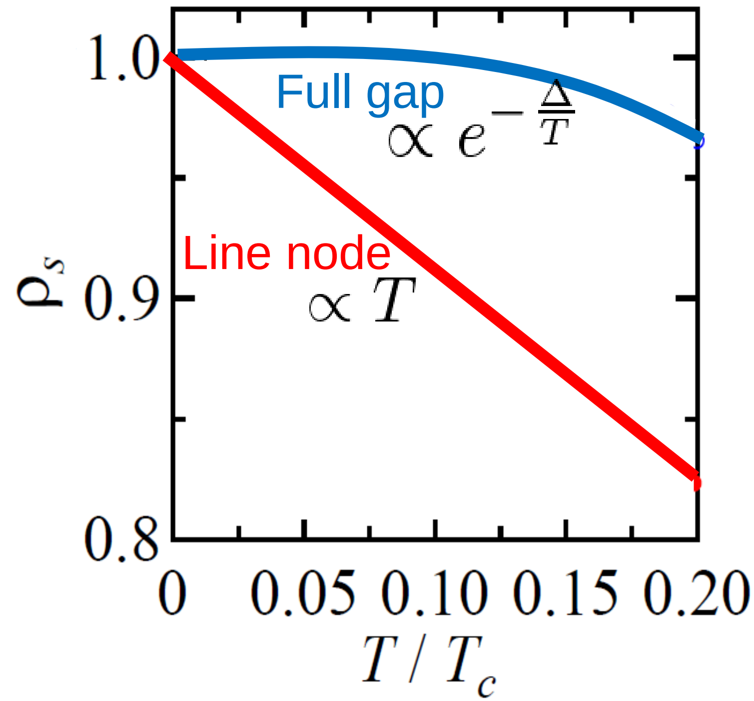

$$\rho_s = \frac{n_s(T)}{n_s(0)}$$

$n_s(T)$ Superfluid density

$$\lambda_L = \left(\frac{m}{\mu_0 n e^2}\right)^{\frac{1}{2}}$$

London penetration depth

$$\rho_s = \frac{\lambda_L^2(0)}{\lambda_L^2(T)}$$

Gap structure

Full gap

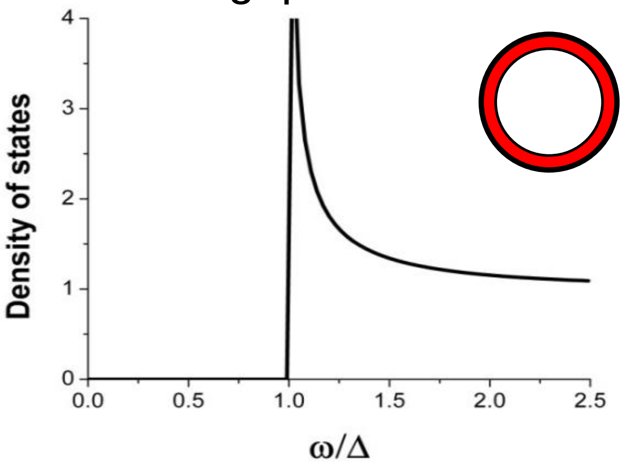

Line node

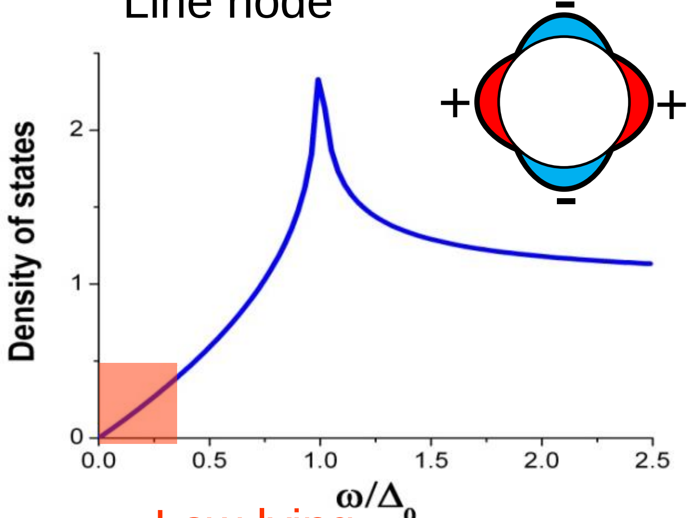

Low-lying excitations

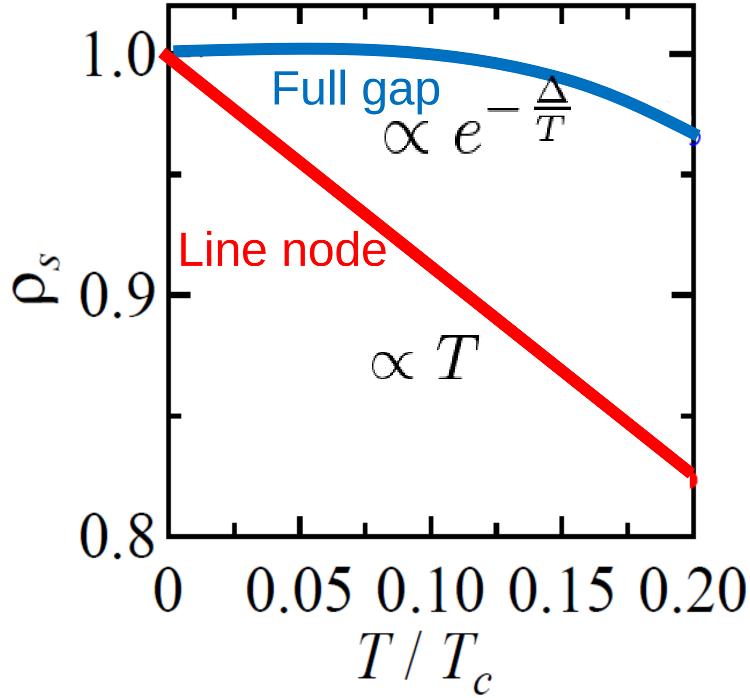

Line node	Full gap
$\lambda_L^{-2} \propto T$	$\lambda_L^{-2} \propto e^{-\frac{\Delta}{T}}$
$C \propto T^2$	$C \propto e^{-\frac{\Delta}{T}}$
$1/T_1 \propto T^3$	$1/T_1 \propto e^{-\frac{\Delta}{T}}$

Gap structure

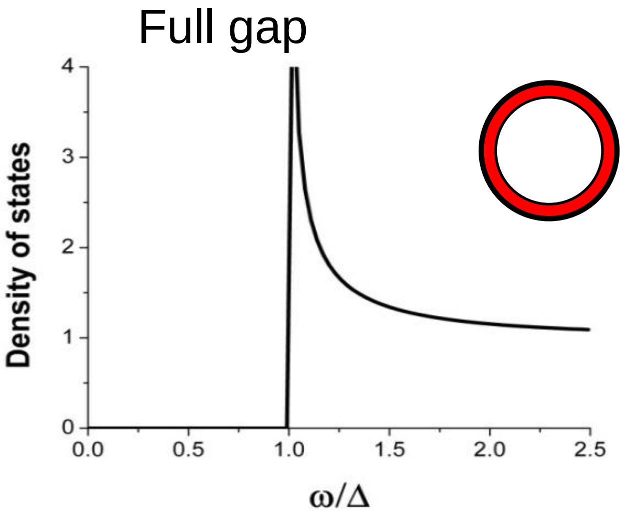

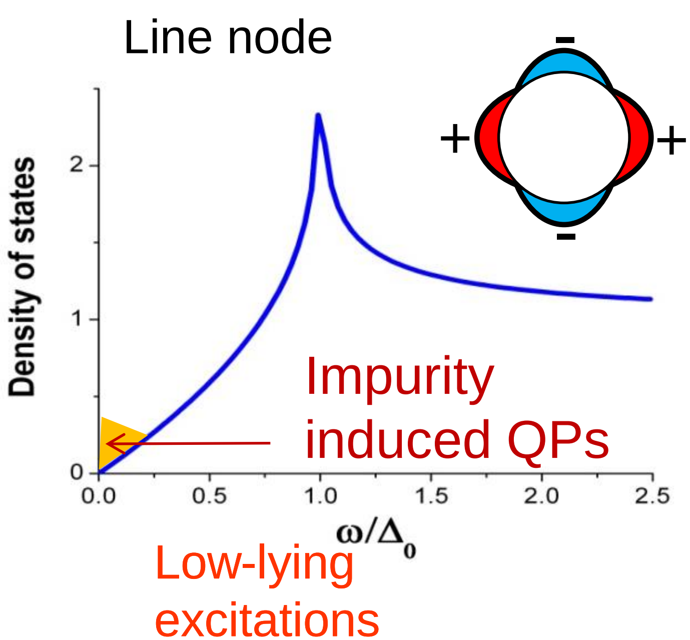

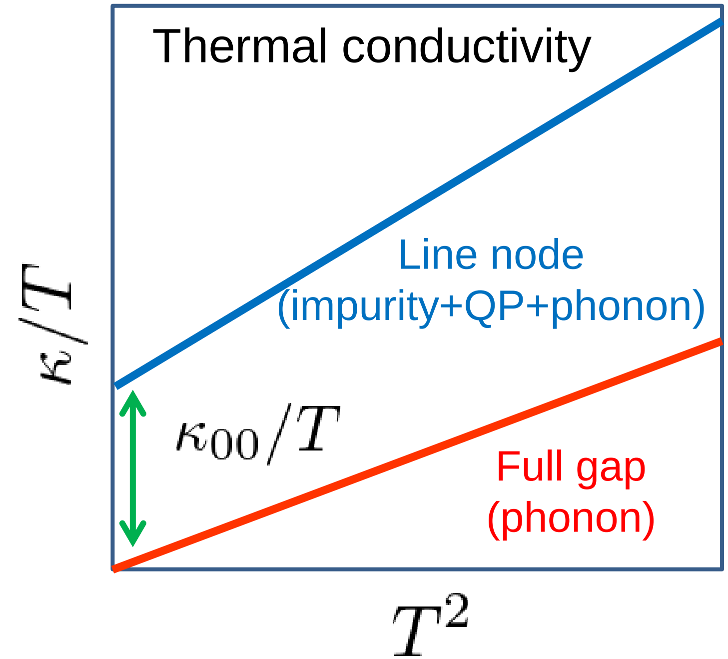

Superfluid does not carry the heat

$$\kappa_e = C_e v_F^2 \tau \qquad \kappa/T = \alpha + \beta T^2$$

$$\alpha = \kappa_{00}/T$$

$$\kappa_{00}/T = N_{imp}(0) v_F^2 \tau_{imp}$$

$$\tau_{imp} \propto 1/N_{imp}(0)$$

Independent of impurity

Universal thermal conductivity

Doppler shift of QP excitations

Full gap

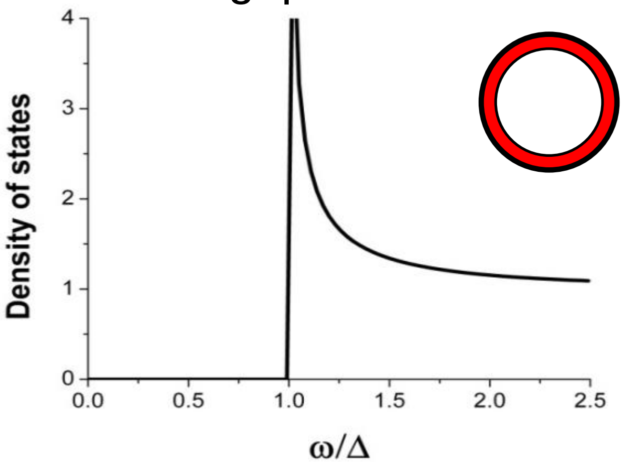

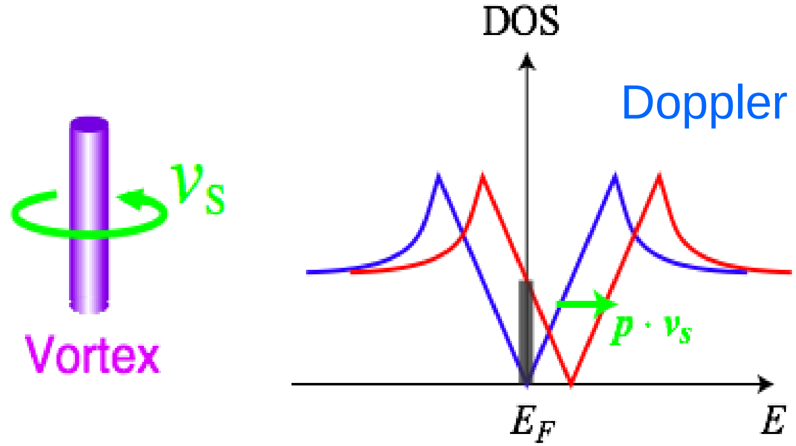

$$E'(\boldsymbol{p}) \rightarrow E(\boldsymbol{p}) + \boldsymbol{v_s} \cdot \boldsymbol{p}$$

v_s: supercurrent

G.E. Volovik, JETP Lett. **58**, 469 (1993)

Line node

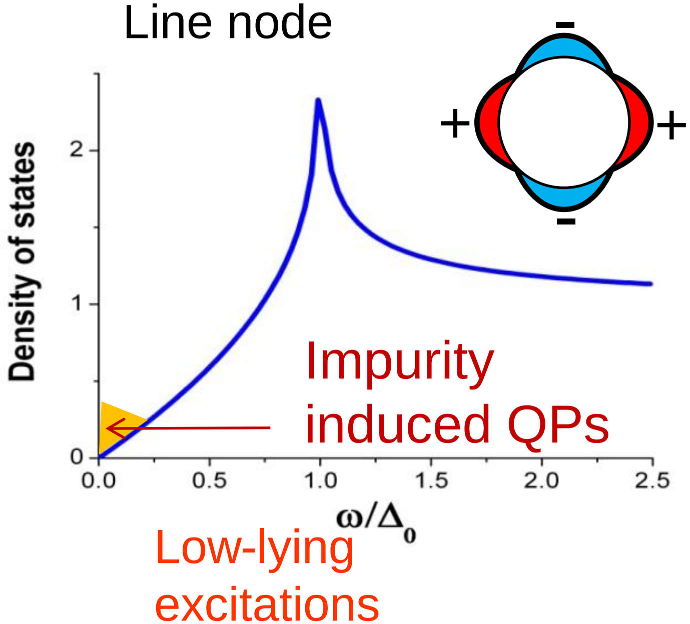

$$N(0) \sim \sqrt{H} \;\longrightarrow\; C(H),\; \kappa(H) \sim \sqrt{H}$$

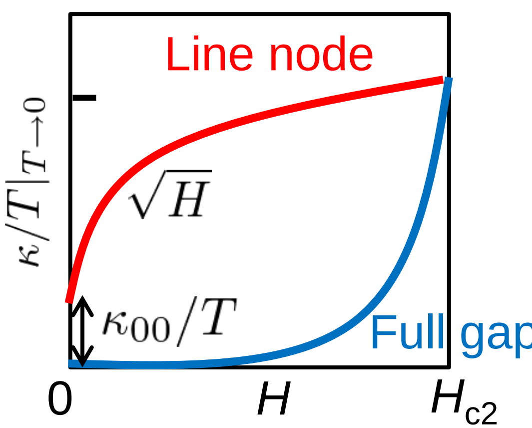

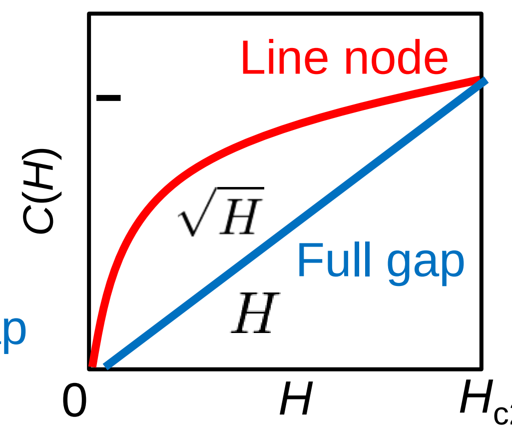

Thermal conductivity is governed by QPs **outside** of vortex core.

Thermal conductivity Measurement below 1 K

dilution refrigerator

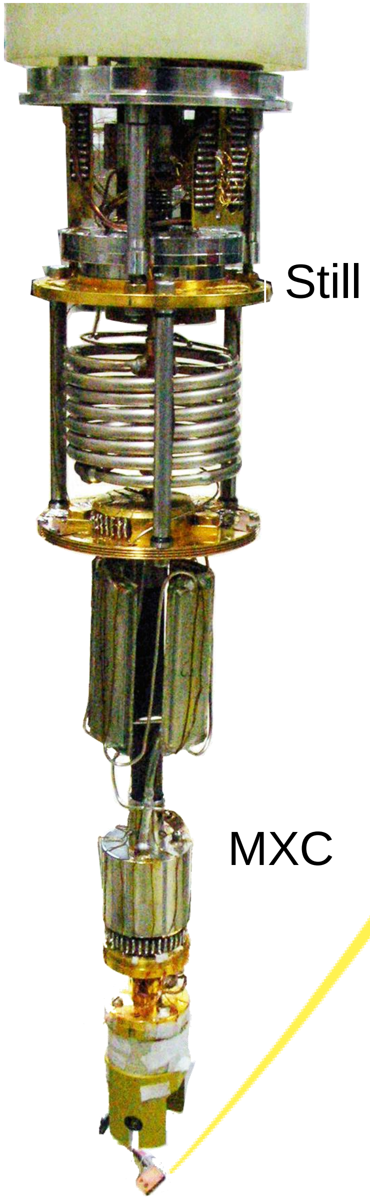

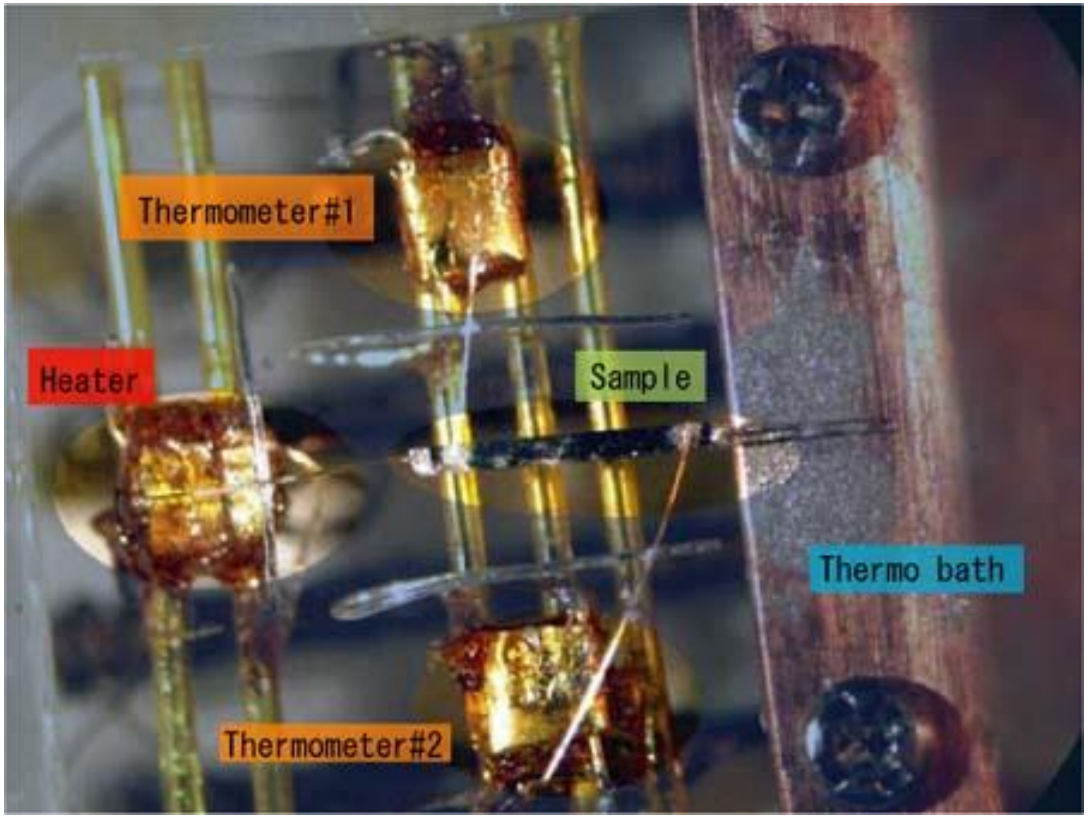

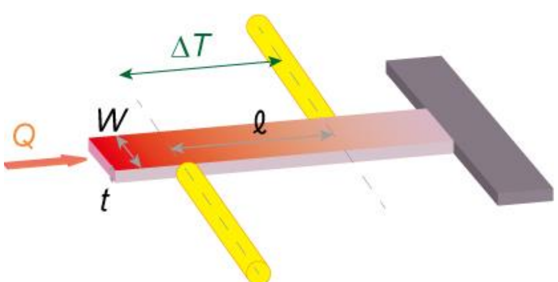

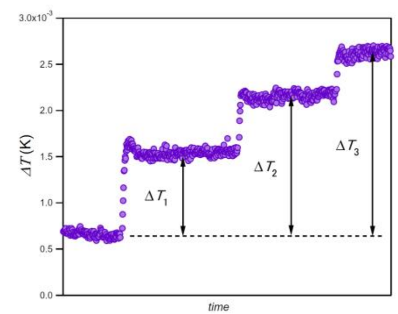

Full gap superconductivity

hole doped $Ba_{1-x}K_xFe_2As_2$

Penetration depth

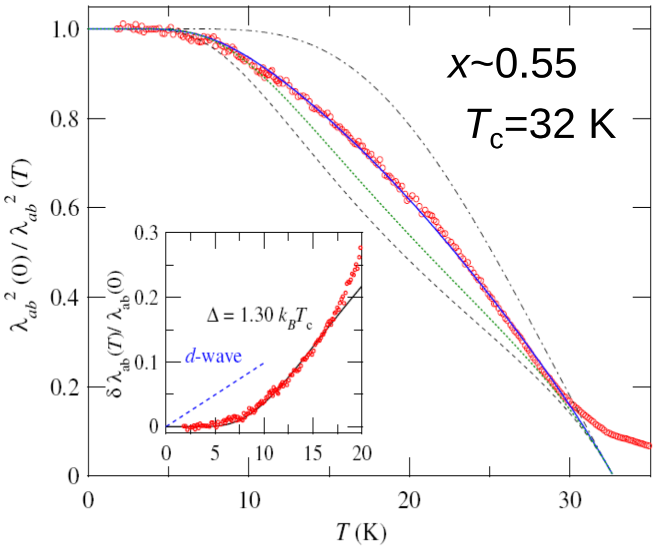

K. Hashimoto, *et al.*, PRL **102**, 027001 (2009).

Thermal conductivity

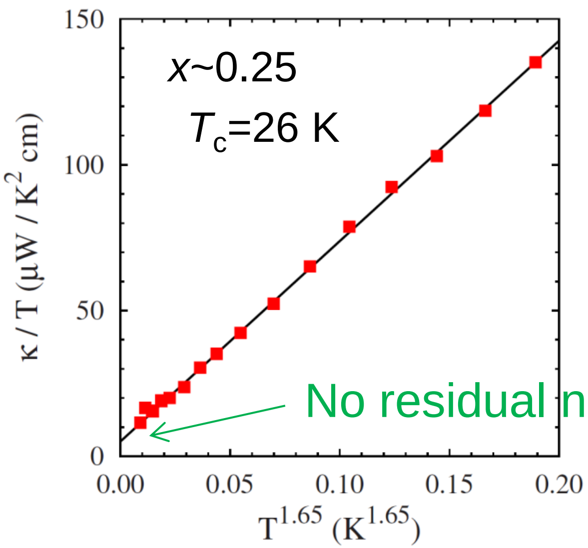

No residual normal fluid

X.G. Luo *et al*. PRB 80, 140503 (2009).

ARPES

x~0.4
T_c=37 K

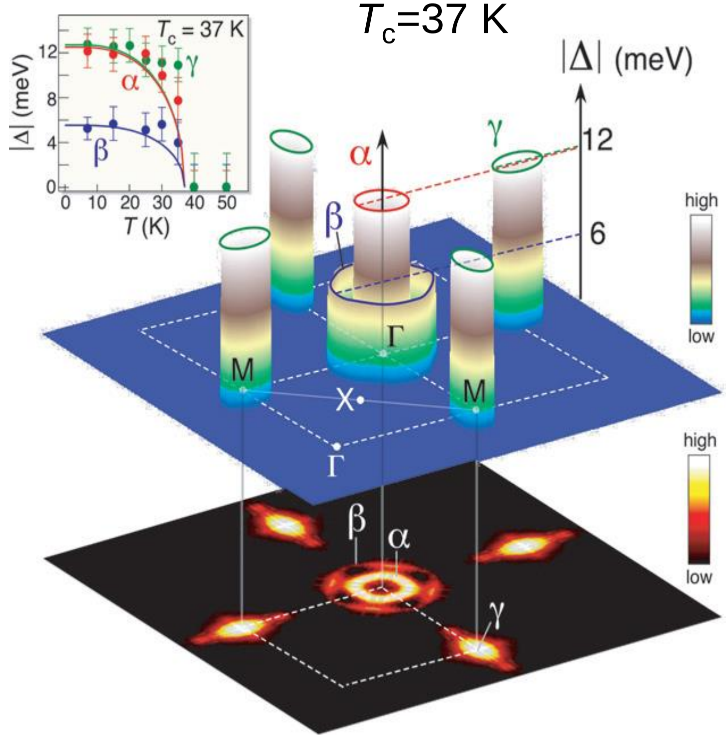

H. Ding *et al.*, EPL **83**, 47001 (2008).

Superconducting gap structure of $BaFe_2As_2$ systems

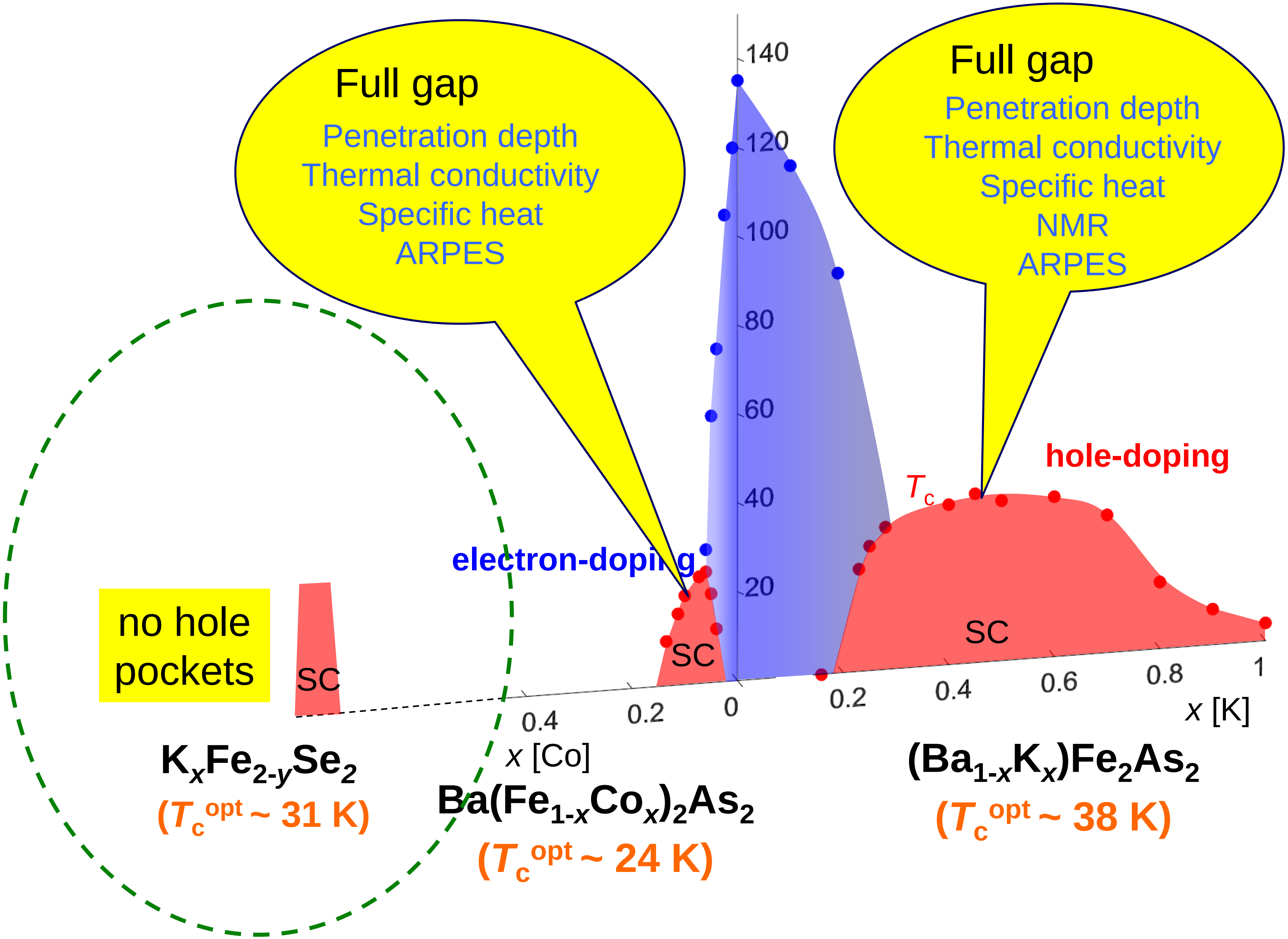

Superconducting gap structure of $BaFe_2As_2$ systems

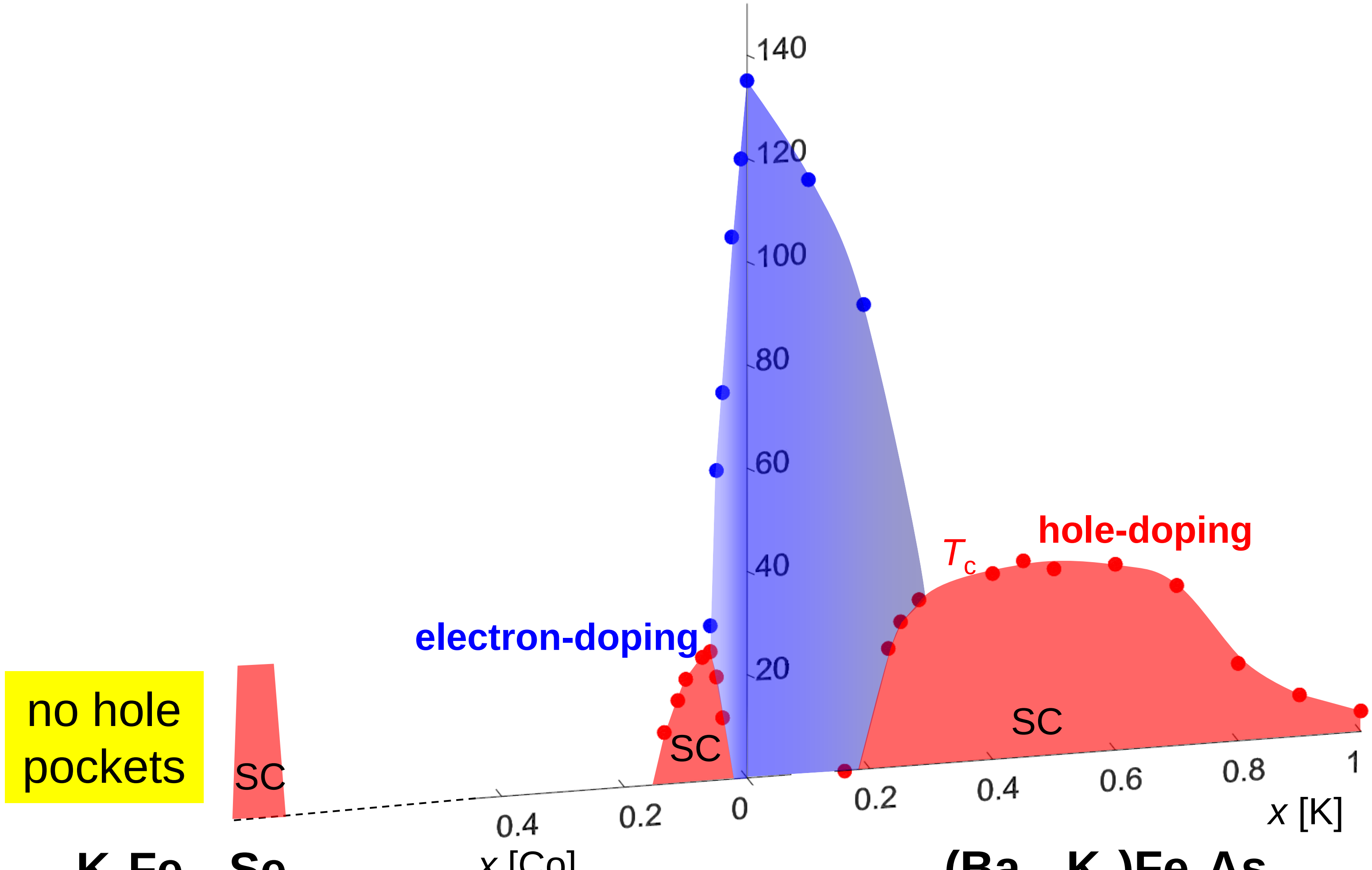

$K_xFe_{2-y}Se_2$
(T_c^{opt} ~ 31 K)

$Ba(Fe_{1-x}Co_x)_2As_2$
(T_c^{opt} ~ 24 K)

$(Ba_{1-x}K_x)Fe_2As_2$
(T_c^{opt} ~ 38 K)

SC gap structure in heavily electron doped systems

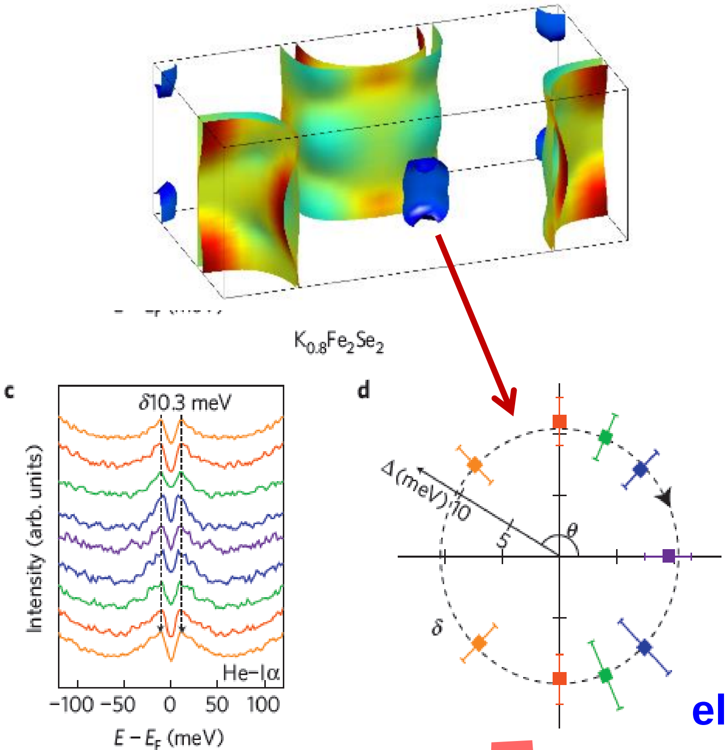

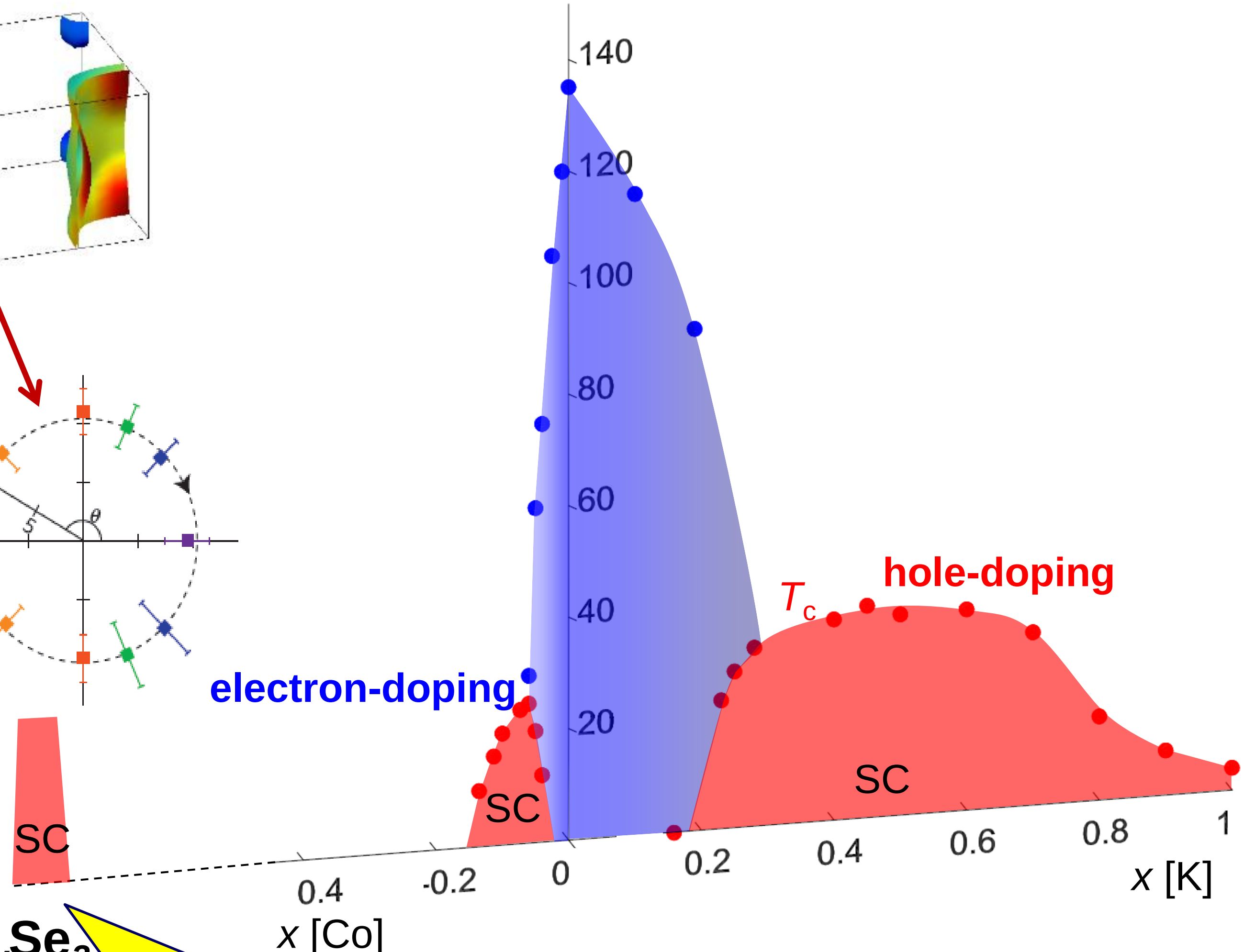

no hole pockets

$K_xFe_{2-y}Se_2$

(T_c^{opt} ~ 31 K)

Y. Zhang *et al.*,
Nature Materials (2011).

Full gap

Heavily electron doping

Full gap in inner electron pocket around *Z*-point

s-wave symmetry

Superconducting gap structure of $BaFe_2As_2$ systems

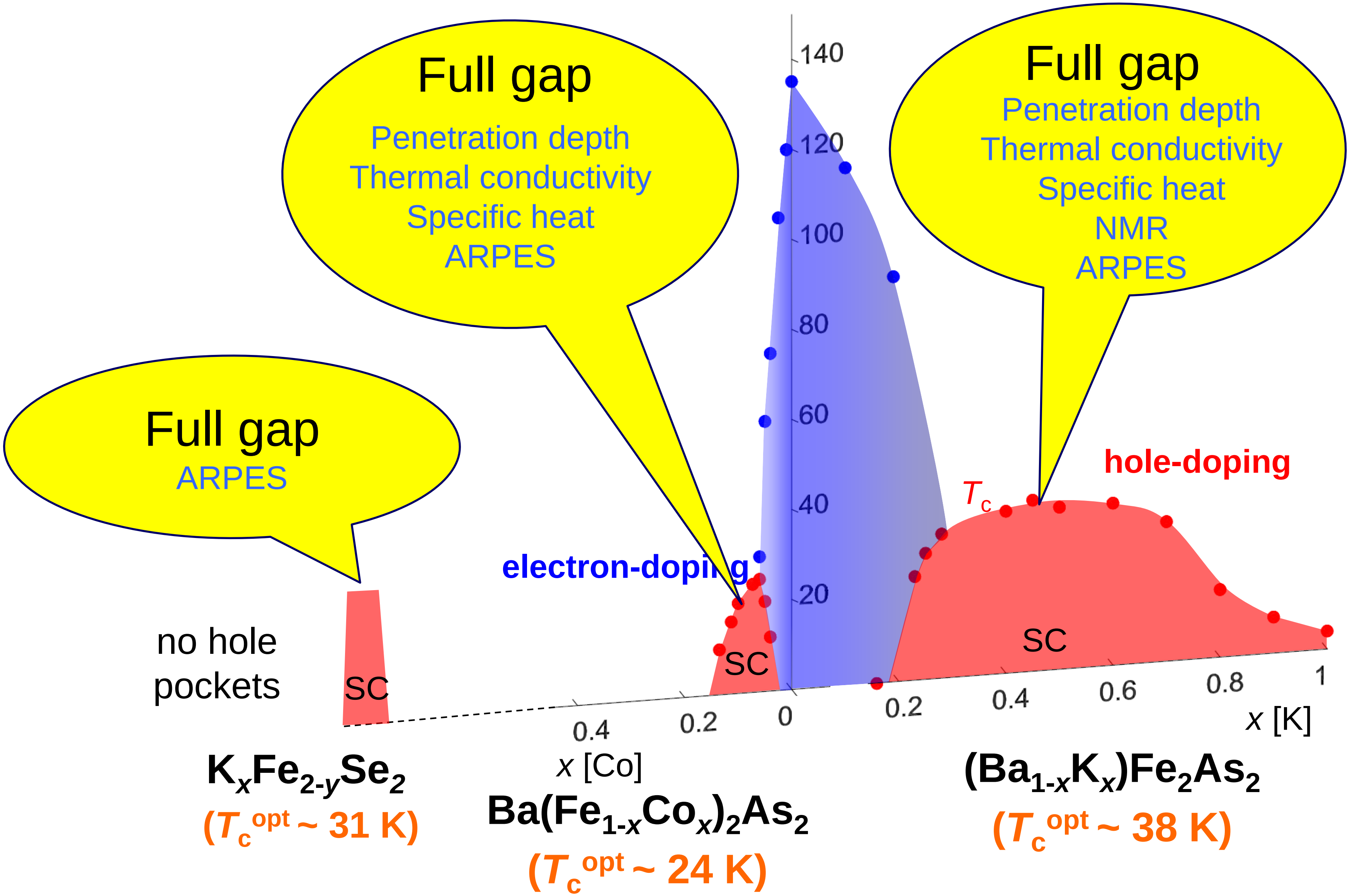

Sign change or no sign change?

S_{+-} or S_{++} ?

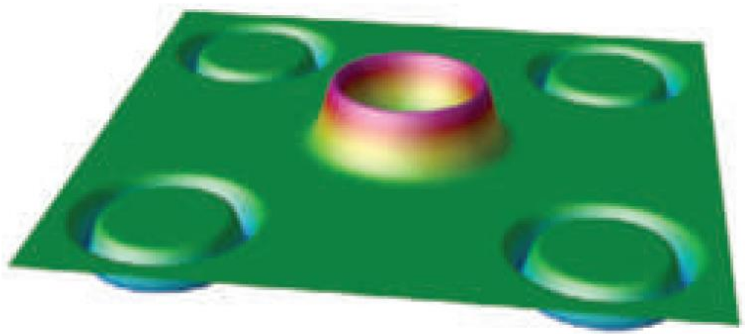

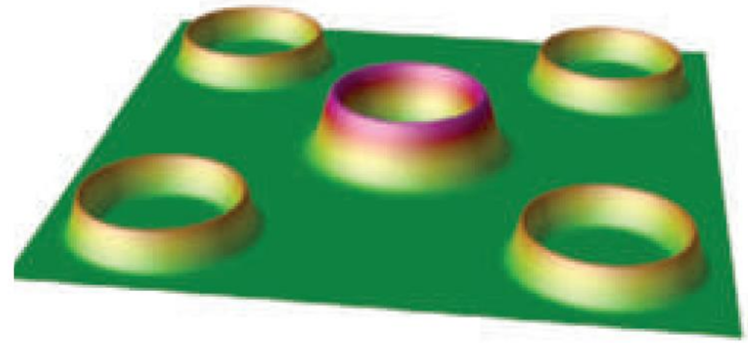

Spin fluctuations

Orbital fluctuations
(Quadrupole fluctuation)

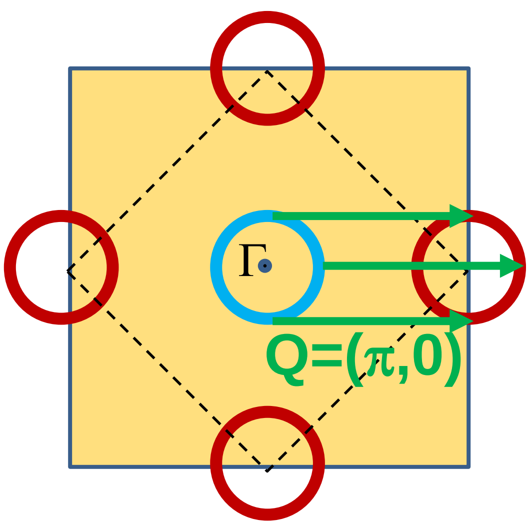

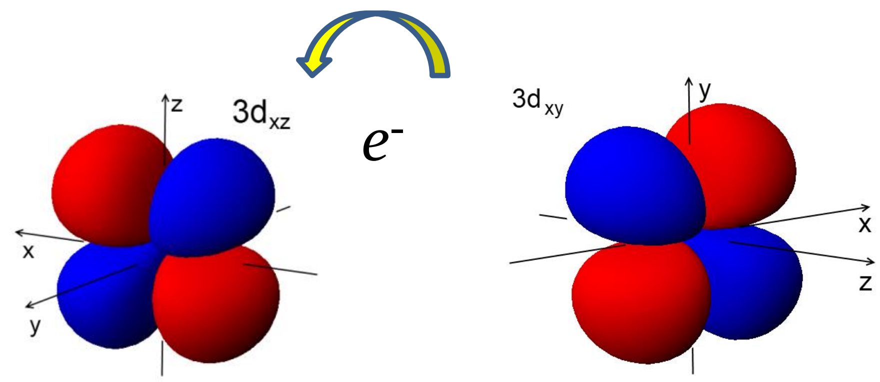

Charge up

Charge down

S+- or S++?

1. Phase sensitive test
2. NMR
3. Neutron scattering
4. Quasi-particle interference
5. Impurity effect

S+- or S++?: Phase sensitive tests

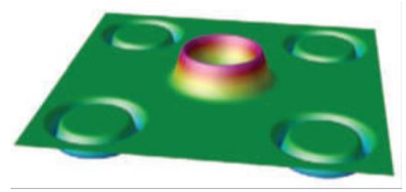

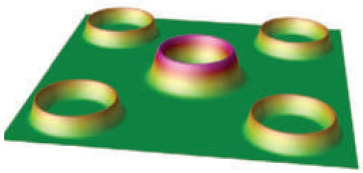

d-wave

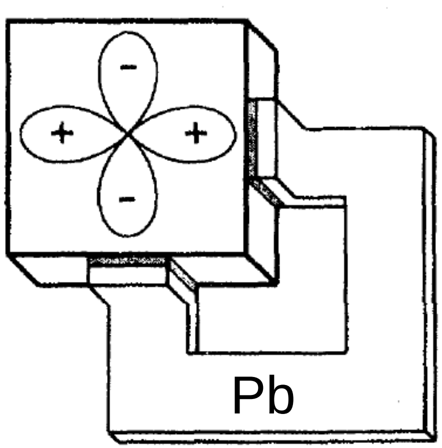

PRL **102,** 227007 (2009) PHYSICAL REVIEW LETTERS week ending 5 JUNE 2009

Possible Phase-Sensitive Tests of Pairing Symmetry in Pnictide Superconductors

D. Parker[1] and I. I. Mazin[1]

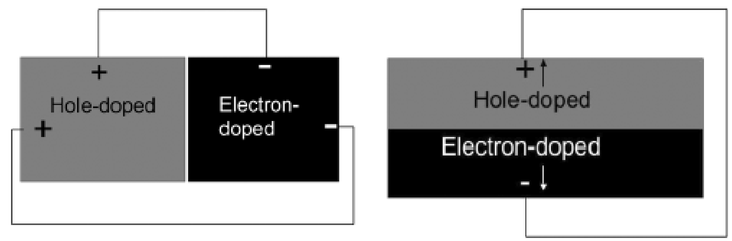

FIG. 3. A schematic view of the tunneling geometry for the proposed bicrystal experiments. Left: an *ab*-plane orientation with two possible lead orientations; right: a *c*-axis orientation.

Practically very difficult to fabricate such junctions

S+- or S++?: Phase sensitive tests

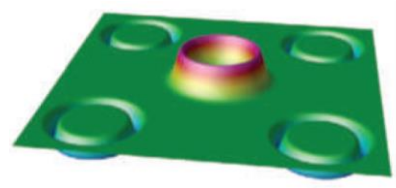

S_{+-}

d-wave

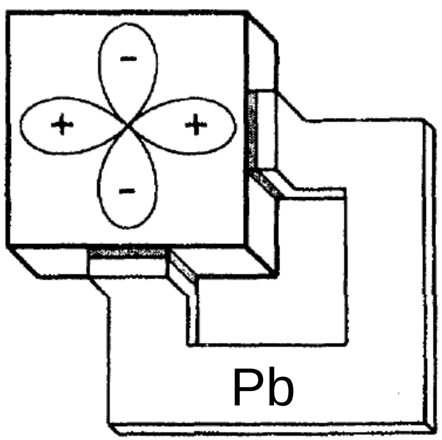

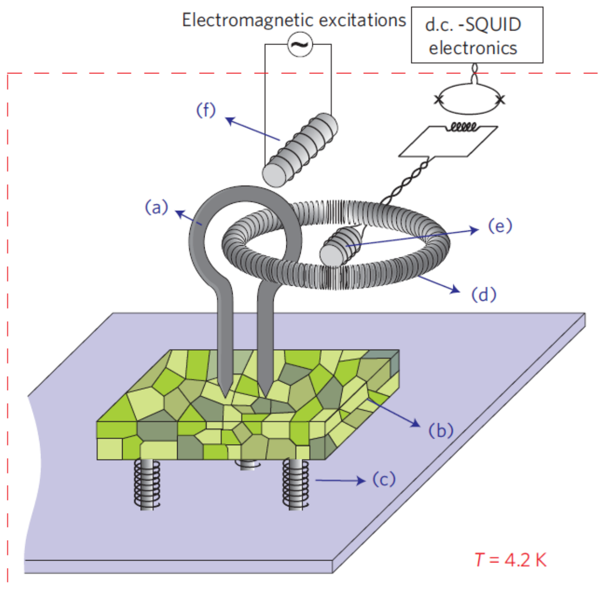

$NdFeAsO_{0.88}F_{0.12}$

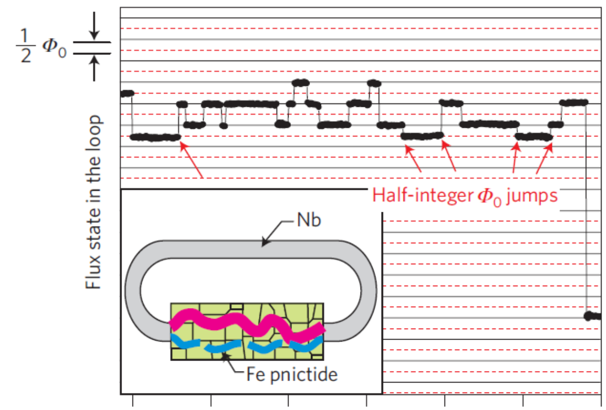

C.T. Chen et al. Nature Phys. (10)

Experiments have been performed on polycrystals

Sign change or no sign change?

Quasiparticle excitations from the SC ground state

$$\gamma^\dagger_{k0} = u_k c^\dagger_{k\uparrow} - v_k c_{-k\downarrow}$$
$$\gamma^\dagger_{k1} = u_k c^\dagger_{-k\downarrow} + v_k c_{k\uparrow}$$

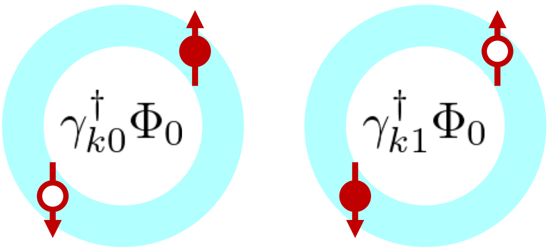

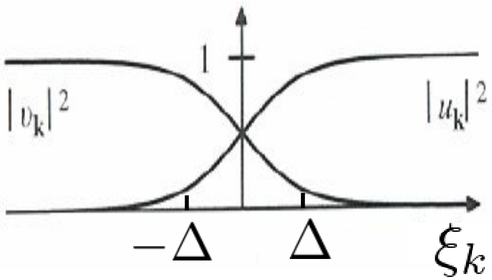

$$|u_k|^2 = \frac{1}{2}\left(1 + \frac{\xi_k}{\sqrt{\Delta_k^2 + \xi_k^2}}\right) \qquad |v_k|^2 = \frac{1}{2}\left(1 - \frac{\xi_k}{\sqrt{\Delta_k^2 + \xi_k^2}}\right) \qquad \xi_k \equiv \frac{\hbar^2 k^2}{2m} - \varepsilon_F$$

B-quasiparticle: a superposition of an electron and a hole

$$\mathbf{k}\sigma \rightarrow \mathbf{k}'\sigma'$$

$$\mathcal{H}_1 = \sum_{k\sigma,k'\sigma'} B_{k\sigma,k'\sigma'} c^\dagger_{k\sigma} c_{k'\sigma'} - \begin{cases} B_{k\sigma,k'\sigma'} c^\dagger_{k\sigma} c_{k'\sigma'} \\ B_{-k'-\sigma',-k-\sigma} c^\dagger_{-k'-\sigma'} c_{-k-\sigma} \end{cases}$$

connected by time-reversal symmetry

Coherence factor

Scattering of QPs
$$(u_k u_{k'} \pm v_k v_{k'})^2 = \frac{1}{2}\left(1 \pm \frac{\Delta^2}{E_k E_{k'}}\right)$$

Creation and annihilation of two QPs
$$(v_k u_{k'} \pm u_k v_{k'})^2 = \frac{1}{2}\left(1 \pm \frac{\Delta^2}{E_k E_{k'}}\right)$$

S+- or S++?: NMR

$$\frac{1}{T_1T} \propto \sum_{kk'} \left(1 + \frac{\Delta_k \Delta_{k'}}{E_k E_{k'}}\right) \left[-\frac{\partial f(E_k)}{\partial E_k}\right] \delta(E_k - E_{k'})$$

s-wave

$$\frac{1}{T_1} \propto \int_{\Delta(T)}^{\infty} dE\, \frac{E^2 + \Delta^2}{\underline{E^2 - \Delta^2}}\, \mathrm{sech}^2\left(\frac{E}{2T}\right)$$

Hebel-Slichter peak

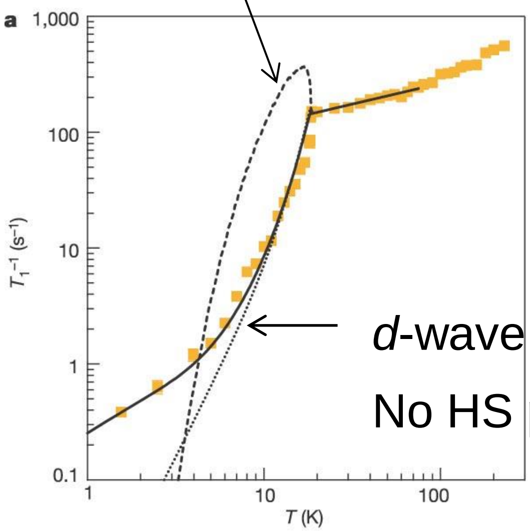

d-wave

No HS peak

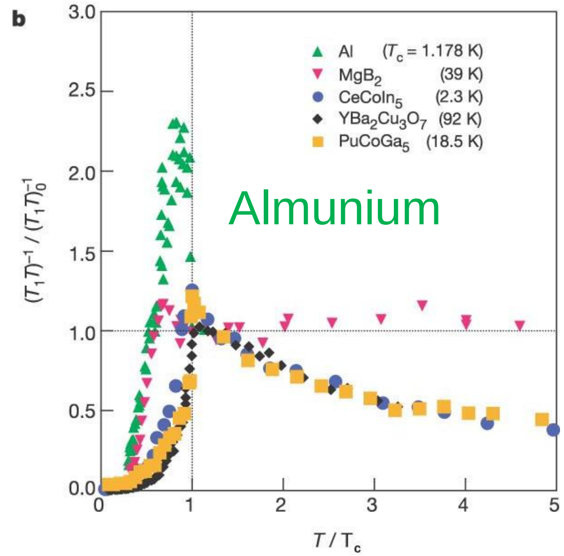

N. Curro *et al*. Nature (12)

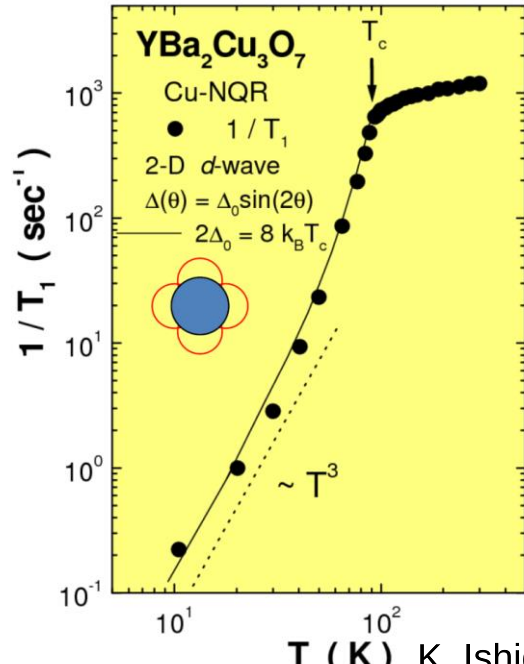

K. Ishida *et al*. JPSJ (93)

S+- or S++?: NMR

$$\frac{1}{T_1 T} \propto \sum_{kk'} \left(1 + \frac{\Delta_k \Delta_{k'}}{E_k E_{k'}}\right) \left[-\frac{\partial f(E_k)}{\partial E_k}\right] \delta(E_k - E_{k'})$$

S_{++} $\quad \Delta_k = \Delta_{k'} = \Delta$

$$\frac{1}{T_1} \propto \int_{\Delta(T)}^{\infty} dE \, \frac{E^2 + \Delta^2}{E^2 - \Delta^2} \, \mathrm{sech}^2 \left(\frac{E}{2T}\right)$$

S_{+-} $\quad \Delta_k = -\Delta_{k'} = \Delta$

$$\frac{1}{T_1} \propto \int_{\Delta(T)}^{\infty} dE \, \mathrm{sech}^2 \left(\frac{E}{2T}\right)$$

No HS peak

Hebel-Slichter peak

No HS peak

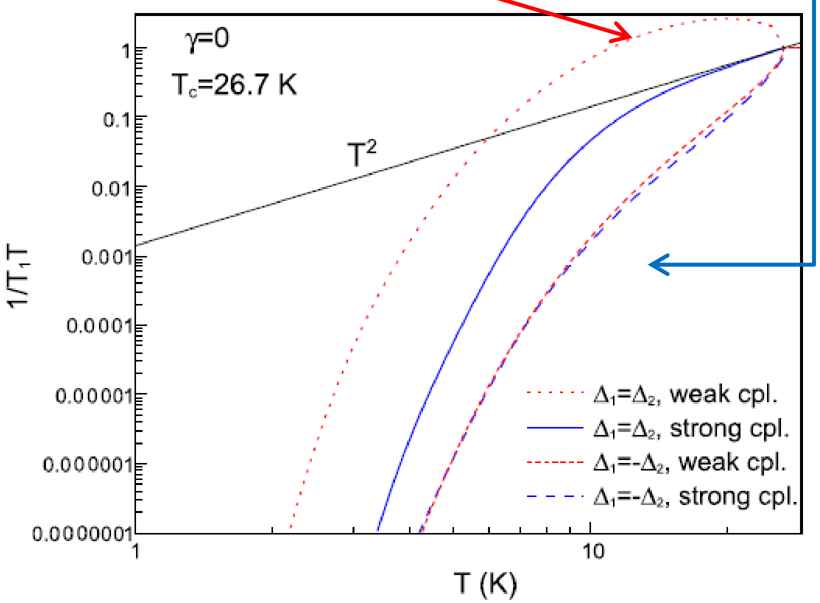

D. Parker *et al*.
PRB (08)

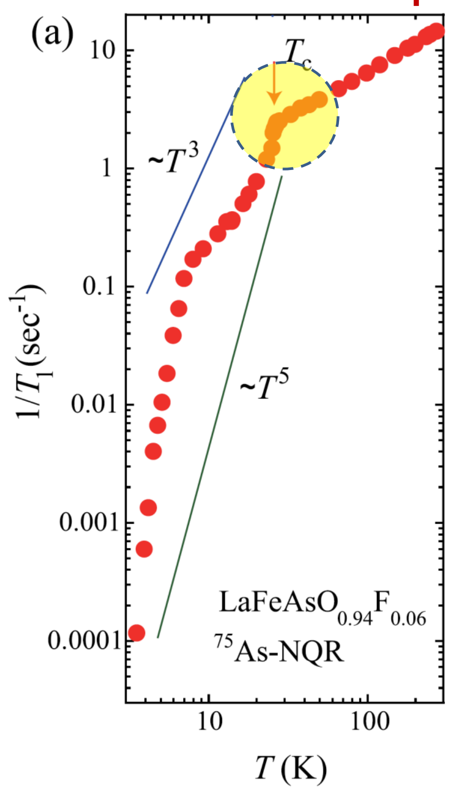

T. Oka *et al*.
PRL (12)

However, the HS peak readily disappears by inelastic scatterings, eg. Pb.

Absence of the coherence peak is not evidence of S_{+-}

S+- or S++?: Neutron resonance peak at *Q*

In the superconducting state

$$\mathrm{Im}\chi_0(\mathbf{q},\omega) = \frac{1}{4}\frac{1}{(2\pi)^3}\int d^3k \left(1 - \frac{\Delta_k \Delta_{k+q}}{E_{k+q}E_k}\right)\delta(\omega - E_{k+q} - E_k) \qquad E_{\mathbf{k}} = \sqrt{\xi_{\mathbf{k}}^2 + \Delta_{\mathbf{k}}^2}$$

The coherence factor becomes 2 for $\boxed{\Delta_{\mathbf{k+Q}} = -\Delta_{\mathbf{k}}}$

Sharp resonance peak at $\omega_{res} < 2\Delta$

$CeCoIn_5$ *d*-wave

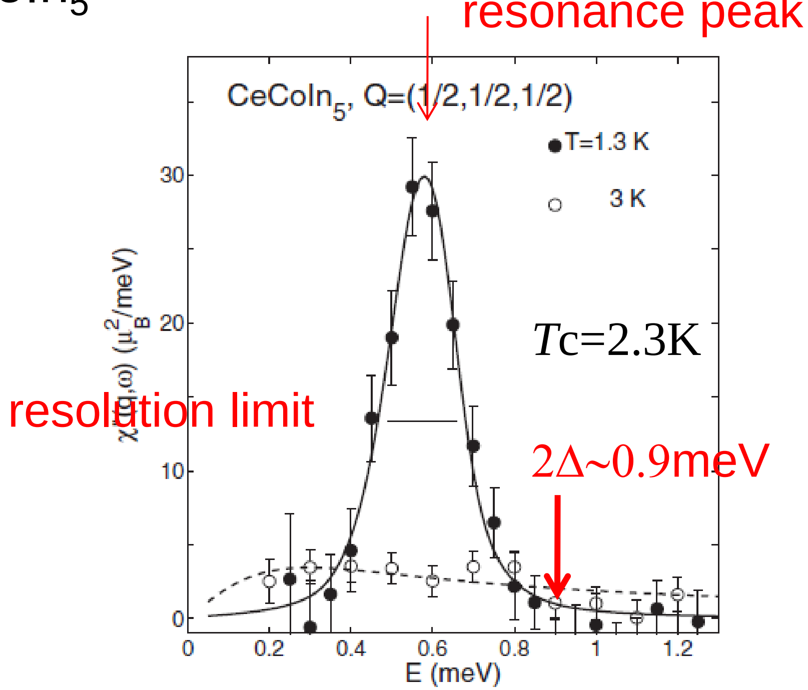

Stock *et al.*, PRL **100**, 087001 (2008)

S+- or S++?: Neutron resonance peak at $\boldsymbol{Q}$

In the superconducting state

$$\mathrm{Im}\chi_0(\mathbf{q},\omega) = \frac{1}{4}\frac{1}{(2\pi)^3}\int d^3k \left(1 - \frac{\Delta_k\Delta_{k+q}}{E_{k+q}E_k}\right)\delta(\omega - E_{k+q} - E_k) \qquad E_{\mathbf{k}} = \sqrt{\xi_{\mathbf{k}}^2 + \Delta_{\mathbf{k}}^2}$$

The coherence factor becomes 2 for $\boxed{\Delta_{\mathbf{k+Q}} = -\Delta_{\mathbf{k}}}$

S_{+-} Sharp resonance peak at $\omega_{res} < 2\Delta$ $(\Delta_{el}+\Delta_{hole})$

S_{++} Broad peak at $\omega_{res} > 2\Delta$ $(\Delta_{el}+\Delta_{hole})$

$BaFe_{1.85}Co_{0.15}As_2$ Inosov *et al*., Nat. Phys. (10).

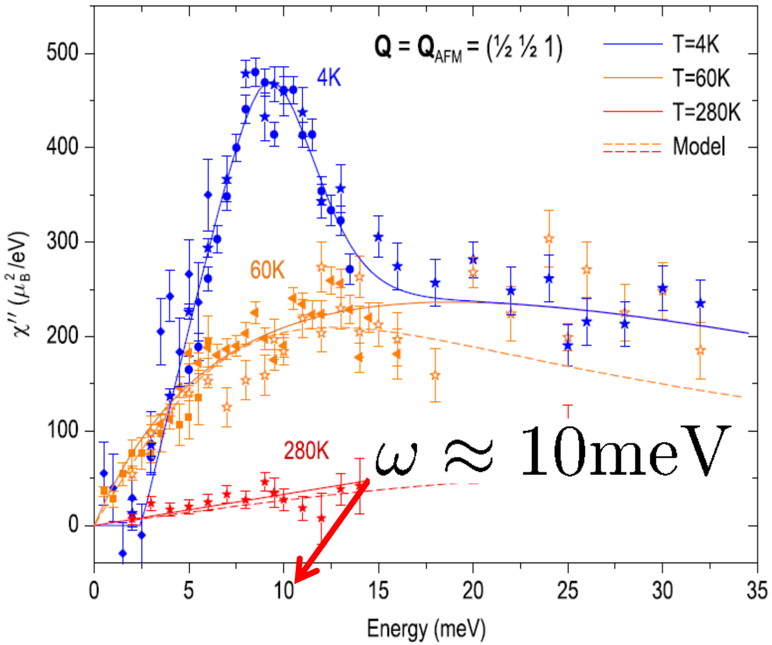

ARPES（bulk-sensitive）:

$$\Delta_{\mathrm{el}} + \Delta_{\mathrm{hole}} \approx 11.6\mathrm{meV}$$

Terashima *et al*., PNAS 2009

penetration depth:

$$\Delta_{\mathrm{el}} + \Delta_{\mathrm{hole}} \approx 8.4\mathrm{meV}$$

Luan *et al*., PRL 2011

specific heat:

$$\Delta_{\mathrm{el}} + \Delta_{\mathrm{hole}} \approx 7\mathrm{meV}$$

Hardy *et al*., EPL 2010

S+- or S++?: Neutron resonance peak at *Q*

In the superconducting state

$$\mathrm{Im}\chi_0(\mathbf{q},\omega) = \frac{1}{4}\frac{1}{(2\pi)^3}\int d^3k\left(1-\frac{\underline{\Delta_k\Delta_{k+q}}}{E_{k+q}E_k}\right)\delta(\omega - E_{k+q} - E_k) \qquad E_{\mathbf{k}} = \sqrt{\xi_{\mathbf{k}}^2+\Delta_{\mathbf{k}}^2}$$

The coherence factor becomes 2 for $\boxed{\Delta_{\mathbf{k+Q}} = -\Delta_{\mathbf{k}}}$

S_{+-} Sharp resonance peak at $\omega_{res} < 2\Delta$ ($\Delta_{el}+\Delta_{hole}$)

S_{++} Broad peak at $\omega_{res} > 2\Delta$ ($\Delta_{el}+\Delta_{hole}$)

$BaFe_{1.85}Co_{0.15}As_2$ Inosov *et al.*, Nat. Phys. (10).

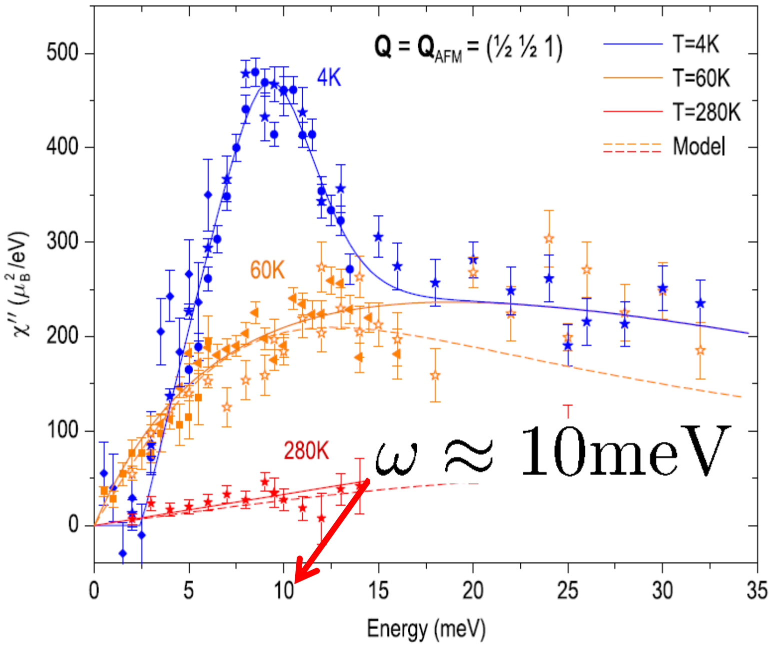

S. Onari and H. Kontani, PRB (11)

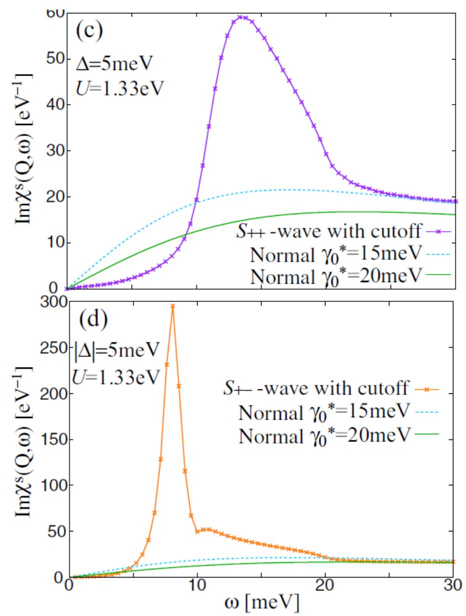

Neutron scattering experiments can be explained by either models.

S+- or S++?: Quasiparticle interference (QPI)

Quasi-Particle Interference

Tunnel conductance

$$Z(\mathbf{r},E) \equiv \frac{dI/dV(\mathbf{r},+E)}{dI/dV(\mathbf{r},-E)} = \frac{\rho(\mathbf{r},+E)}{\rho(\mathbf{r},-E)} \xrightarrow{\text{FT}} \boxed{Z(\mathbf{q},E)}$$

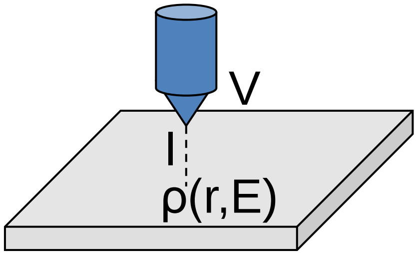

No impurity (no scattering) $Z(\mathbf{q},E)=0$ for $\mathbf{q}\neq 0$

Nonmagnetic impurity

QP scattering probability (SC state)

$$w(\mathbf{k}\sigma \to \mathbf{k}'\sigma) \propto \underbrace{|V(\mathbf{k},\mathbf{k}')|^2}_{\text{matrix element}} \underbrace{(u_k u_{k'} - v_k v_{k'})^2}_{\text{coherence factor}}$$

Nonmagnetic (no spin flip)

matrix element

coherence factor

$$\boxed{(u_k u_{k'} - v_k v_{k'})^2 = \frac{1}{2}\left(1 - \frac{\Delta_k \Delta_{k'}}{E_k E_{k'}}\right)}$$

sign-preserving scattering

$\Delta_k \Delta_{k'} > 0$ $\quad (u_k u_{k'} - v_k v_{k'})^2$ small

sign-reversing scattering

$\Delta_k \Delta_{k'} < 0$ $\quad (u_k u_{k'} - v_k v_{k'})^2$ large

S+- or S++?: Quasiparticle interference (QPI)

Quasi-Particle Interference

Tunnel conductance

$$Z(\mathbf{r},E) \equiv \frac{dI/dV(\mathbf{r},+E)}{dI/dV(\mathbf{r},-E)} = \frac{\rho(\mathbf{r},+E)}{\rho(\mathbf{r},-E)} \xrightarrow{\text{FT}} \boxed{Z(\mathbf{q},E)}$$

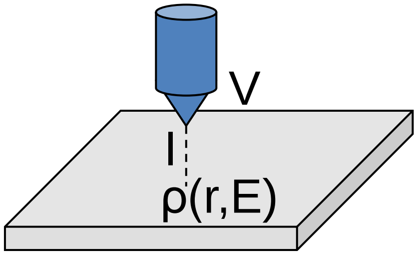

No impurity (no scattering) $Z(\mathbf{q},E)=0$ for $\mathbf{q}\neq 0$

Nonmagnetic impurity

Cuprate : Octet Model

J. Hoffman *et al.*, Science (2002), K. McElroy, *et al.*, Nature (2003).

Δ_k and Δ_{k+q} $\begin{cases} \text{sign-preserving scattering} \Rightarrow \text{suppression} \\ \text{sign-reversing scattering} \Rightarrow \text{enhancement} \end{cases}$

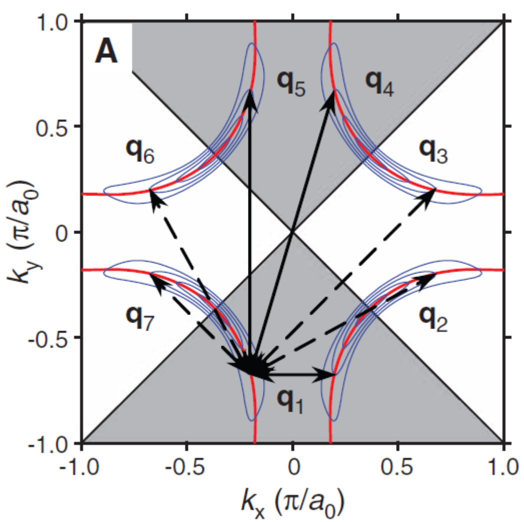

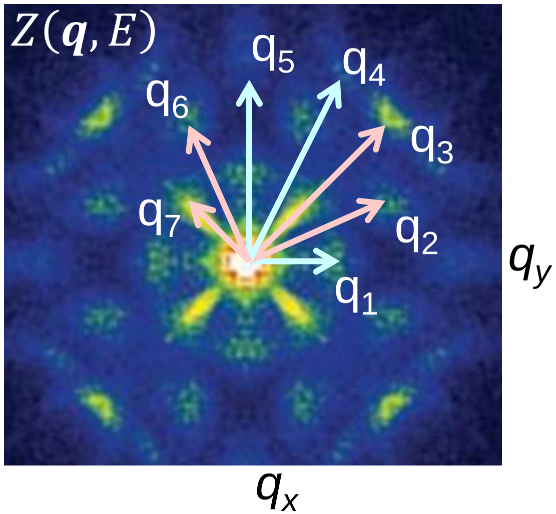

sign-preserving
($\mathbf{q}_1$, $\mathbf{q}_4$, $\mathbf{q}_5$)

sign-reversing
($\mathbf{q}_2$, $\mathbf{q}_3$, $\mathbf{q}_6$, $\mathbf{q}_7$)

T. Hanaguri *et al.*

S+- or S++?: Quasiparticle interference (QPI)

Quasi-Particle Interference

Tunnel conductance

$$Z(\mathbf{r}, E) \equiv \frac{dI/dV(\mathbf{r}, +E)}{dI/dV(\mathbf{r}, -E)} = \frac{\rho(\mathbf{r}, +E)}{\rho(\mathbf{r}, -E)} \xrightarrow{\text{FT}} \boxed{Z(\mathbf{q}, E)}$$

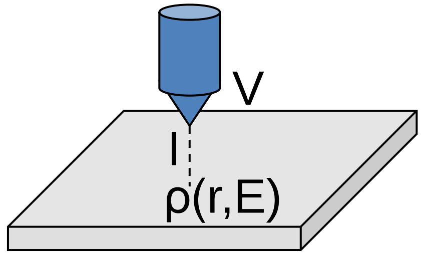

No impurity (no scattering) $Z(\mathbf{q}, E) = 0$ for $\mathbf{q} \neq 0$

Nonmagnetic impurity

Fe-based superconductor

Δ_k and Δ_{k+q} $\begin{cases} \text{sign-preserving scattering} \Rightarrow \text{suppression} \\ \text{sign-reversing scattering} \Rightarrow \text{enhancement} \end{cases}$

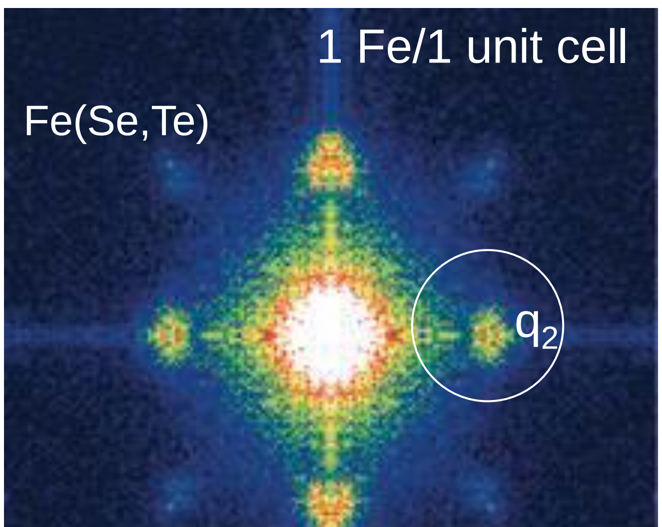

T. Hanaguri, *et al.*, Science **328**, 474 (2010).

q_y

S_{++}-wave SC $\quad$ $S_{\pm}$-wave SC

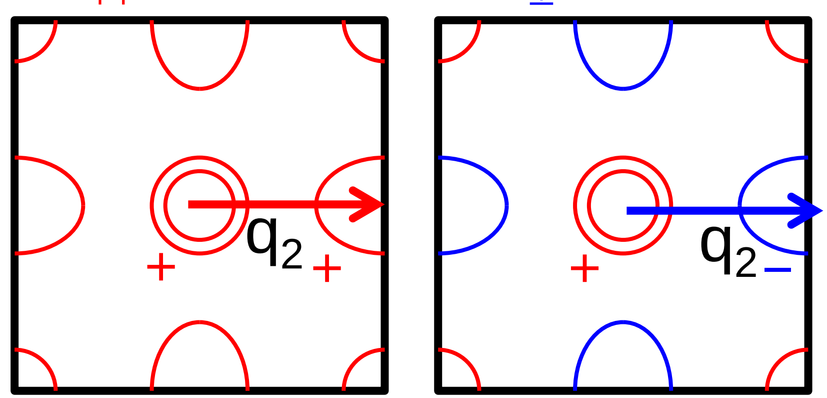

Zero at q_2 $\quad$ Peak at q_2

However, $\mathbf{q}_2$ spot can appear even in S++ case when $\Delta_e \neq \Delta_h$

S+- or S++?: Impurity effect

$Ba(Fe_{1-x}Co_x)_2As_2$

Nakajima *et al.*, Phys. Rev. B 82, 220504(R)

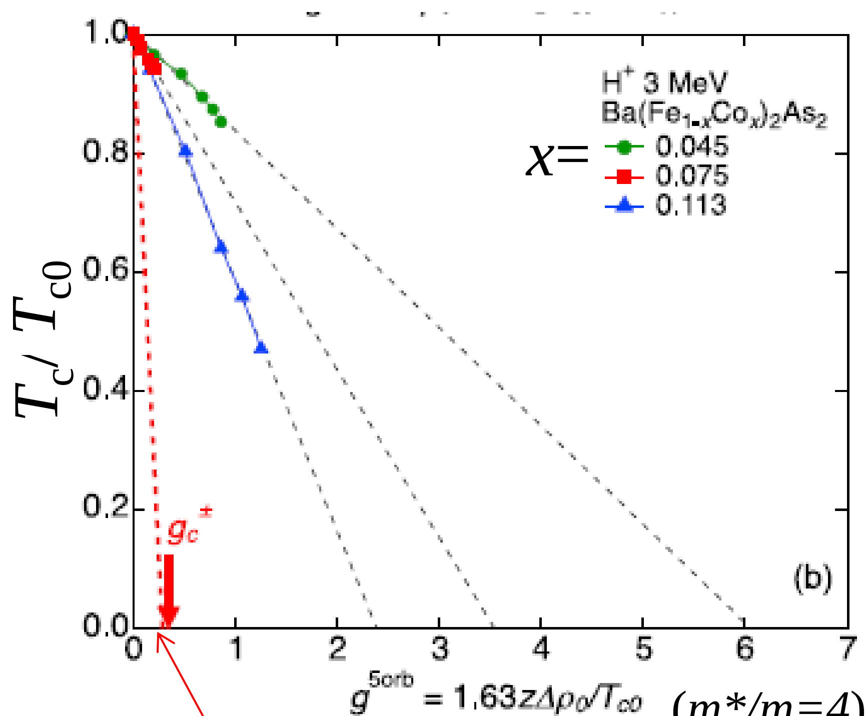

(*m*/m*=4)

normalized scattering ratio

$Ba_{1-x}K_xFe_2As_2$

Taen *et al.*, Phys. Rev. B 88, 224514

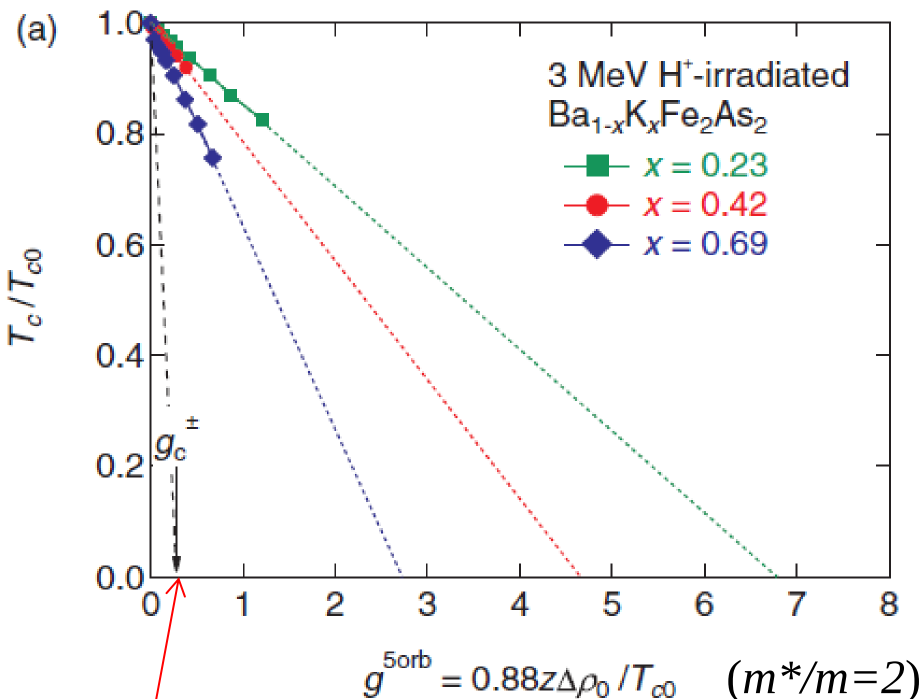

(*m*/m*=2)

normalized scattering ratio

theoretical prediction for S_{+-} wave (Onari and Kontani, PRL 2009)

The robustness of the SC state against impurity contradicts with the S+-wave state.

S_{+-}

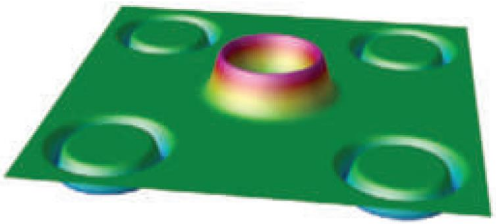

?

S_{++}

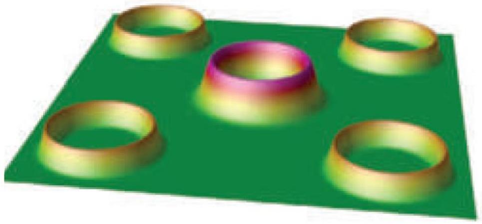

?

No conclusive experimental evidence so far

Are all iron-based high-T_c superconductors fully gapped?

If some are nodal

→ Presence of repulsive interaction

Accidental or symmetry protected?

If accidental

→ Presence of two (or more) competing pairing interactions

Superconducting gap structure of $BaFe_2As_2$ systems

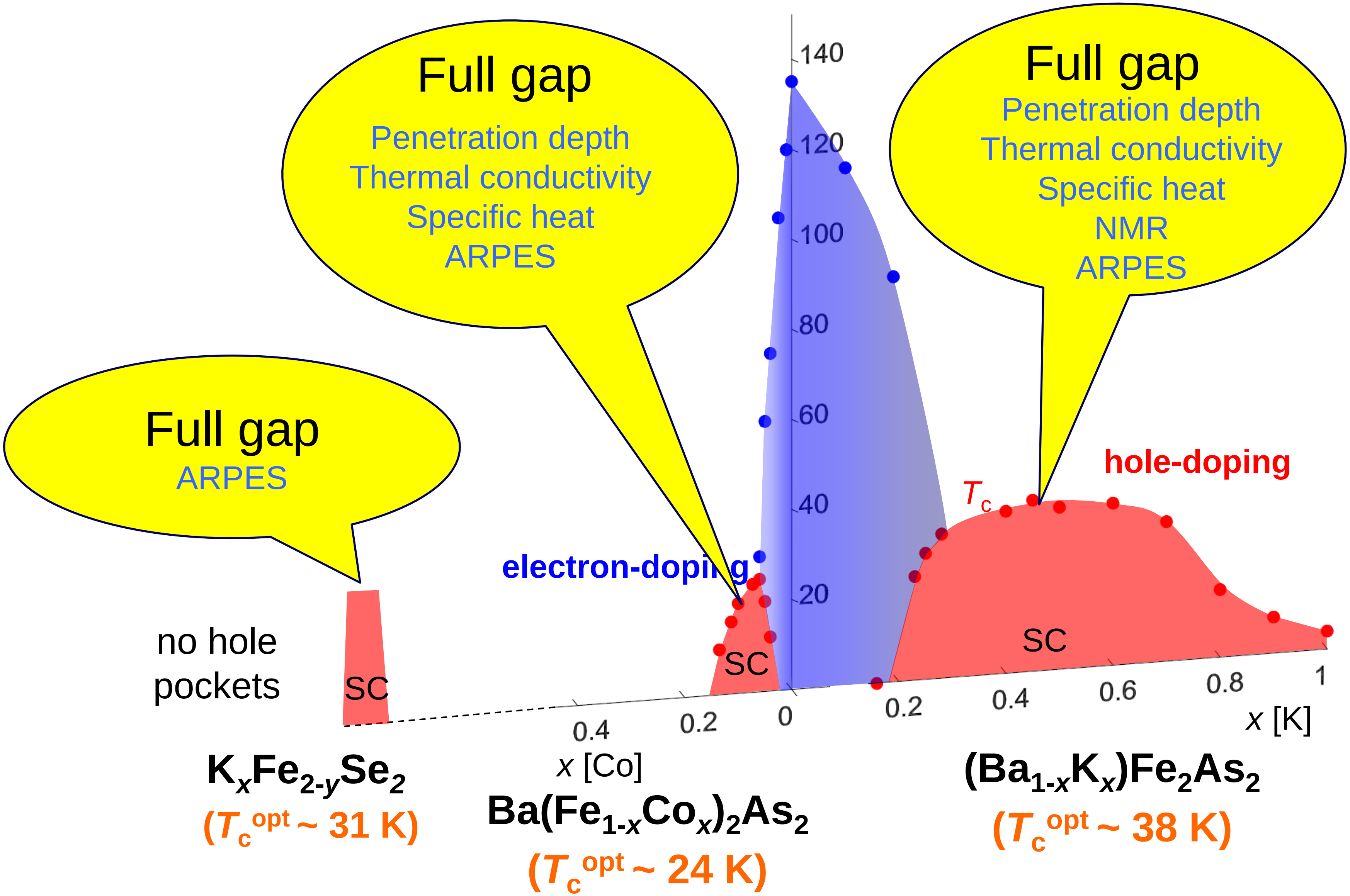

SC gap structure in isovalent doped systems

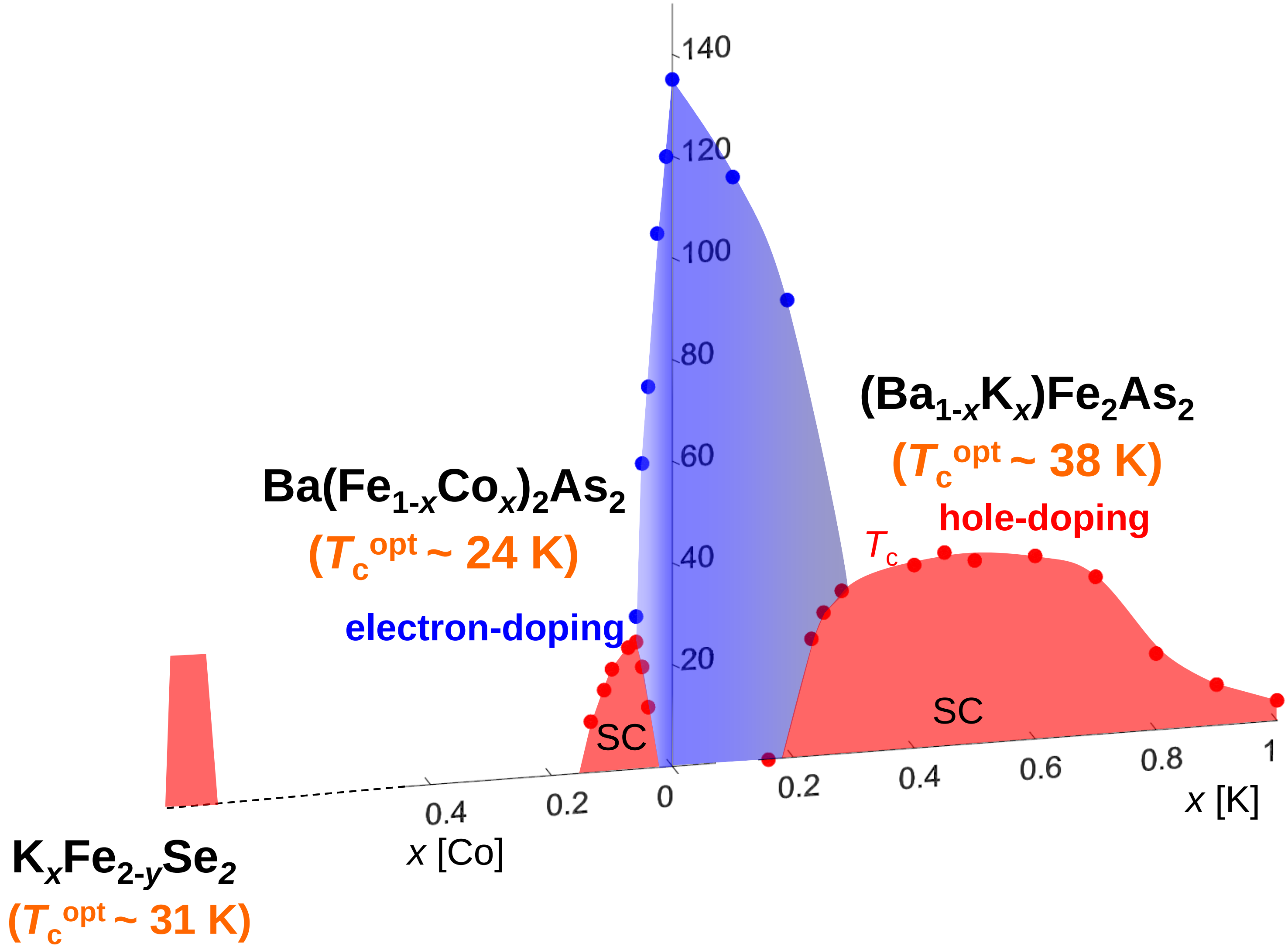

SC gap structure in isovalent doped systems

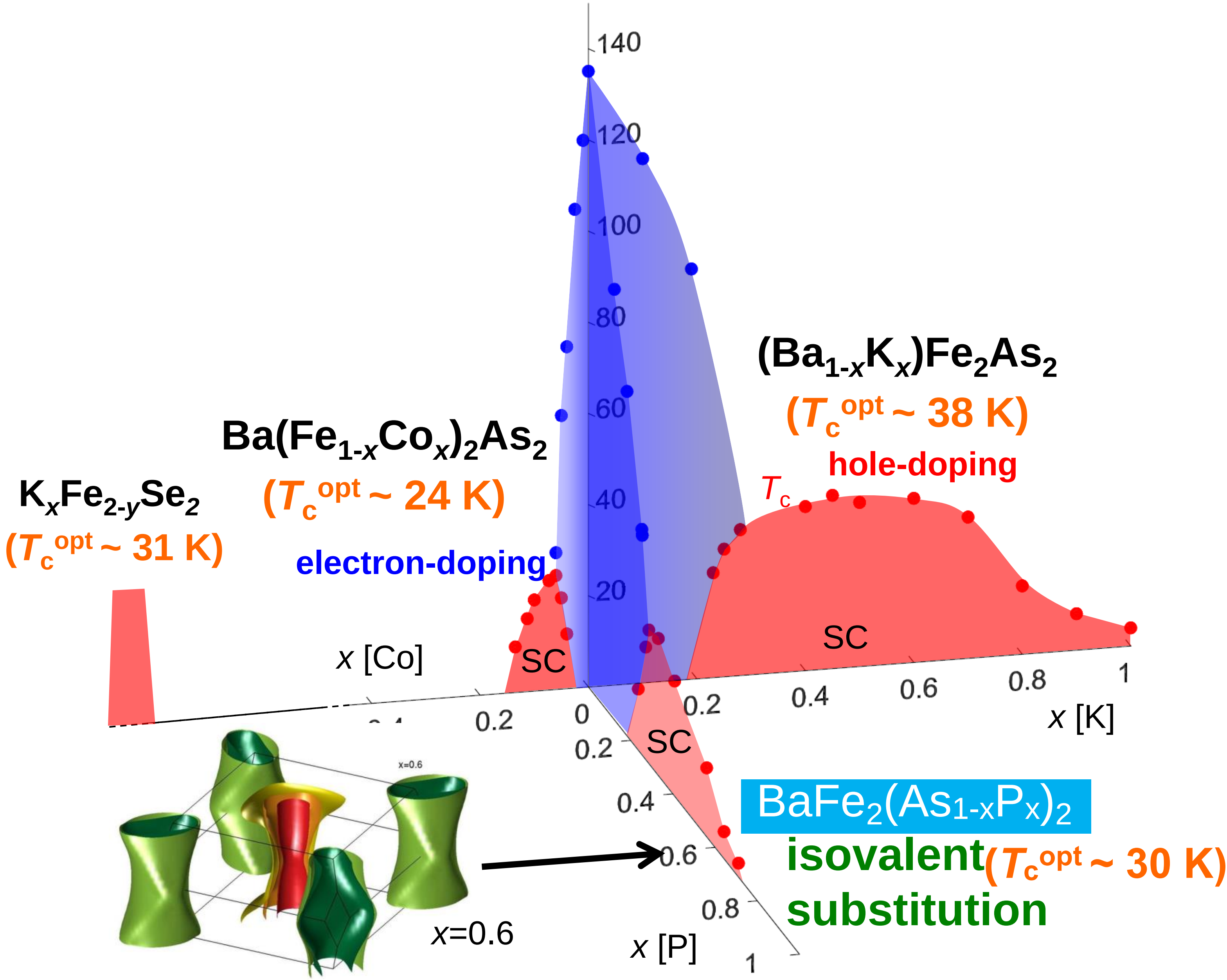

SC gap structure in isovalent doped systems

Penetration depth

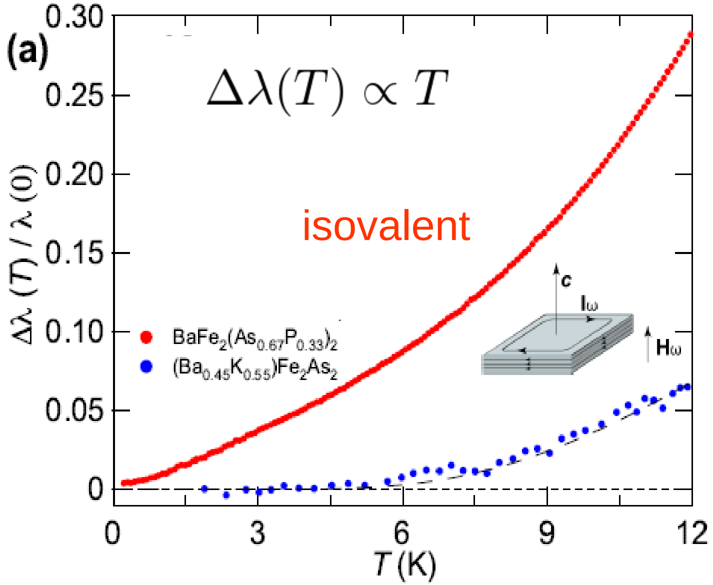

Specific heat $BaFe_2(As_{0.53}P_{0.47})_2$

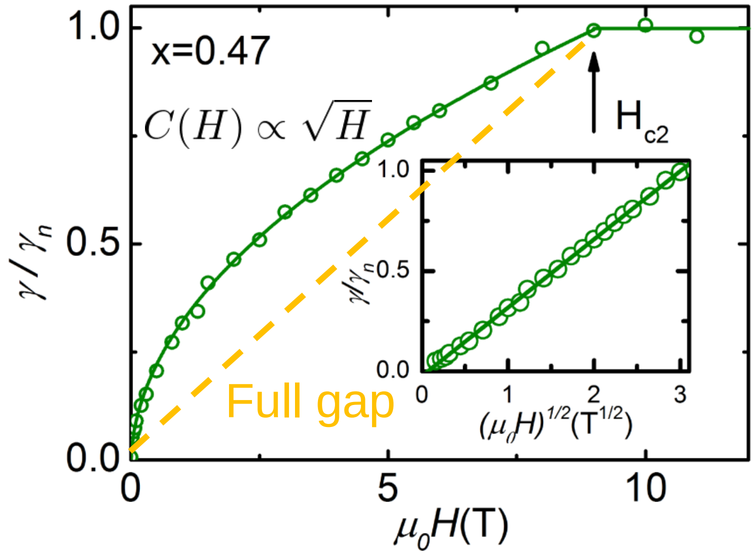

Thermal conductivity

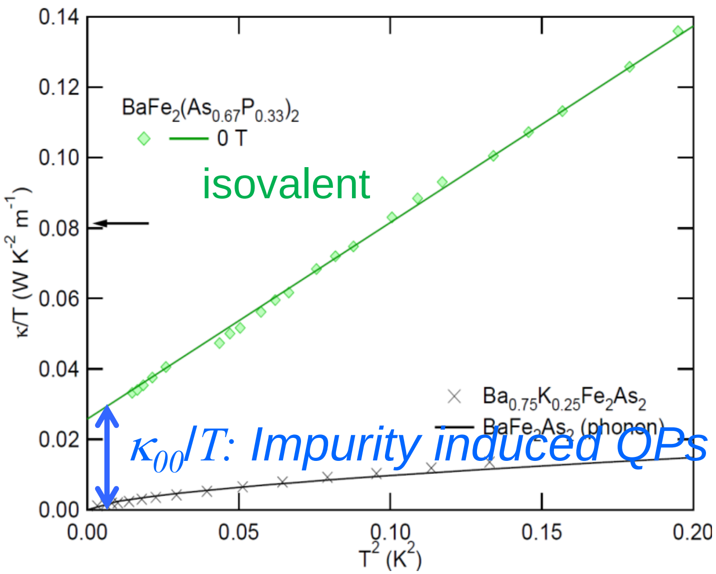

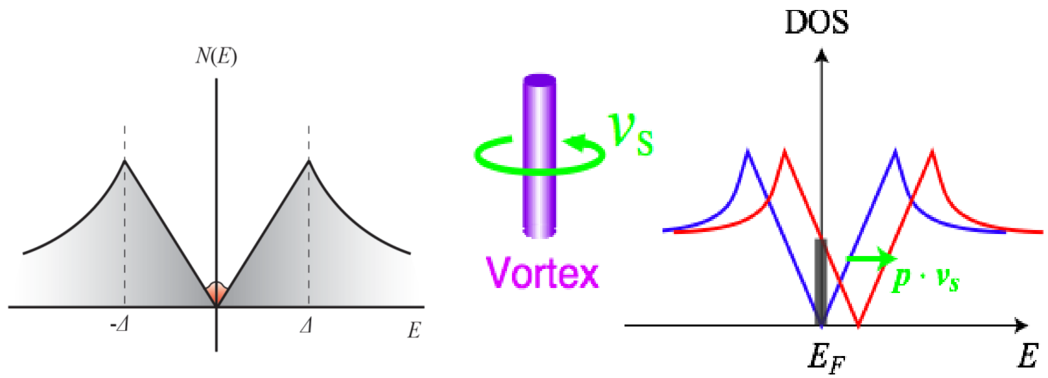

Luo *et al.*
Kurita *et al.*

Doppler shift

K. Hashimoto *et al*., PRB (2010)
K. Hashimoto *et al*., PRL (2009)
K. Hashimoto *et al*., Science (2012)
A. Carrington *et al*. (2014)

SC gap structure in isovalent doped systems

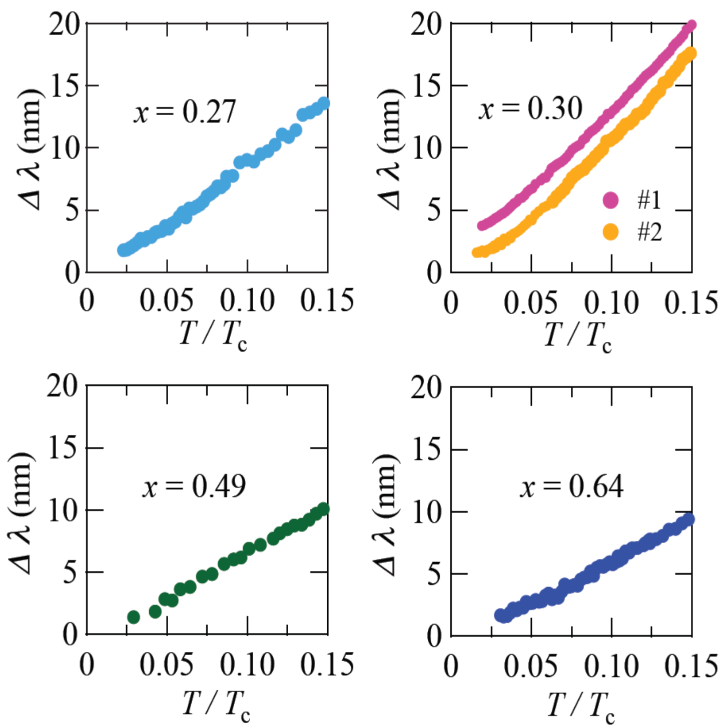

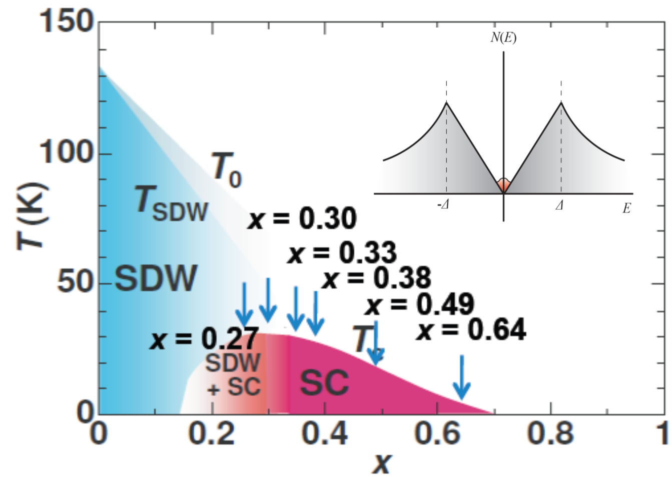

K. Hashimoto *et al*., Science (2012)

- The presence of line nodes is a robust feature for all *x*.

Presence of repulsive interaction

non-phononic (magnetic) pairing interaction

Non-universal gap structure in $BaFe_2As_2$ systems

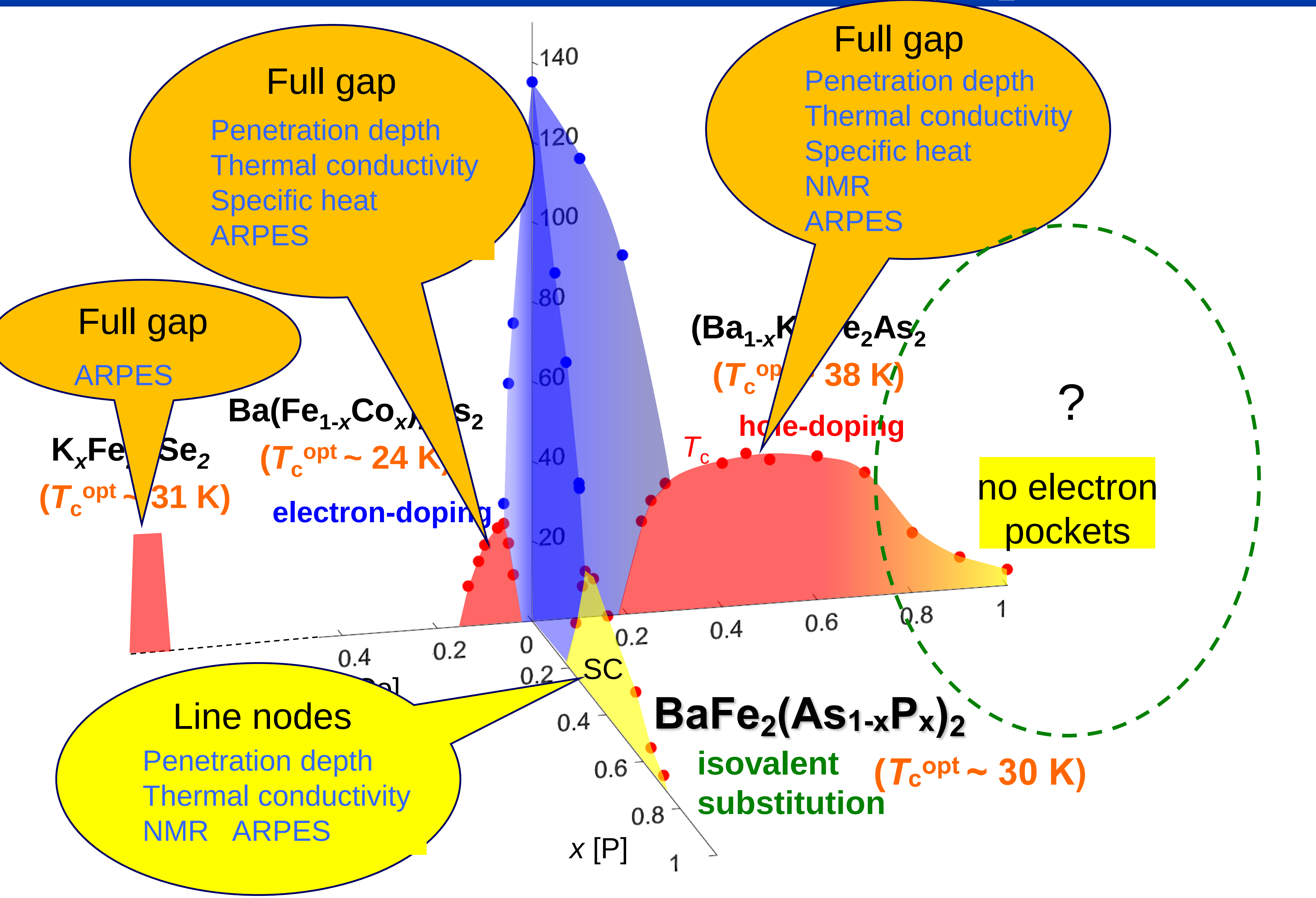

Gap structure of hole doped $Ba_{1-x}K_xFe_2As_2$

D. Watanabe *et al.* PRB (2014)

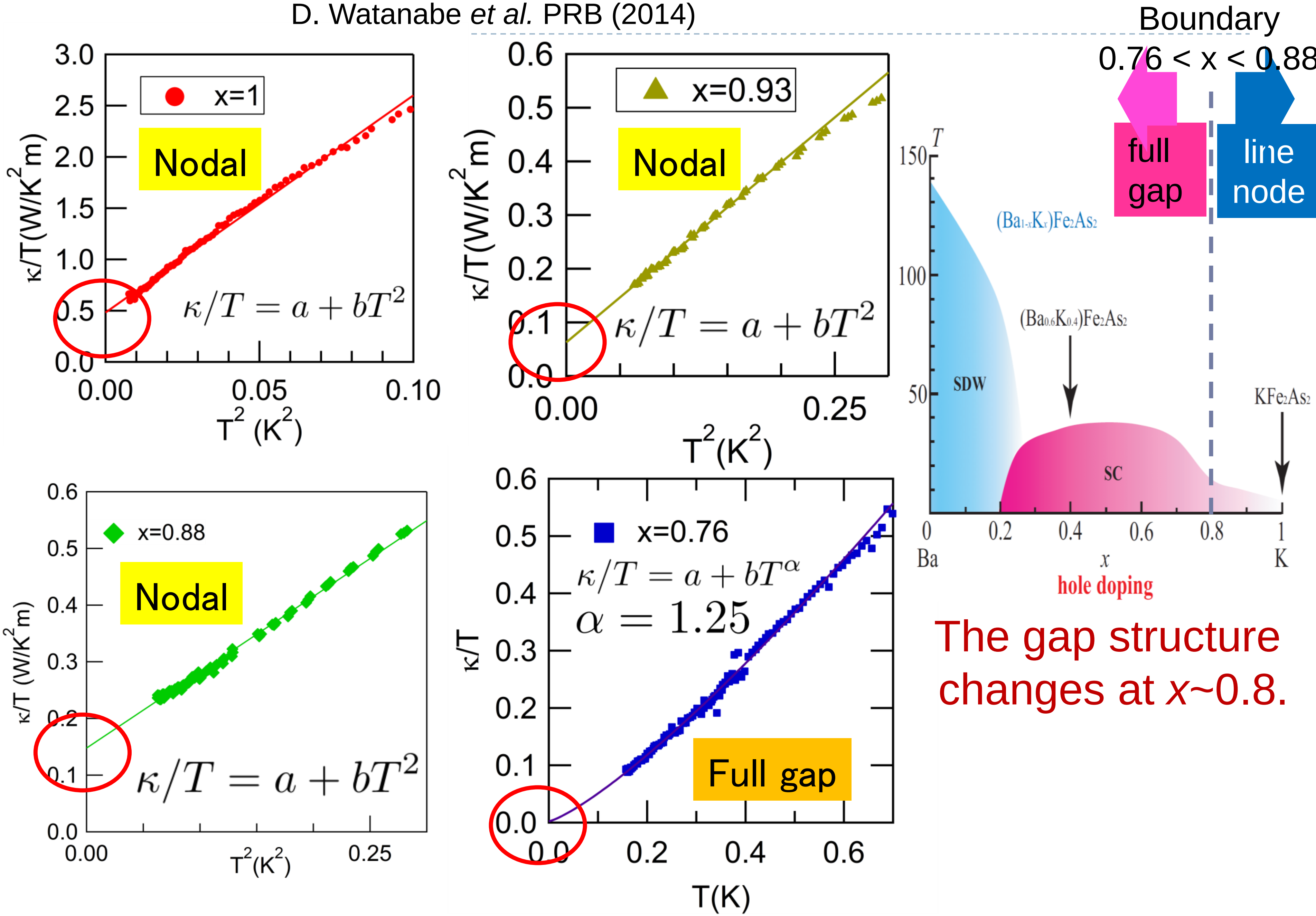

The gap structure changes at *x*~0.8.

Non-universal gap structure in $BaFe_2As_2$ systems

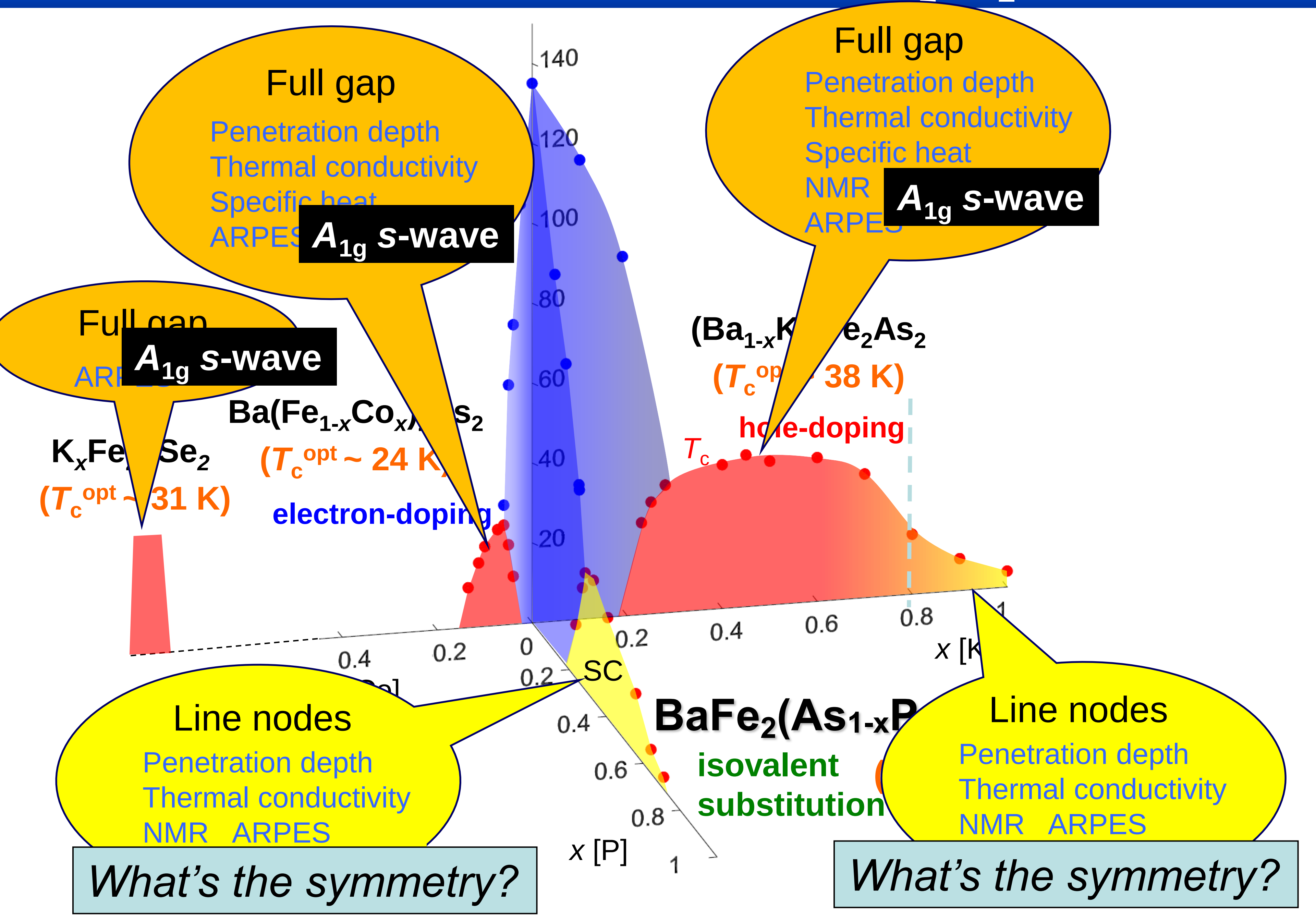

Non-universal gap structure in $BaFe_2As_2$ systems

_s_-wave (A_{1g})
Nodes: Accidental

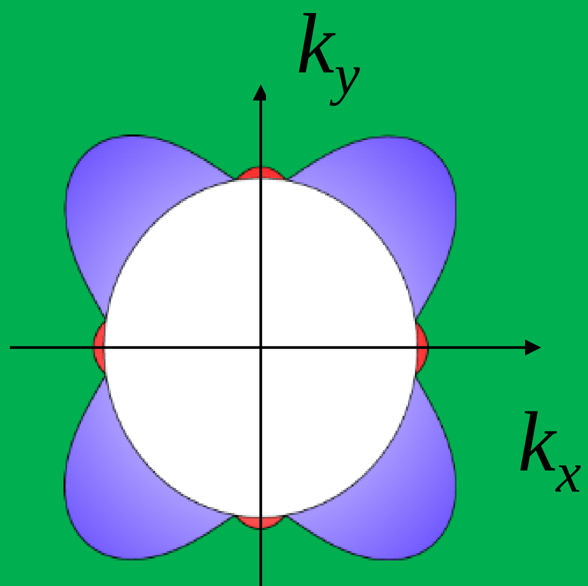

or

_d_–wave (B_{1g} or B_{2g})
Nodes: Symmetry-protected

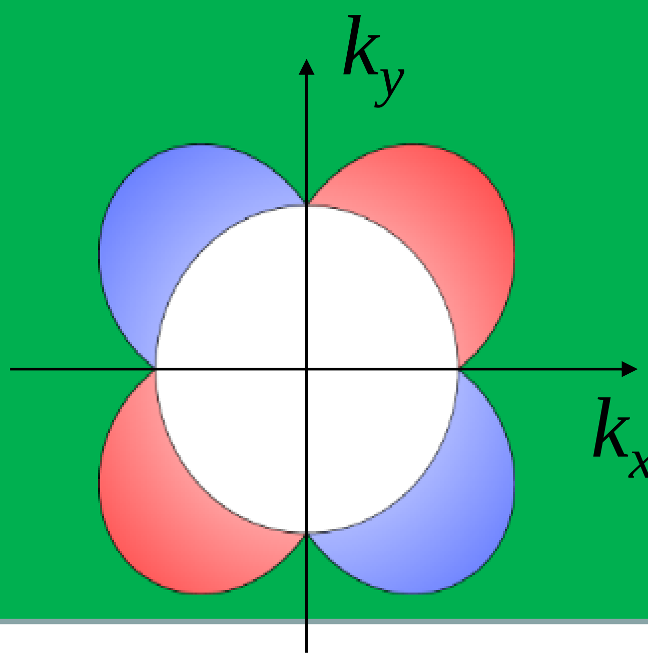

What's the symmetry?

What's the symmetry?

Are the nodes accidental or symmetry protected?

Impurity scattering dependence of gap structure can be a powerful probe of symmetry

Γ : impurity scattering rate

d-wave symmetry-protected nodes

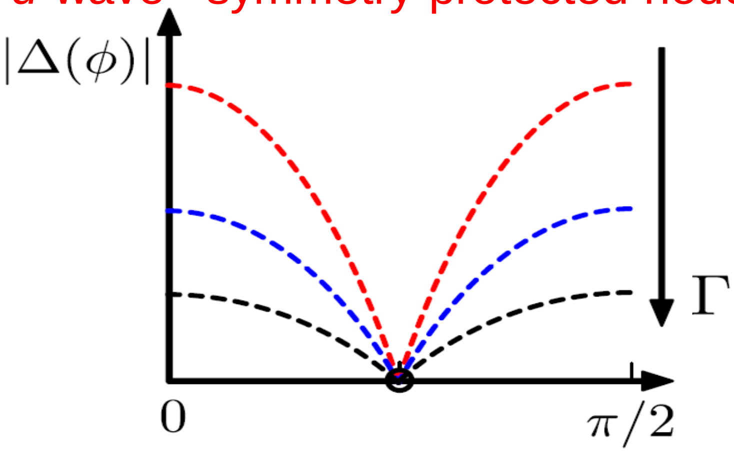

J-Ph Reid *et al*., Supercond. Sci. Technol. **25**,084013 (2012).

Nodes are robust against disorder

s-wave accidental nodes

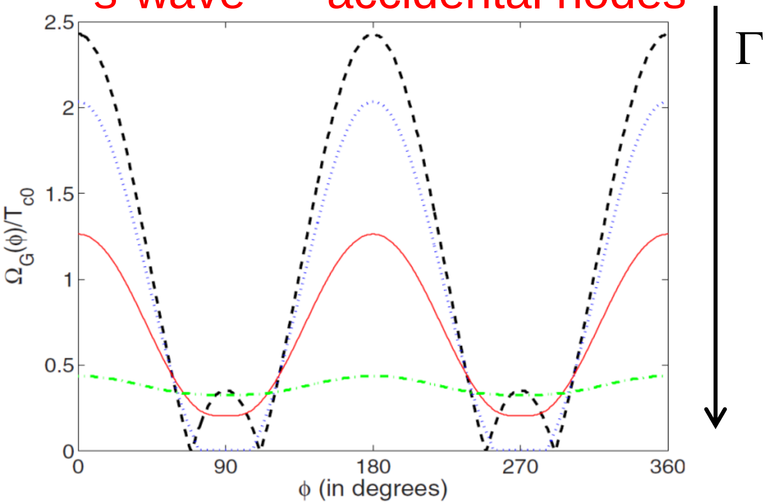

V. Mishra *et al*., PRB **79**, 094521 (2009).

Nodes can be lifted by disorder

Are the nodes accidental or symmetry protected?

Impurity scattering dependence of gap structure can be a powerful probe of symmetry

Γ : impurity scattering rate

d-wave   symmetry-protected nodes

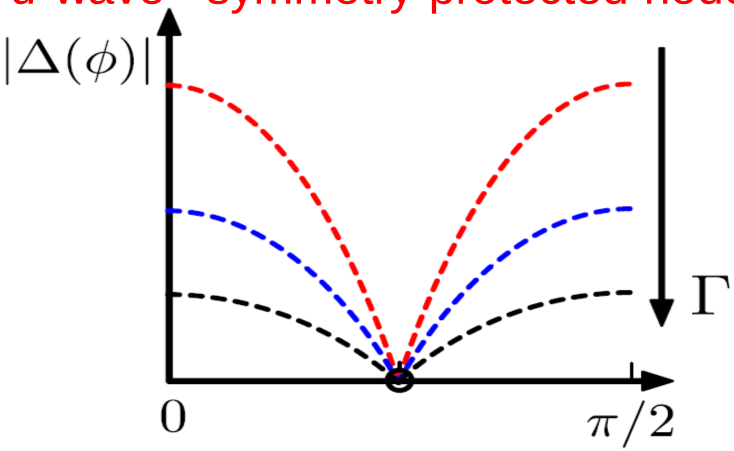

J-Ph Reid *et al*., Supercond. Sci. Technol. **25**,084013 (2012).

Nodes are robust against disorder

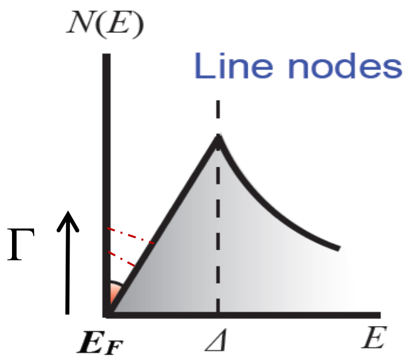

Zn doped $YBa_2Cu_3O_{6.95}$

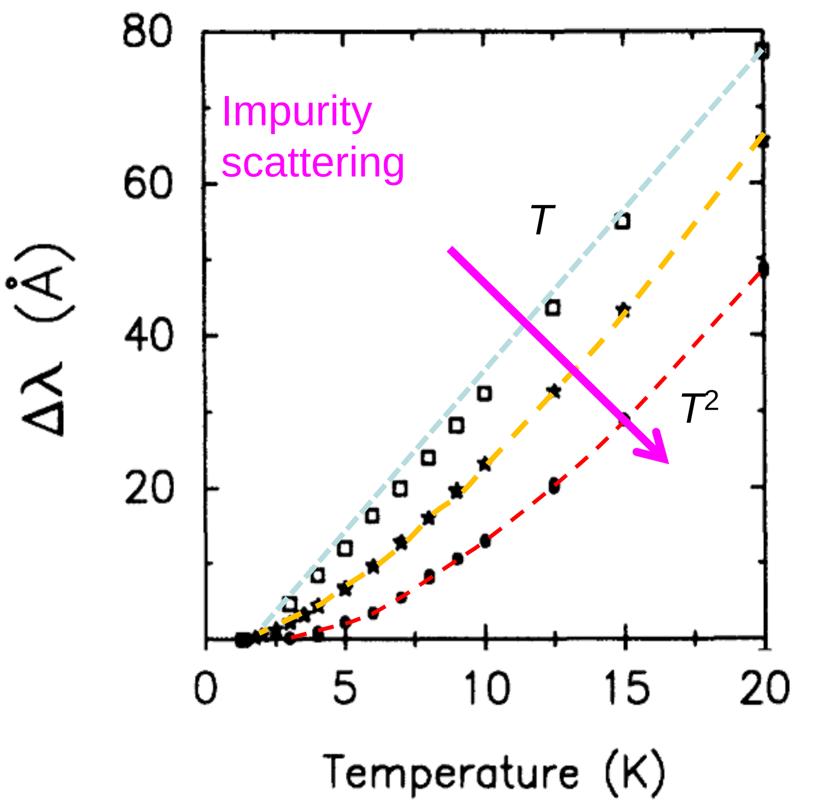

D. A. Bonn *et al*., PRB **50**,4051 (1993).
P. J. Hirschfeld and N. Goldenfeld, PRB **48**, 4219 (1993).

Are the nodes accidental or symmetry protected?

Impurity scattering dependence of gap structure can be a powerful probe of symmetry

Γ : impurity scattering rate

"*Nonmagnetic*" disorder

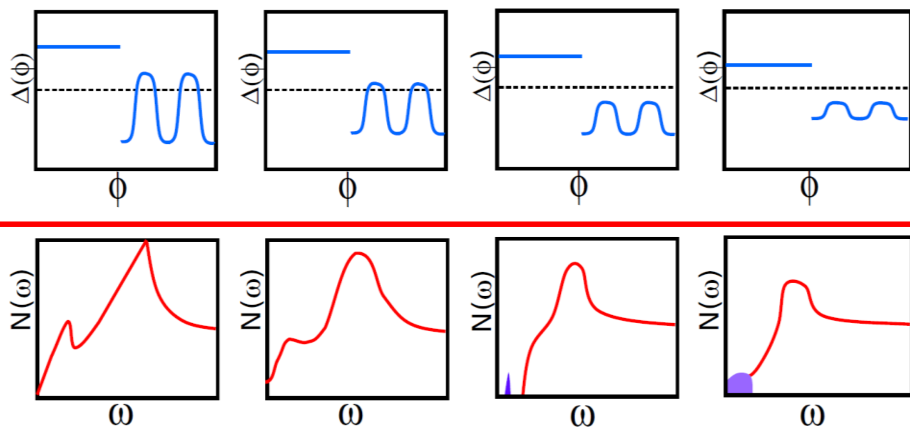

$\Delta\lambda(T)$ T T^2 $\exp(-\Delta/k_B T)$ T^2

S±

Y. Wang *et al.*, PRB **87**, 094504 (2013).

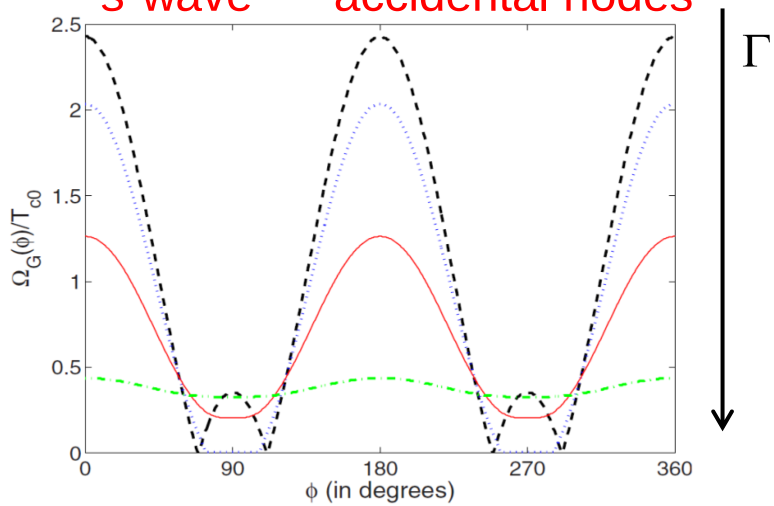

V. Mishra *et al.*, PRB **79**, 094521 (2009).

Nodes can be lifted by disorder

Are the nodes accidental or symmetry protected?

Impurity scattering dependence of gap structure can be a powerful probe of symmetry

Γ : impurity scattering rate

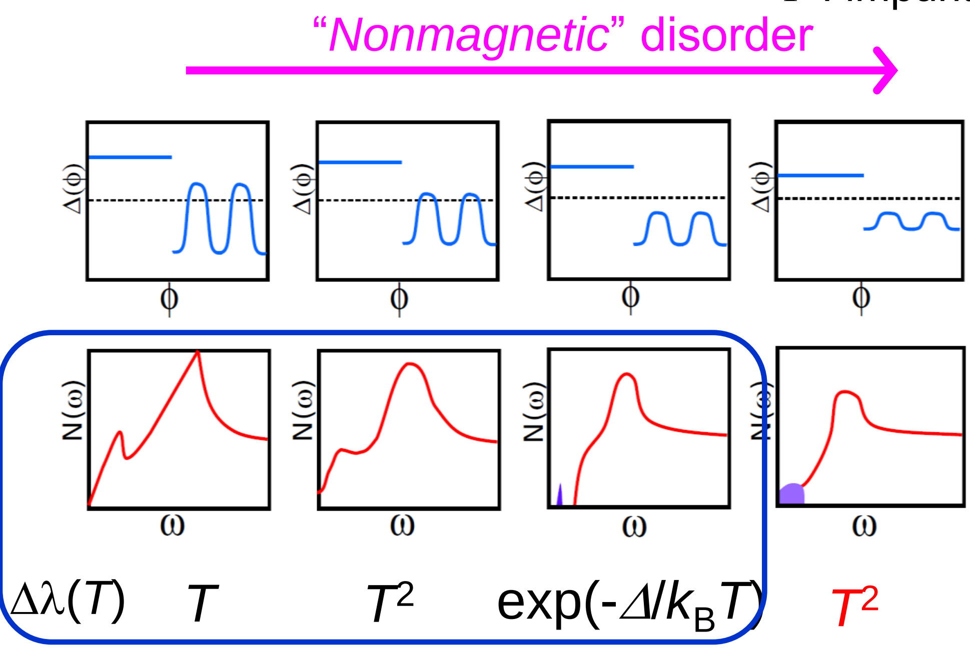

S++

Y. Wang *et al*., PRB **87**, 094504 (2013).

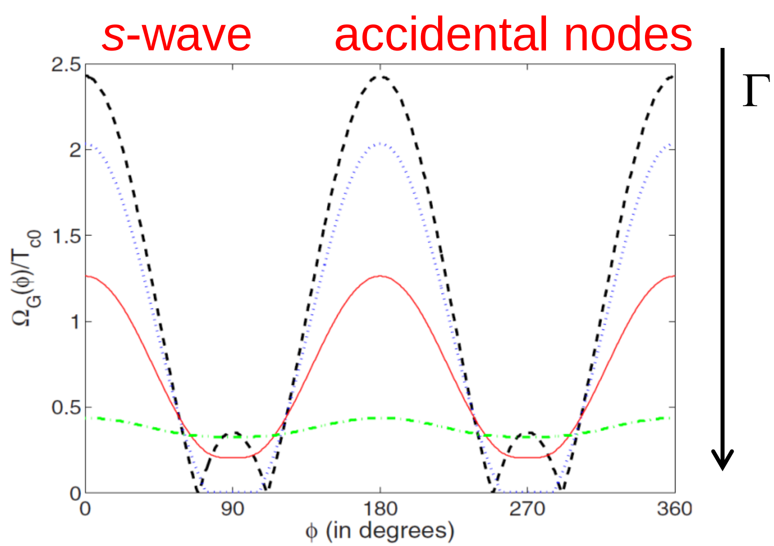

V. Mishra *et al*., PRB **79**, 094521 (2009).

Nodes can be lifted by disorder

Introducing controlled point defects by electron irradiation

Single crystals

$BaFe_2(As_{1-x}P_x)_2$

x = 0.33, 0.36

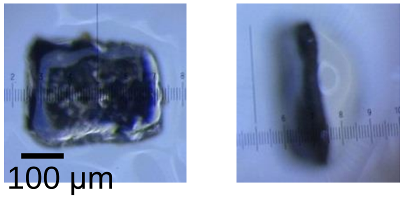

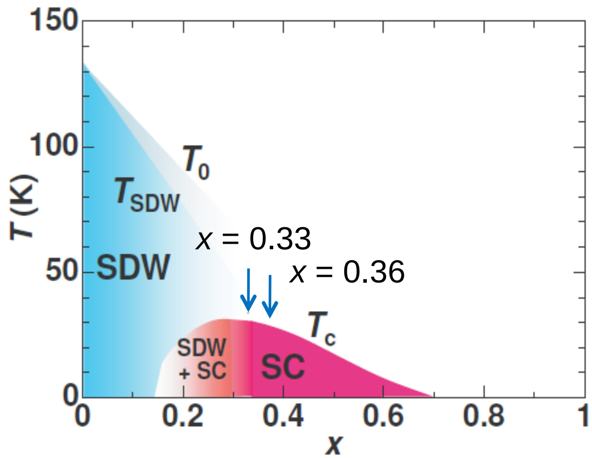

Electron irradiation

T = 20 K 2.5 MeV

✓No change of lattice constants

✓No significant change of carrier density

✓Controlled disorder on the same sample

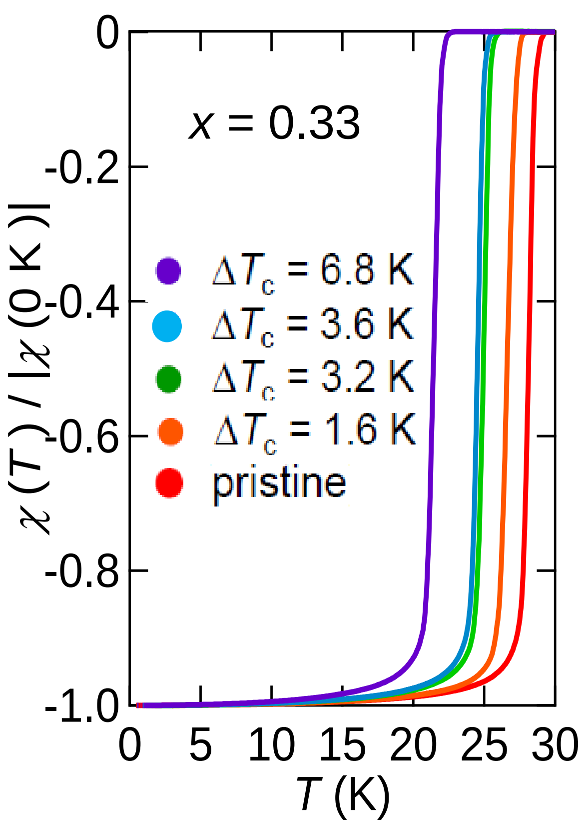

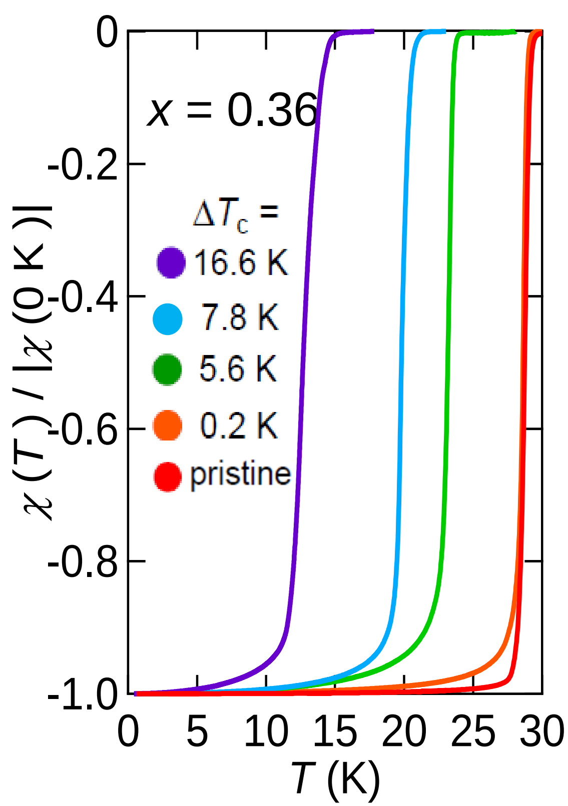

Point defects

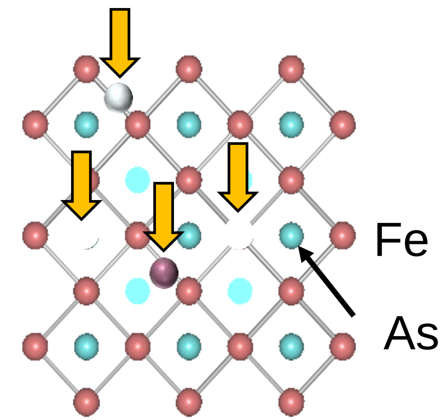

1C/cm^2 0.23 at%

Fe: 0.06% Ba: 0.10%

As: 0.07%

Sharp SC transitions

Homogeneous point defects

Observation of node lifting by electron irradiation

Y. Mizukami *et al.*

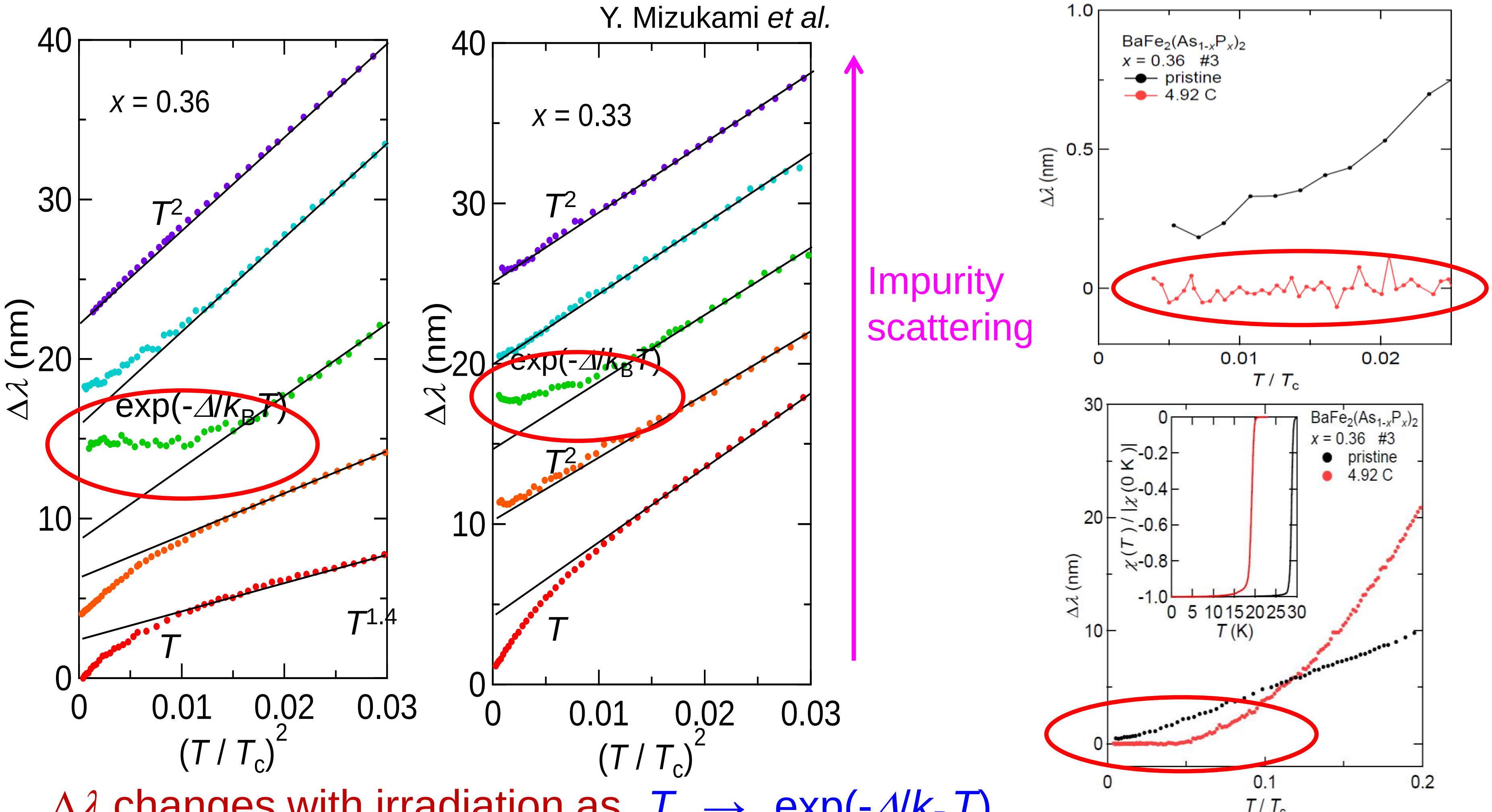

$\Delta\lambda$ changes with irradiation as $T \rightarrow \exp(-\Delta/k_B T)$

Disorder-induced transformation from (line) nodal to nodeless state: Node is not symmmetry protected

Bulk evidence for *s*-wave (A_{1g}) symmetry

Observation of node lifting by disorder

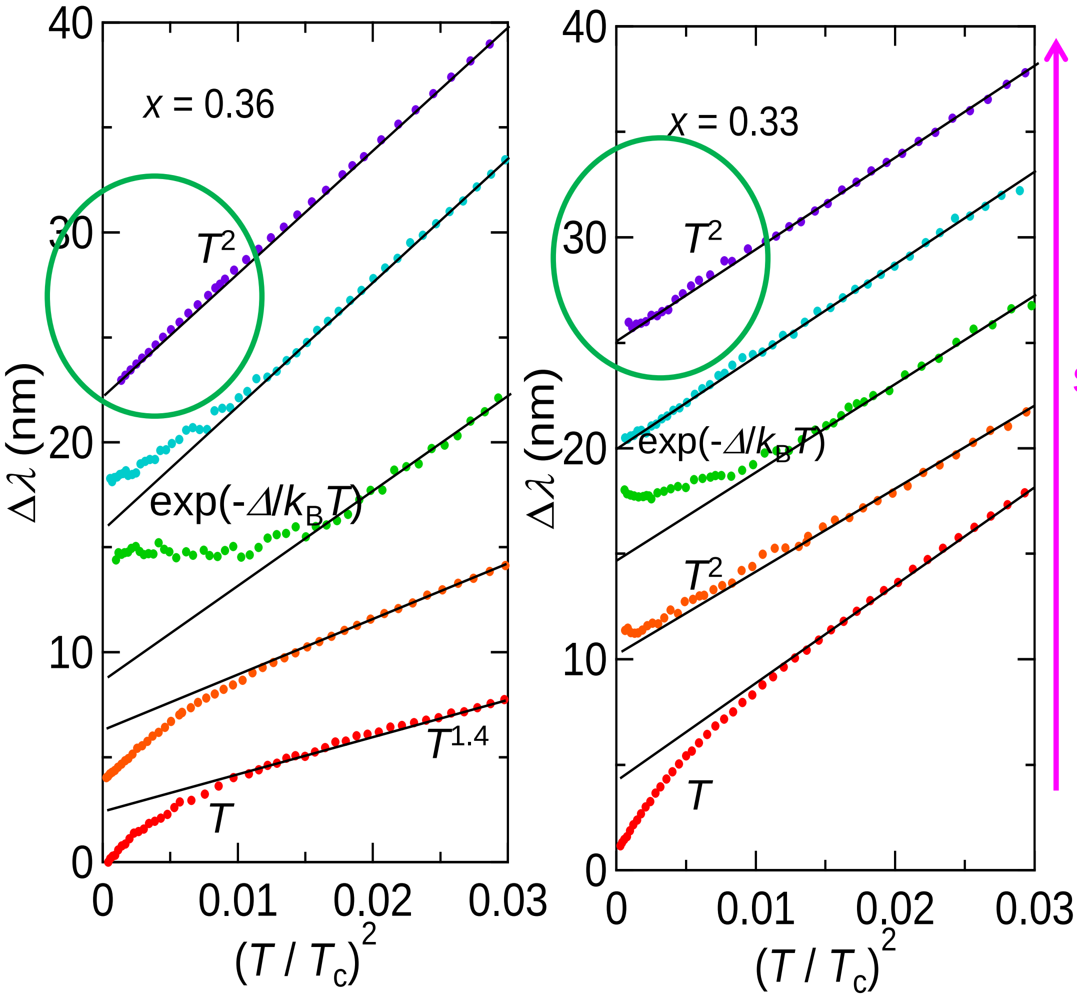

Impurity scattering

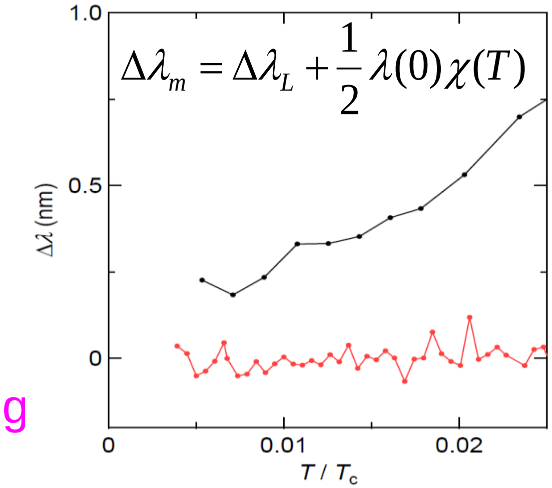

no evidence of Curie upturn down to ~80 mK

magnetic moment of point disorder is smaller than ~ 0.2-0.4μ_B

"*Nonmagnetic*" disorder

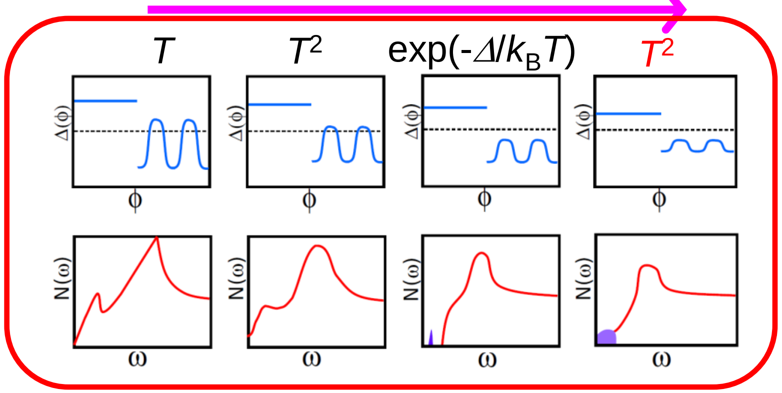

$\Delta\lambda$ changes with irradiation as

$T \;\rightarrow\; T^2 \;\rightarrow\; \exp(-\Delta/k_BT) \;\rightarrow\; T^2$

Y. Mizukami *et al.*

Y. Wang *et al.*, PRB **87**, 094504 (2013). **S±**

Non-universal gap structure in $BaFe_2As_2$ systems

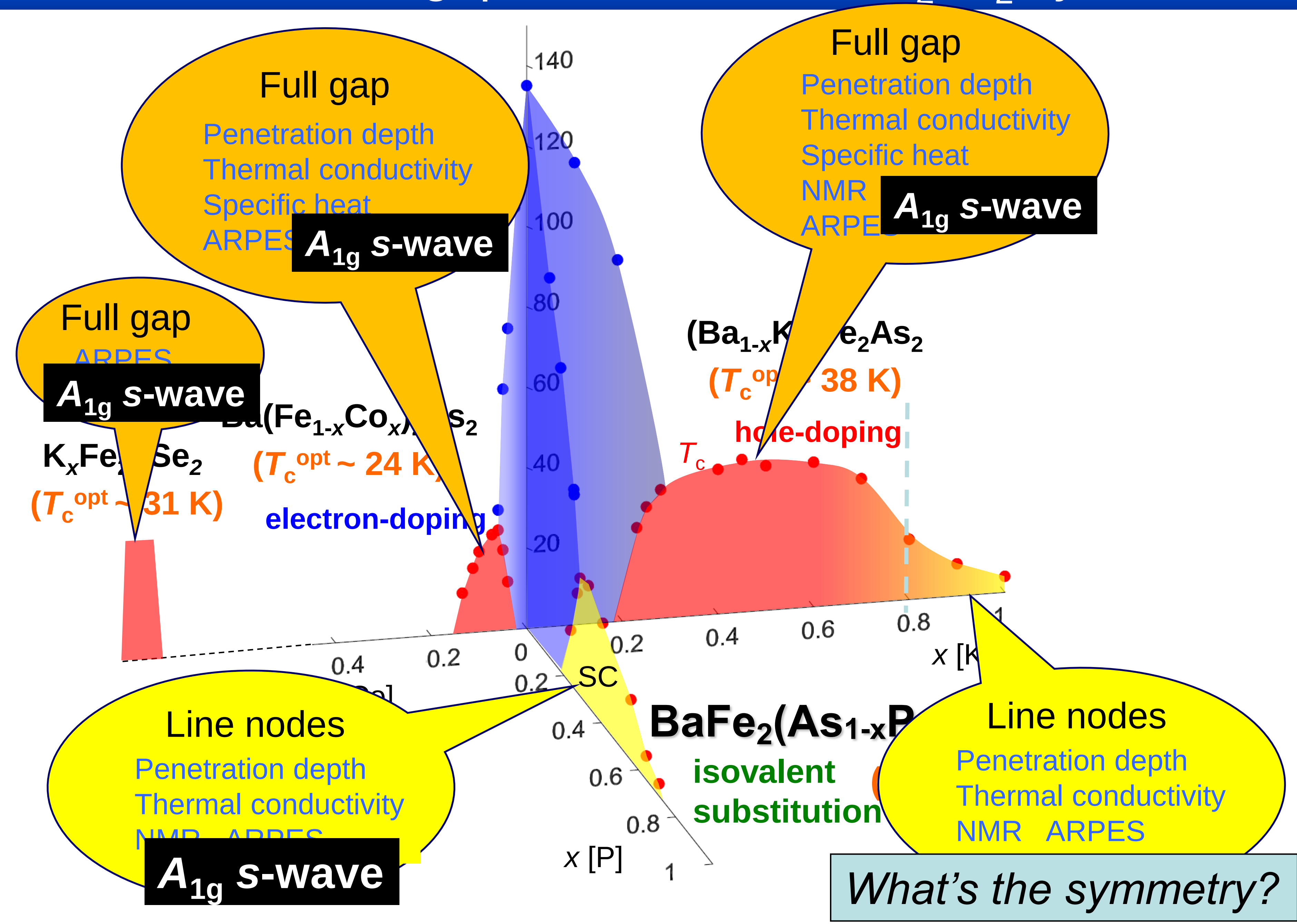

Gap symmetry in KFe_2As_2

Nodal *s*-wave

Laser ARPES

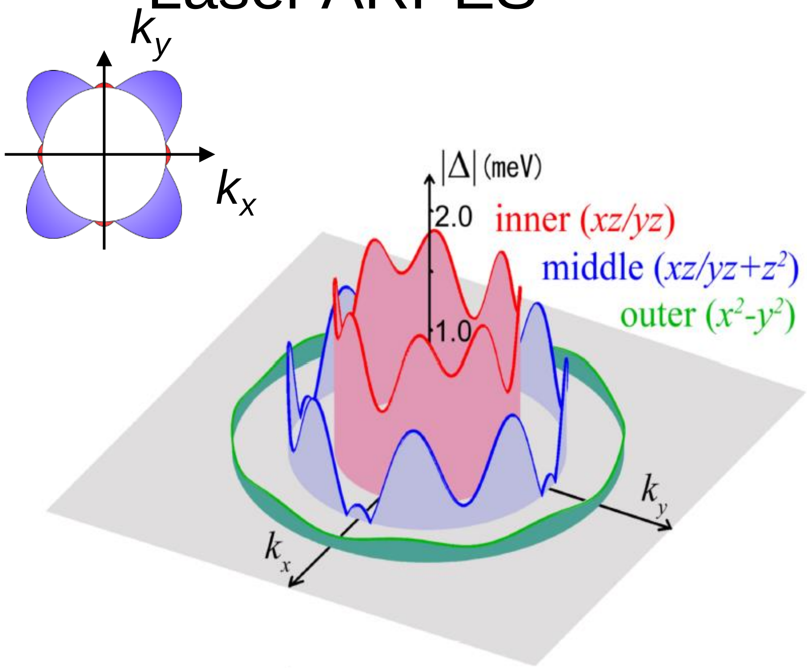

Octet-Line Node

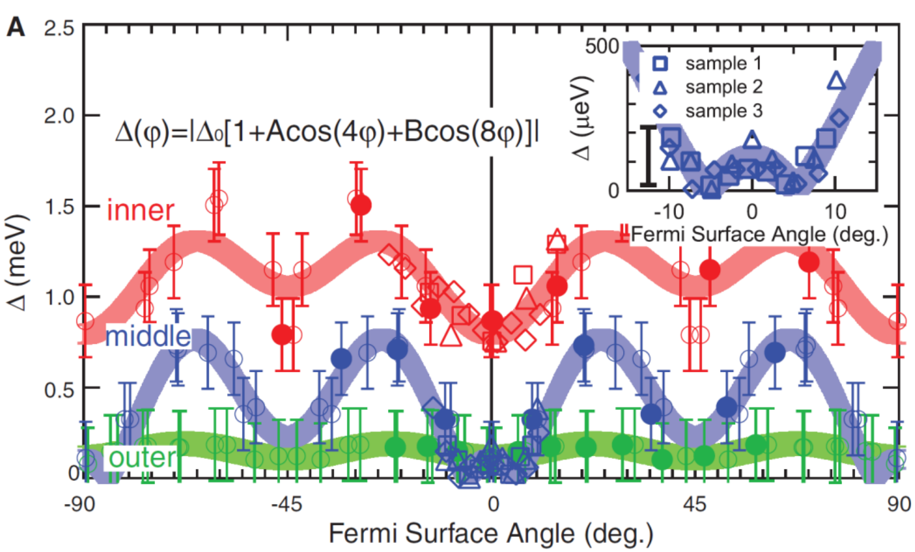

K. Okazaki *et al.*, Science (2012).

Gap symmetry in KFe_2As_2

Nodal *s*-wave

Laser ARPES

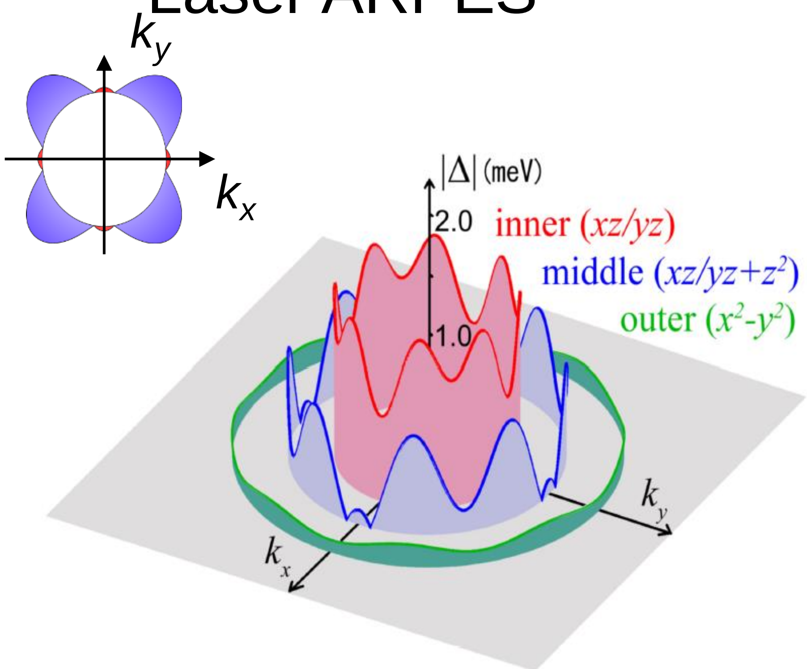

K. Okazaki *et al.*, Science (2012).

Specific heat

F. Hardy *et al*. JPSJ (2013)

d–wave

Thermal conductivity

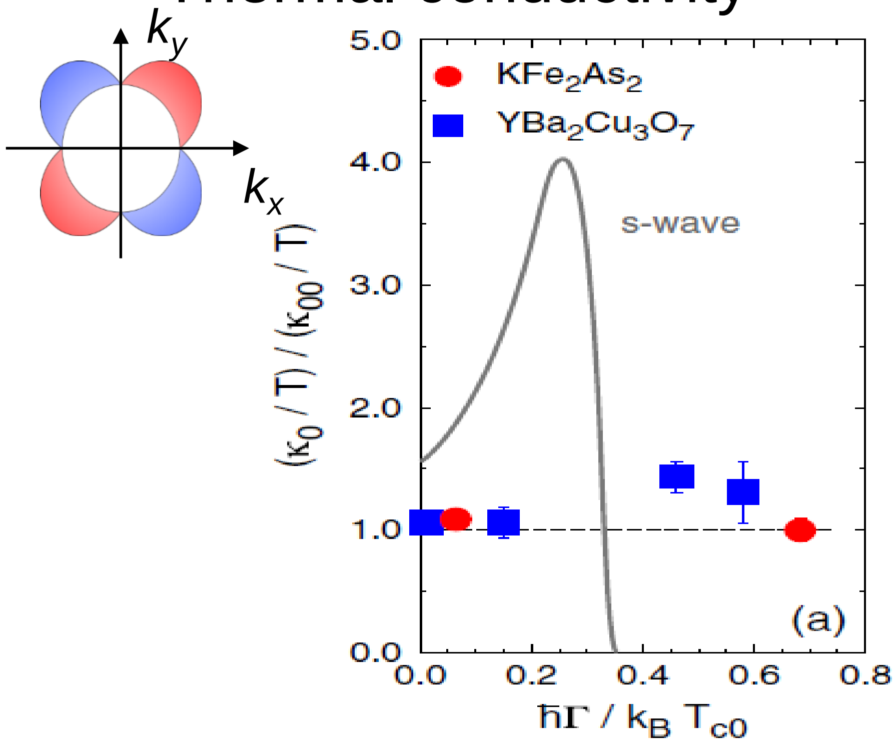

J.P.Reid *et al*. PRL (2012)

Doping evolution of SC gap structure in $(Ba_{1-x}K_x)Fe_2As_2$

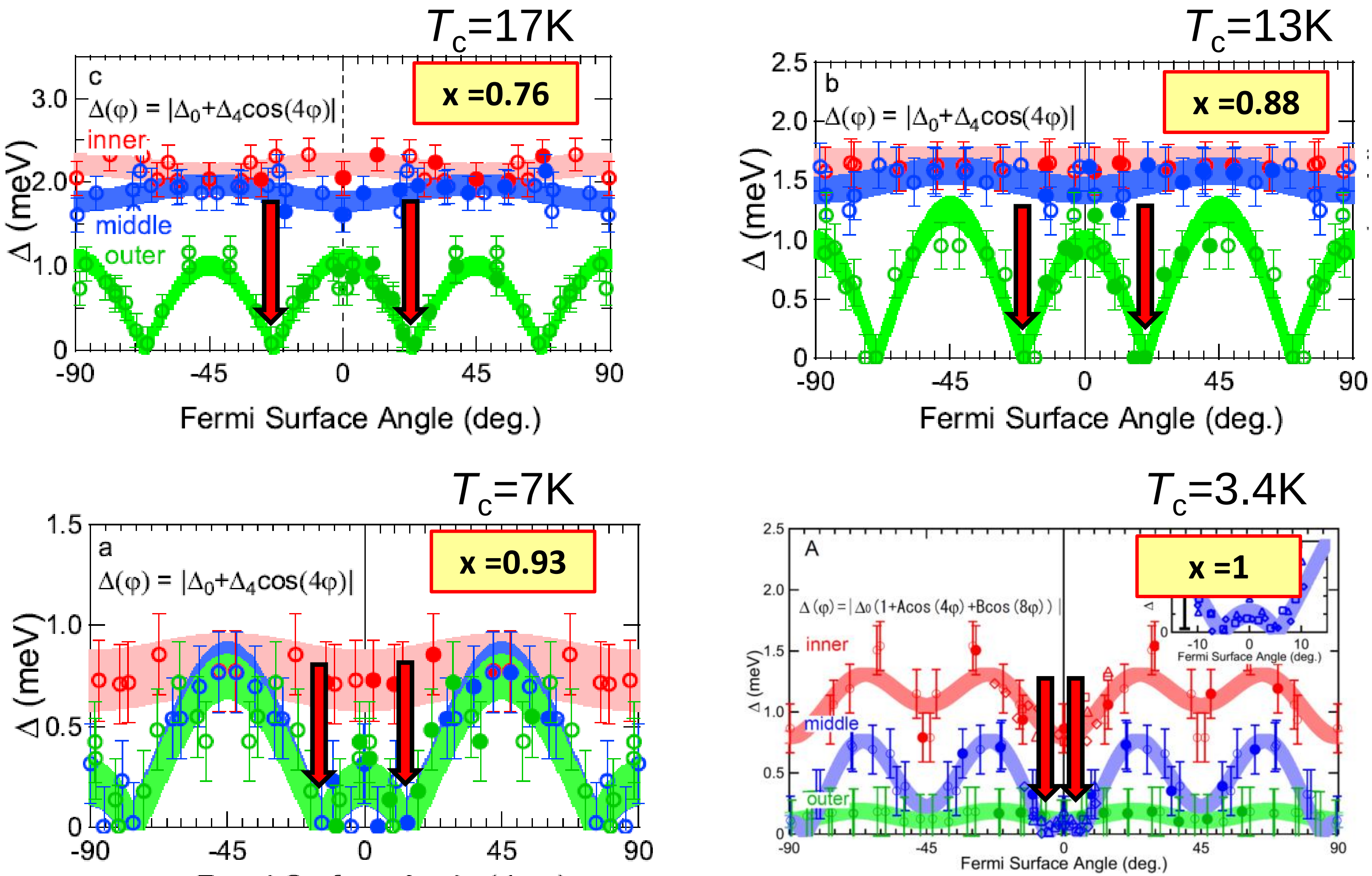

No discontinuous change of the gap function with doping.

K. Okazaki *et al.*, Science 337, 1314 (2012)
Y. Ota *et al.*, (submitted) arXiv:1307.7922

Non-universal gap structure in $BaFe_2As_2$ systems

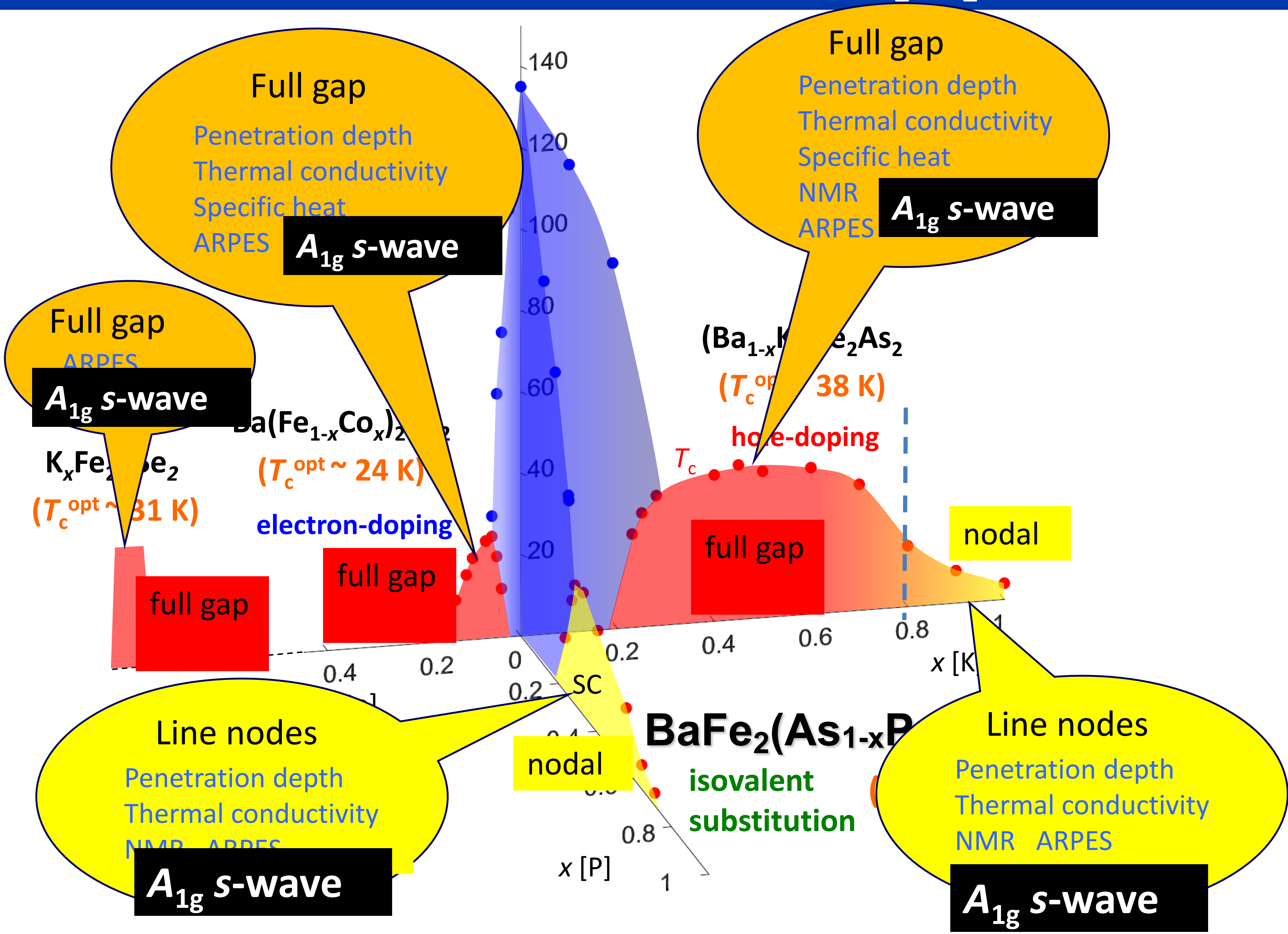

Superconducting gap structure of $BaFe_2As_2$ systems

The nodes are not symmetry protected but accidental.

SC gap structure is *not universal*
but
SC gap symmetry is *universal*,
i.e. A_{1g}-symmetry.

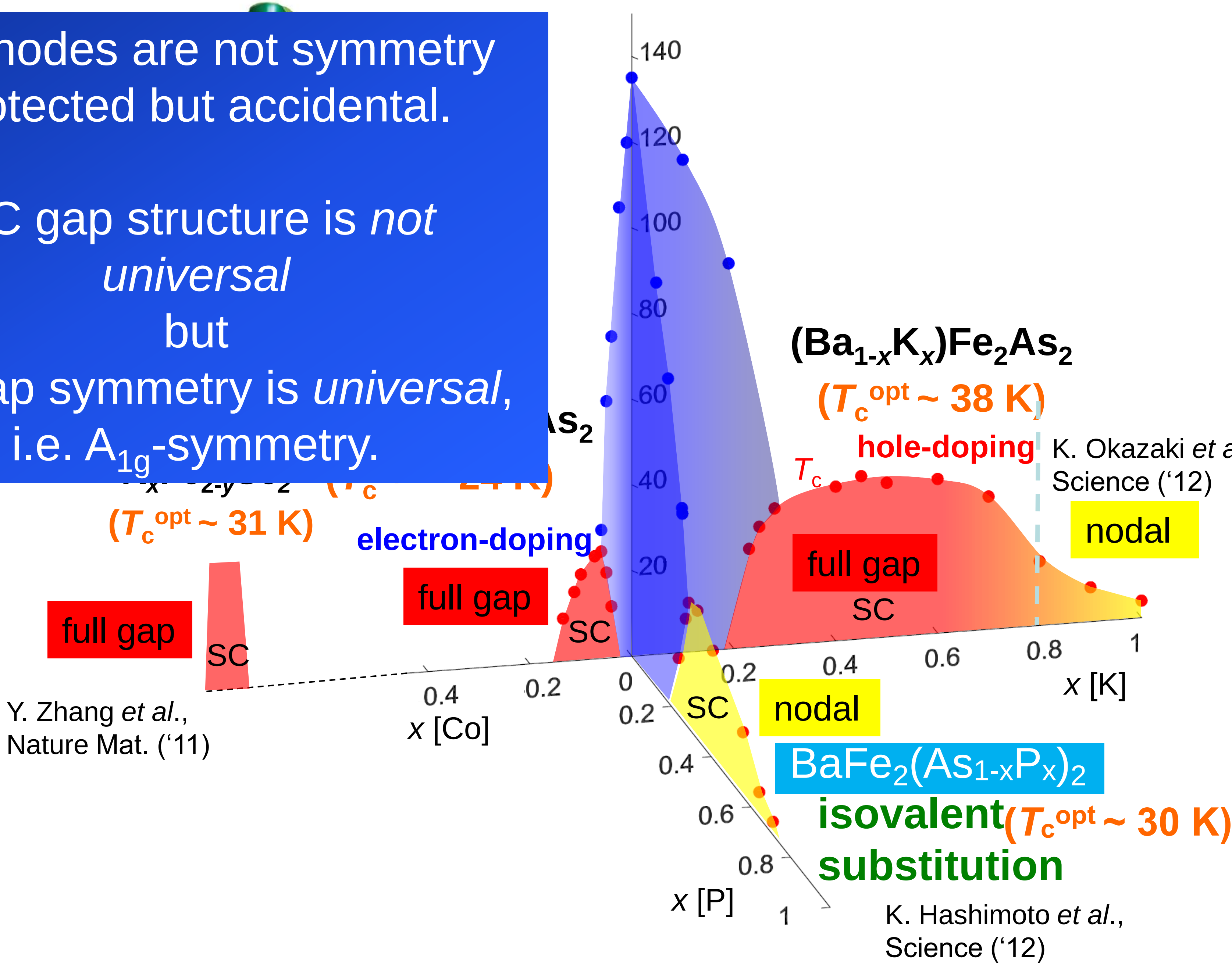

Nodal structure of $BaFe_2(As_{1-x}P_x)_2$

Specific heat

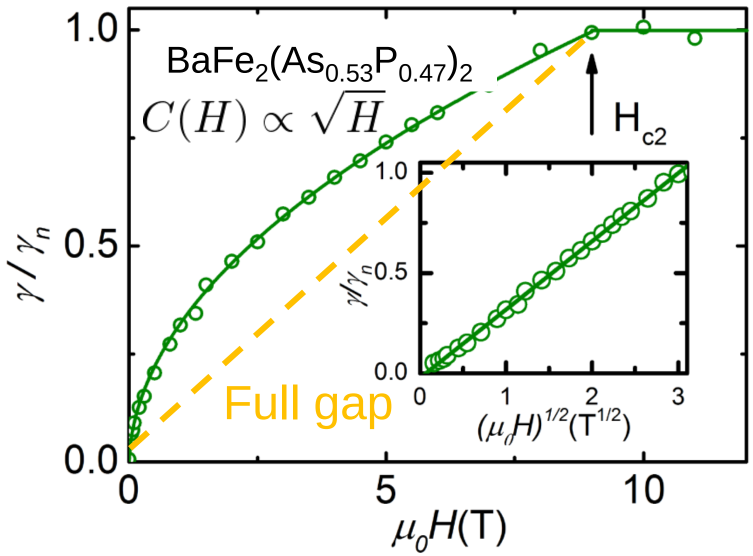

$C(H) \propto \sqrt{H}$ up to H_{c2}

Line nodes in all FSs

Laser ARPES

$BaFe_2(As_{0.35}P_{0.65})_2$
(T_c=30 K)

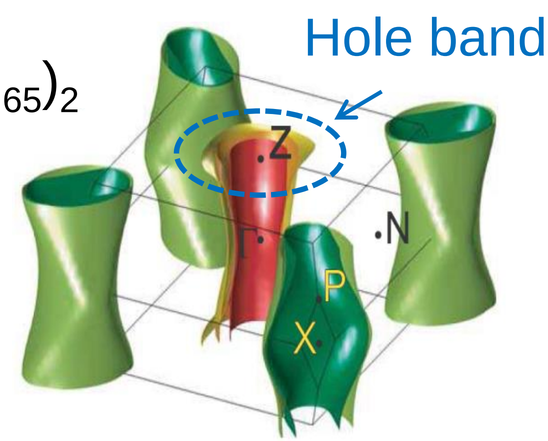

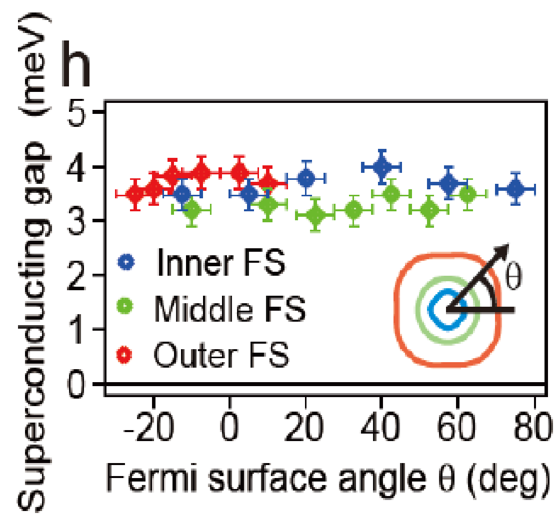

Hole

Horizontal

Full gap in all three hole bands around *Z*-point

Where is the line node ?
Pinpointing line node by angle-resolved thermal conductivity

Doppler shift $E'(\mathrm{k},\mathrm{r}) = E(\mathrm{k}) + \mathrm{v}_S(\mathrm{r}) \cdot \mathrm{v}_F$

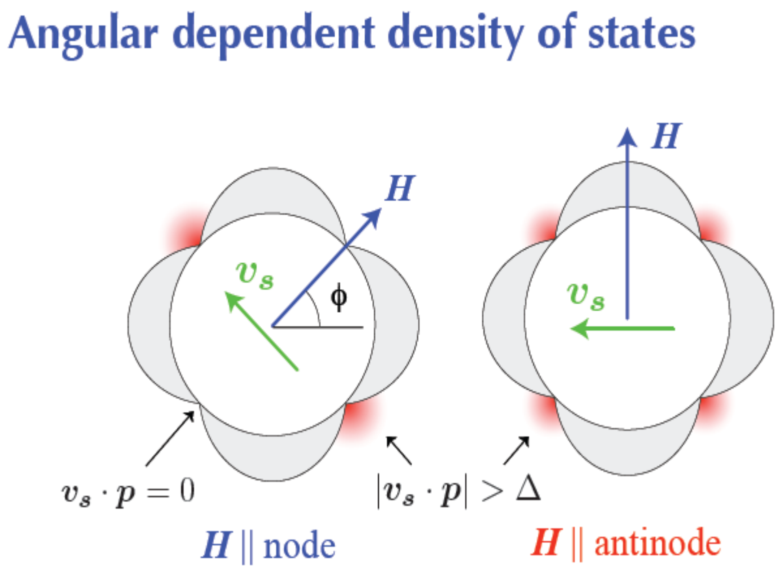

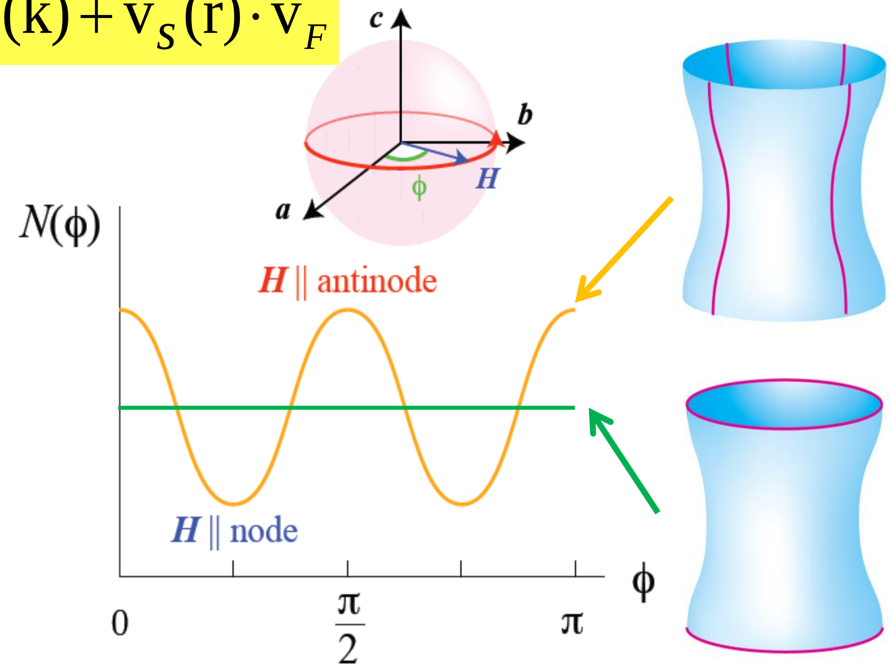

Fourfold oscillation, minima for ***H*** // node

theory I.Vekhter *et al.* 1999-2002
K.Maki *et al*. 2000-2004
P.Thalmeier *et al*. PRB (01)
H.Kusunose JPSJ (04)
T. Nakai *et al*. PRB (04)
L.Tewordt and Fay PRB (05)
A.B. Vorontsov and I.Vekhter, PRL (06), PRB (07)
Y. Nagai and N. Hayashi, PRL (08)
G.R. Boyd *et al*. PRB (09)
review Y. Matsuda *et al*. J. Phys. C 18, R705 (06)

Quasiparticles are not generated at nodal locations where $\boldsymbol{v}_F$ // **H** ($\boldsymbol{v}_s \cdot \boldsymbol{v}_F = 0$)

Pnictide

A.B. Vorontsov and I.Vekhter, PRL (10)
S. Graser et al. PRB (08)
A.V. Chubukov and I. Eremin, PRB (10)

Where is the line node ?
Pinpointing line node by angle-resolved thermal conductivity

Doppler shift $E'(\mathrm{k},\mathrm{r}) = E(\mathrm{k}) + \mathrm{v}_S(\mathrm{r})\cdot\mathrm{v}_F$

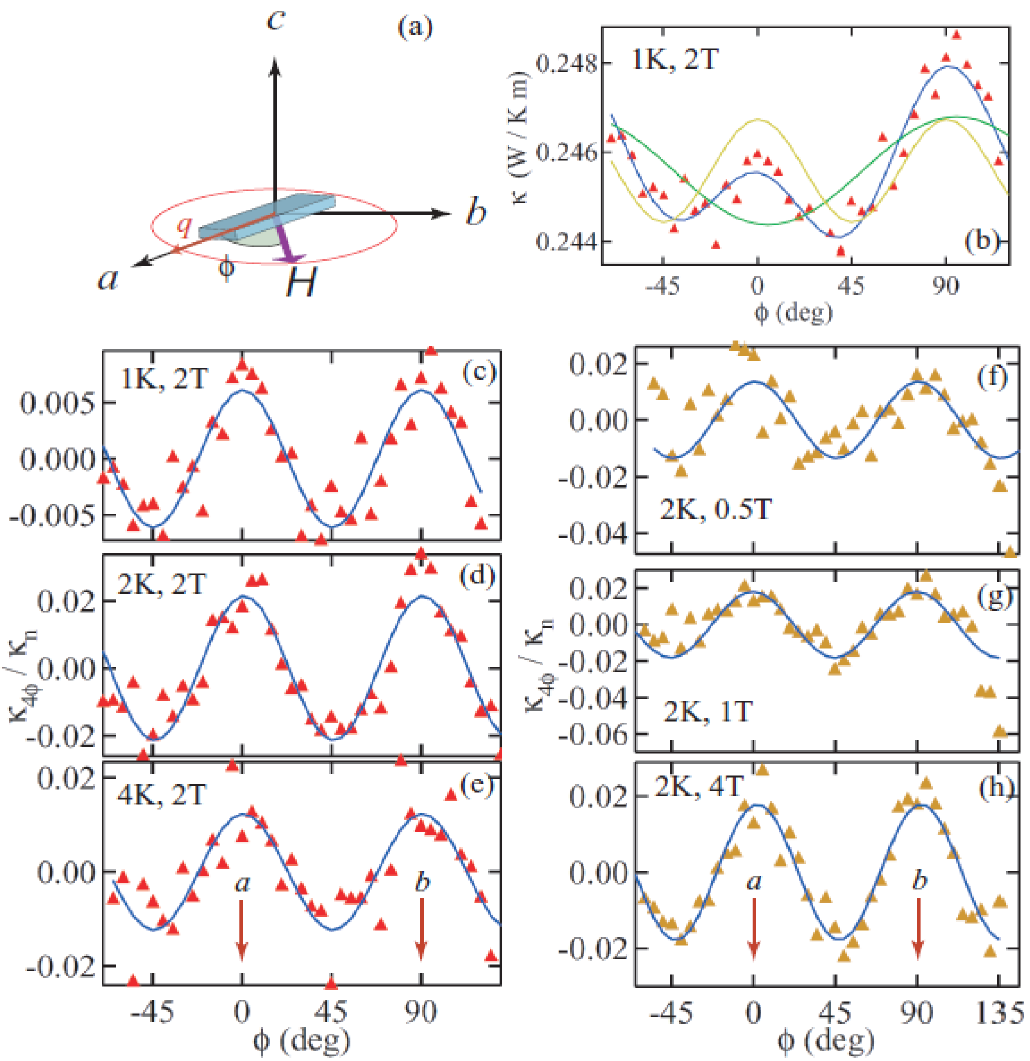

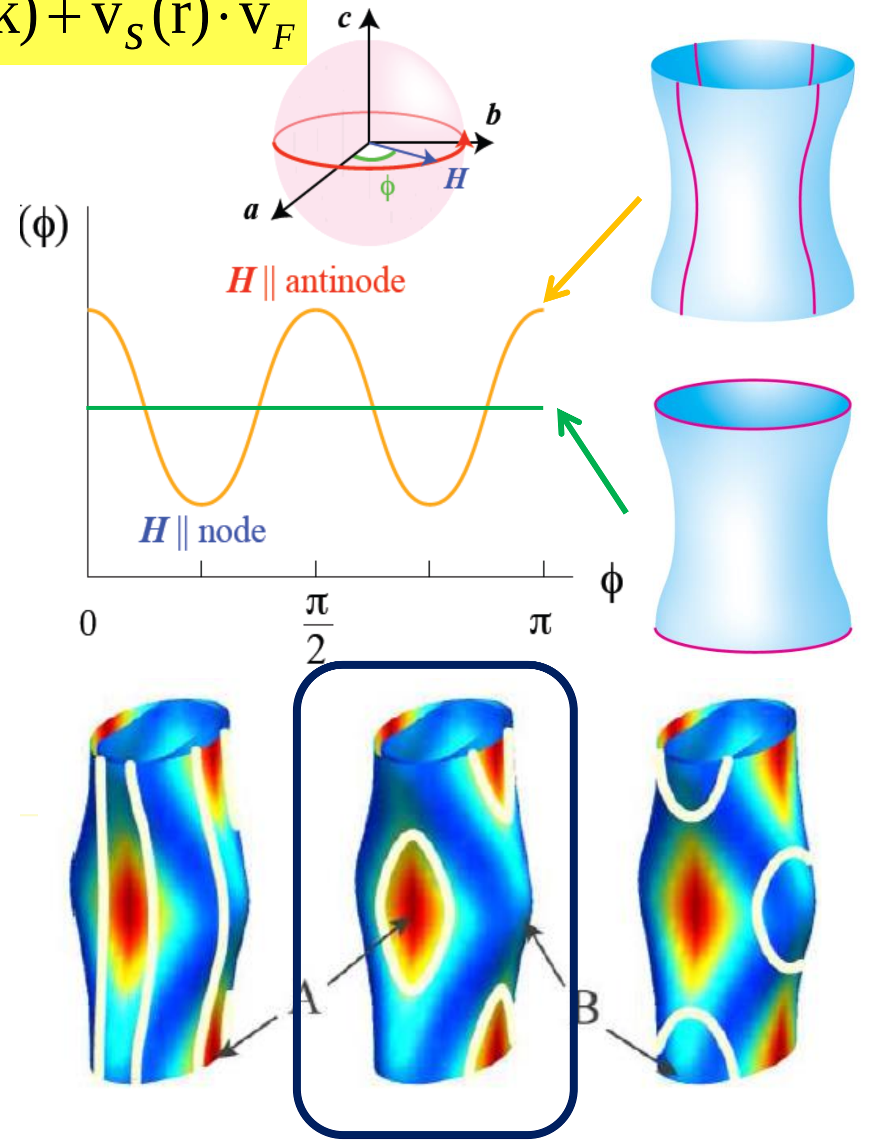

M. Yamashita *et al*. PRB (2011)

Nodal structure of $BaFe_2(As_{1-x}P_x)_2$

$BaFe_2(As_{0.3}P_{0.70})_2$
(T_c=31 K)

Electron

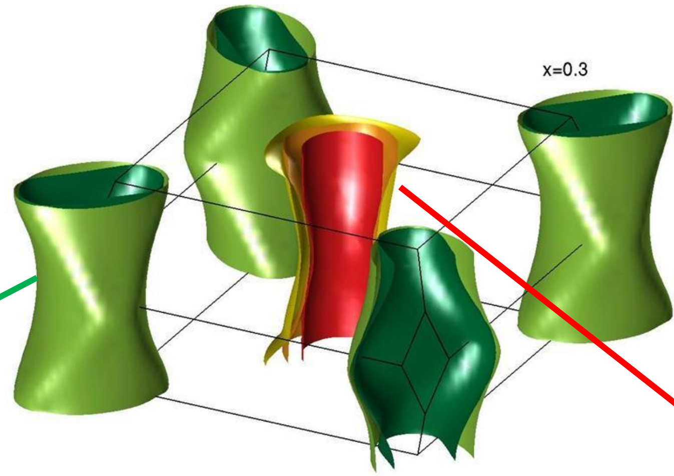

Hole

Nodal loop

Horizontal lines

What is the implication of line node?

Line node → Presence of repulsive pairing interaction

Accidental line node (not symmetry protected)

→ Presence of two (or more) competing pairing interactions

Possible scenarios

1) Frustration

el-h: repulsive S_{+-}

el-el : repulsive

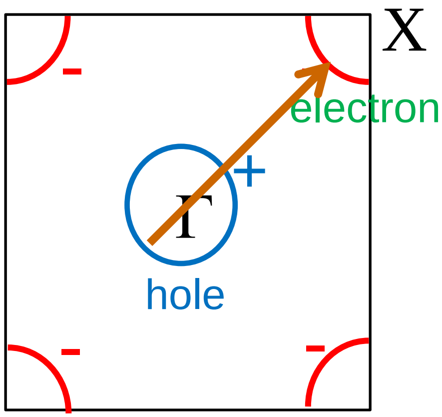

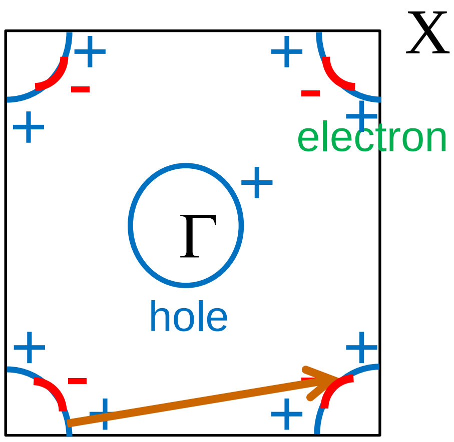

2)Competition

Orbital : attractive S_{++}

Spin : repulsive S_{+-}

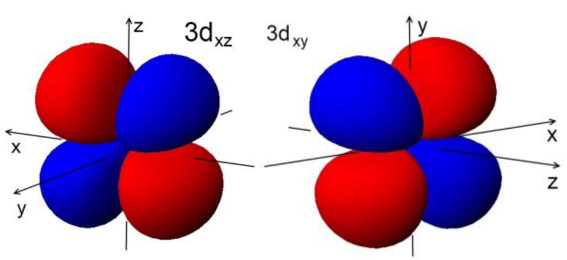

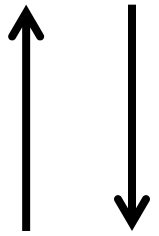

Summary: Superconducting gap structure

Full gap superconductivity

S_{+-}

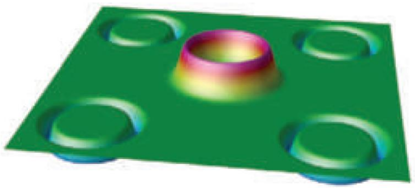

?

Repulsive
Spin fluctuations

S_{++}

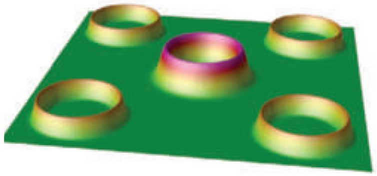

?

Attractive
Orbital fluctuations

No conclusive experimental evidence so far

Some pnictides have line nodes

Presence of repulsive pairing interaction

Line node is accidental (not symmetry protected)

Presence of two (or more) competing pairing interactions

Physics of iron-based high temperature superconductors (III)

Yuji Matsuda

Department of Physics
Kyoto University
Kyoto, Japan

Physics of iron-based high-T_c superconductors

Selected recent topics

1. Quantum critical point

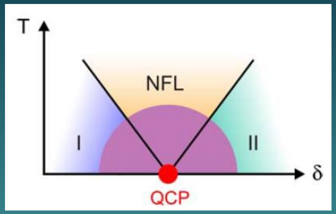

2. BCS-BEC crossover and a novel high field SC phase

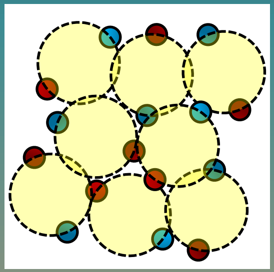

3. Nematicity

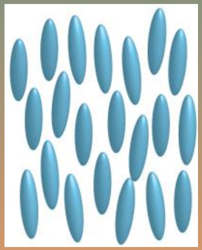

Quantum Critical Point (QCP)

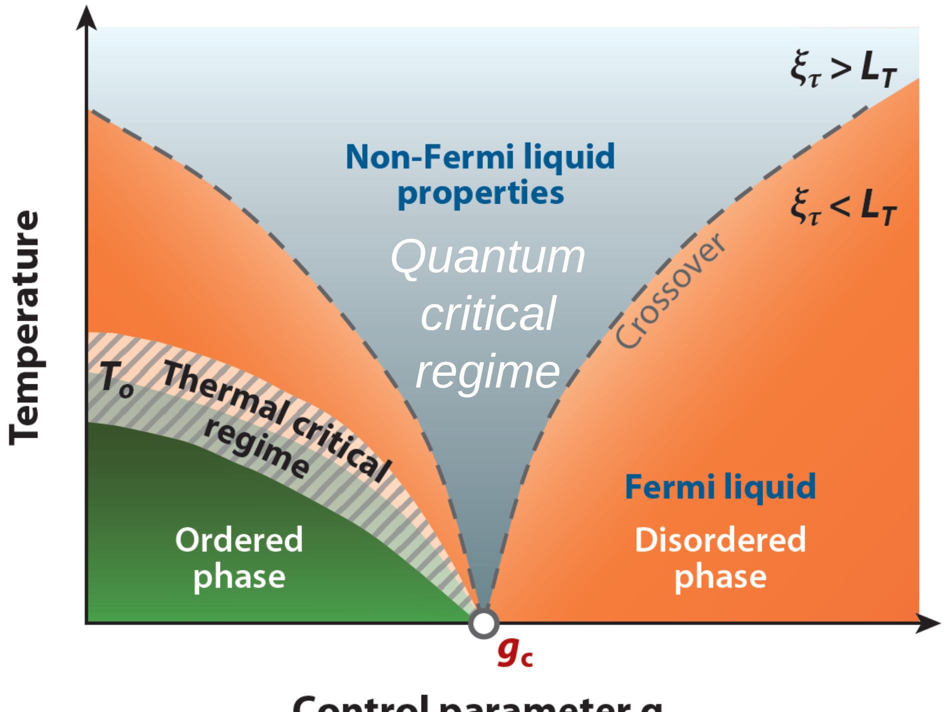

(Quantum critical point)

g: pressure, chemical substitution, magnetic field

S. Sachdev, Quantum Phase Transitions

Quantum time scale

$$\xi \propto |g - g_c|^\nu \qquad \xi_\tau \propto \xi^z$$

Thermal time scale

$$L_T = \frac{\hbar}{k_B T}$$

$\xi_\tau < L_T$

QP excitations are well defined

$\xi_\tau > L_T$

Physical properties are seriously influenced by QCP at $g = g_c$.

Ordinary phase transition – driven by thermal fluctuations

Quantum phase transition – driven by zero temperature quantum fluctuations associated with Heisenberg's Uncertainty Principle

Quantum Critical Point (QCP)

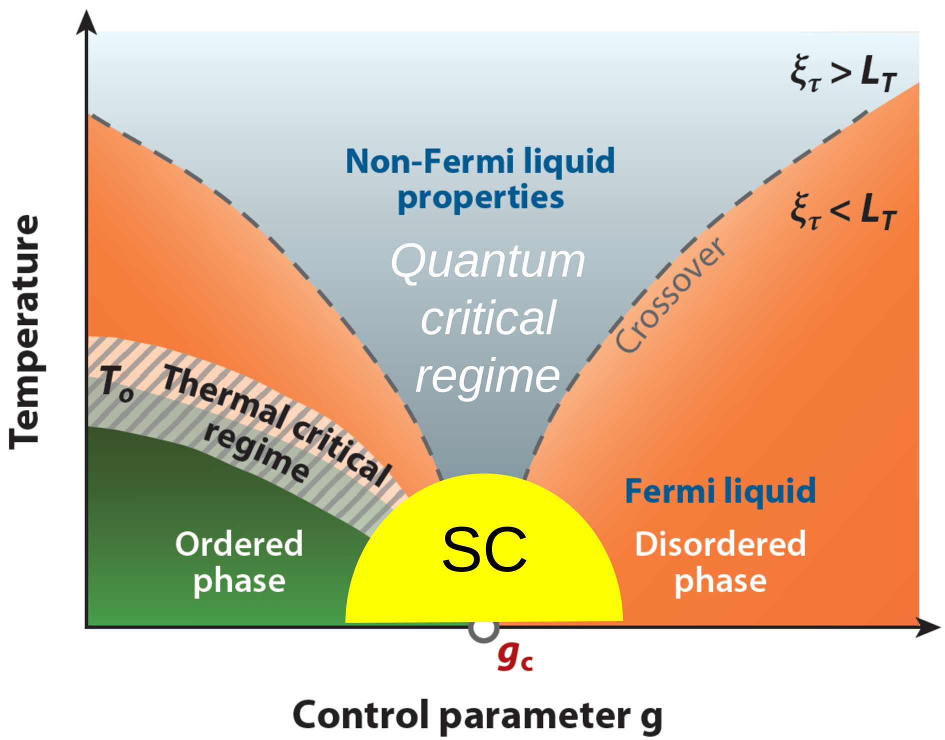

(Quantum critical point)

g: pressure, chemical substitution, magnetic field

S. Sachdev, Quantum Phase Transitions

Fe-pnictide

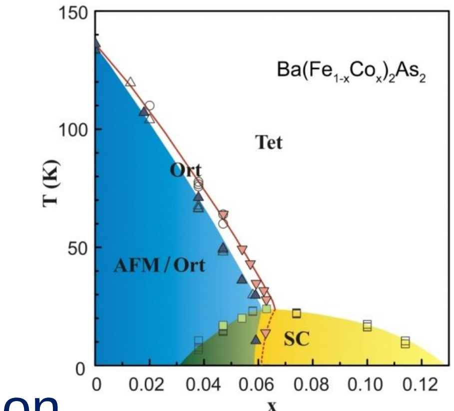

Heavy Fermion

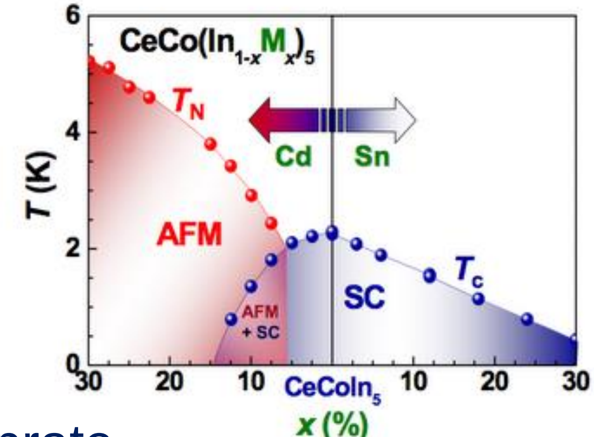

Cuprate

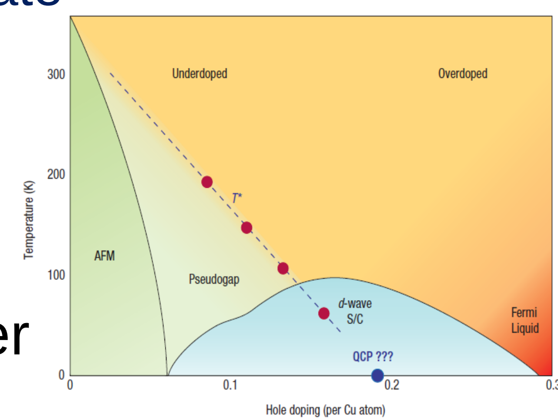

Does the QCP lie beneath the SC dome?

1. Mechanism of superconductivity
2. non-Fermi liquid properties
3. Coexistence of SC and magnetic (exotic) order

What lies beneath the SC dome?

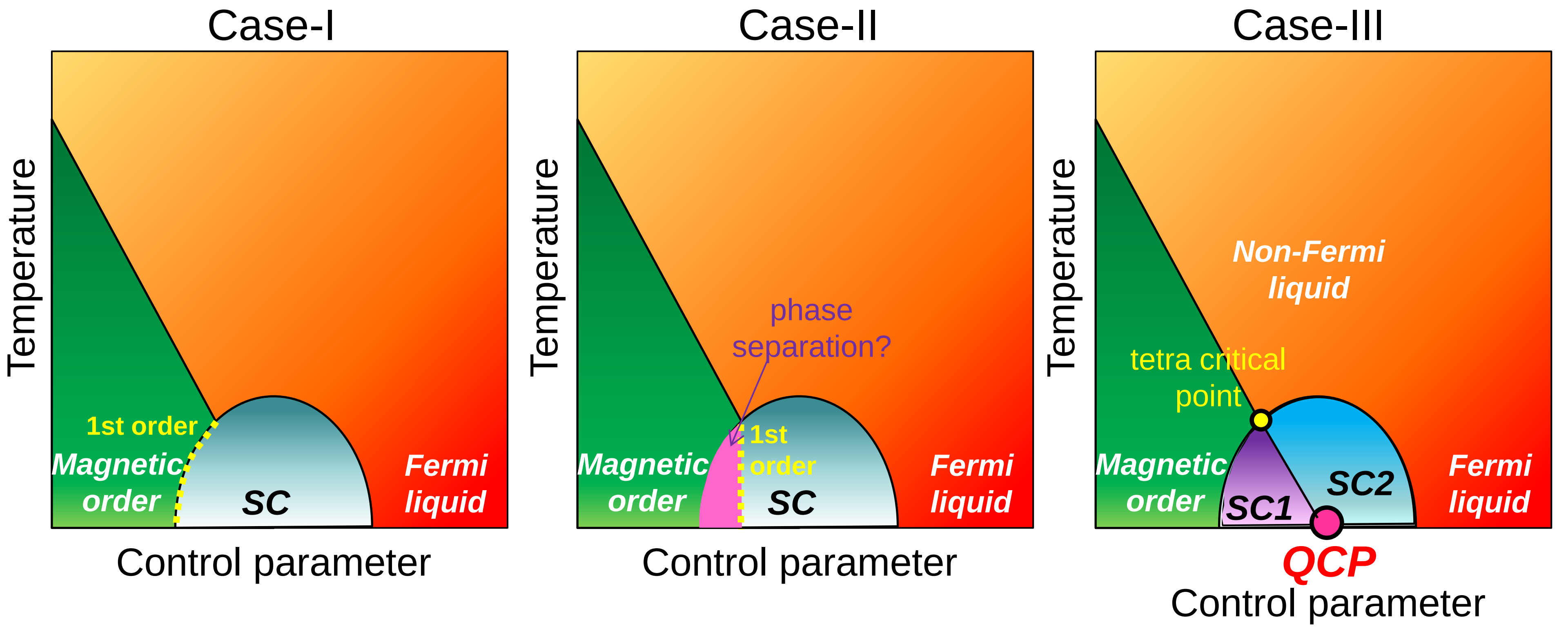

Criticality avoided by the transition to the SC state

Origin of non-Fermi liquid properties, if observed, is not clear.

QCP lying beneath the SC dome

1. Non-Fermi liquid properties
2. Mechanism of unconvensional SC
3. Microscopic coexistence of SC and magnetic (exotic) order

What lies beneath the SC dome?

QCP hidden in the SC dome has been highly controversial

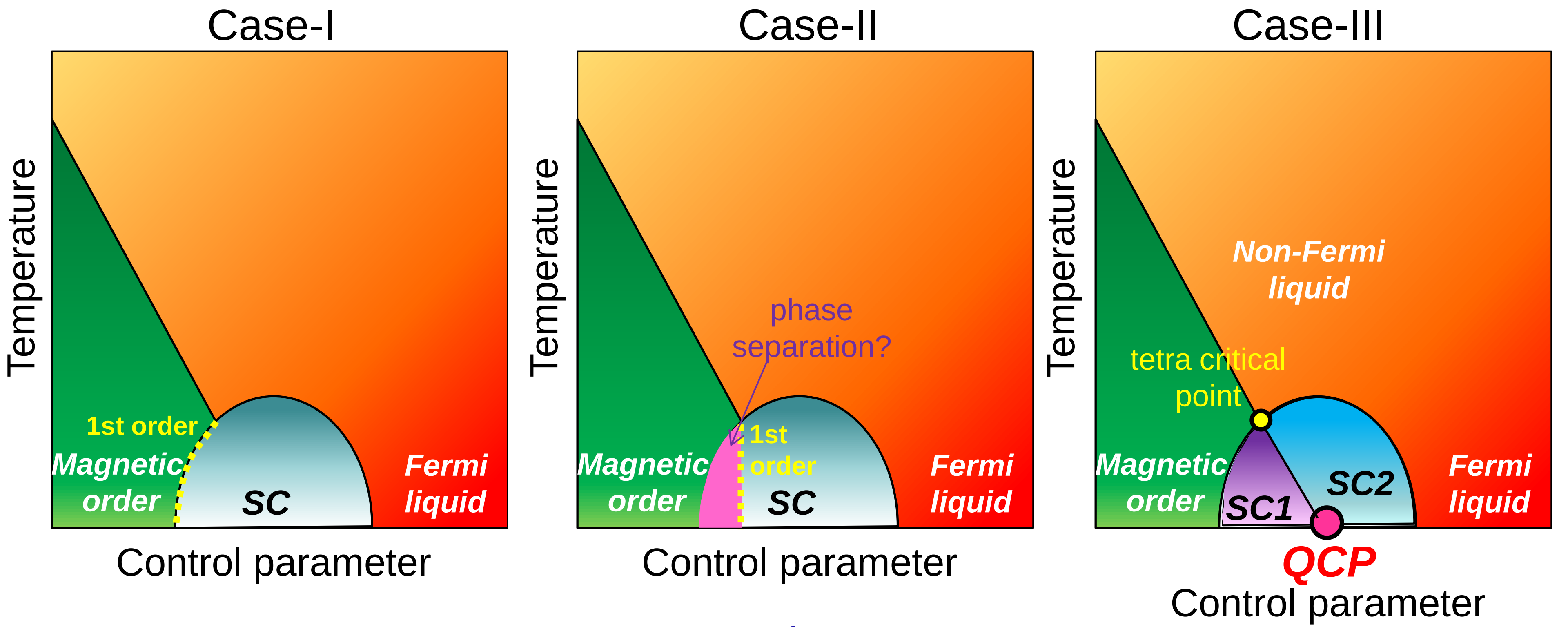

$CeIn_3$,$CePd_2Si_2$

NMR

T. Kawasaki *et al*. J. Phys. Soc. Jpn (04)

$CeRhIn_5$

Specific heat

T. Park *et al*. Nature (06)

G. Knebel *et al*. Phys. Rev. B (06)

Other heavy fermions ??

Pnictides ??

Cuprates ??

Fe-based high-T_c superconductors

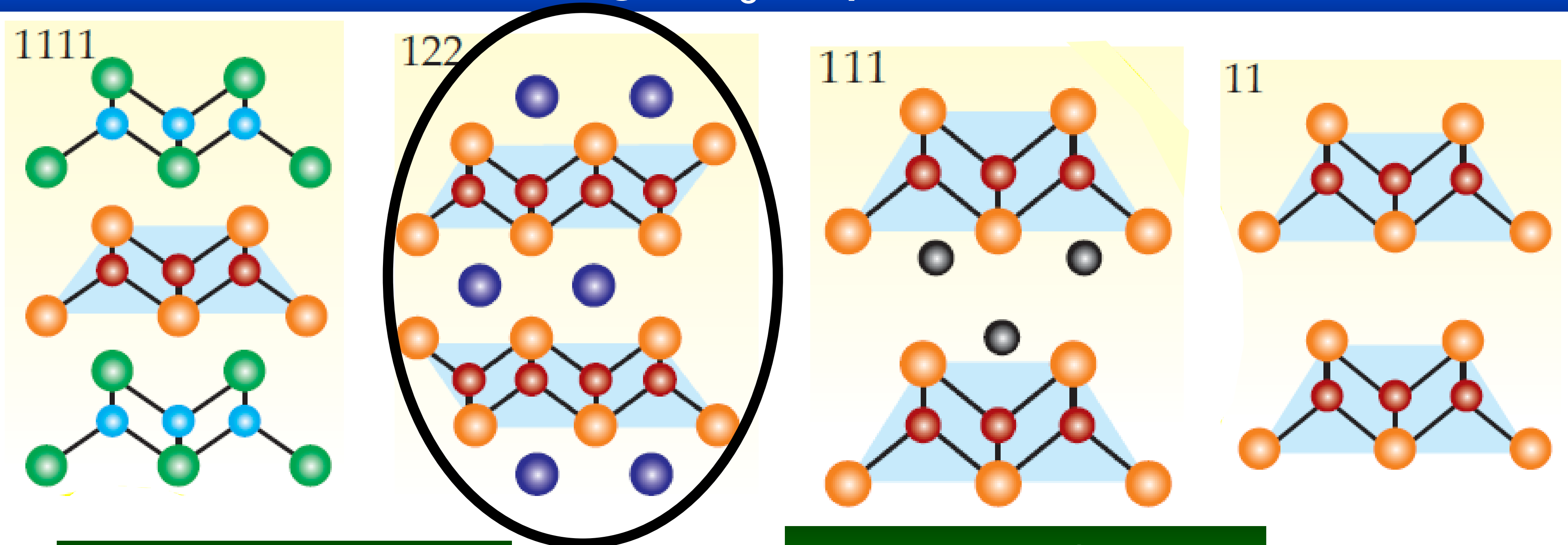

Well separated electron and hole sheets

2D square lattice of Fe

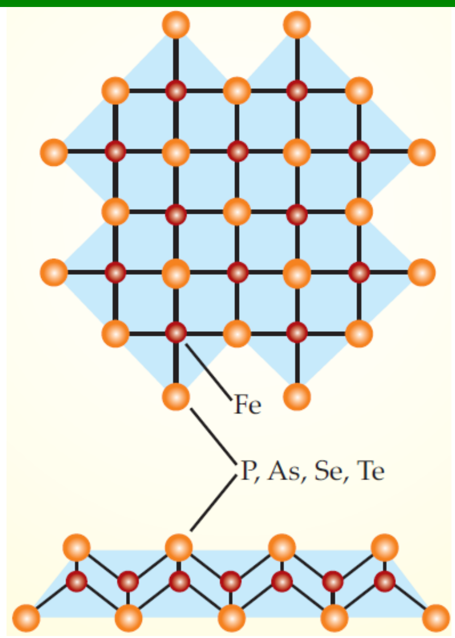

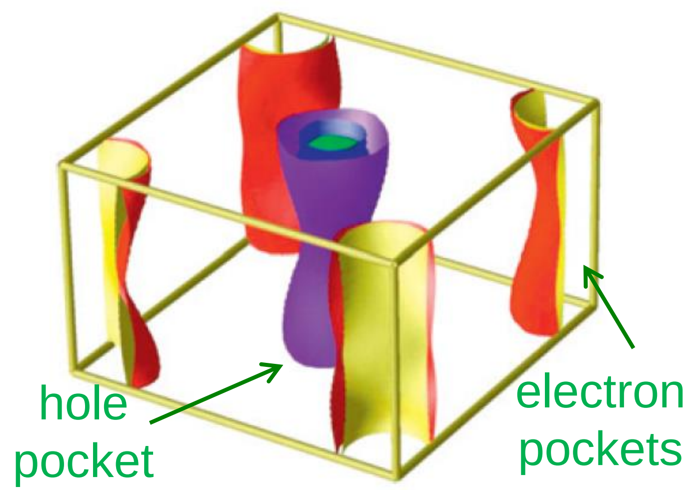

Superconductivity in $BaFe_2As_2$ systems

Parent compound

$BaFe_2As_2$

(AF Metal)

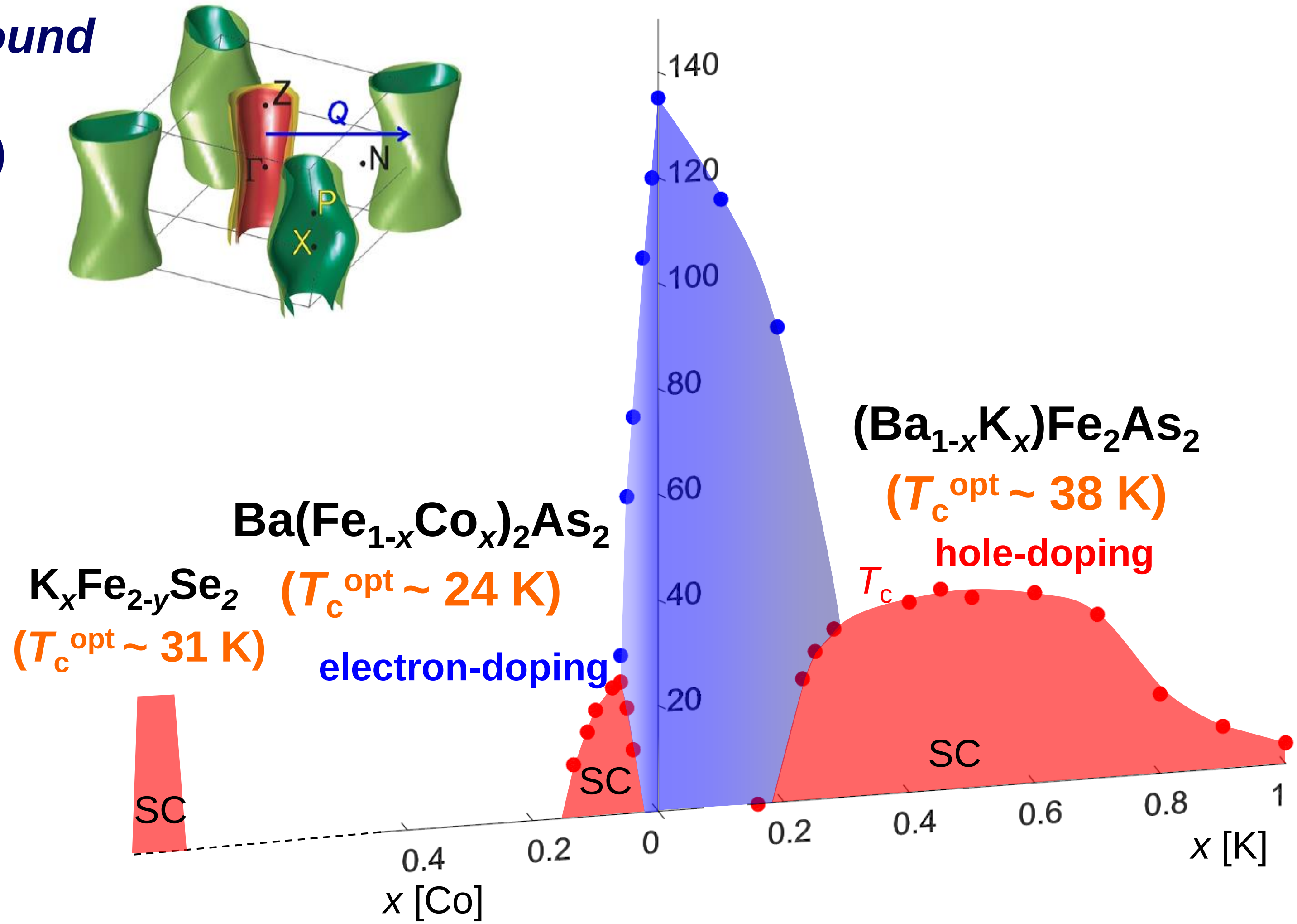

Superconductivity in $BaFe_2As_2$ systems

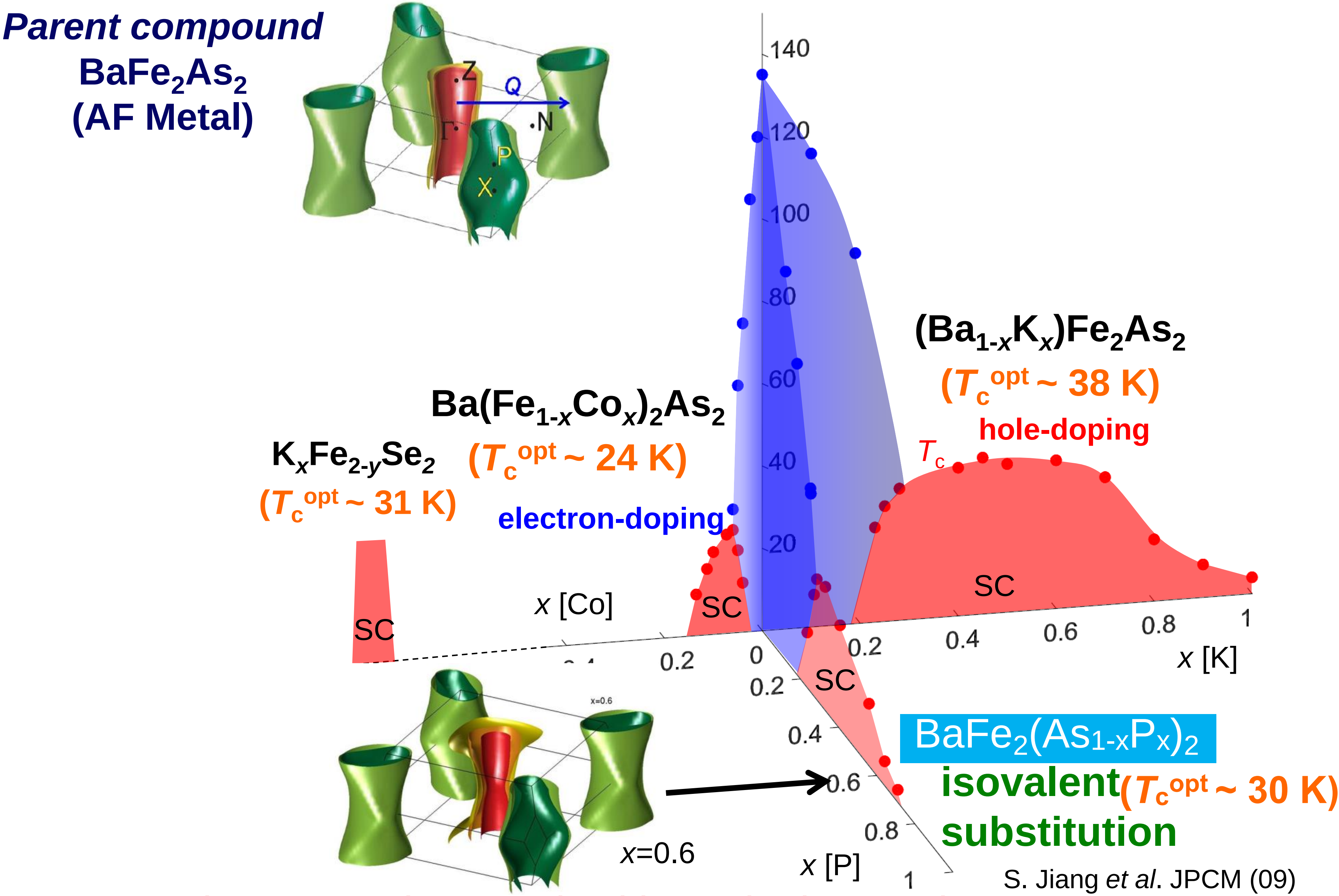

Ground state can be tuned without doping carriers

Superconductivity in $BaFe_2As_2$ systems

Parent compound

$BaFe_2As_2$

(AF Metal)

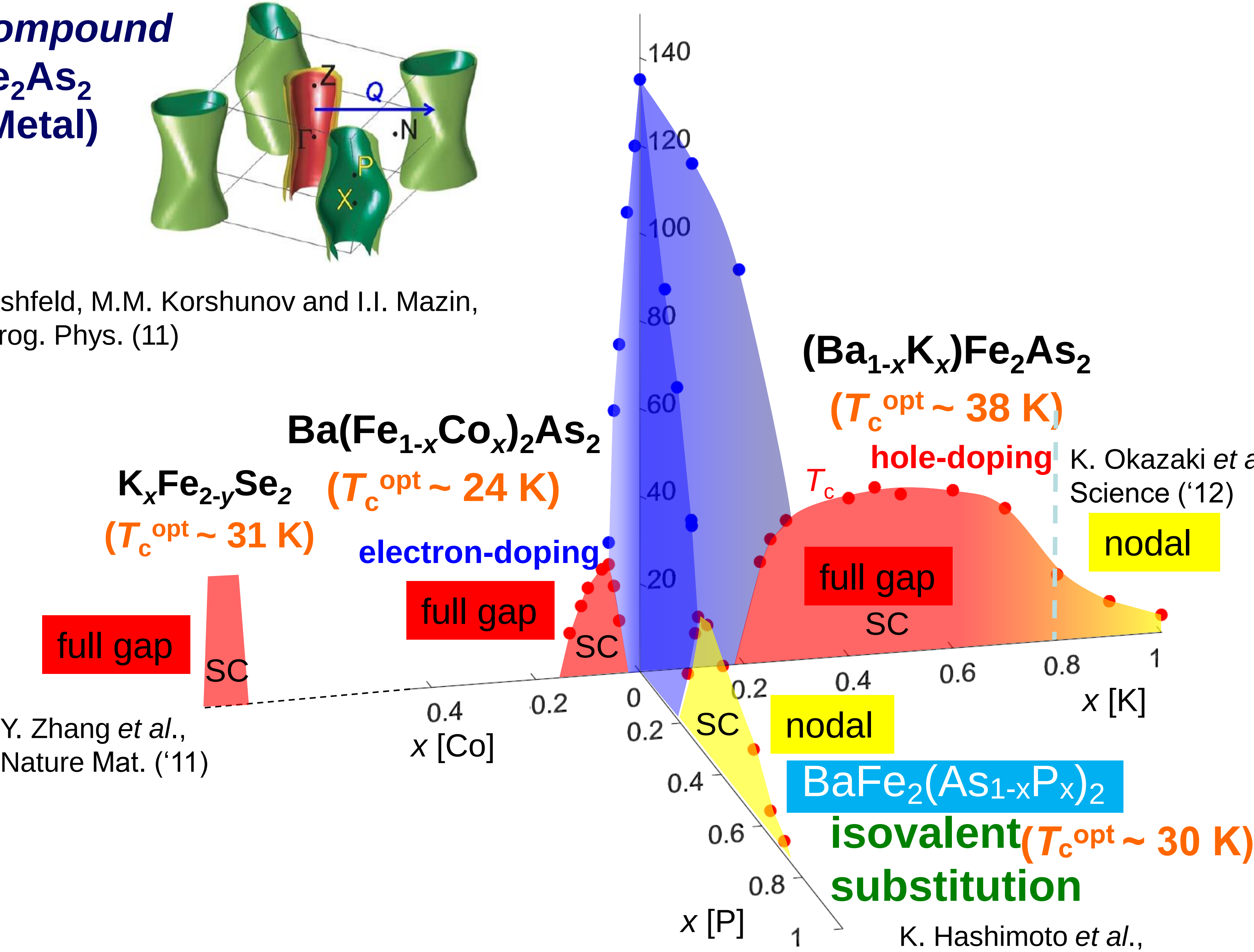

P.J. Hirshfeld, M.M. Korshunov and I.I. Mazin, Rep. Prog. Phys. (11)

K. Okazaki *et al.*, Science ('12)

Y. Zhang *et al.*, Nature Mat. ('11)

K. Hashimoto *et al.*, Science ('12)

$BaFe_2(As_{1-x}P_x)_2$: a clean system

Parent compound
$BaFe_2As_2$
(AF Metal)

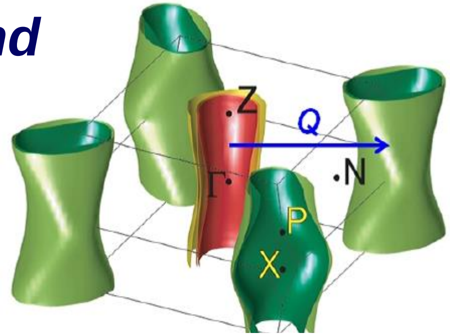

$BaFe_2(As_{1-x}P_x)_2$

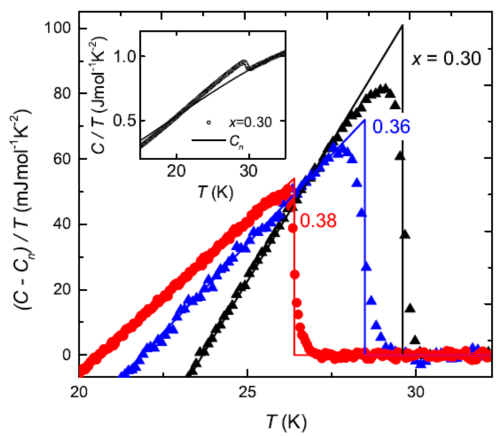

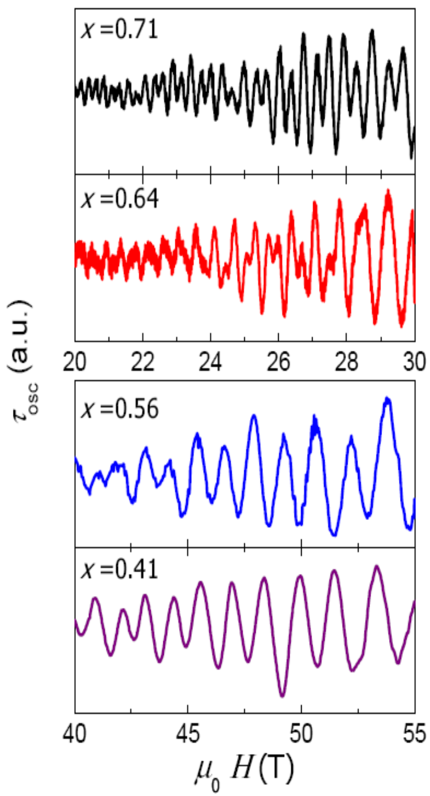

H. Shishido *et al*. PRL (10)
J.G. Analytis et al. PRL (11)
P. Walmsley *et al*. PRL (13)

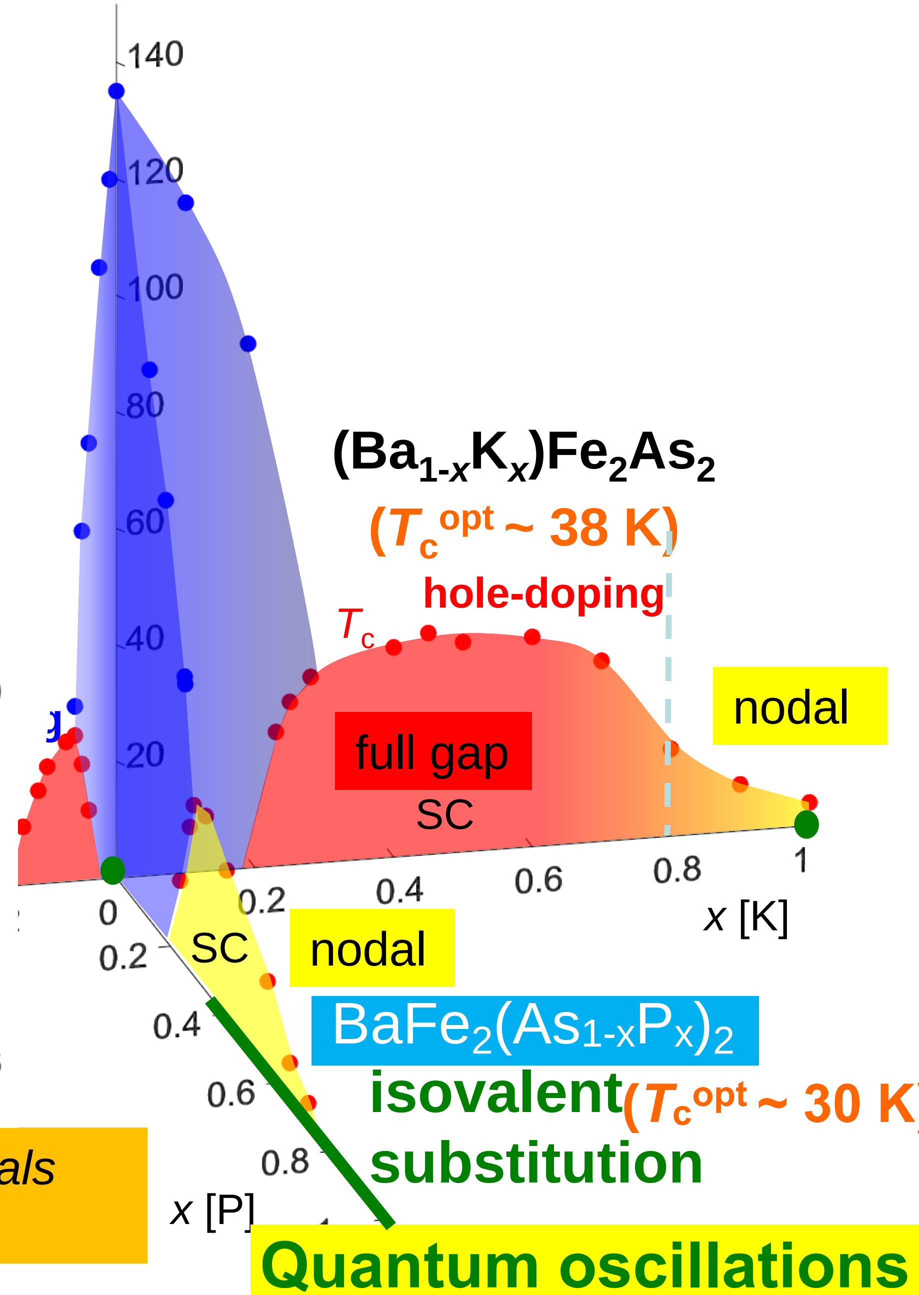

Clean and homogeneous single crystals have been available.

Quantum phase transition lurking inside the superconducting dome

Influence of quantum critical fluctuations on *normal and superconducting* electrons

Doping evolution of the transport property

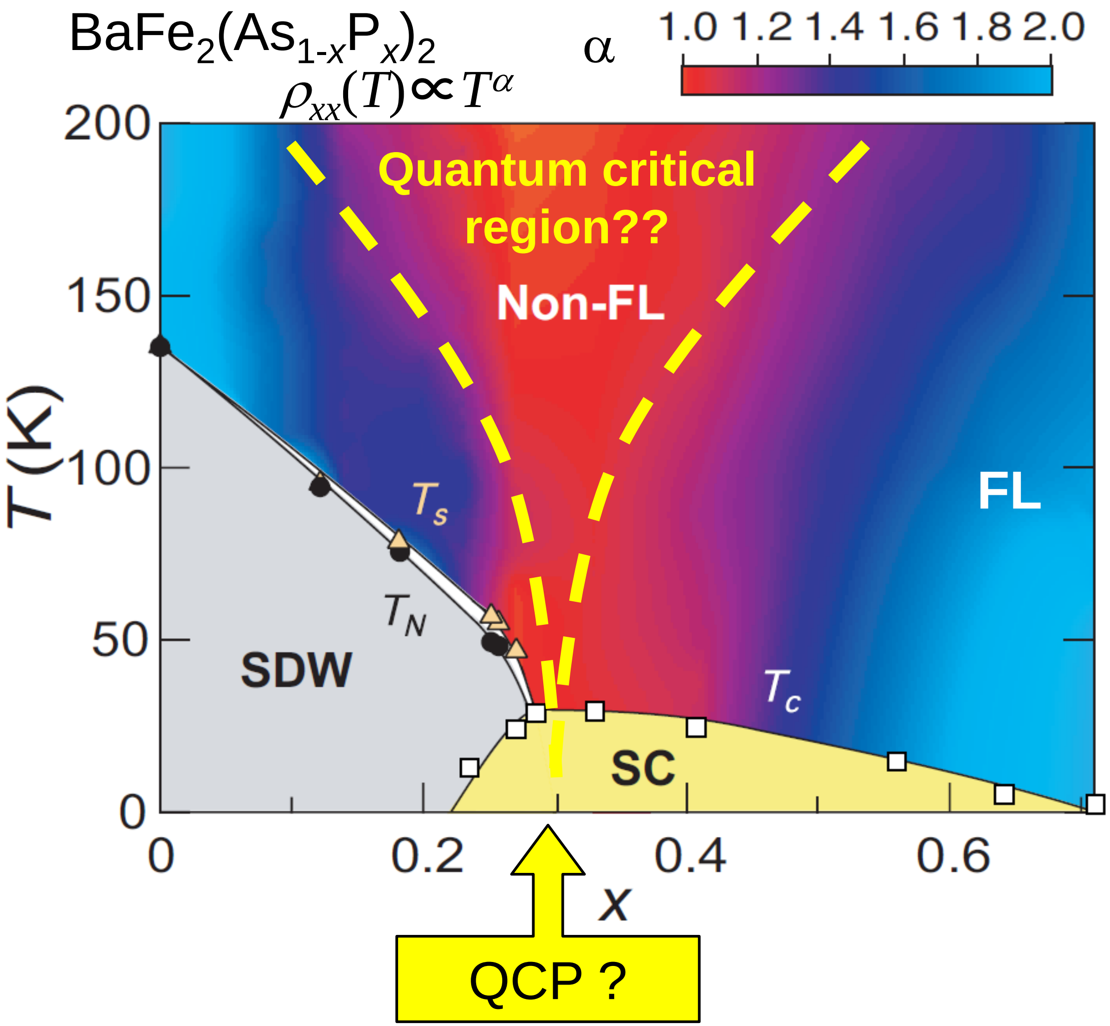

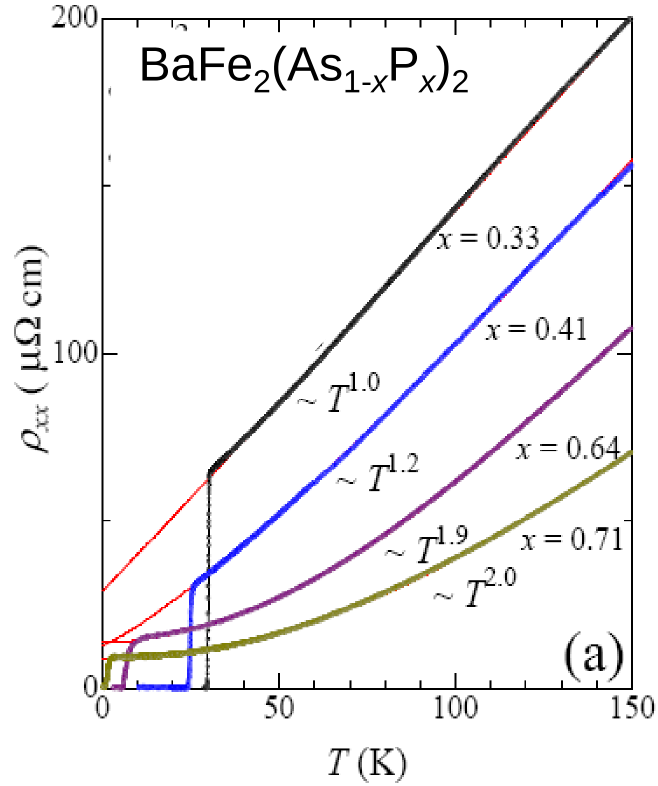

S. Kasahara *et al*., PRB **81**, 184519 (10)

A.E. Böhmer *et al*. Phys. Rev. B 86, 094521 (12)

T-linear resistivity at *x*=0.33 just beyond SDW end point (x_c=0.3)

Hallmark of non-Fermi liquid

T^2-dependence at *x*=0.71

Fermi-liquid behavior

See also

S. Sachdev and B. Keimer, Physics Today (11)

J. Dai, Q. Si, J.-X. Zhu, and E. Abrahams, PNAS (09)

Fermi surface and mass renormalization

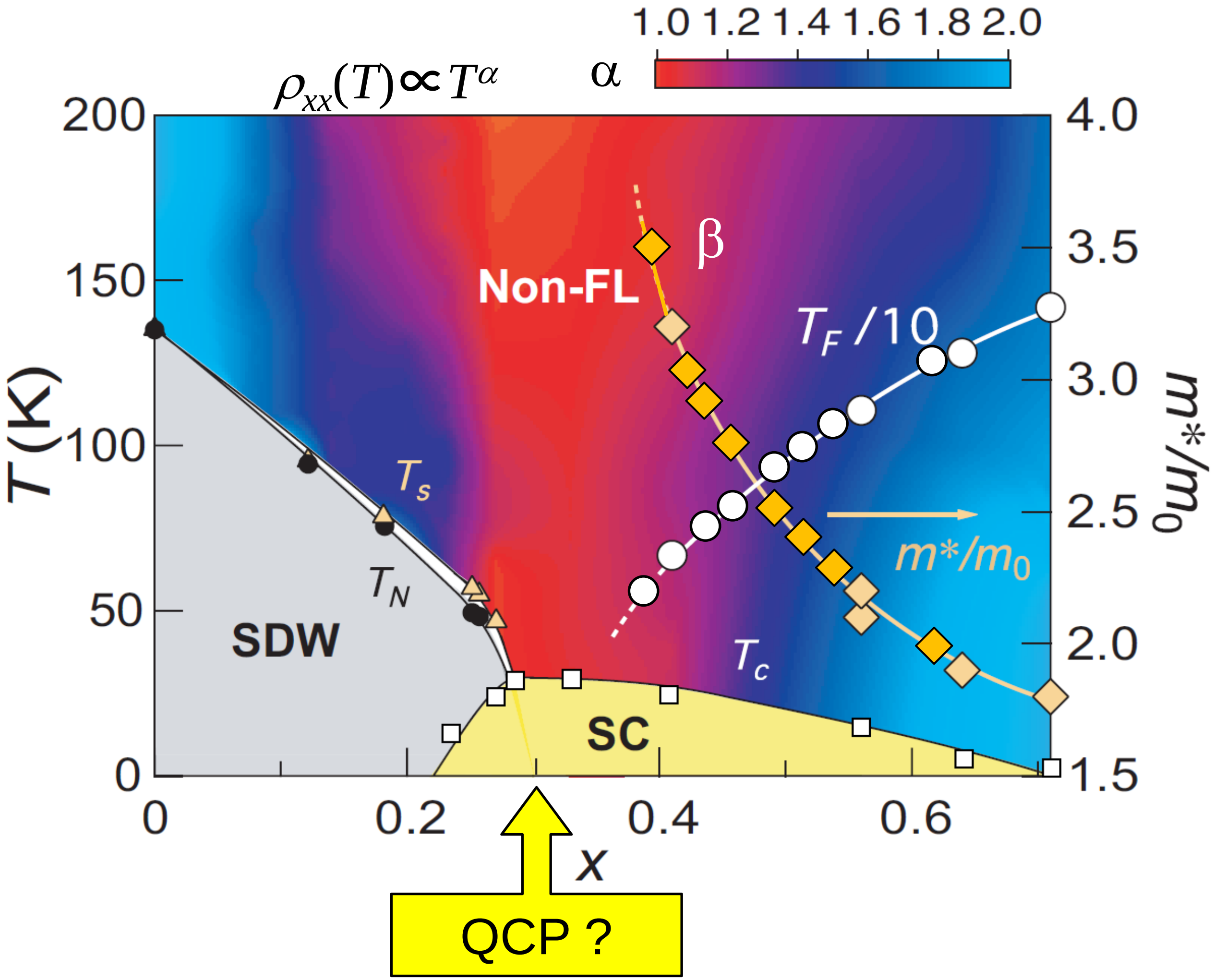

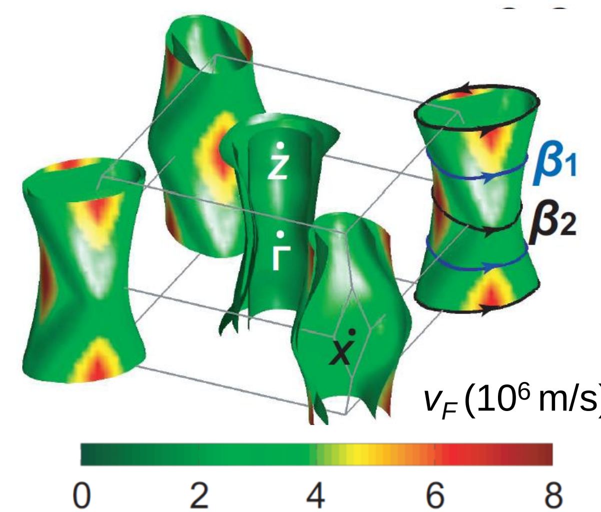

Effective mass

Fermi temperature

$$T_F = \hbar eF / m^* k_B$$

dHvA

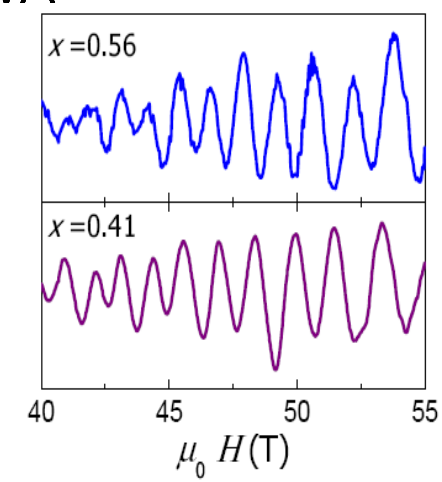

As x is tuned towards the maximum T_c,

Effective mass m^* is strongly enhanced

Fermi temperature $T_F = heF/m^*k_B$ tends to zero

H.Shishido *et al*. PRL (09) B. J. Arnold *et al*. PRB (R)(11), P. Walmsley *et al*. PRL(13)

Doping evolution of the specific heat jump at T_c

$BaFe_2(As_{1-x}P_x)_2$

P. Walmsley *et al*. PRL(13)

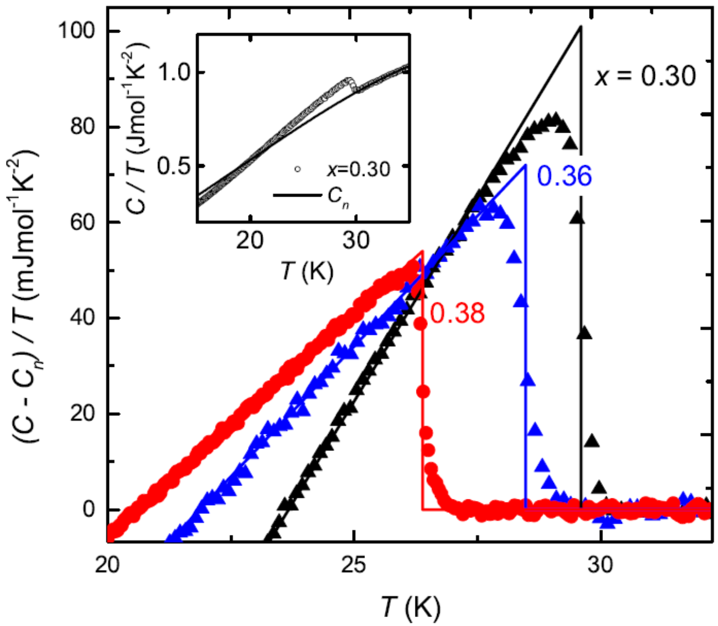

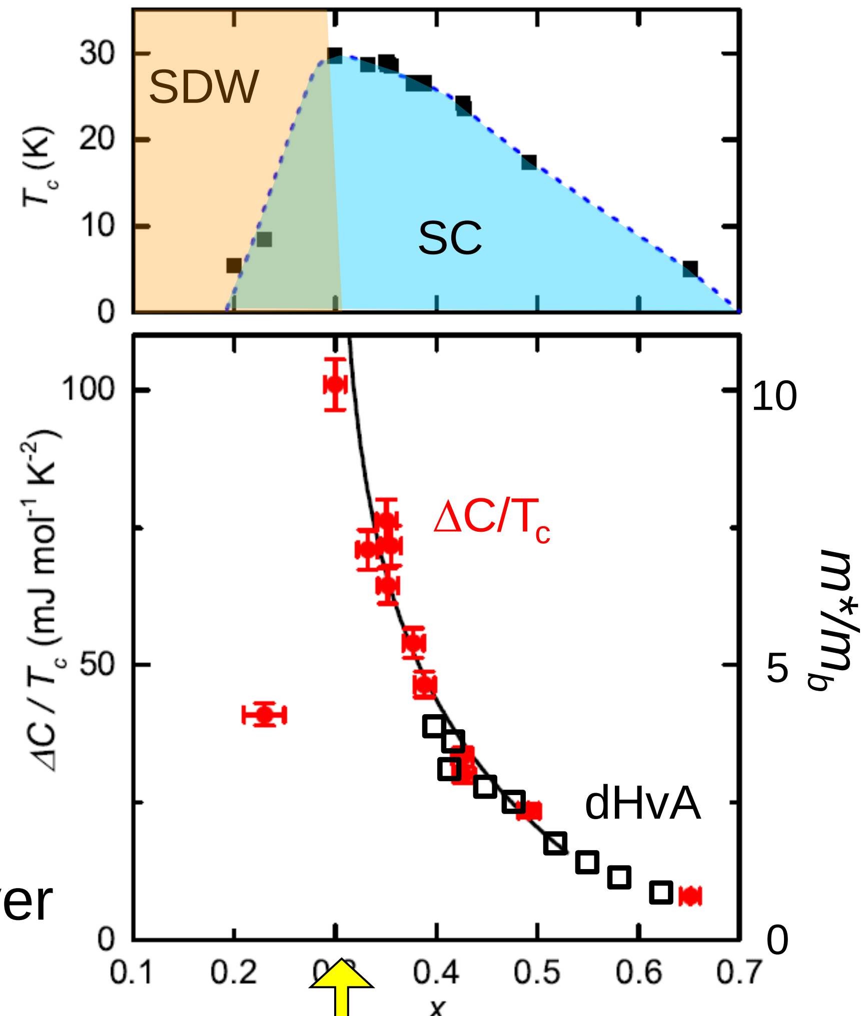

$$\frac{\Delta C}{T_c} \propto \gamma \propto m^*$$

QCP?

The uniform mass enahancement over the Fermi surface

Strong mass enhancement at x=0.30

γ~70 mJ/K^{2}mol

Doping evolution of the specific heat jump at T_c

$BaFe_2(As_{1-x}P_x)_2$

P. Walmsley *et al*. PRL(13)

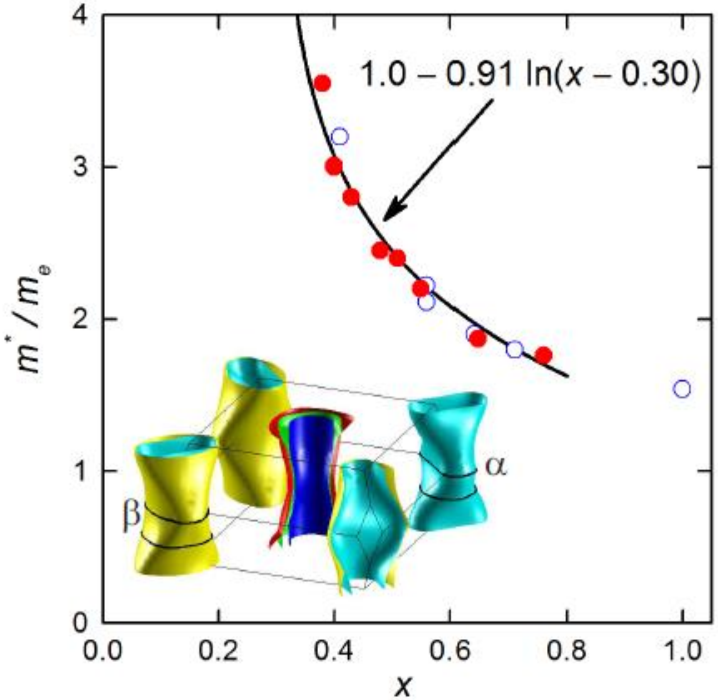

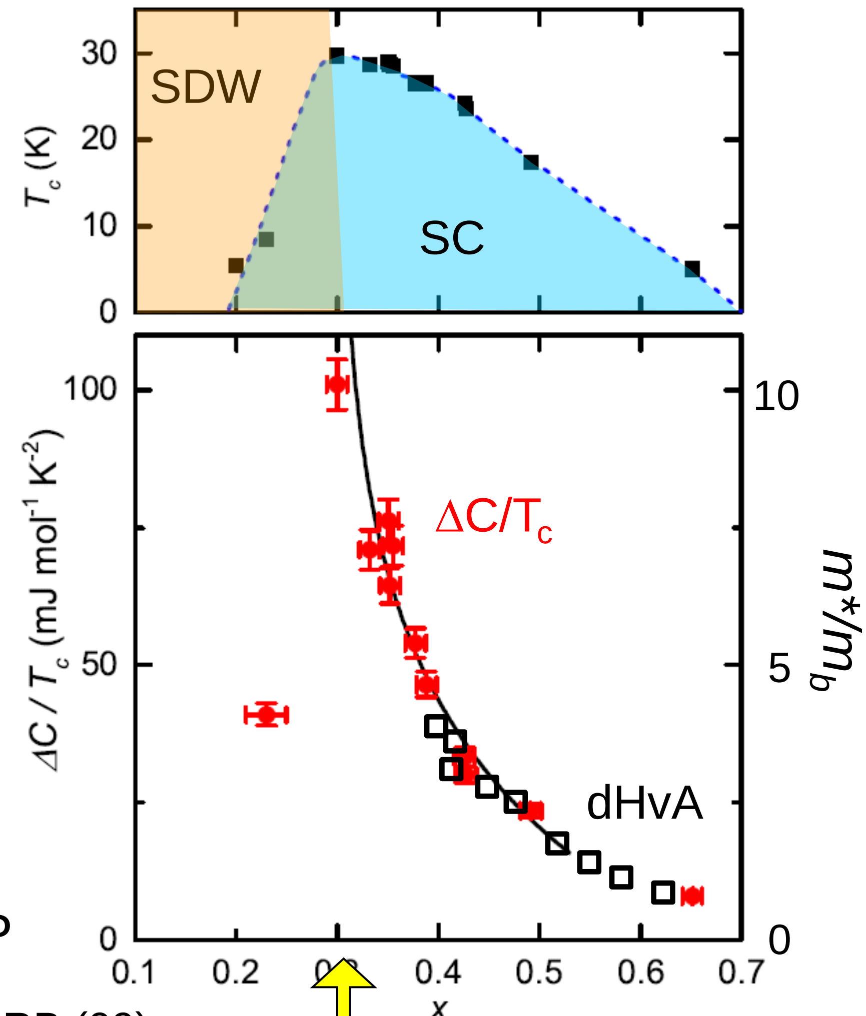

$$\frac{m^*}{m_b} = c_0 + c_1 \ln(x - x_c)$$

expected *x*-dependence close to a QCP

QCP?

$$\Delta C/T_c \propto T_c^2$$

S. L. Bud'ko *et al.* PRB (09)
J. Zaanen PRB (09)

$$\Delta C/T_c \propto T_c^{5-6}$$

for 30K> T_c >23K   present results

Doping evolution of the magnetic fluctuations (^{31}P NMR)

$1/T_1T \sim \chi(\pi,\pi)$

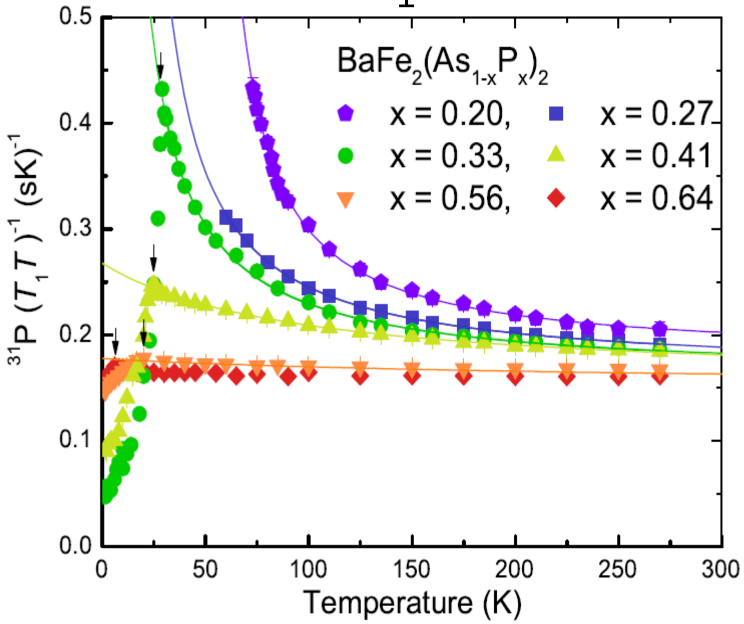

θ: Weiss temperature

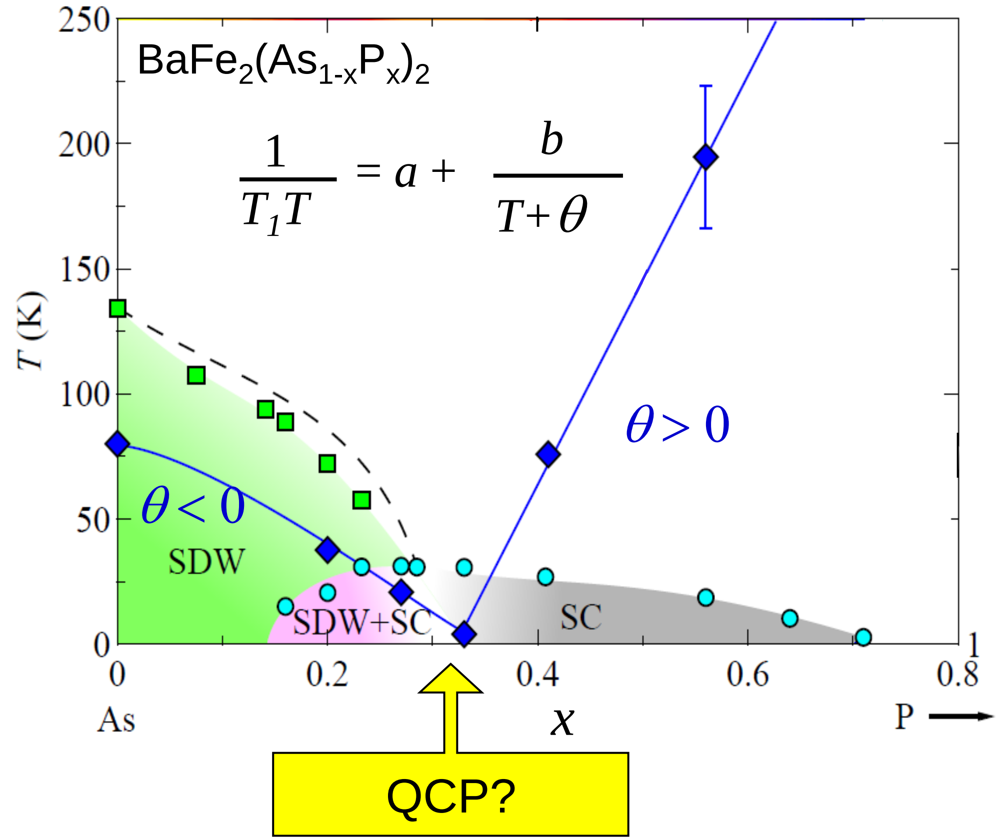

θ goes to zero at x~0.3

Dynamical susceptibility diverse at T=0 K.

Y. Nakai *et al*. PRL (10)

Doping evolution of normal electrons

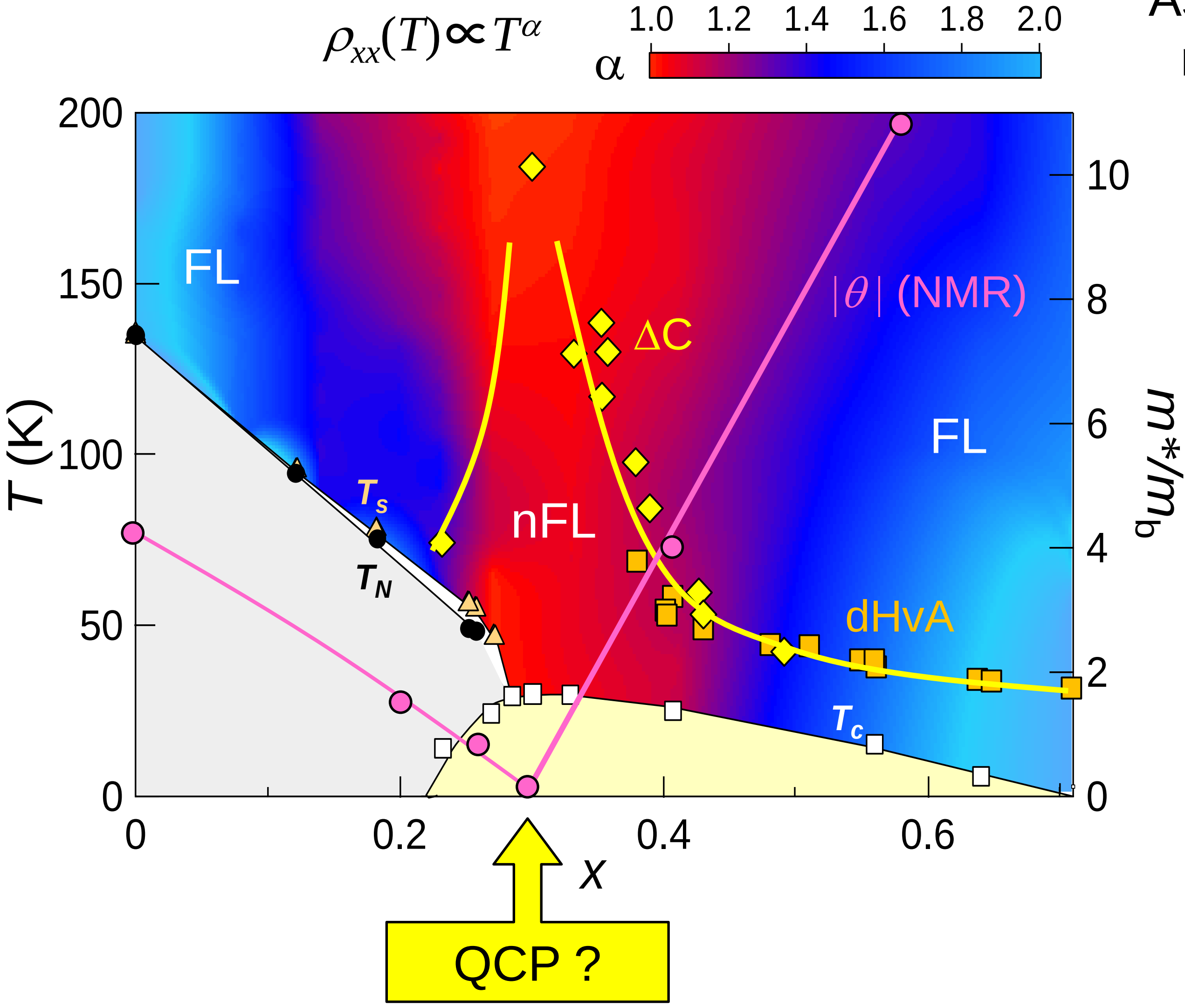

As x is tuned towards the maximum T_c at x=0.30

Hallmark of non-Fermi liquid behavior

Resistivity

Effective mass m is strongly enhanced*

dHvA

Specific heat

Weiss temperature goes to zero

NMR

We need evidence at zero temperature and zero field.

Quantum phase transition lurking inside the superconducting dome

Influence of quantum critical fluctuations on *normal and superconducting* electrons

Doping evolution of the London penetration depth at T=0

London penetration depth λ_L is the quantity that can probe the electronic structure at zero temperature limit.

Number of superfluid

$$\lambda_L^{-2}(0) = \frac{\mu_0 n_s e^2}{m^*}$$

Mass of superfluid

1. Tunnel diode oscillator (13MHz, 70 mK)

Al coated method

2. Microwave surface impedance

Rutile cavity resonator (5 GHz, Q~10^6, 350 mK)

3.Nodal superconducting gap structure

Line node
$$\frac{\delta\lambda_L(T)}{\lambda_L(0)} \approx \frac{\ln 2}{\Delta} k_B T$$

Determination of the London penetration depth at T=0

Very small single crystals

Typical crystal size ~200x200x10μm^3

Rectangular shape

Cleaved just before the measurements

$225.9 \times 217.6 \times 10\ \mu m^3$

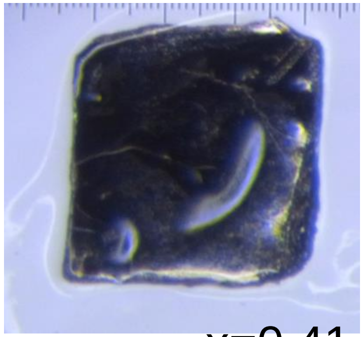

x=0.41

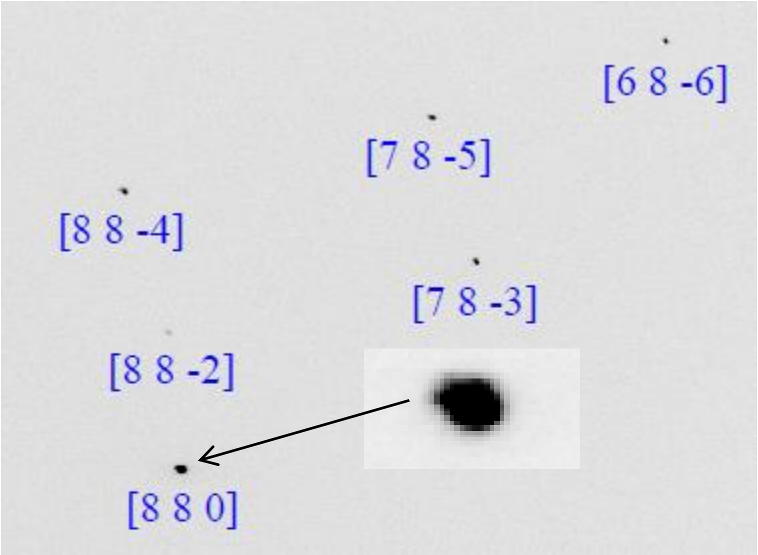

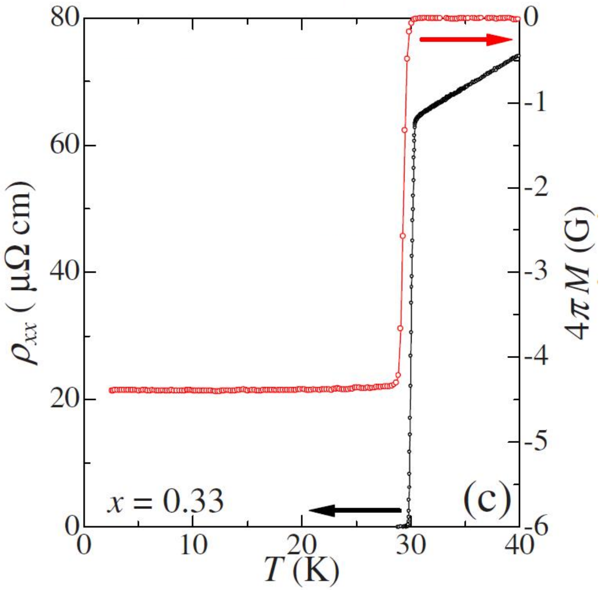

Synchrotron X-ray diffraction pattern shows high crystalline quality

Sharp SC transition

Nearly perfect Meissner state with negligibly small non-SC region

Determination of the London penetration depth at T=0

1. Al coated method (Tunnel diode oscillator, 13MHz)

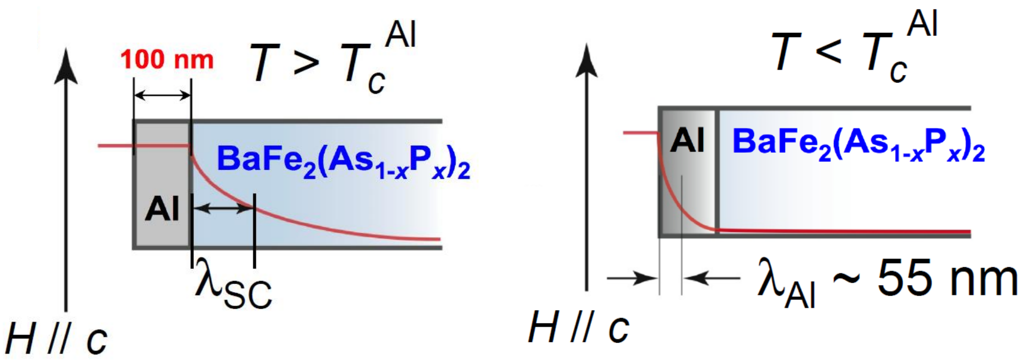

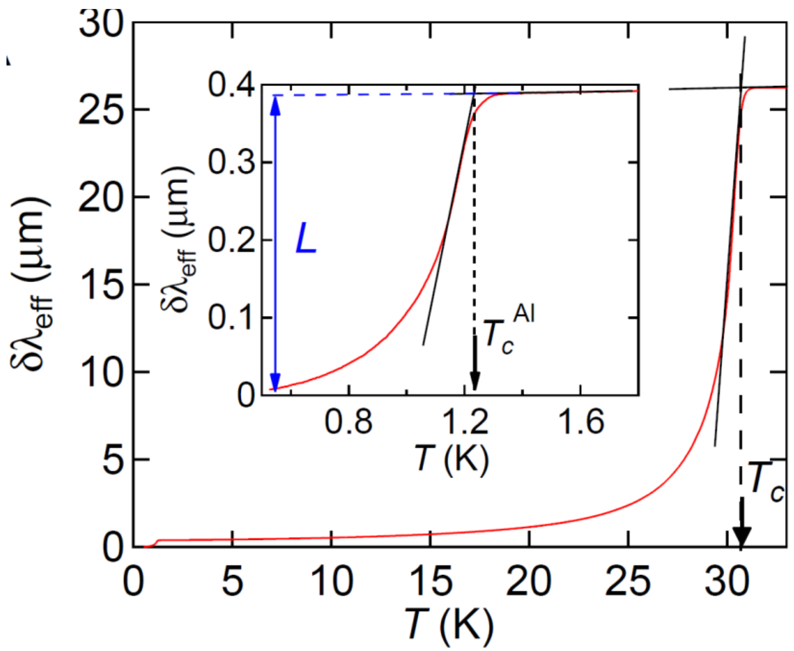

$$\lambda_{\rm eff}(T) = \lambda_{\rm Al}(T)\frac{\lambda(T) + \lambda_{\rm Al}(T)\tanh\frac{t}{\lambda_{\rm Al}(T)}}{\lambda_{\rm Al}(T) + \lambda(T)\tanh\frac{t}{\lambda_{\rm Al}(T)}},$$

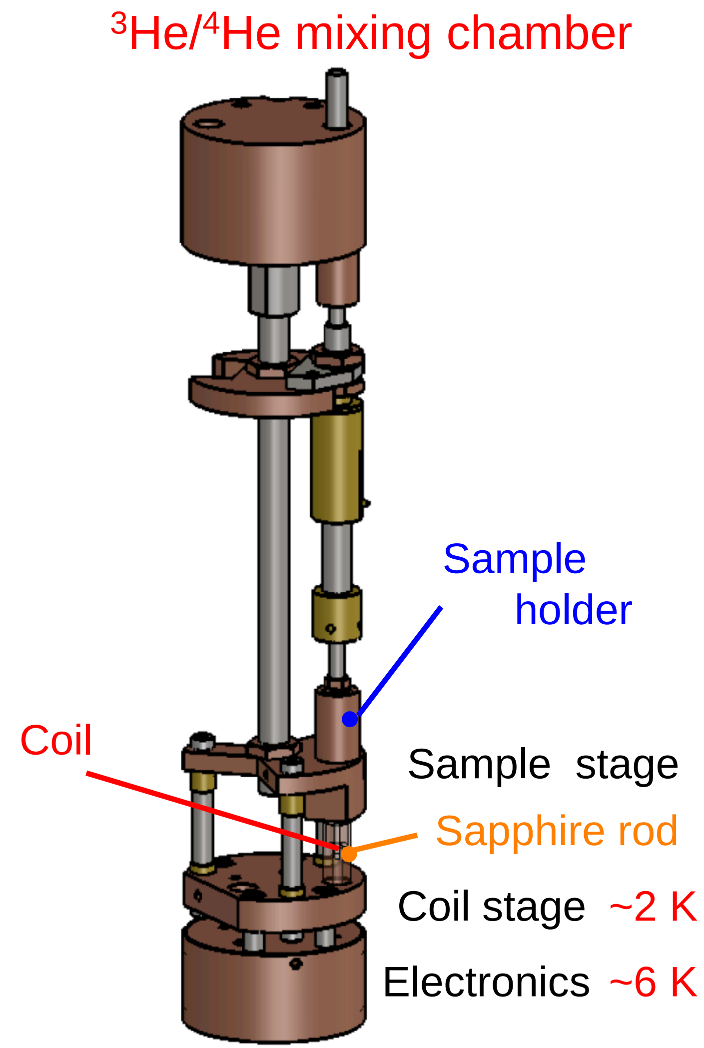

Error bar of $\lambda_L(0)$: ±15%

Determination of the London penetration depth at T=0

2. Microwave surface impedance

$$R_s = G_1\left(\frac{1}{2Q_s} - \frac{1}{2Q_0}\right) \quad X_s = G_2\left(-\frac{f_s - f_0}{f_0}\right) + C$$

Normal state $$R_s = X_s$$

Superconducting state $$\lambda_{ab} = \frac{X_s}{\mu_0 \omega}$$

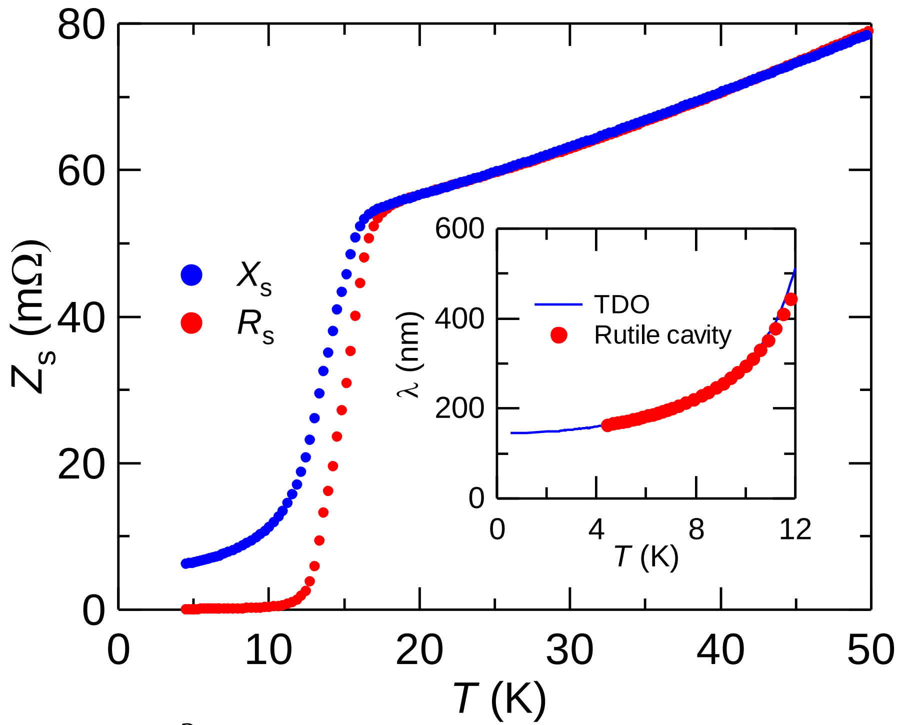

$R_s(0) < 10^{-3} R_s(T>T_c)$

Rutile cavity resonator

(5 GHz, Q~10^6)

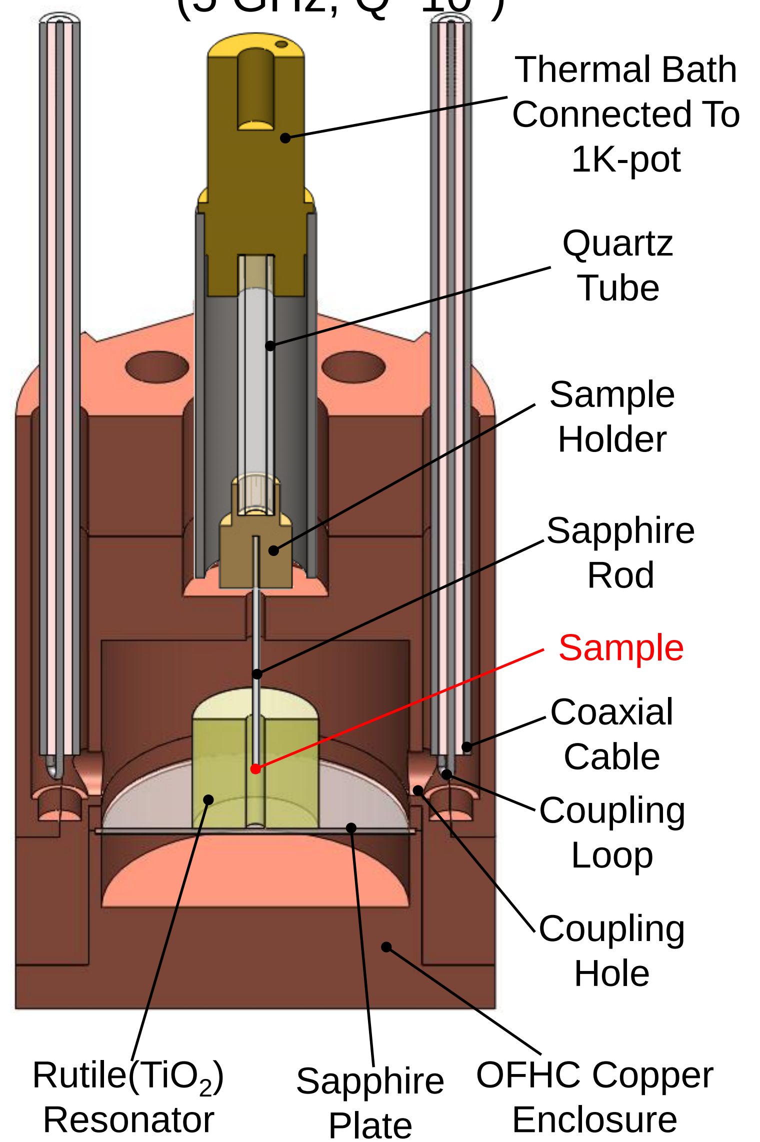

Error bar of $\lambda_L(0)$: ±15%

W.A. Huttema *et al*. Rev. Sci. Instrum (06)

Determination of the London penetration depth at T=0

3.Nodal superconducting gap structure

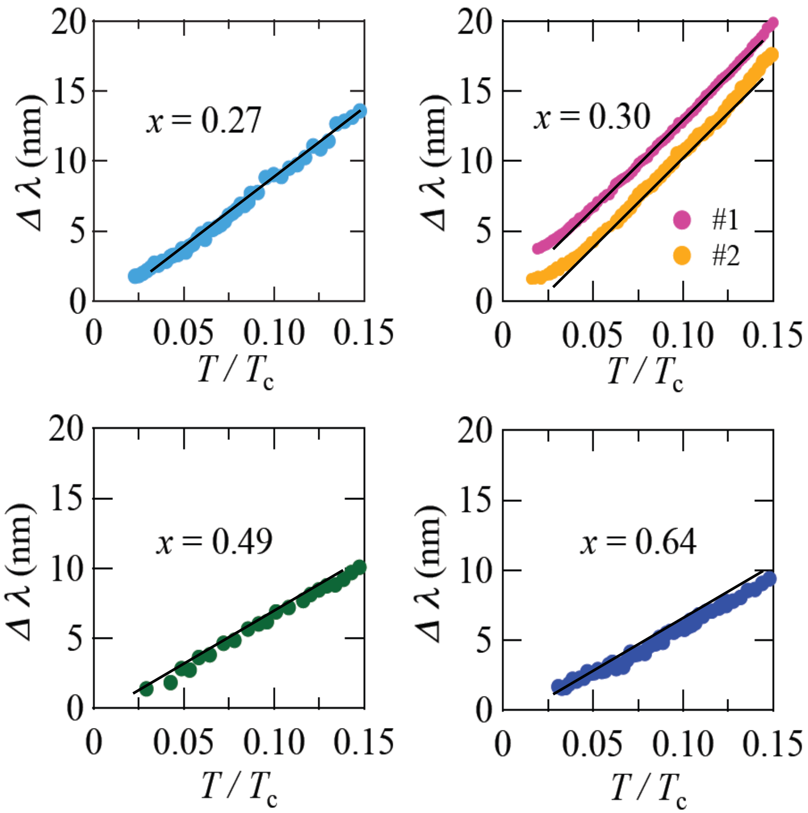

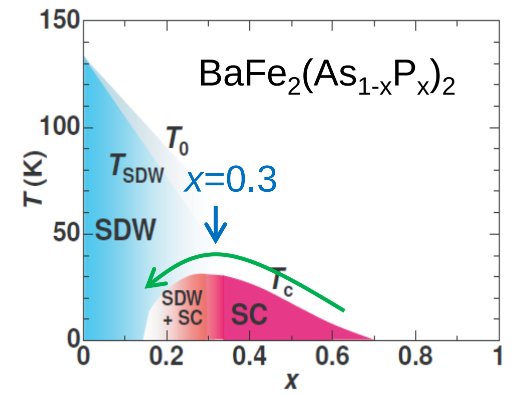

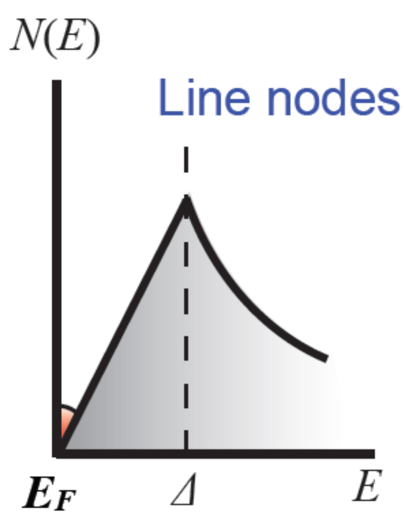

$$\frac{\delta\lambda_L(T)}{\lambda_L(0)} \approx \frac{\ln 2}{\Delta} k_B T$$

$$\lambda_L(0) \approx 2.5 \frac{d\delta\lambda_L(T)}{d(T/T_c)}$$

Error bar of $\lambda_L(0)$ ±10%

Doping evolution of the London penetration depth at T=0

K. Hashimoto *et al*. Science (12)

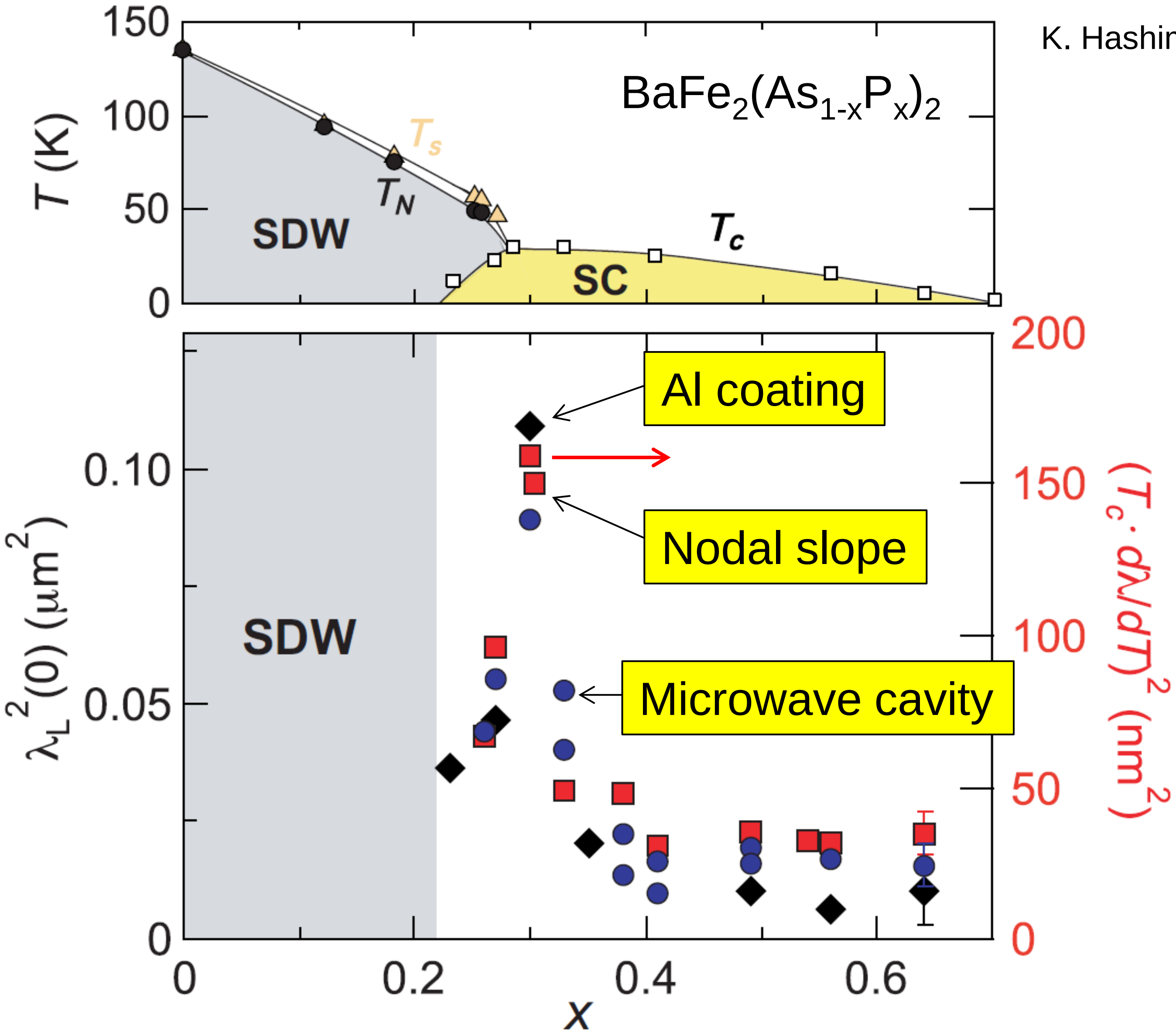

All three methods give very similar x-dependence

Doping evolution of the London penetration depth at T=0

QCP at x=0.3

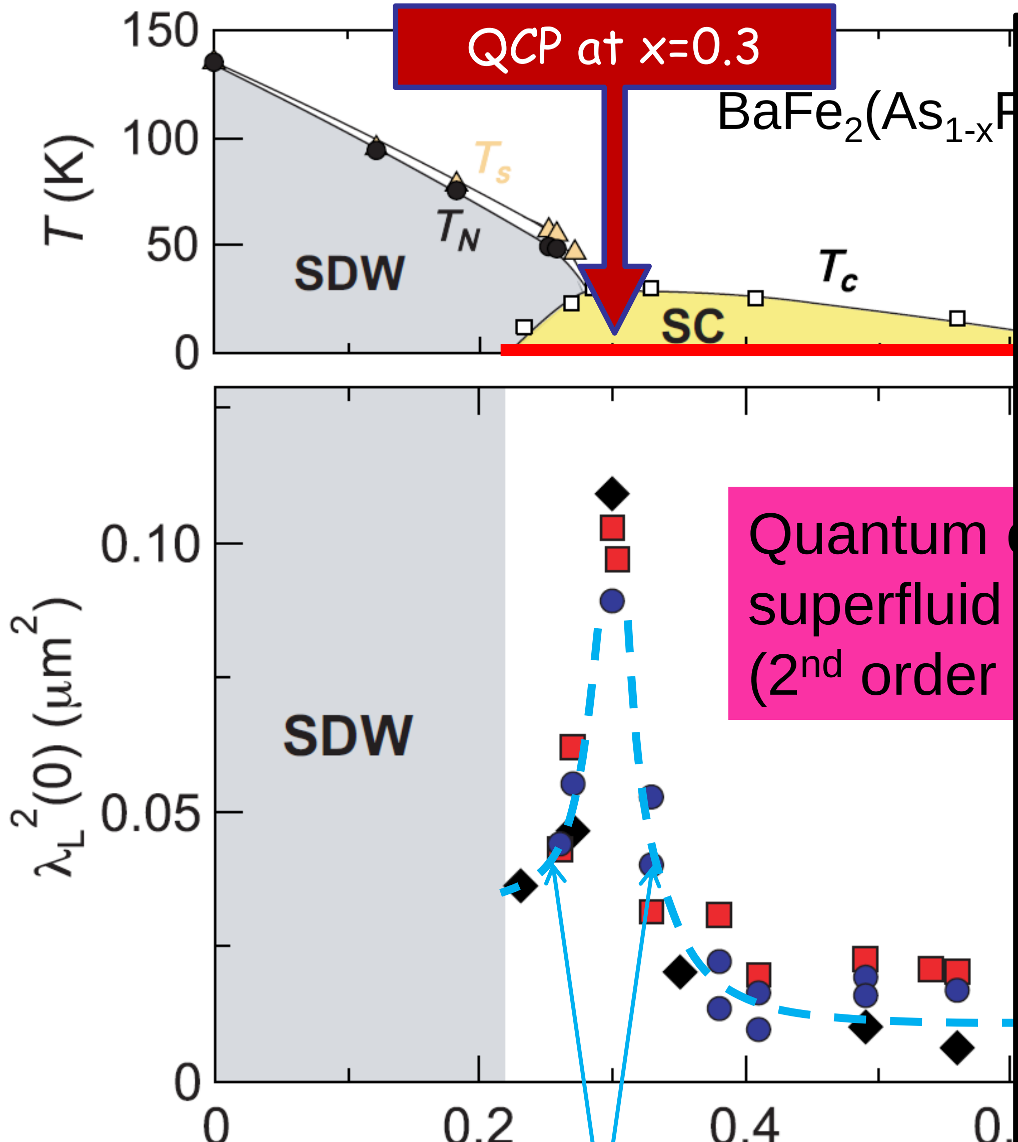

Quantum
superfluid
(2nd order

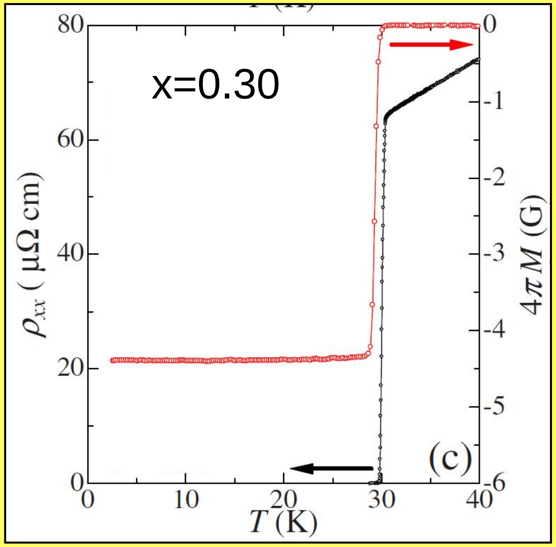

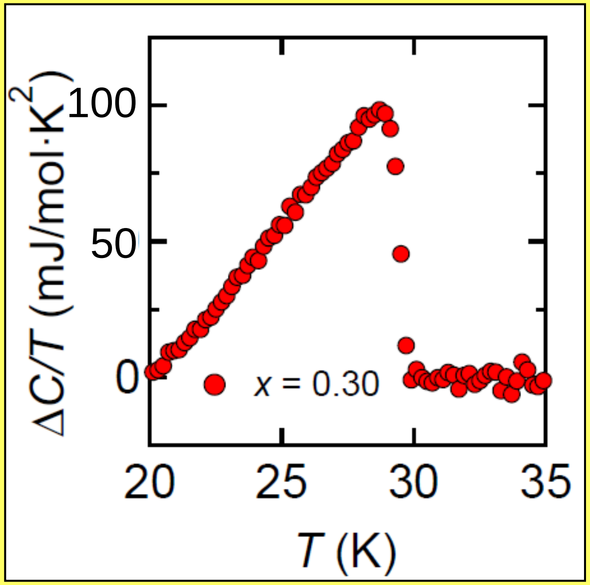

Striking enhancement of $\lambda_L^2(0)$ on approachi

The data represents the behavior at the zero temperature limit.

Singularity of the London penetration depth at QCP

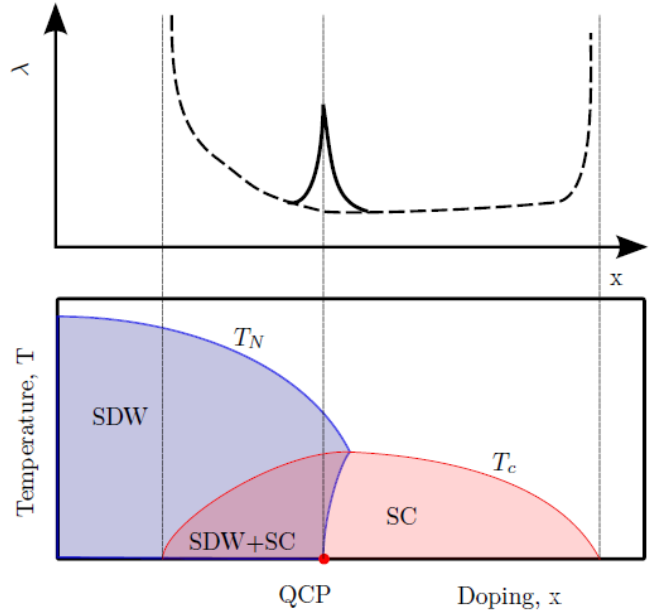

1) Mass renormalization of superfluid by critical magnetic fluctuations

A. Levchenko, M. G. Vavilov, M. Khodas, and A. V. Chubukov, PRL (13)
T. Nomoto and H. Ikeda, PRL (13)

2) SDW fluctuations + nematic order

D.Chowdhury, B. Swingle, E. Berg, and S. Sachdev, PRL (13)

What lies beneath the SC dome?

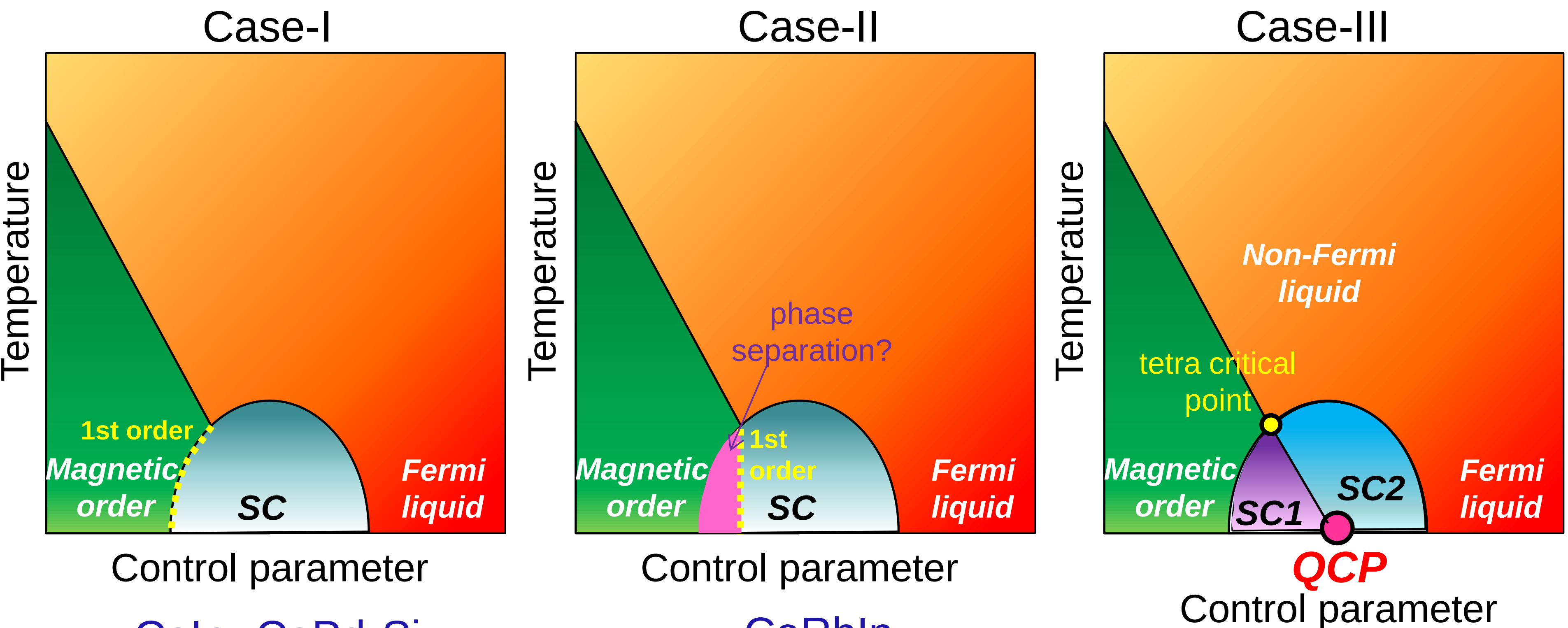

$CeIn_3$, $CePd_2Si_2$

NMR

T. Kawasaki *et al*. J. Phys. Soc. Jpn (04)

$CeRhIn_5$

Specific heat

T. Park *et al*. Nature (06)

G. Knebel *et al*. Phys. Rev. B (06)

$Ba(Fe_{1-x}Ni_x)_2As_2$

Neutron

Xingye Lu *et al*. PRL (13)

$Ba\ (Fe_{1-x}Co_x)_2As_2$

No anomaly in λ_L

$BaFe_2(As_{1-x}P_x)_2$

K. Hashimoto *et al*. Science (12)

QCP lies beneath the dome

Normal electrons

$\rho_{xx}(T) \propto T^{\alpha}$

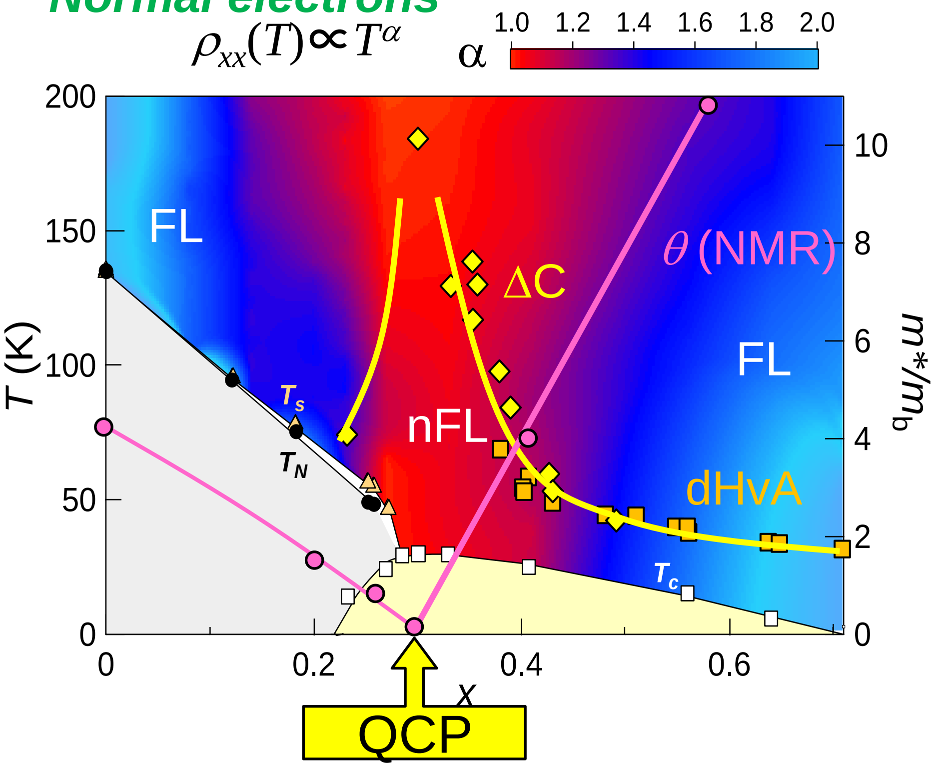

Hallmark of non-Fermi liquid behavior

S. Kasahara *et al*. PRB (10)

Enhancement of normal electron mass

H. Shishido *et al*. PRL (10), P. Walmsley *et al*. PRL(13)

Vanishing of Weiss temperature

Y. Nakai *et al*. PRL (10)

Superconducting electrons

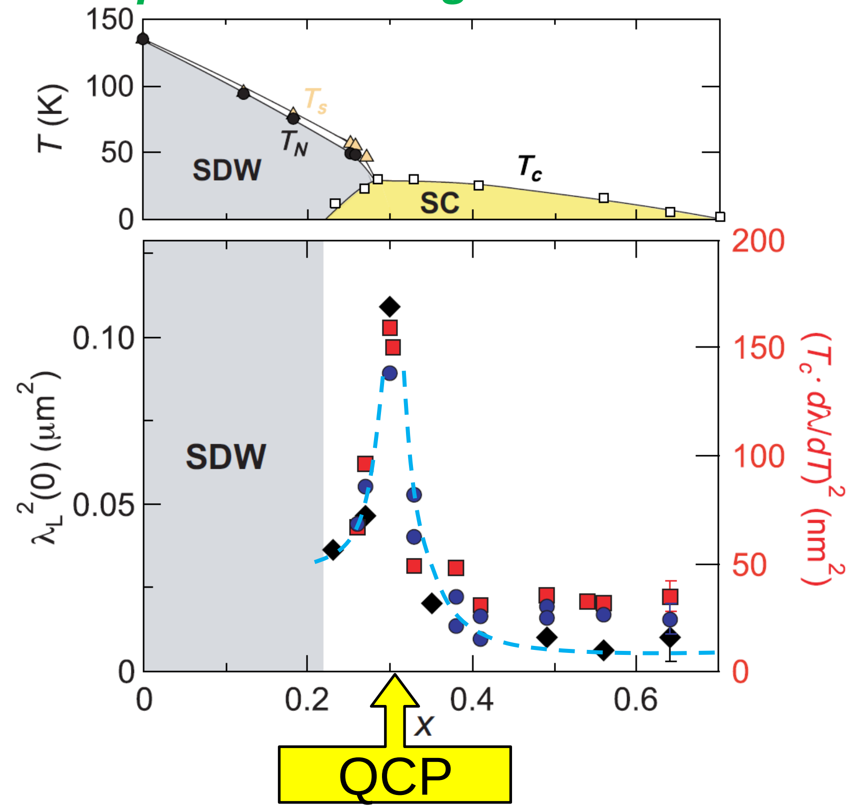

Striking enhancement of superfluid mass

K. Hashimoto *et al*. Science (12), PNAS (13)

QCP lies beneath the superconducting dome

T. Shibauchi, A. Carrington and Y. Matsuda, Annu. Rev. Condens. Matter Phys. 5, 113 (14)

QCP lies beneath the dome

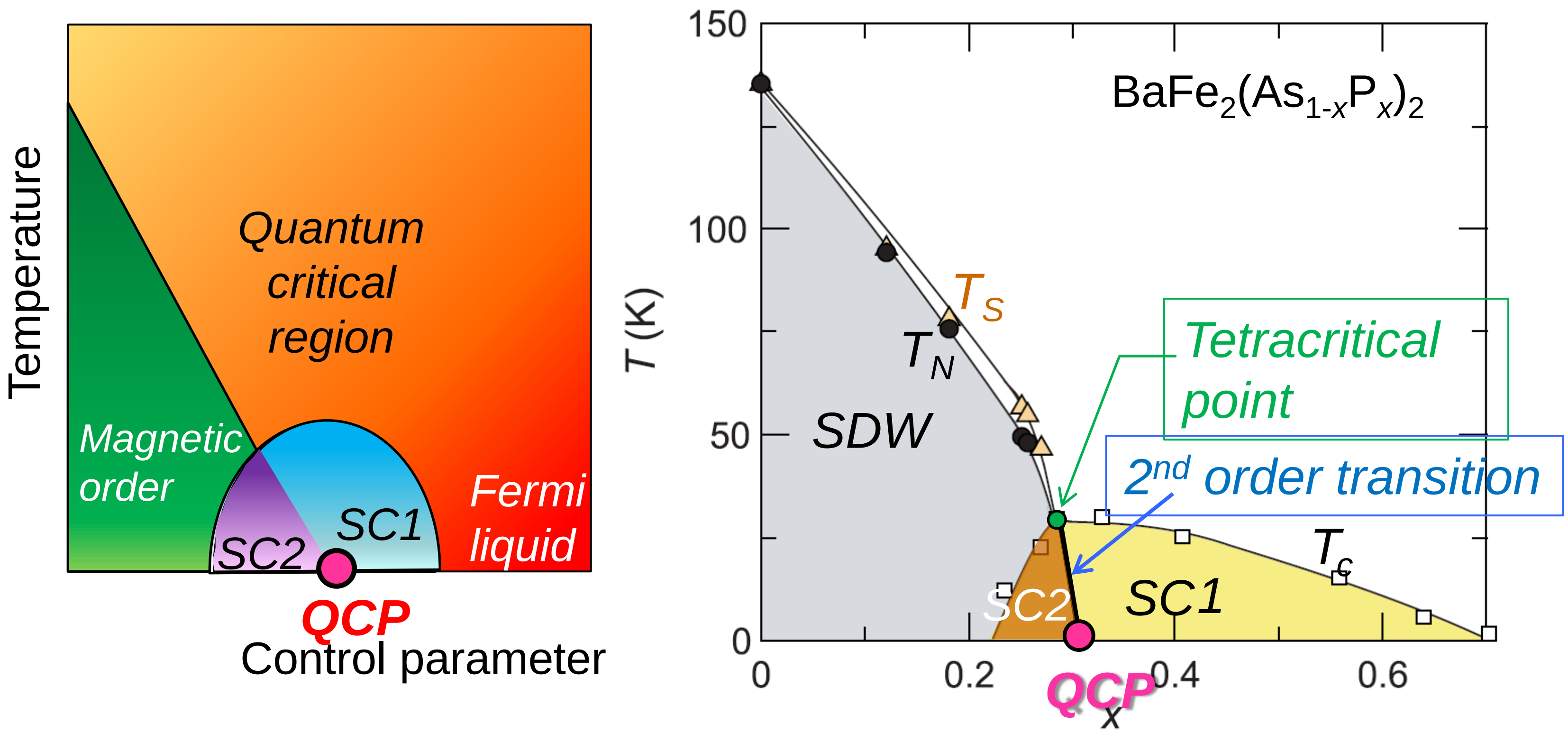

1. The QCP is the origin of the non-Fermi liquid behavior above T_c.

2. Microscopic coexistence of superconductivity and SDW.

3. The quantum critical fluctuations help to enhance the high-T_c superconductivity.

Changes in the phase diagram by point disorder

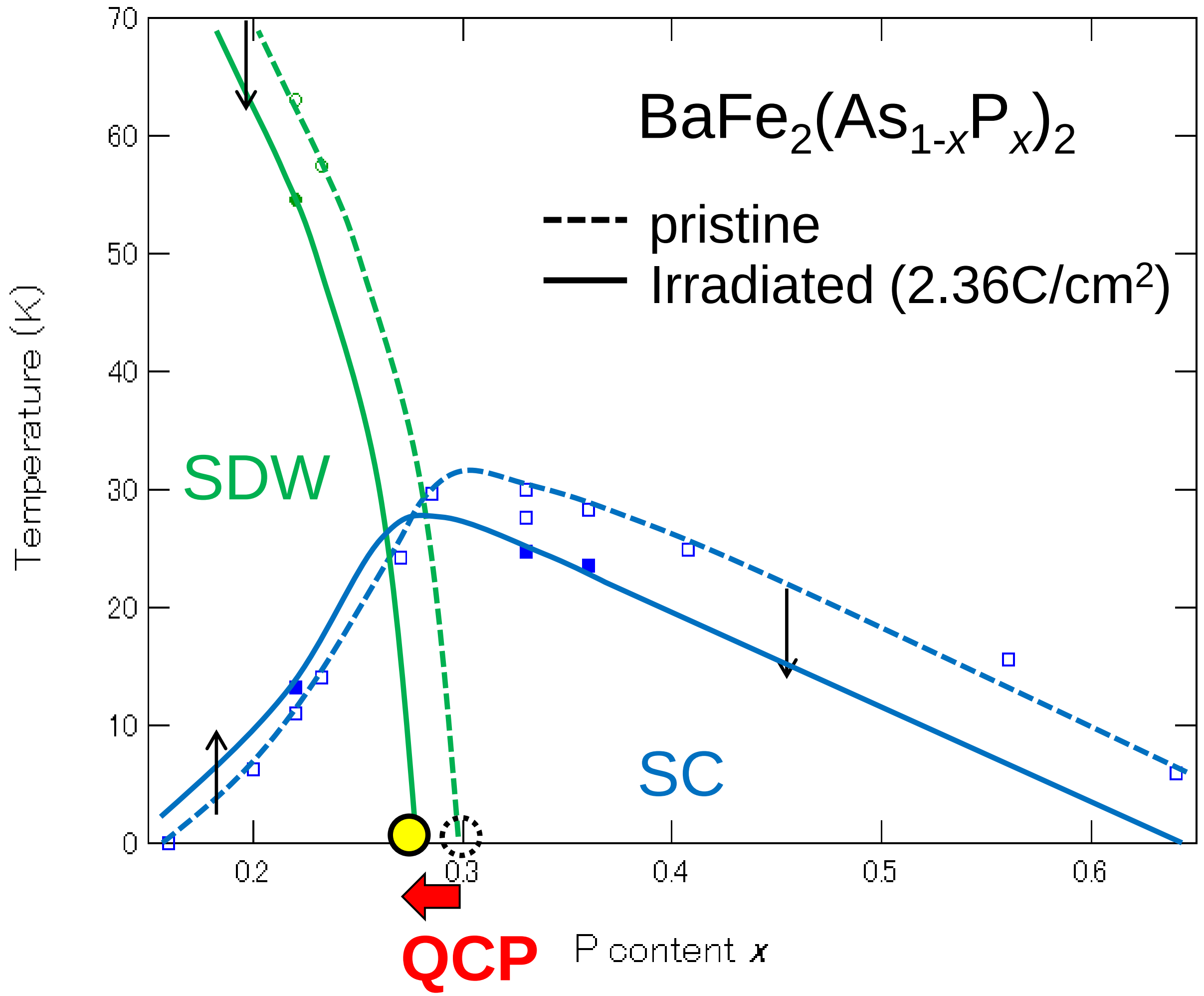

Suppression of SDW moves the QCP toward left, which can consistently explain the shift of SC dome.
A close link between the QCP and SC.

Quantum critical fluctuations are definitely important for the high-T_c superconductivity

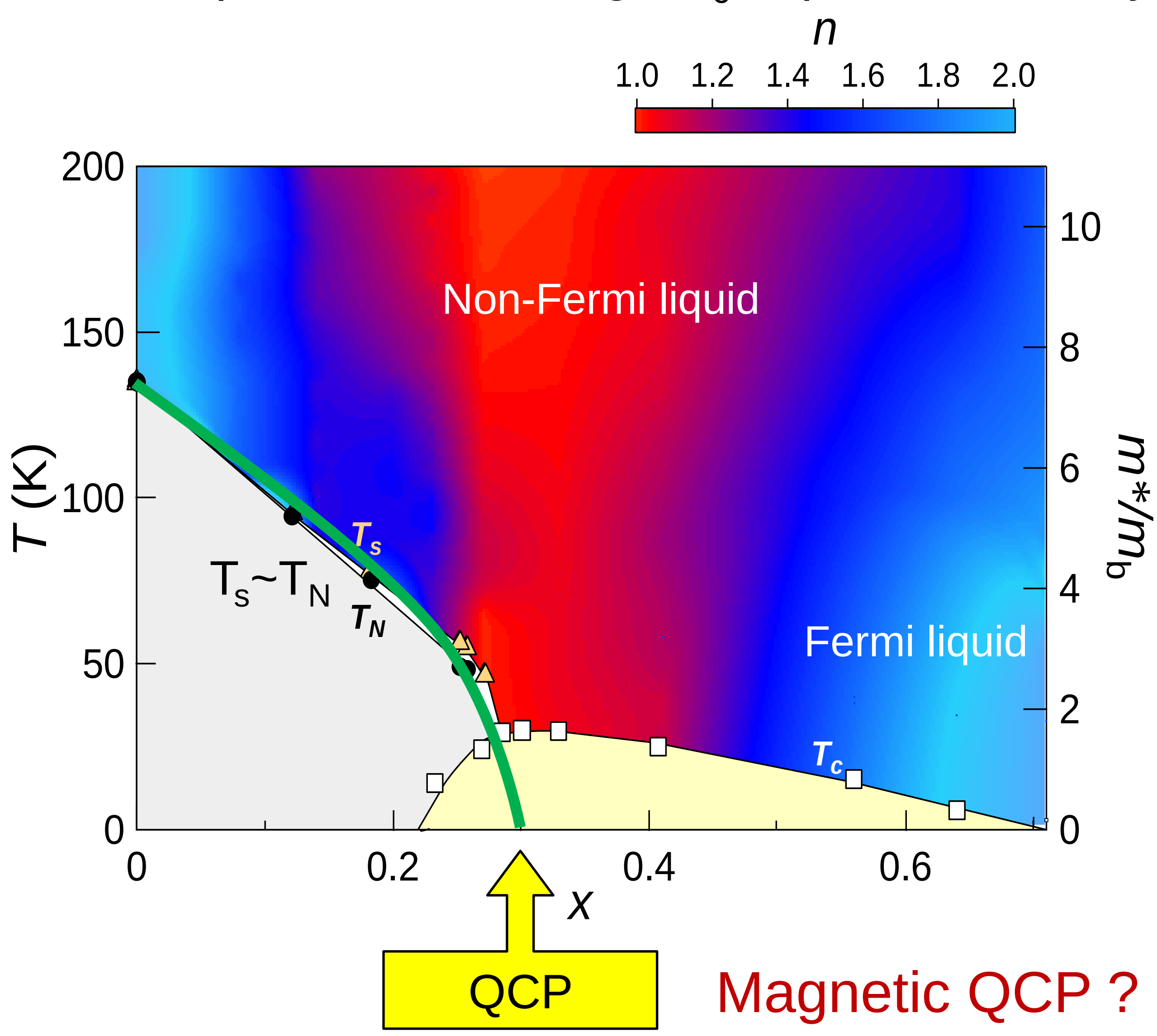

Magnetic QCP ?   orbital QCP?

Doping evolution of the London penetration depth at T=0

$BaFe_2(As_{1-x}P_x)_2$

$Ba(Fe_{1-x}Co_x)_2As_2$

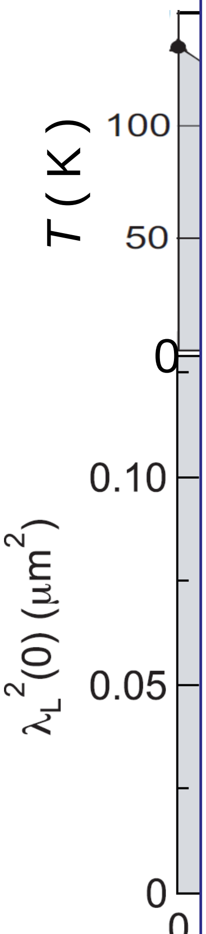

Inhomogeneity?

SC gap map

STM

SC gap map

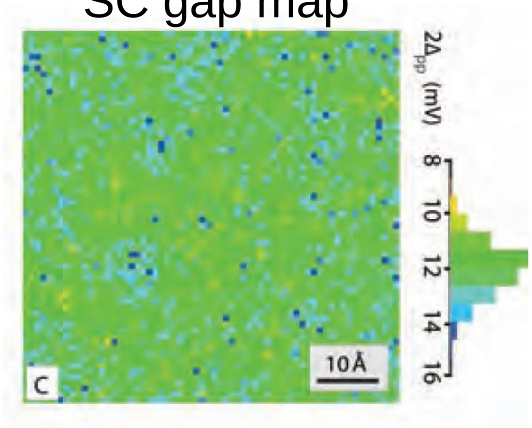

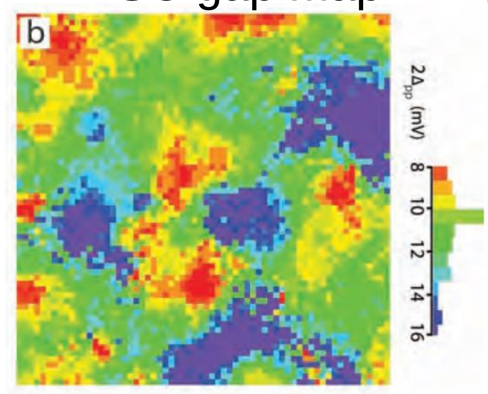

F. Massee, Ph.D thesis, Amsterdam

Gap structure?

Line node

Full gap

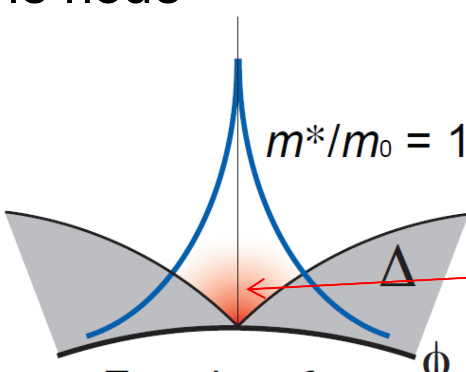

Quantum critical fluctuations

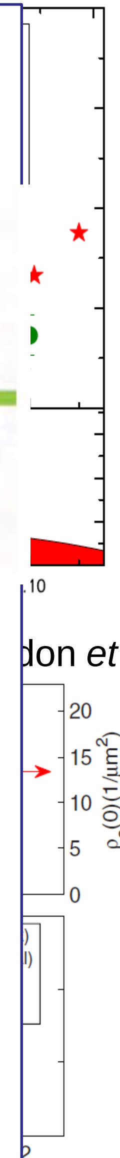

don *et al*. PRB (10)

uan *et al.* PRL (11)

Critical

been re

Doping evolution of the London penetration depth at T=0

$BaFe_2(As_{1-x}P_x)_2$

High-T_c cuprates

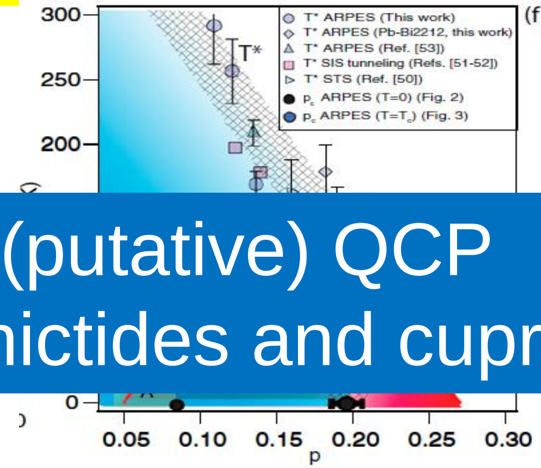

I. M. Vishik *et al*., PNAS (2012).

Superfluid density n_s/m^* at (putative) QCP
Contrasting behavior between pnictides and cuprates

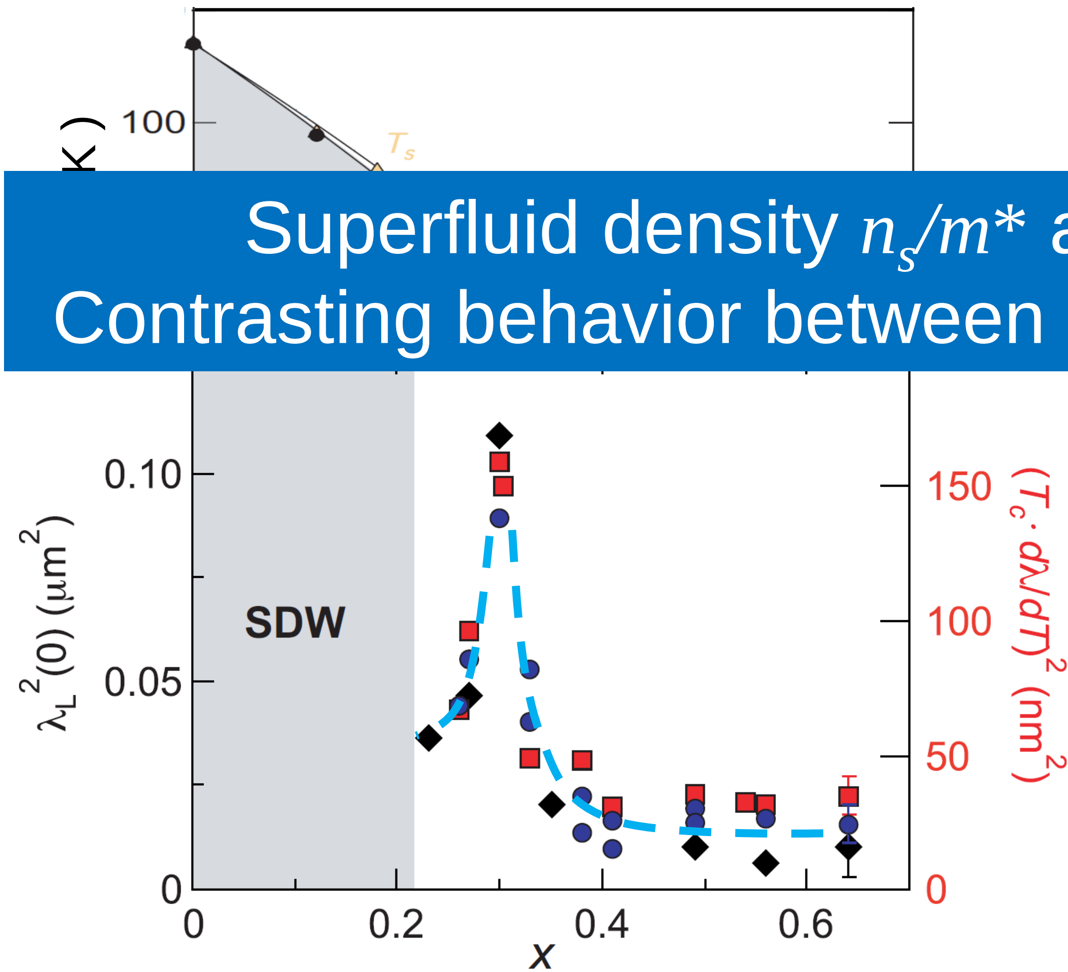

Bi:2212

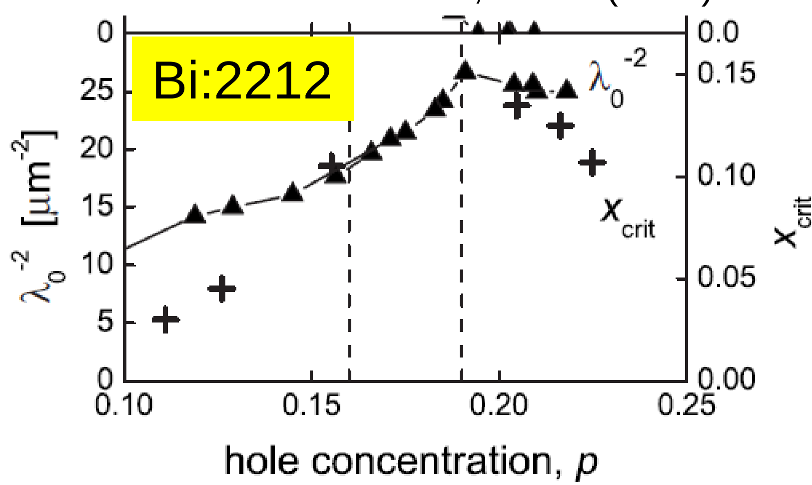

J.G.Storey *et al*. PRB (07)

Bi:2212 : broad maximum in $1/\lambda_L^2(0)$ (enhancement of n_s/m^*) at p~0.19

$BaFe_2(As_{1-x}P_x)_2$: sharp peak in $\lambda_L^2(0)$ (suppression of n_s/m^*) at x=0.3

Physics of iron-based high-T_c superconductors

Selected recent topics

1. Quantum critical point

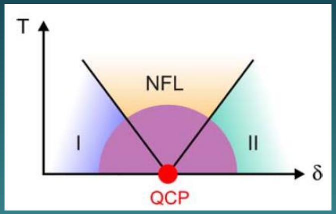

2. BCS-BEC crossover and a novel high field SC phase

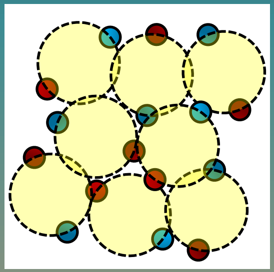

3. Nematicity

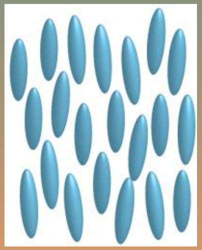

BCS-BEC crossover

M. Randeria, E. Taylor, Annu. Rev. Condens. Matter Phys. (14)

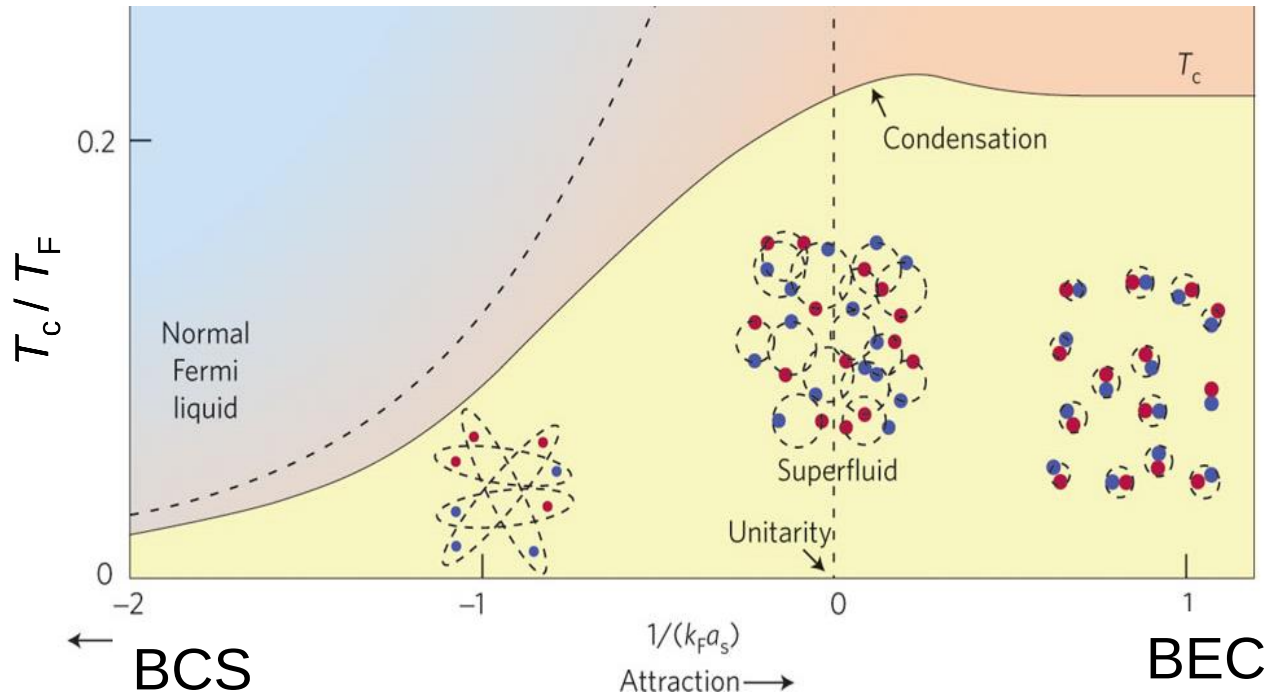

← BCS

BEC

$k_F\xi \gg 1$

$k_F\xi \sim 1$

$k_F\xi \ll 1$

Cooper pairs

strongly interacting pairs

diatomic molecules

$$\frac{\Delta}{\varepsilon_F} \sim \frac{T_c}{T_F} \sim \frac{1}{\xi k_F}$$

Conventional superconductors

$\Delta/\varepsilon_F \sim 10^{-4} - 10^{-5}$

High-T_c cuprates

$\Delta/\varepsilon_F \sim 10^{-2} - 10^{-3}$

Doping evolution of the superfluid density

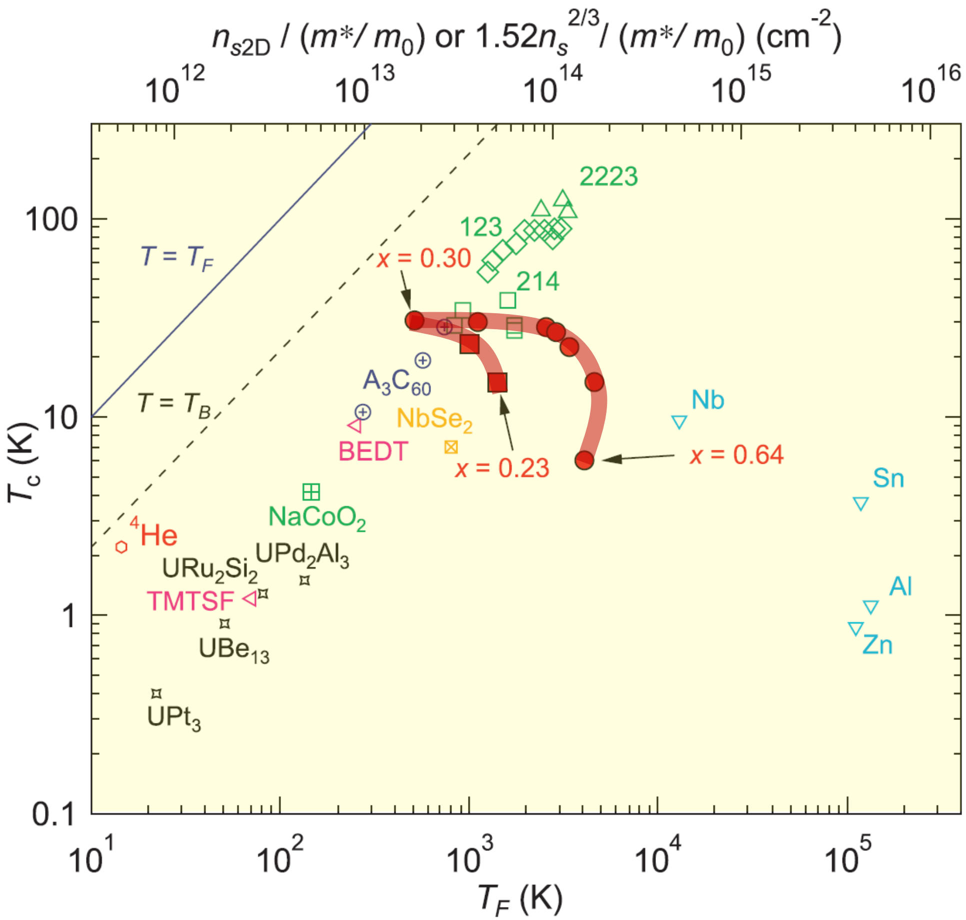

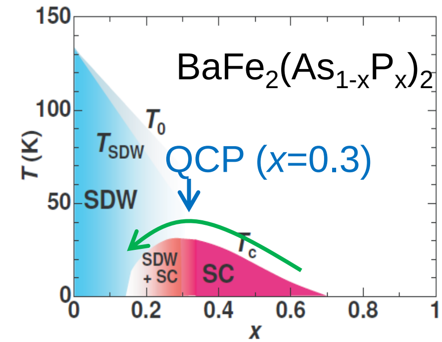

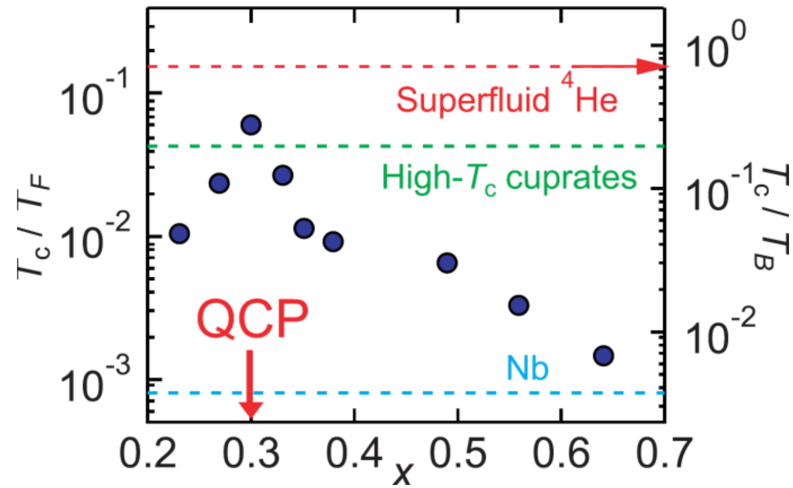

The strongest pairing interaction at the QCP.

High-T_c SC is driven by the QCP

T_c/ T_B=1/4 at the QCP
40% of superfluid ^{4}He

A possible crossover towards the BEC driven by quantum criticality

Fe-based high-T_c superconductors

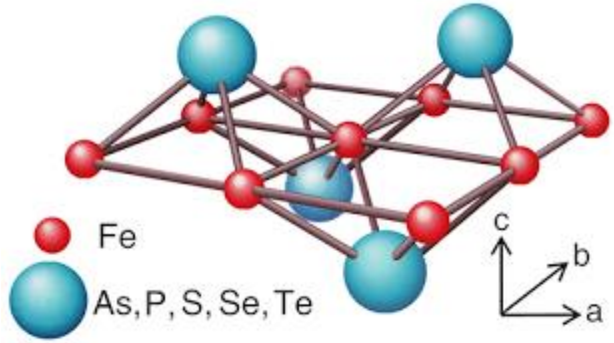

42622

(32522)

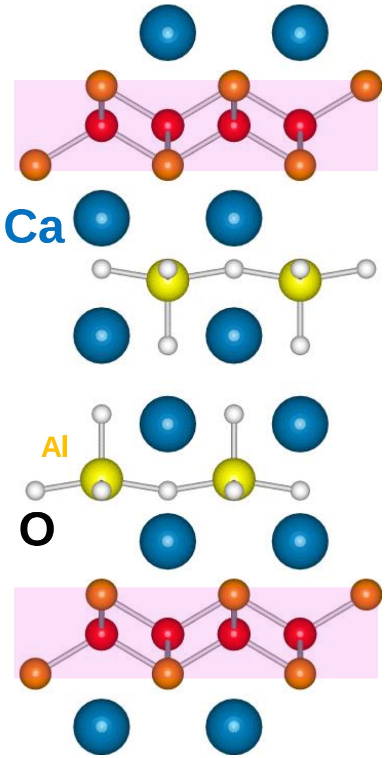

$(A_4M_2O_6)\ Fe_2As_2$

T_c(max)=47K

Zhu et al.(2009)

Ogino et al. (2009)

1111

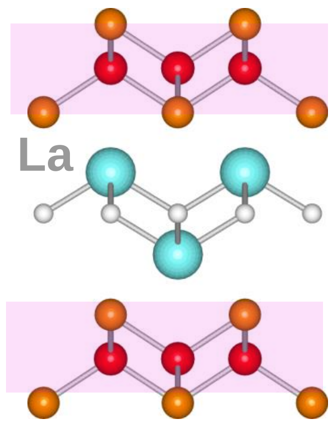

Ln FeAsO

T_c(max)=55K

Y. Kamihara et al.(2008)

122

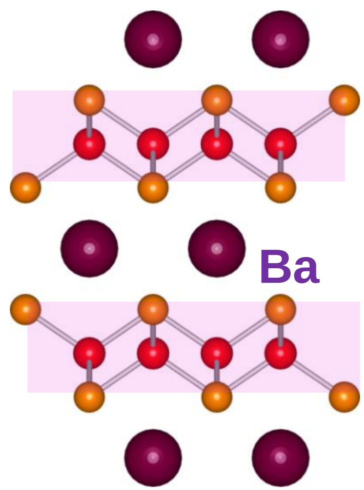

$BaFe_2As_2$

T_c(max)=38K

M. Rotter et al.(2008)

111

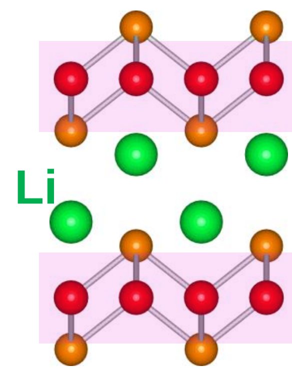

LiFeAs

T_c= 18 K

X.C.Wang et al.(2008)

11

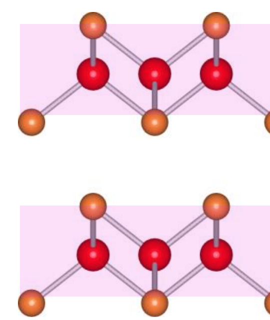

FeSe

T_c= 9 K

F.C.Hsu et al.(2008)

FeSe: A candidate system near BCS-BEC crossover

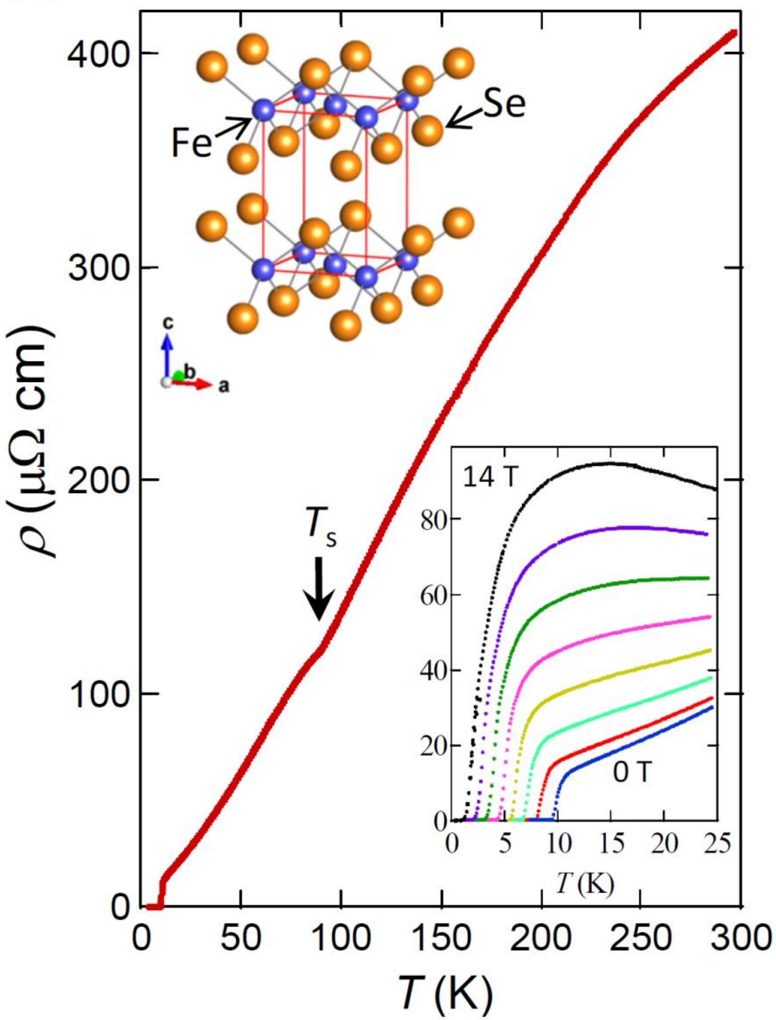

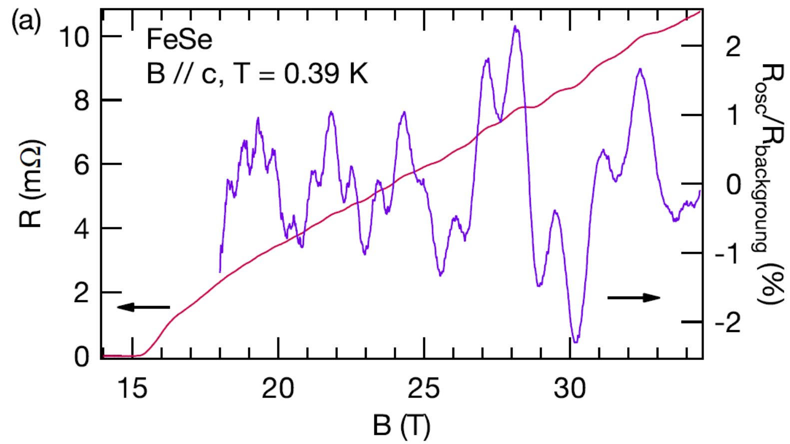

✓ 1:1 stoichiometry within experimental error

A. Böhmer et al. PRB (2013).

✓ Small residual resistivity & large RRR

✓Large magnetoresistance, SdH oscillations

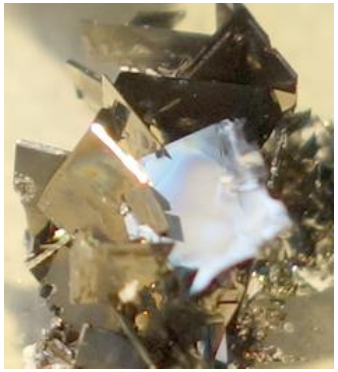

High quality single crystals of FeSe

STM topographic image of FeSe

+95 mV/100 pA $T \sim 0.4$ K

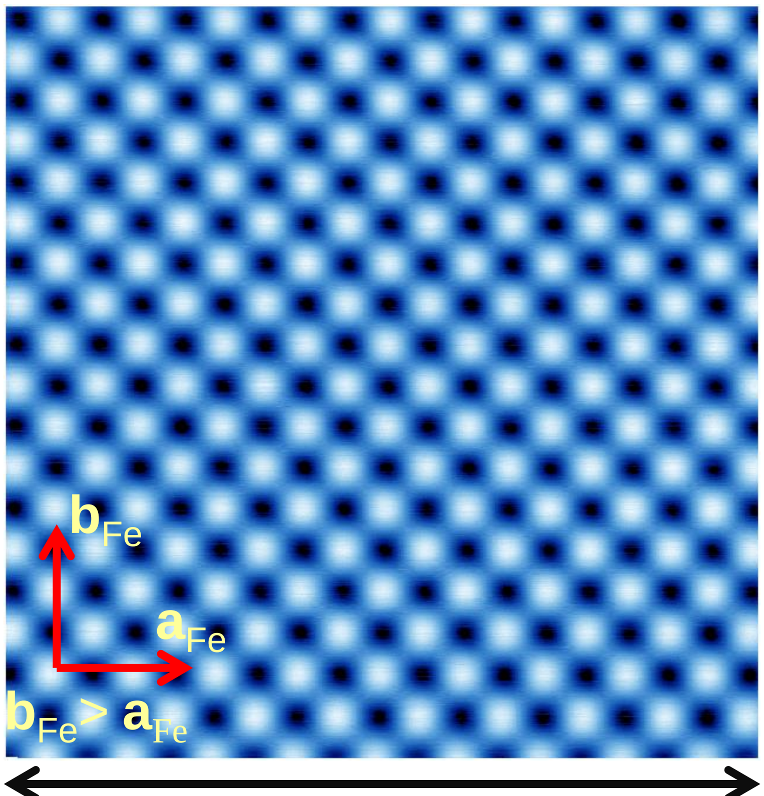

5 nm

+95 mV/100 pA $T \sim 1.5$ K

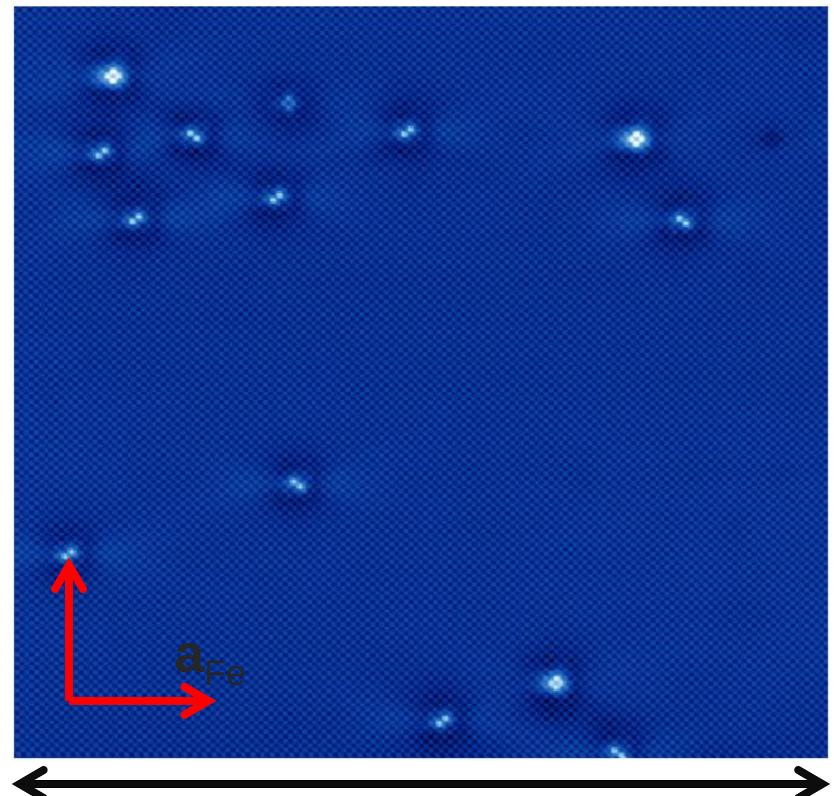

45 nm

- ✓ Surface Se lattice
- ✓ Low defect density (< 1/ 5,000 unit cells) Extremely clean Xtals

Extremely small Fermi energy : QPI

Band dispersion curves obtained by
QPI (Quasi Particle Interference) of STM

S. Kasahara *et al.*,

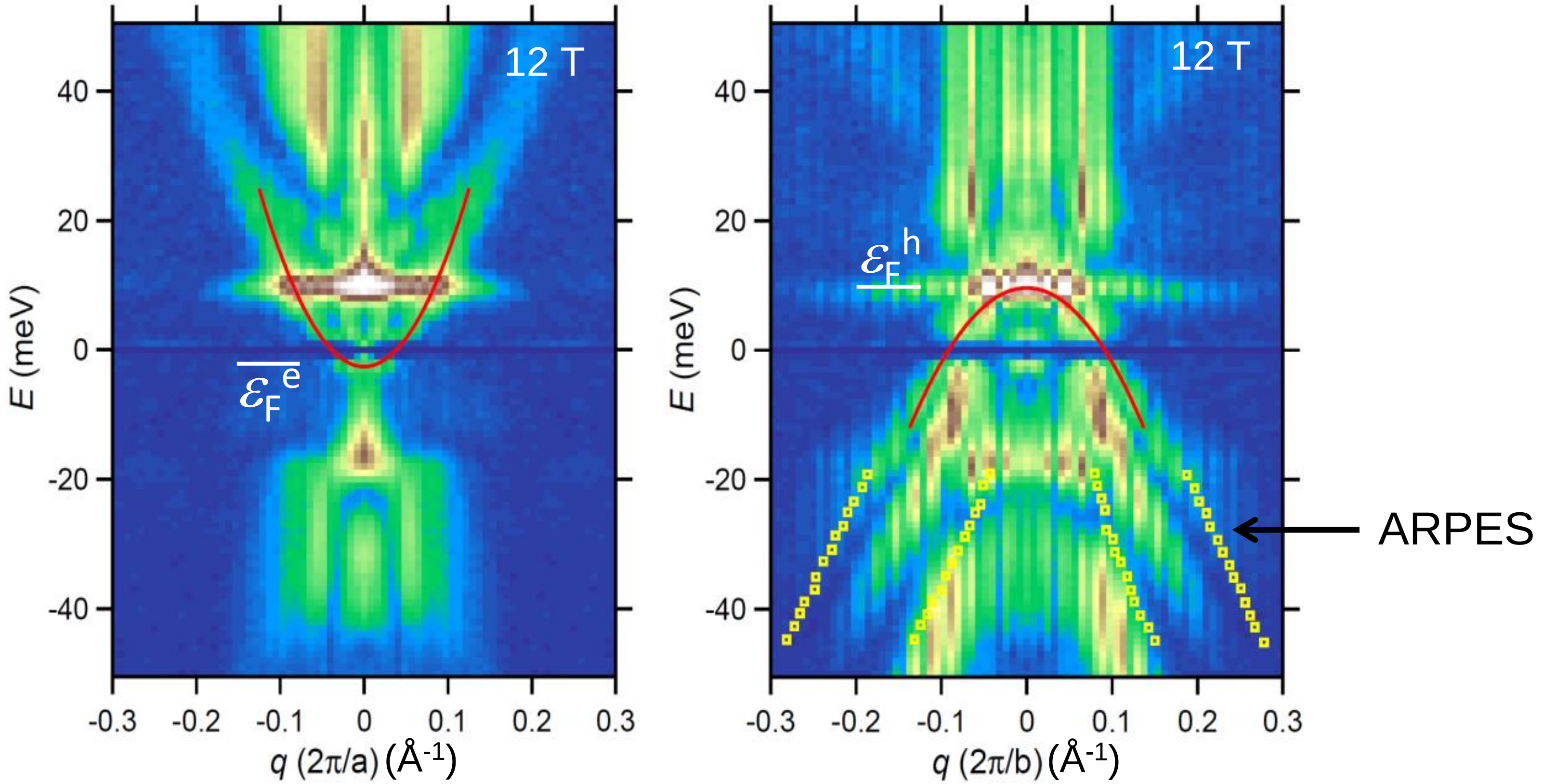

Electron band

$\varepsilon_F \sim 3$ meV

Hole band

$\varepsilon_F \sim 10$ meV

Extremely small Fermi energy: Quamtum oscillations

T. Terashima et al., arXiv.1405.7749.

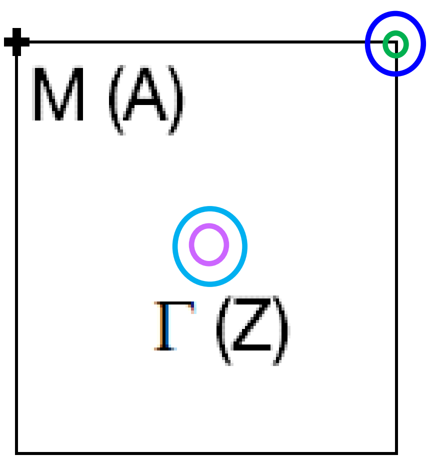

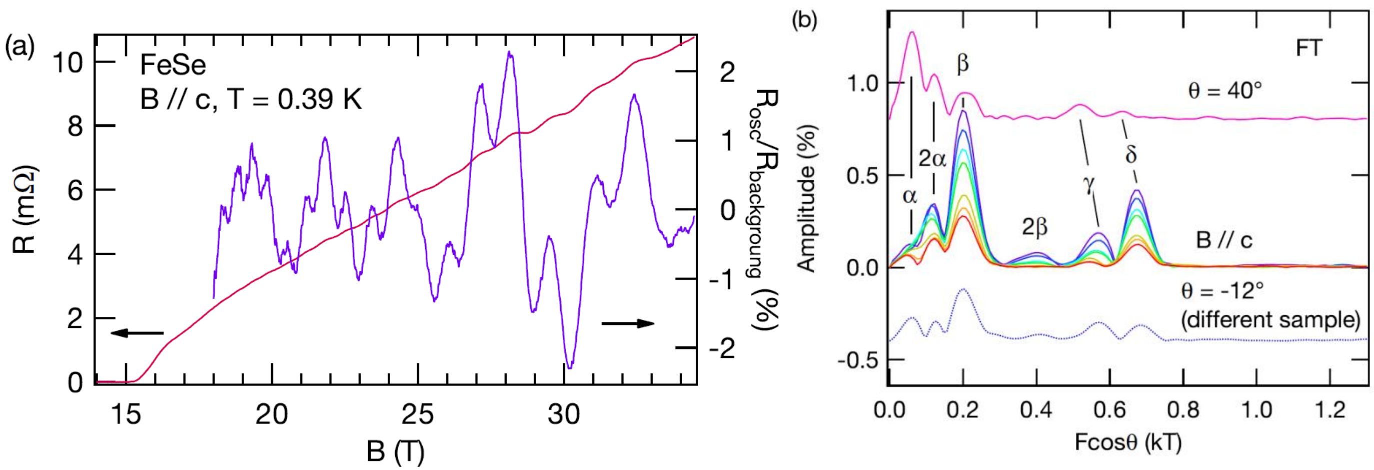

Only two Fermi surface sheets

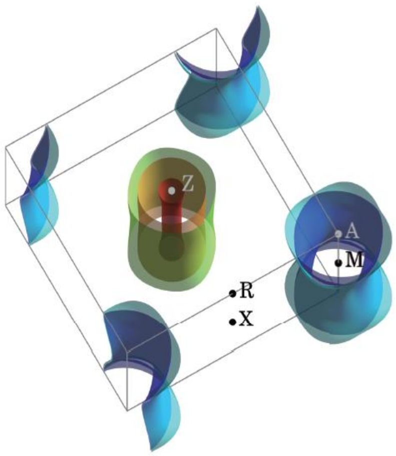

LDA

Branch	F (kT)	m^*/m_e	A (%BZ)	k_F (Å^{-1})	E_F (meV)
α[a]	0.06	1.9(2)	0.20	0.043	3.5
β	0.20	4.5(5)	0.69	0.078	5.1
γ	0.57	7.0(7)	2.0	0.13	9.4
δ	0.67	4.8(5)	2.3	0.14	16

✓ Extremely small Fermi surface and Fermi energy.

Extremely small Fermi energy

Seebeck coefficient

$$S/T = \pm \frac{\pi^2}{2}\frac{k_B}{e}\frac{1}{T_F}$$

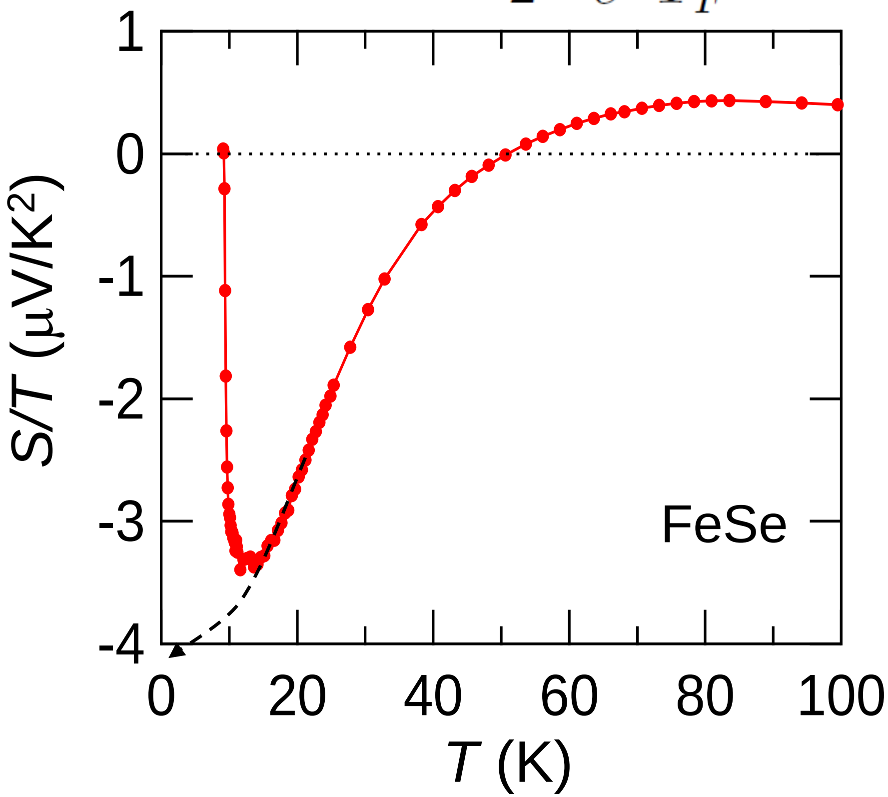

T_F ~100 K

(The upper limit for the electron band)

Penetration depth

$$\varepsilon_F = \frac{\pi\hbar^2 d}{\mu_0 e^2}\lambda_L^{-2}(0)$$

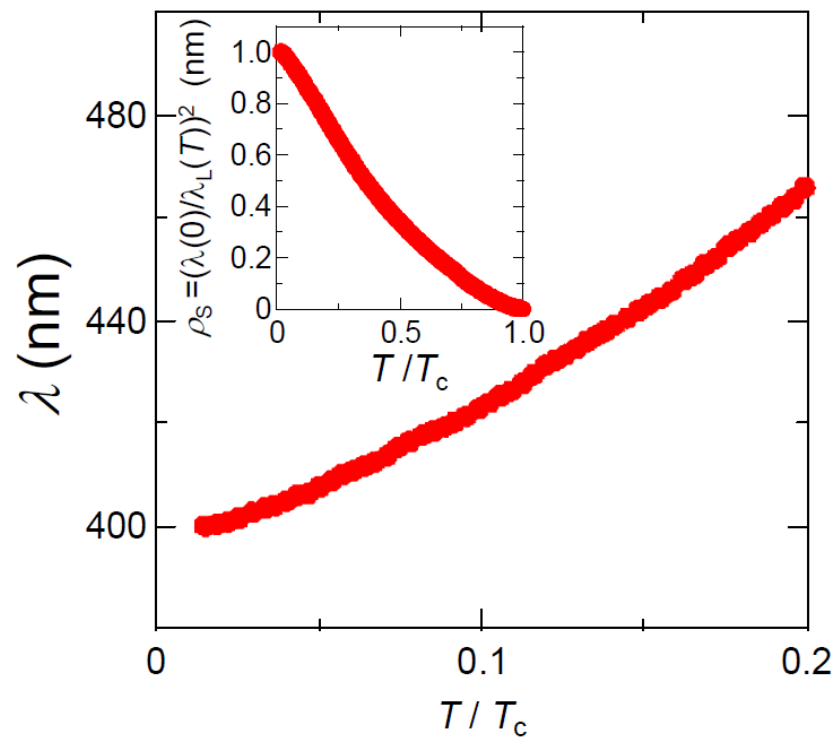

T_F ~100 K

A possible BCS-BEC crossover regime, $\varepsilon_F \sim \Delta$

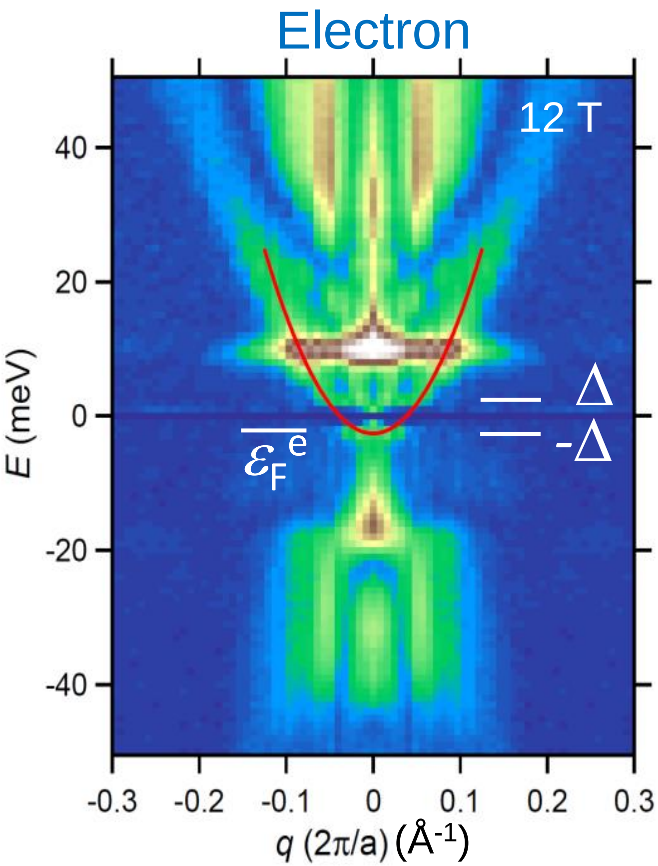

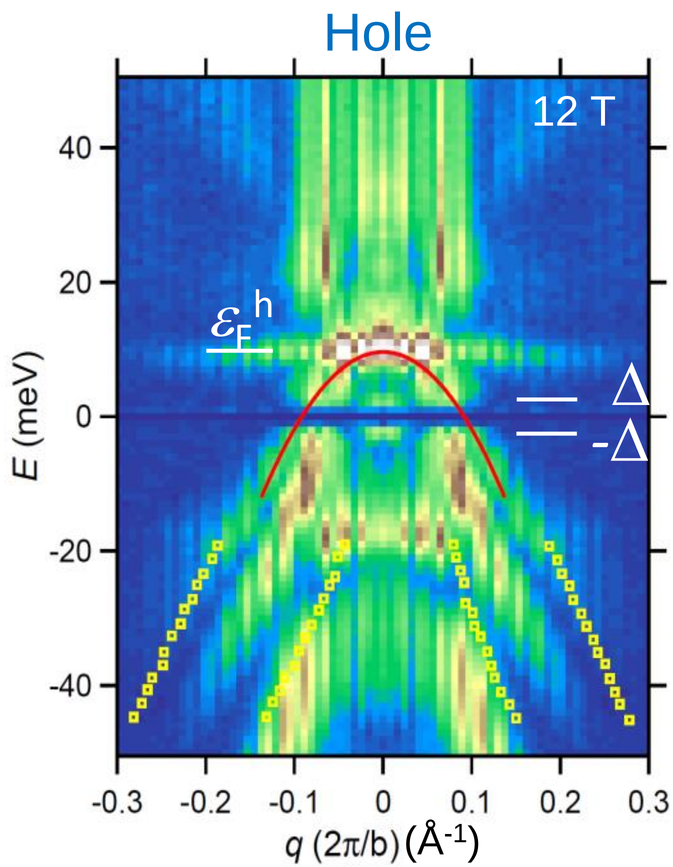

$\Delta \sim 2.5$ meV

Conventional superconductors

$\Delta/\varepsilon_F \sim 10^{-4} - 10^{-5}$

High-T_c cuprates

$\Delta/\varepsilon_F \sim 10^{-2} - 10^{-3}$

$\Delta/\varepsilon_F^{\,e} \sim 1$

$\Delta/\varepsilon_F^{\,h} \sim 0.3$

Never realized in any other superconductors!

cf. Cold atoms

BCS-BEC crossover

FeSe is in the BCS-BEC crossover regime
Close to unitary Fermi gas?

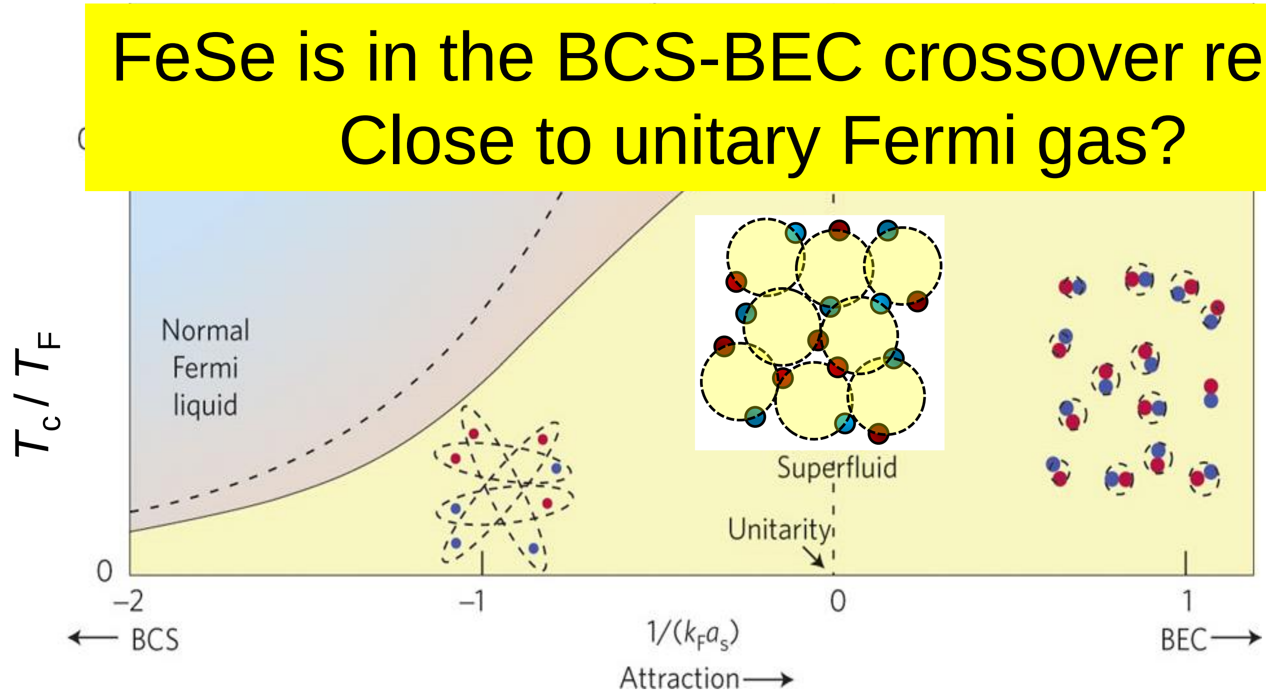

M. Randeria, E. Taylor, Annu. Rev. Condens. Matter Phys. (14)

BCS		BEC
$k_F\xi \gg 1$	$k_F\xi \sim 1$	$k_F\xi \ll 1$
Cooper pairs	strongly interacting pairs	diatomic molecules

$$\frac{\Delta}{\varepsilon_F} \sim \frac{T_c}{T_F} \sim \frac{1}{\xi k_F}$$

FeSe $\Delta/\varepsilon_F^e \sim 1$

$\Delta/\varepsilon_F^h \sim 0.3$

Conventional superconductors
$\Delta/\varepsilon_F \sim 10^{-4}$ - 10^{-5}

High-T_c cuprates
$\Delta/\varepsilon_F \sim 10^{-2}$ - 10^{-3}

A new high-field superconducting phase

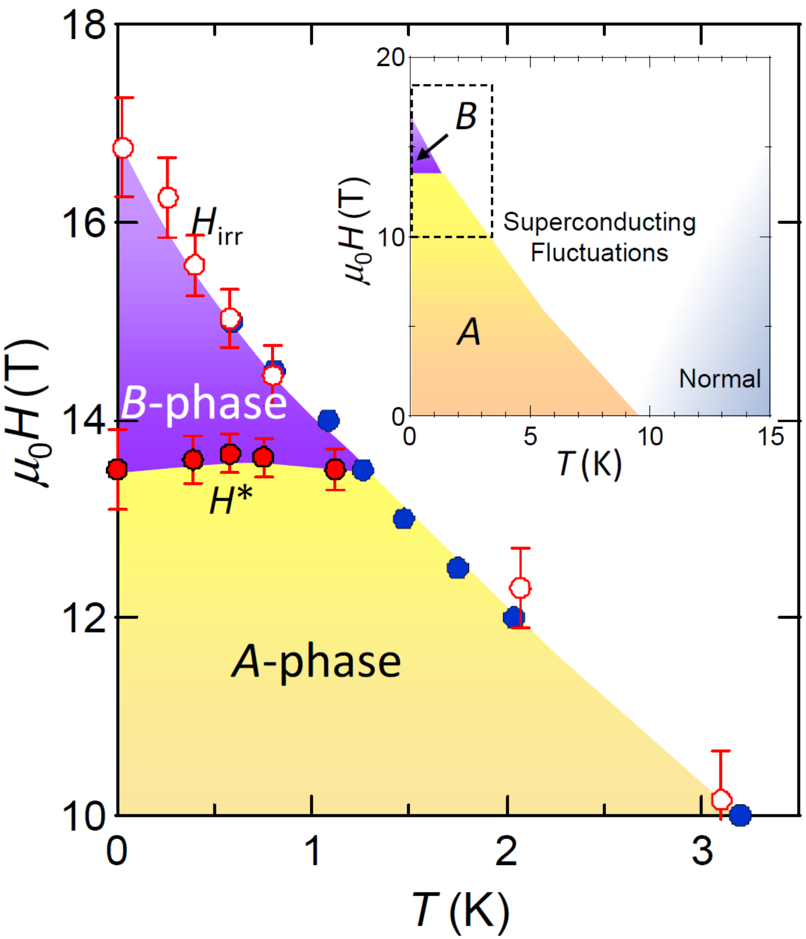

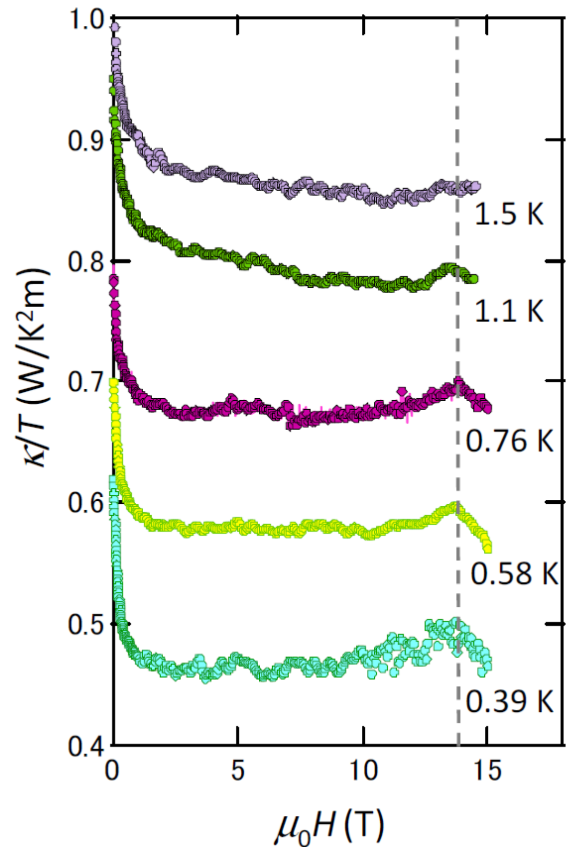

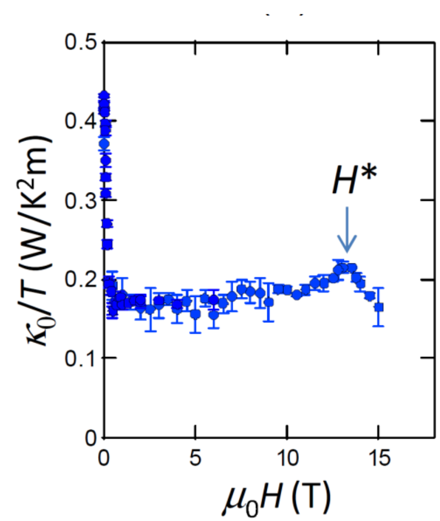

$$\varepsilon_F \sim \Delta \sim \mu_B H$$

Fermi ~ Gap ~ Zeeman

B-phase is induced by strong spin imbalance of the unitary Fermi gas

A new high-field superconducting phase

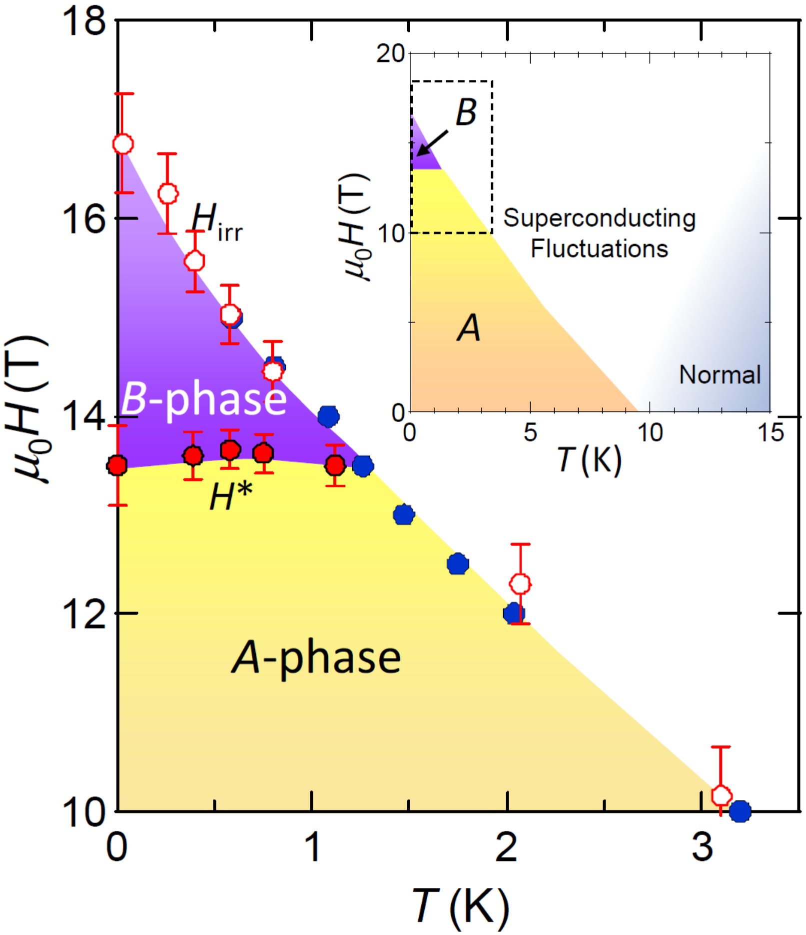

$$\varepsilon_F \sim \Delta \sim \mu_B H$$

Fermi ~ Gap ~ Zeeman

Highly spin-polarized phase

FFLO state ?

(k↑,-k+q↓)

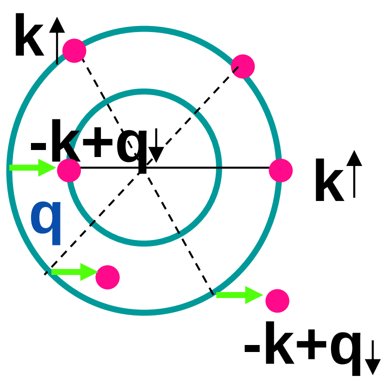

pairing between Zeeman split parts of the Fermi surface

$$\Delta(\mathbf{r}) = \Delta_0 \cos(\mathbf{q} \cdot \mathbf{r})$$

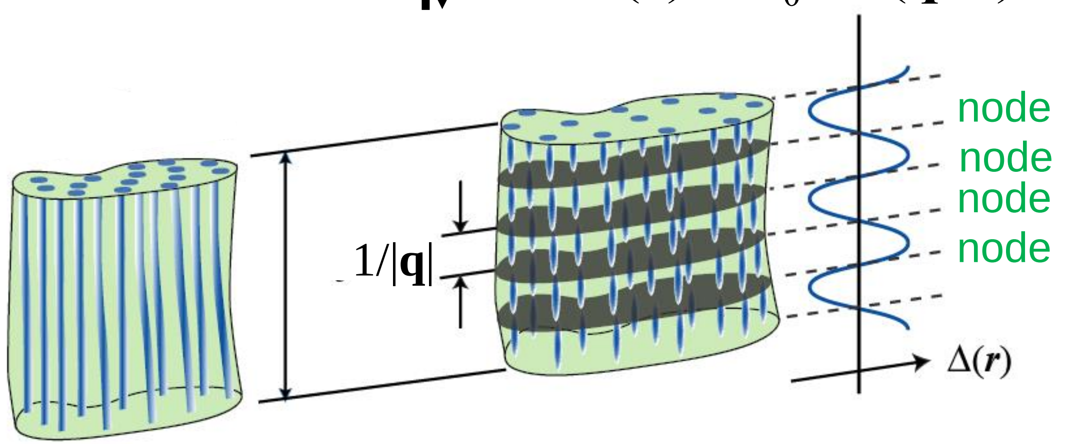

High-T_c superconductivity in single layer FeSe

High-T_c superconductivity in FeSe

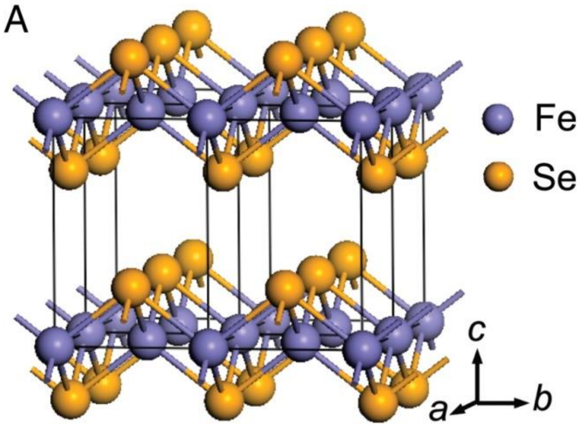

F.-C. Hsu *et al.*,
PNAS **105**, 14262 (2008).

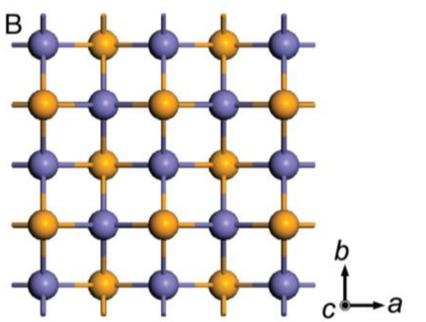

FeSe/$SrTiO_3$

ARPES

1 Monolayer

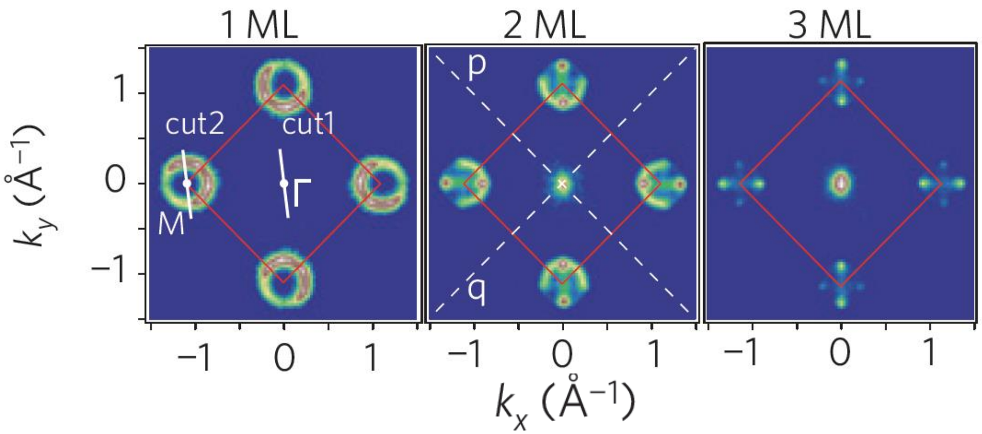

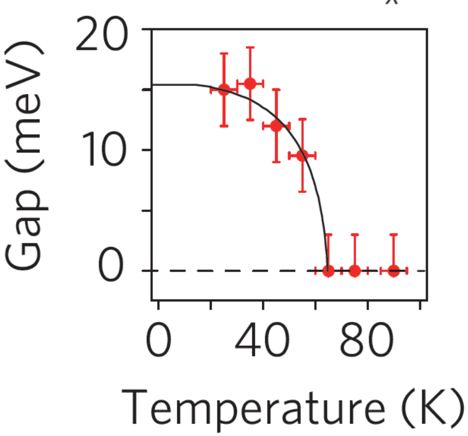

T_c=65K??

S.Tan *et al*. Nature Mat. 12, 634 (2013).

High-T_c superconductivity in FeSe

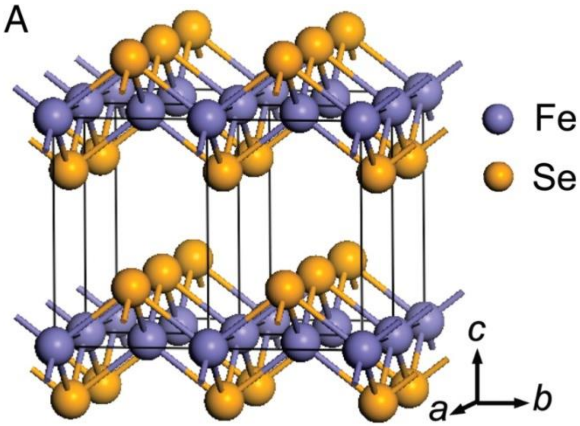

F.-C. Hsu *et al.*,
PNAS **105**, 14262 (2008).

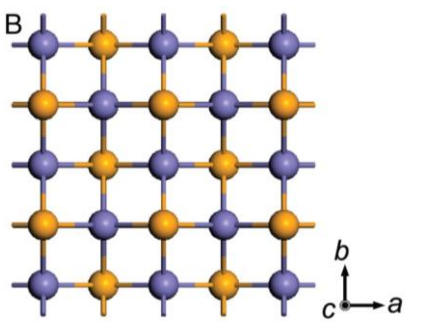

Superconductivity in single-layer films of FeSe with a transition temperature above 100 K

Jian-Feng Ge[1], Zhi-Long Liu[1], Canhua Liu[1]*, Chun-Lei Gao[1], Dong Qian[1], Qi-Kun Xue[2]*, Ying Liu[1,3], Jin-Feng Jia[1]*

arXiv:1406.3435

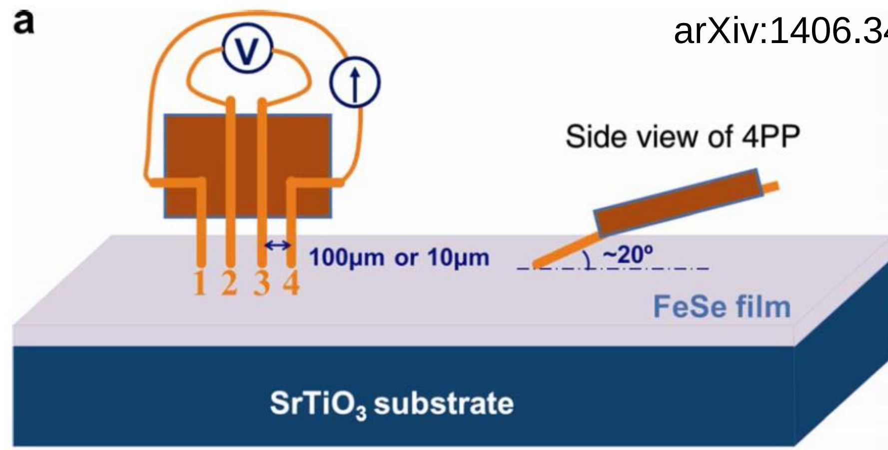

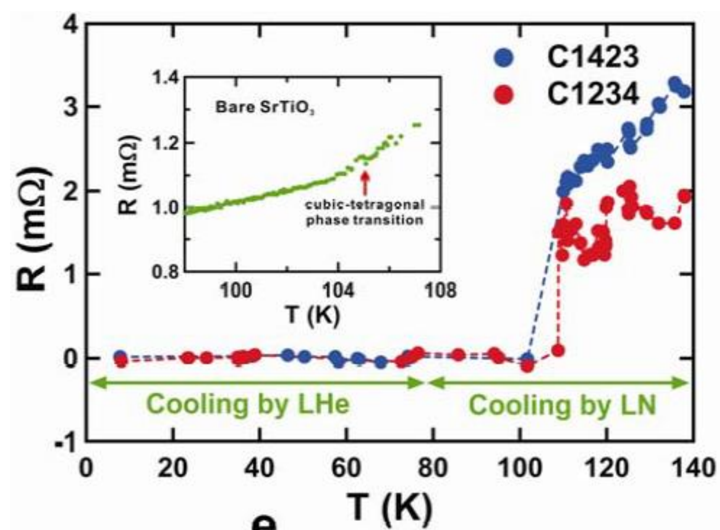

T_c=110 K????

Physics of iron-based high-T_c superconductors

Selected recent topics

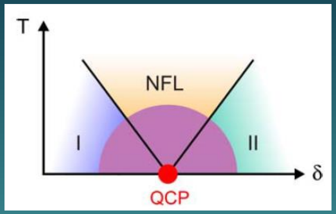

1. Quantum critical point

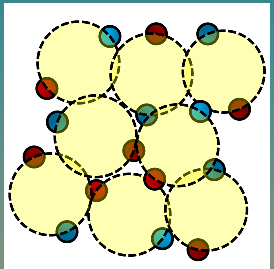

2. BCS-BEC crossover and a novel high field SC phase

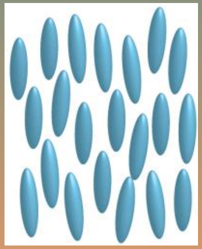

3. Nematicity

Experiments suggesting in-plane anisotropy at $T>T_s$

★**Resistivity** J. Chu *et al*. Science (10). **Detwinned by uniaxial pressure**

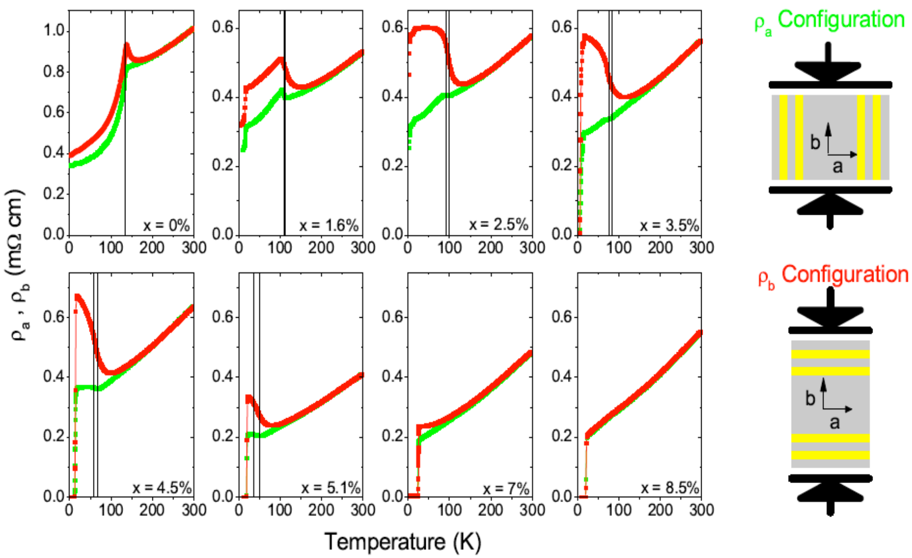

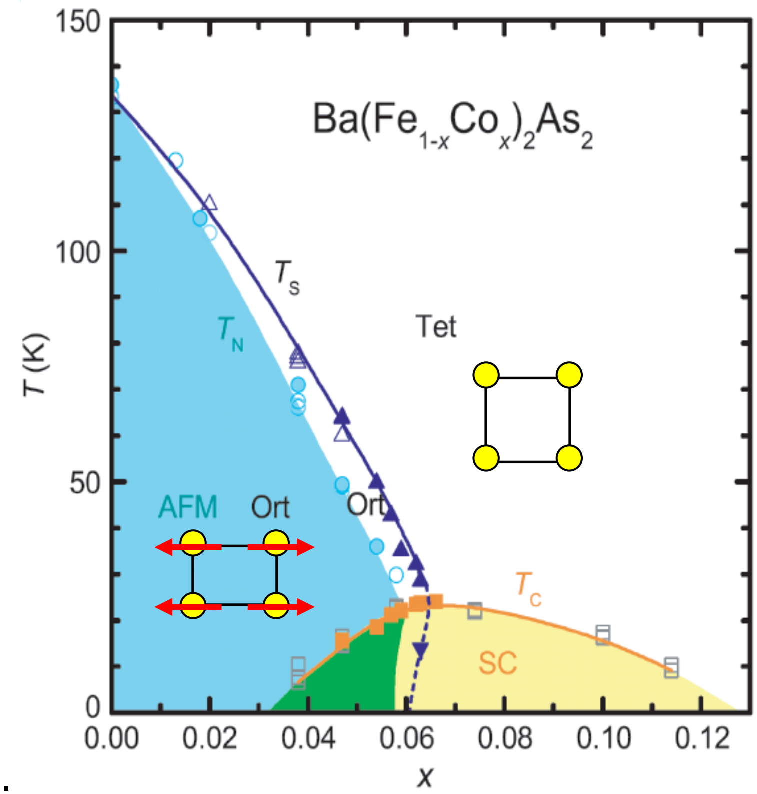

$\rho_b > \rho_a$ **above** T_s

★ **Optical Conductivity** A. Dusza *et al*., EPL (11).
M. Nakajima *et al*., PNAS (11).

★ **Neutron** J. Zhao *et al*., Nature Phys. (09).
L. W. Harriger *et al*. PRB (11).

★ **X-Ray** E.C. Blomberg *et al*. PRB (12)

Experiments suggesting in-plane anisotropy at $T>T_s$

Detwinned by uniaxial pressure

★ **ARPES** M. Yi *et al*., PNAS (11).

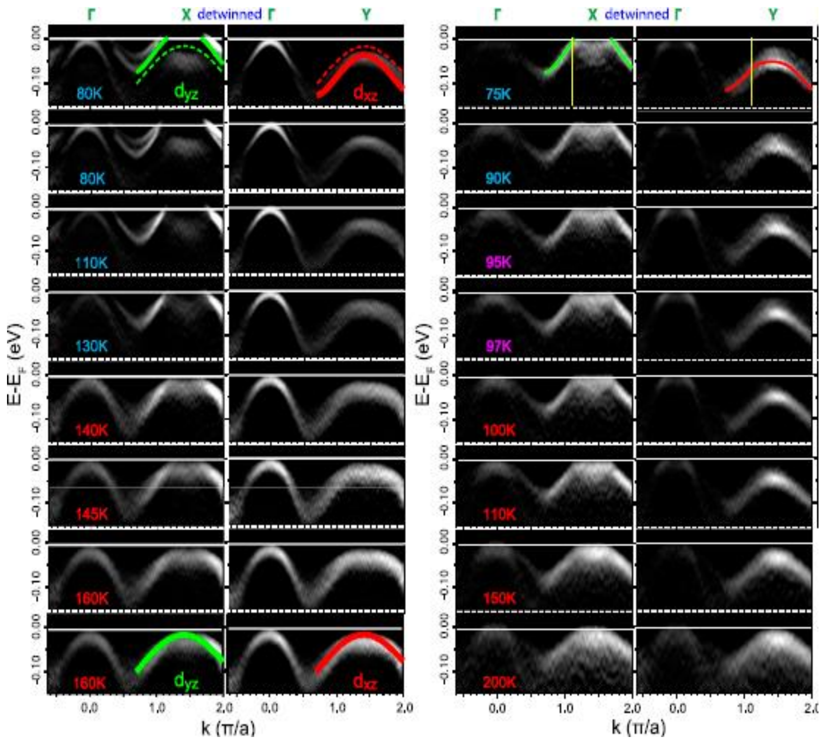

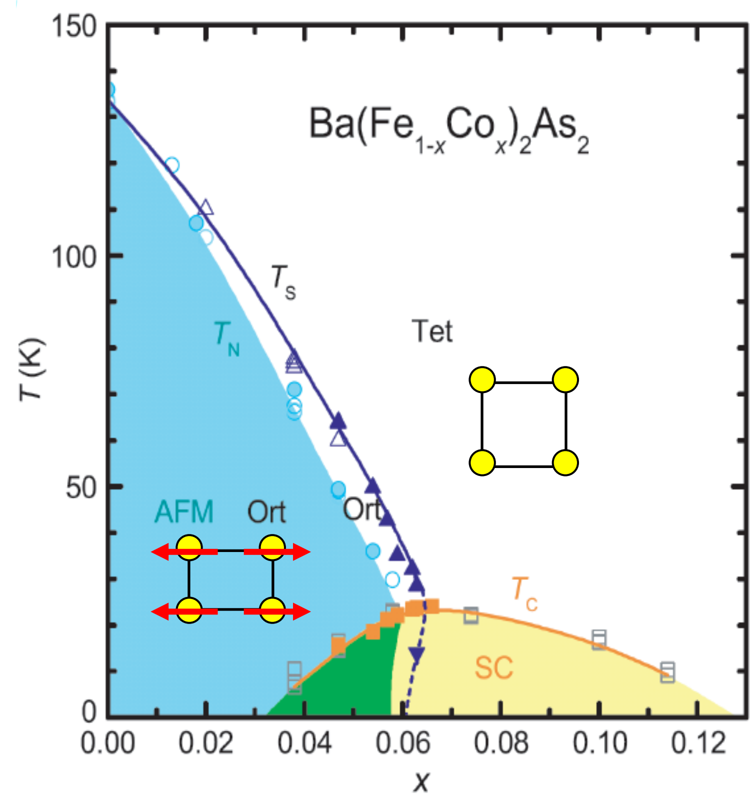

Nematicity appears above T_s in crystals under uniaxial strain. ⇨ Experiments using thermodynamic probe with no uniaxial stress.

Microcantilever torque magnetometry

Micro-chip cantilever

Very high sensitivity

torque	$5\text{x}10^{-12}$ e.m.u.	at $\mu_0 H$=4 T
SQUID	10^{-8} e.m.u.	

Vector magnet and mechanical rotator system

We can rotate ***H*** continuously within the *ab* plane with a misalignment less than 0.01 deg.

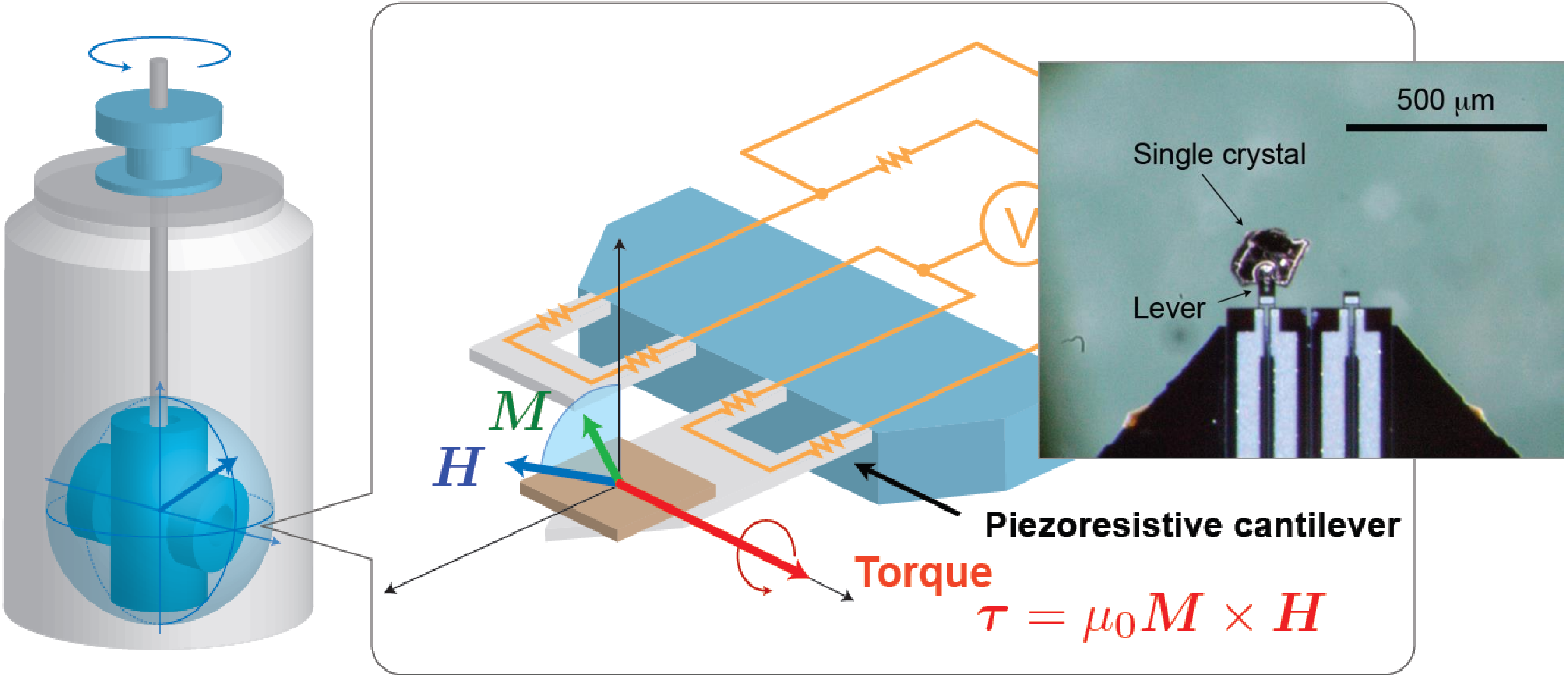

What the magnetic torque tells us

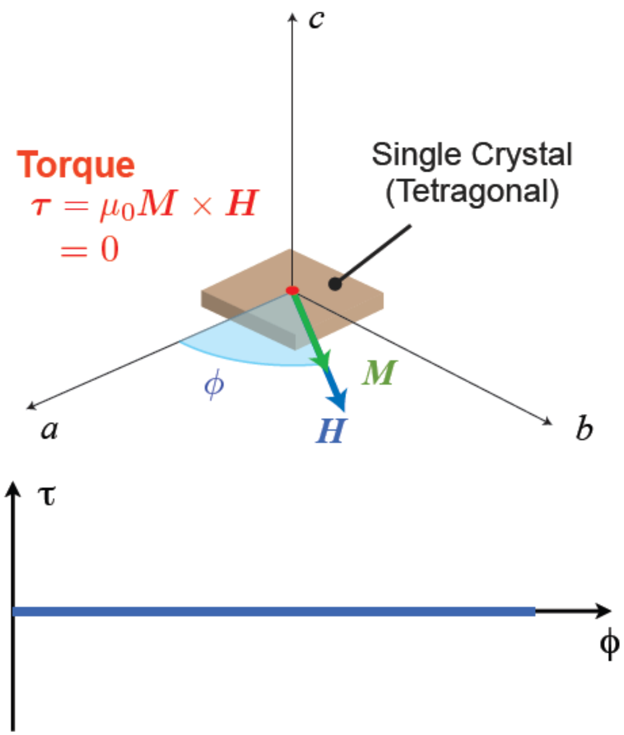

Preserved C_4 symmetry

Torque $\boldsymbol{\tau} = \mu_0 \boldsymbol{M} \times \boldsymbol{H}$

Angle derivative of the free energy

$$\tau(\phi) = -\frac{\partial F_{eq}(\mathbf{H})}{\partial \phi}$$

Direct probe of the
magnetic anisotropy

$$\tau = \frac{1}{2}\mu_0 H^2 V[(\chi_{aa} - \chi_{bb})\sin 2\phi - 2\chi_{ab}\cos 2\phi]$$

$$\chi_{aa} = \chi_{bb}, \quad \chi_{ab} = 0 \quad \rightarrow \quad \tau = 0$$

What the magnetic torque tells us

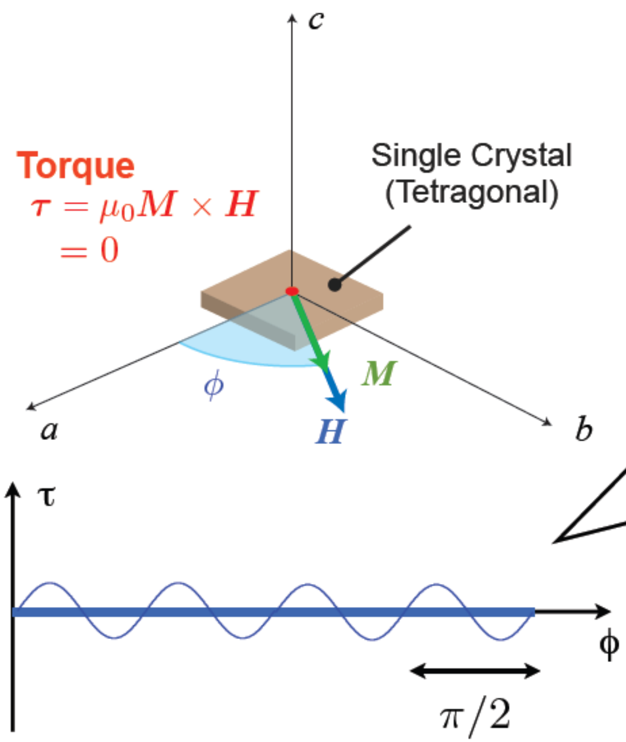

Preserved C_4 symmetry

Nonlinear susceptibility

C_4 symmetry in the *ab* plane: 4-fold oscillation

$$M_i = \chi_{ij} H_j + \chi^{(3)}_{ijkl} H_j H_k H_l + \cdots$$

$\tau = 0$ $\quad$ $\tau \propto \sin 4\phi$

No 2-fold oscillation

$$\tau_{2\phi} = \frac{1}{2}\mu_0 H^2 V[(\chi_{aa} - \chi_{bb})\sin 2\phi - 2\chi_{ab}\cos 2\phi]$$

$$\chi_{aa} = \chi_{bb}, \quad \chi_{ab} = 0$$

What the magnetic torque tells us

If rotational symmetry is broken, twofold oscillation appears in $\tau(\phi)$.

⇩

Torque measurements provide a stringent test for the rotational symmetry breaking (nematicity).

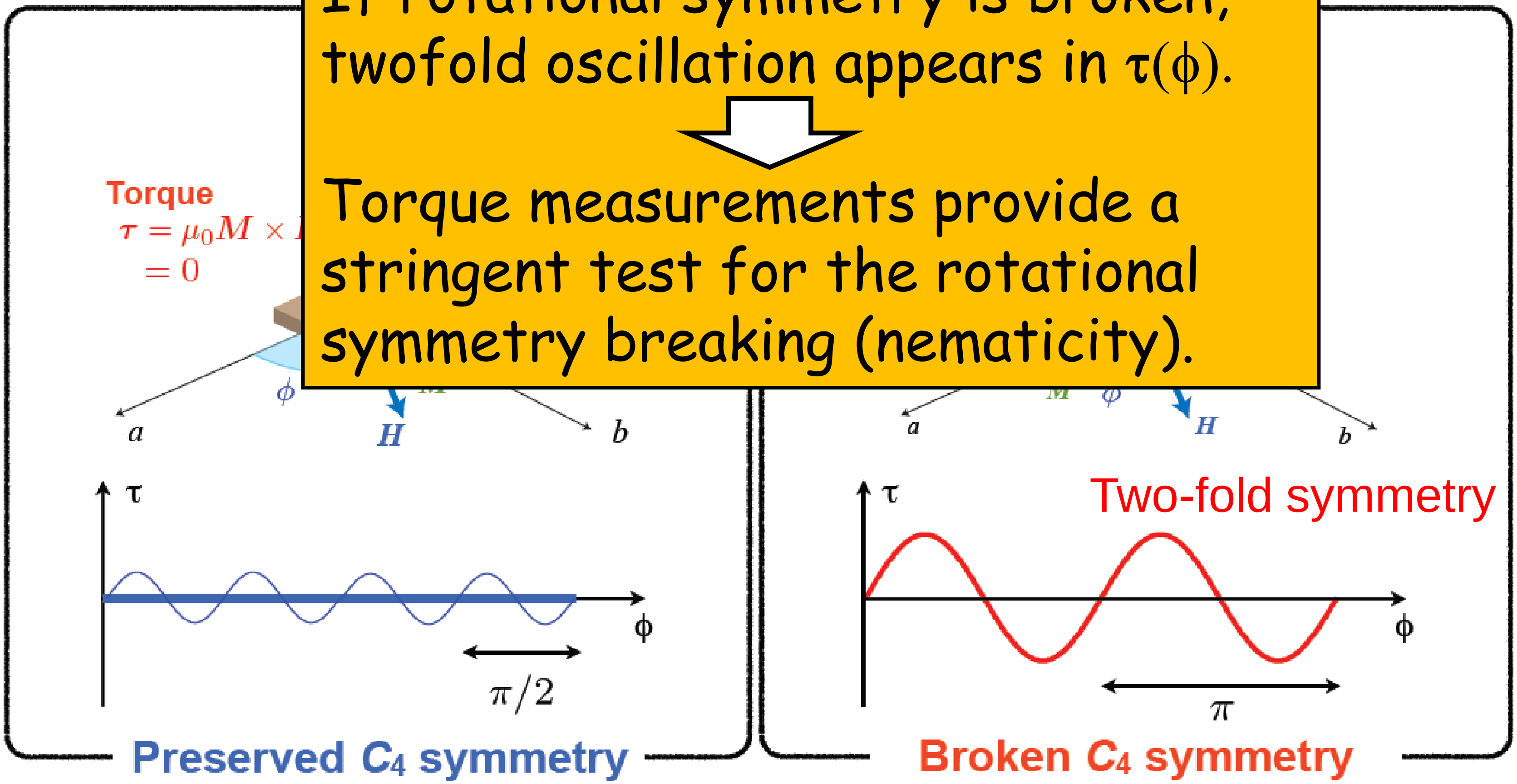

$$\tau_{2\phi} = \frac{1}{2}\mu_0 H^2 V[(\chi_{aa} - \chi_{bb})\sin 2\phi - 2\chi_{ab}\cos 2\phi]$$

$\chi_{aa}=\chi_{bb}$ and $\chi_{ab}=0$

$\chi_{aa}\neq\chi_{bb}$ and/or $\chi_{ab}\neq 0$

In-plane torque magnetometry: a test of nematicity

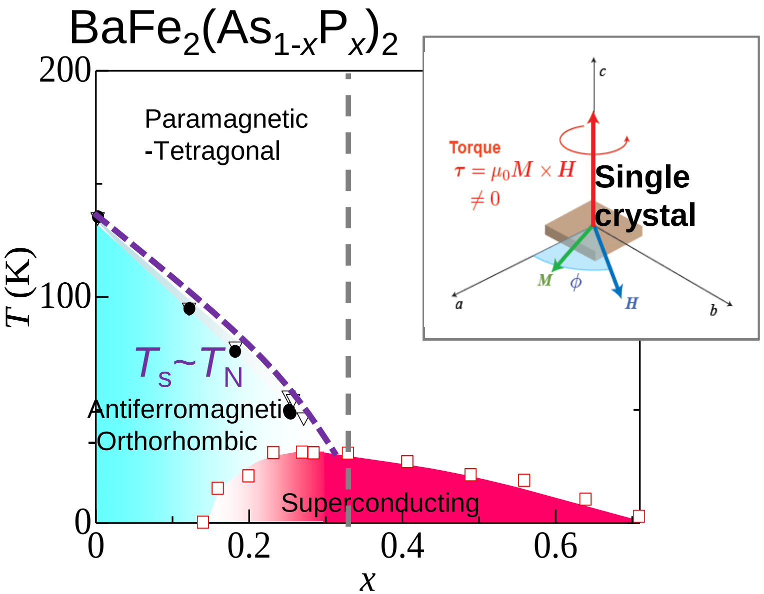

x = 0.33 (no structural and magnetic transitions)

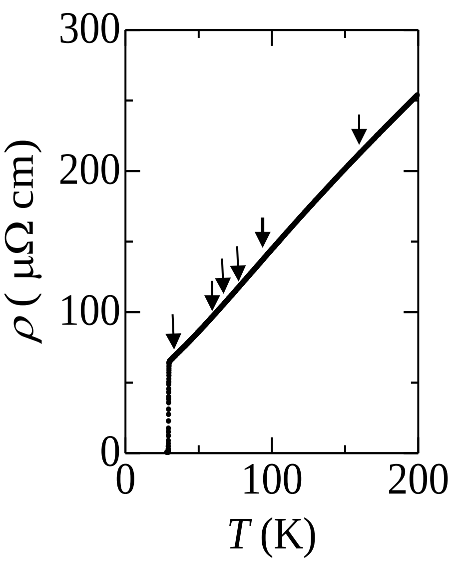

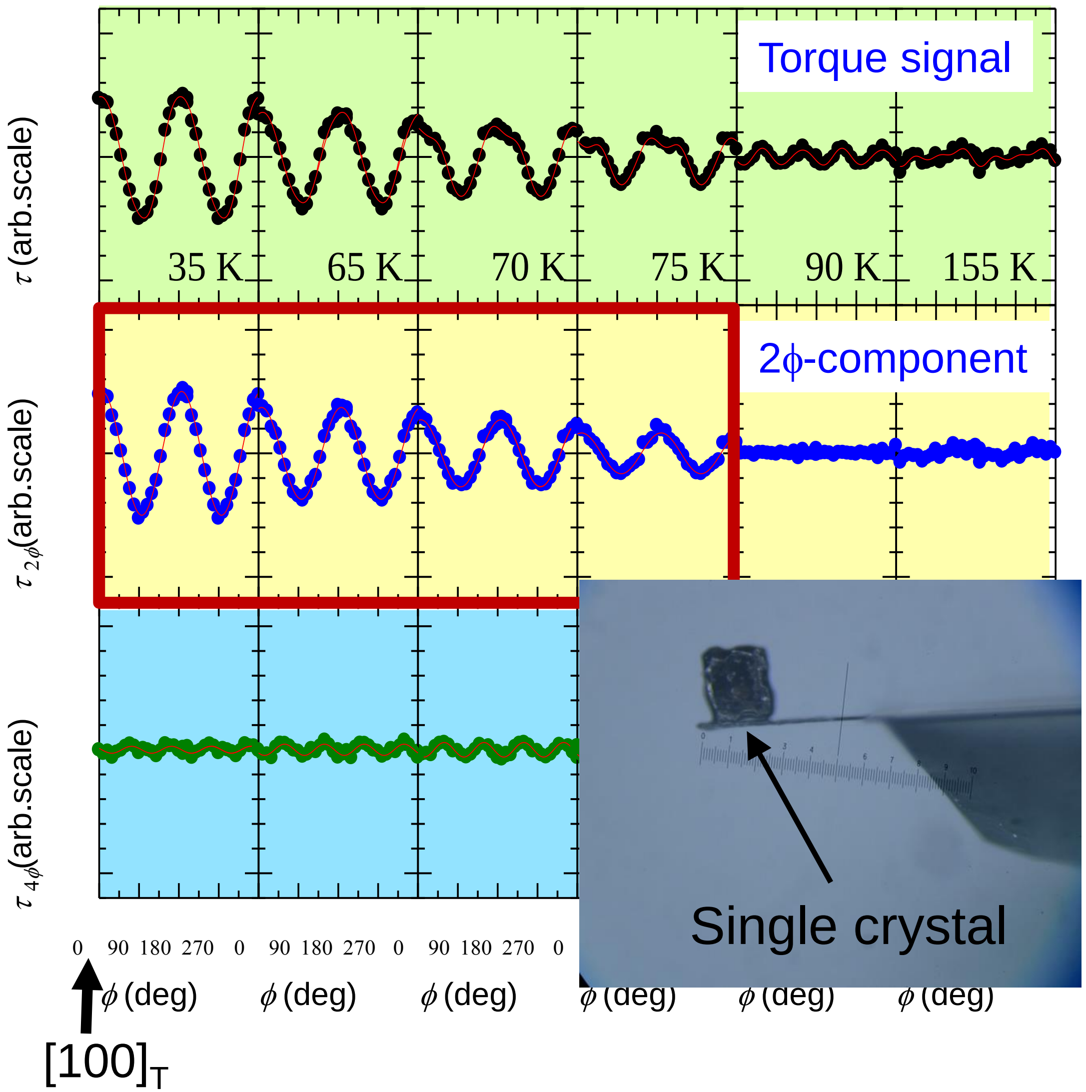

(Typical crystal dimensions: 70 x 70 x 30 um³)

- **2ϕ component at low temperatures**

In-plane torque magnetometry: a test of nematicity

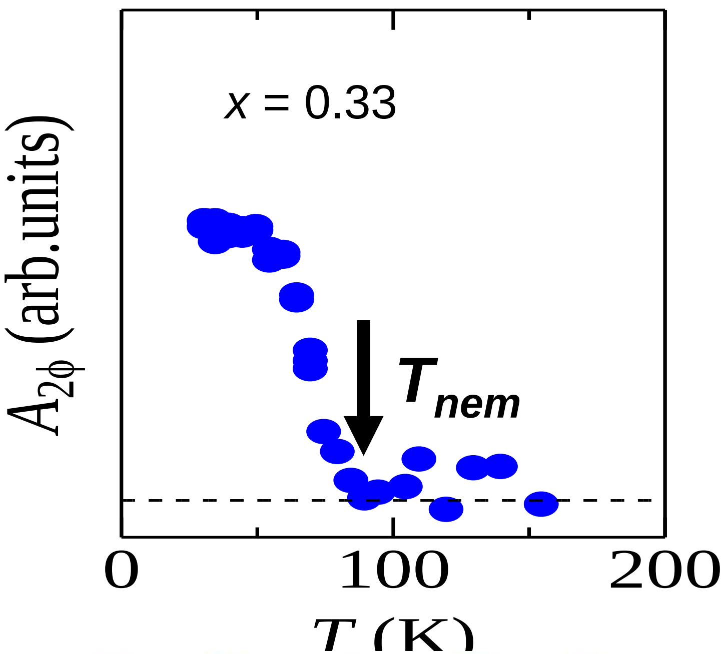

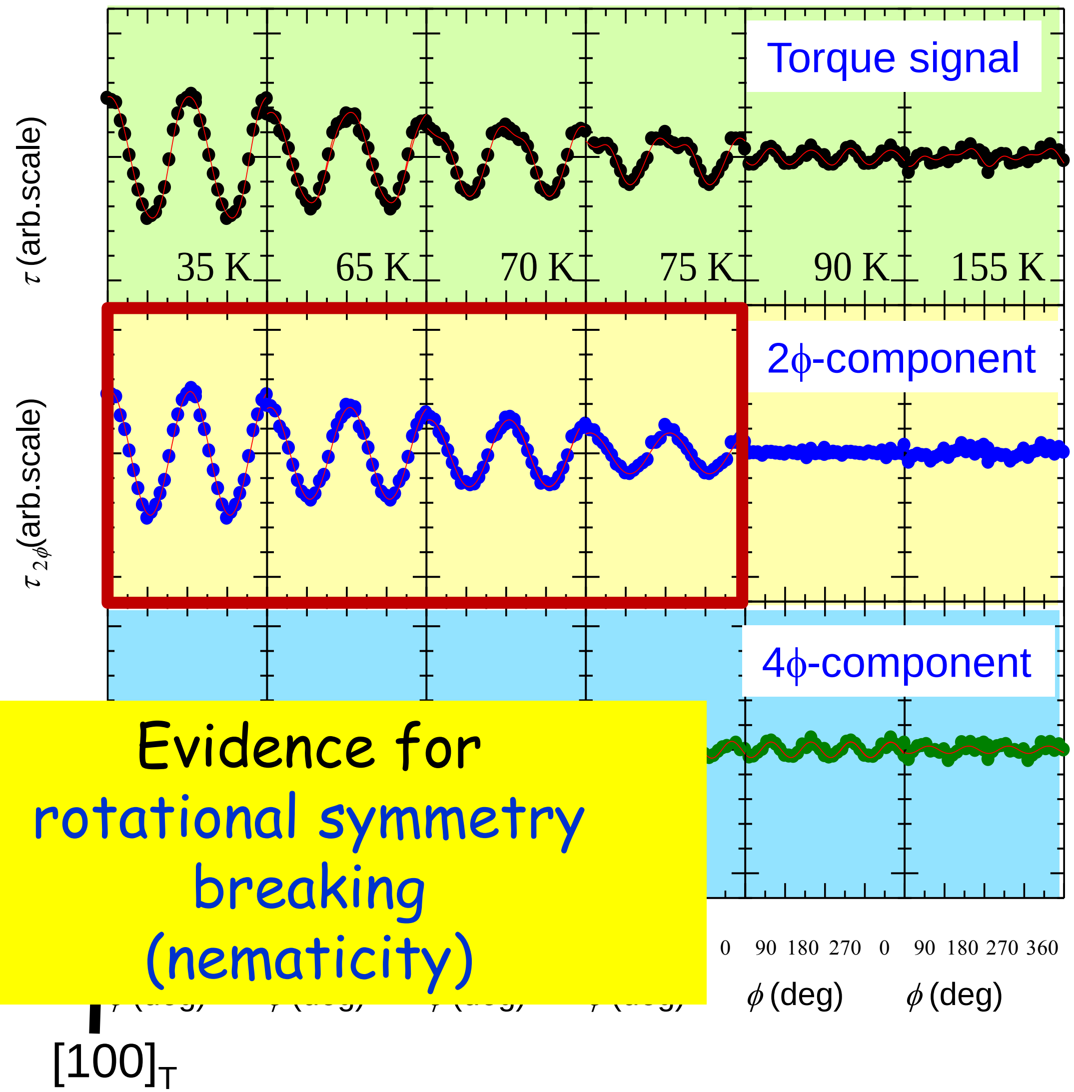

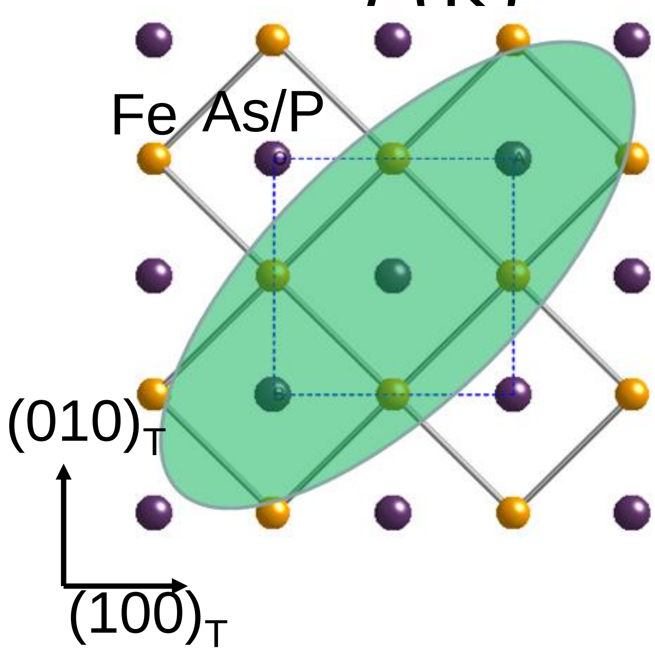

Evidence for
rotational symmetry
breaking
(nematicity)

$$\tau = \frac{1}{2}\mu_0 H^2 V[(\chi_{aa}-\chi_{bb})\sin 2\phi - 2\chi_{ab}\cos 2\phi]$$

$\chi_{ab} \neq 0$

Phase diagram: Nematicity

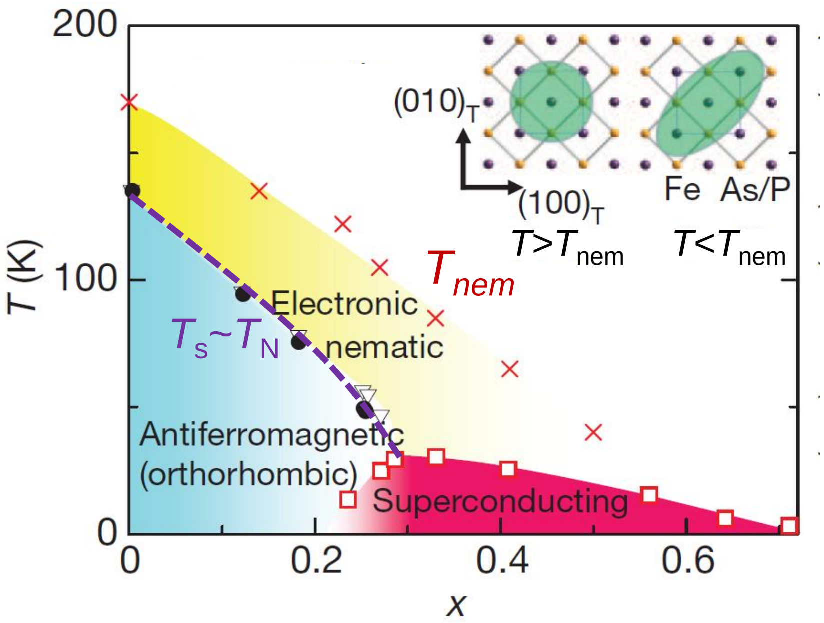

S. Kasahara *et al*. Nature (2012)

Electronic nematic phase persists over a wide range of doping.

Both AFM and SC states are within the nematic phase.

Pseudogap

Laser ARPES in $BaFe_2(As_{1-x}P_x)_2$

T. Shimojima *et al.*, Phys. Rev. B (2014).

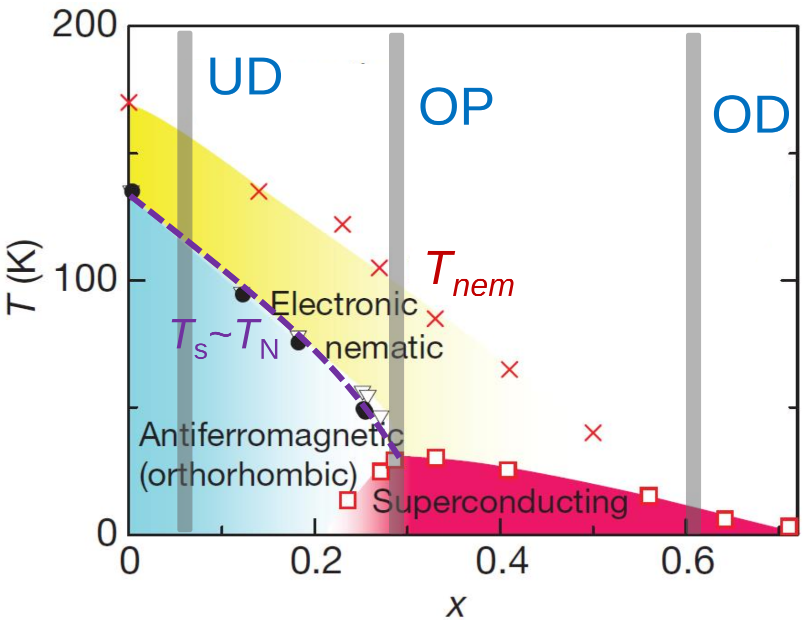

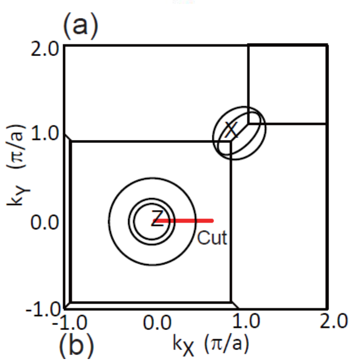

Outer hole band in Z plane

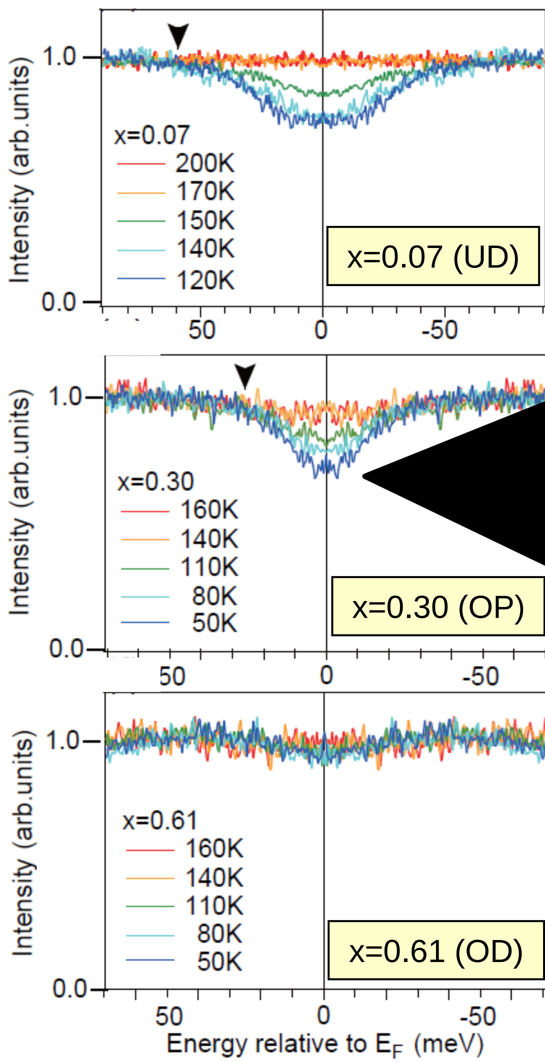

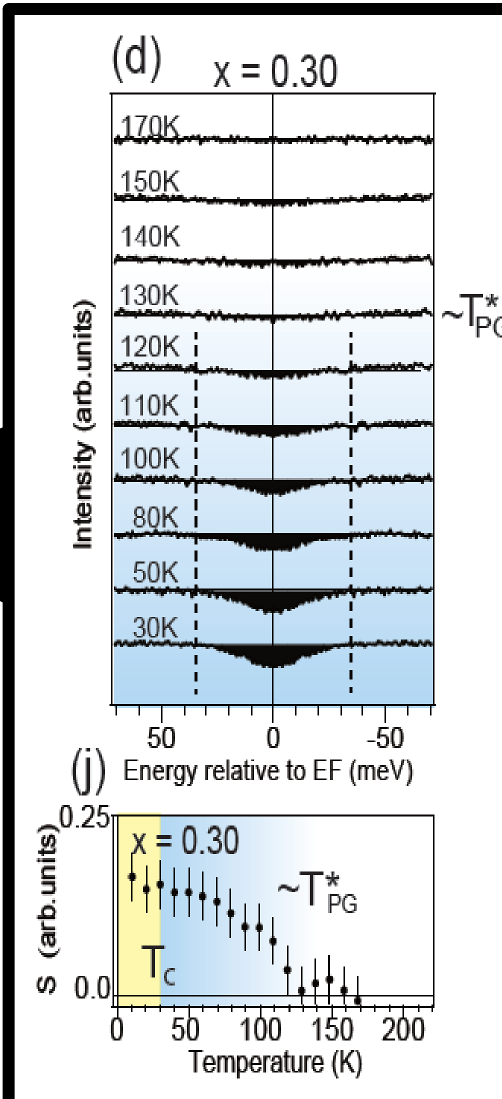

Pseudogap

Laser ARPES in $BaFe_2(As_{1-x}P_x)_2$

T. Shimojima *et al.*, Phys. Rev. B (2014).

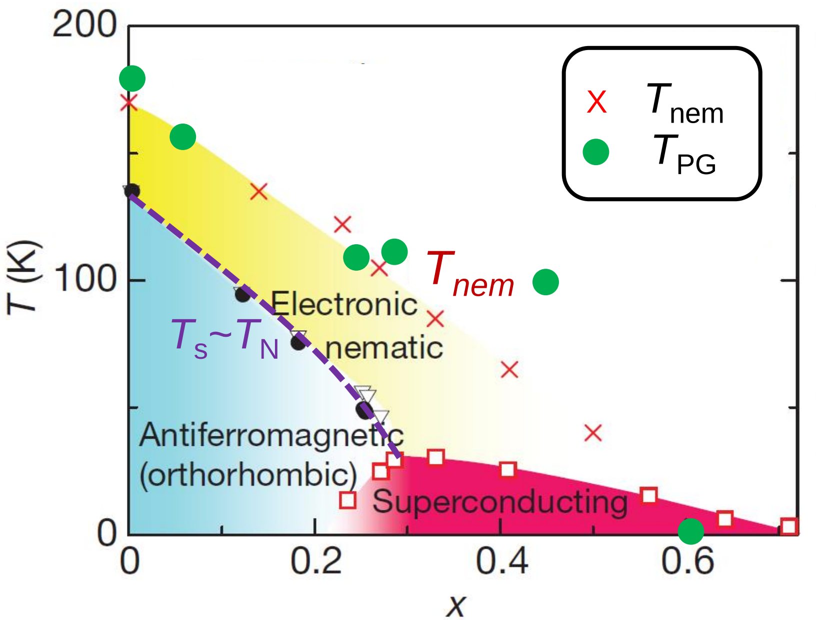

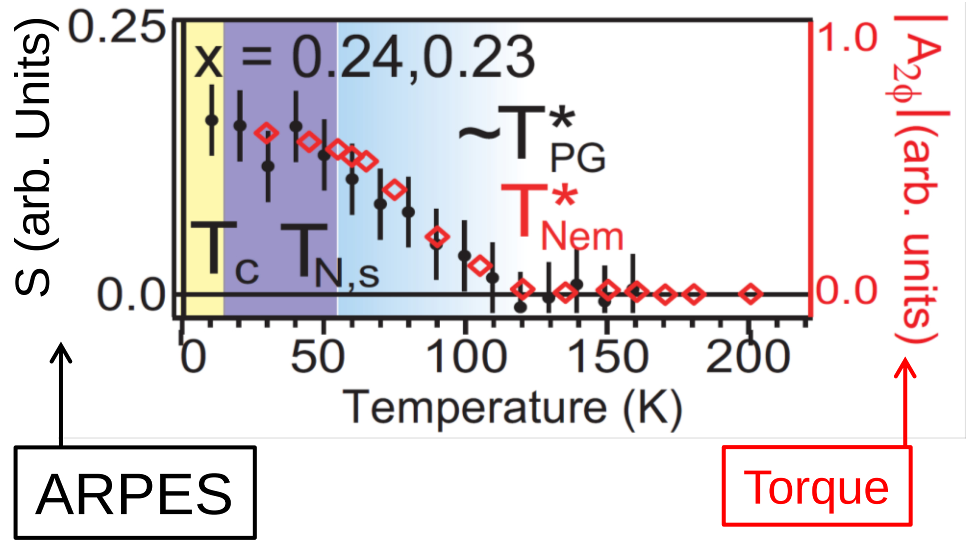

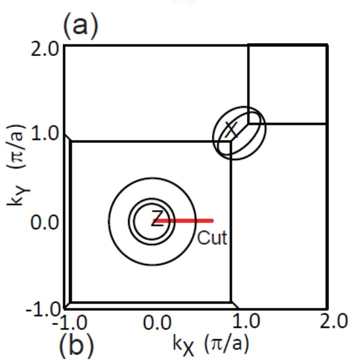

Outer hole band in Z plane

Cuprate

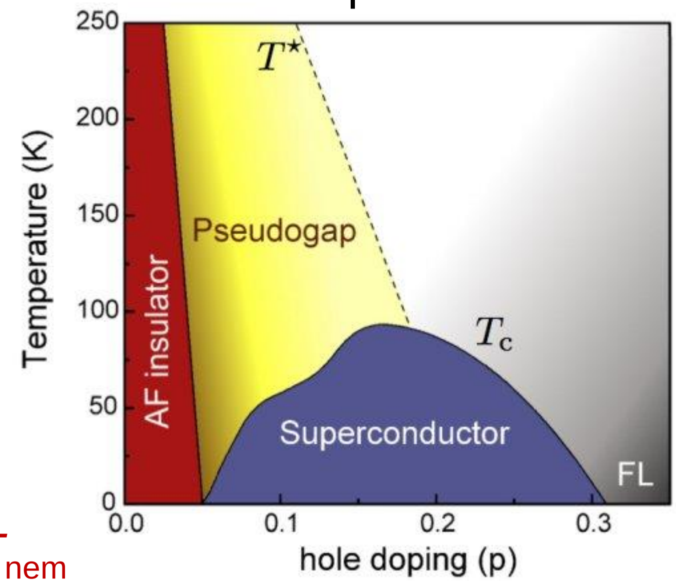

Pseudogap formation at T_{PG}~T_{nem}

Anisotropic electronic occupation in zx/yz orbitals

T. Shimojima *et al.*, Phys. Rev. B (2014).

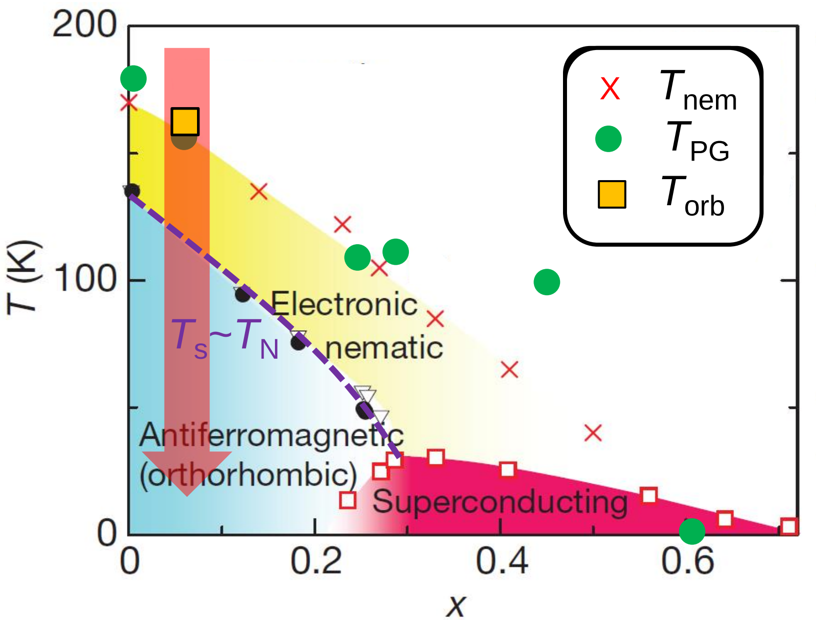

Inequivalent energy shifts for xz/yz orbitals below T_{orb}

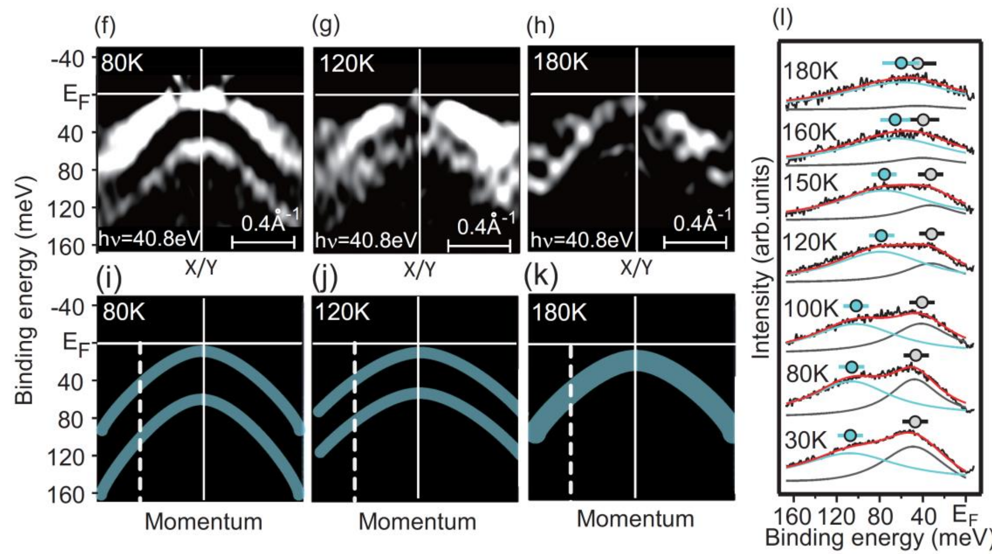

orbital ordering?

Nematic transition T_{nem}
Pseudogap formation T_{PG}
Orbital ordering T_{orb}

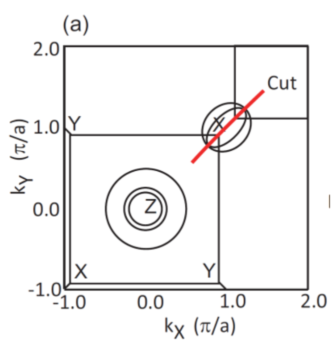

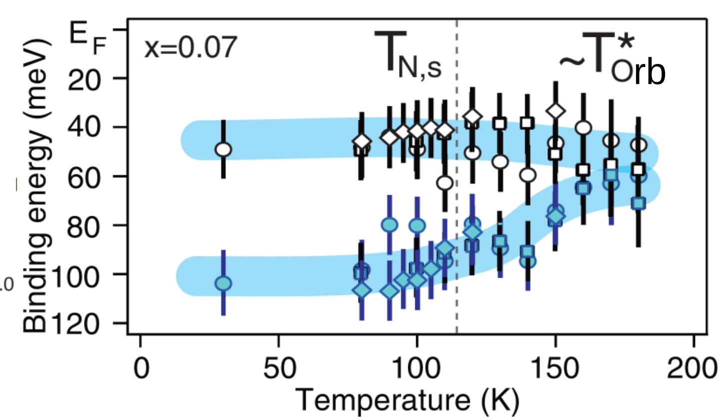

T_{nem} ~ T_{PG} ~T_{orb}

Nematicity and AFM fluctuations

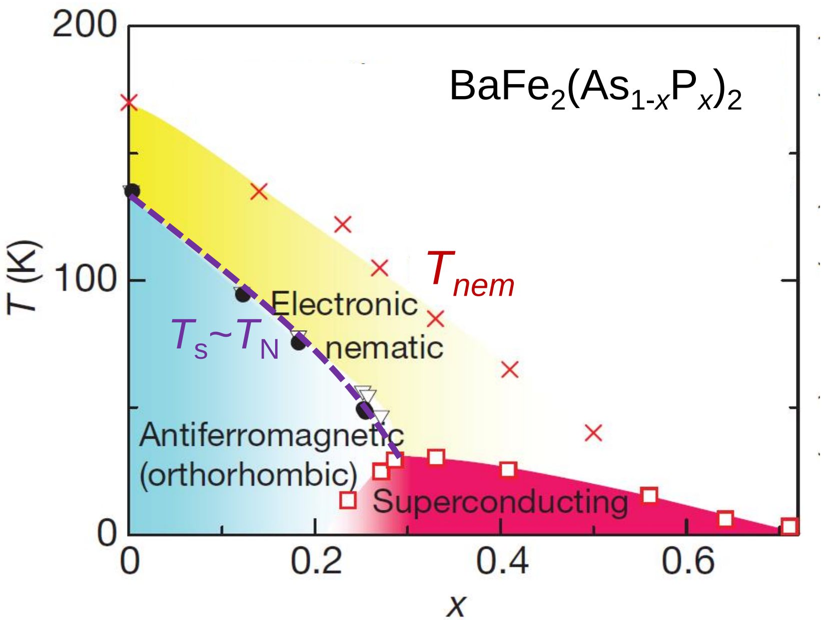

Y. Nakai et al., PRB **87**, 174507 (2013)

NMR $(T_1T)^{-1} \sim \chi(\pi,\pi)$

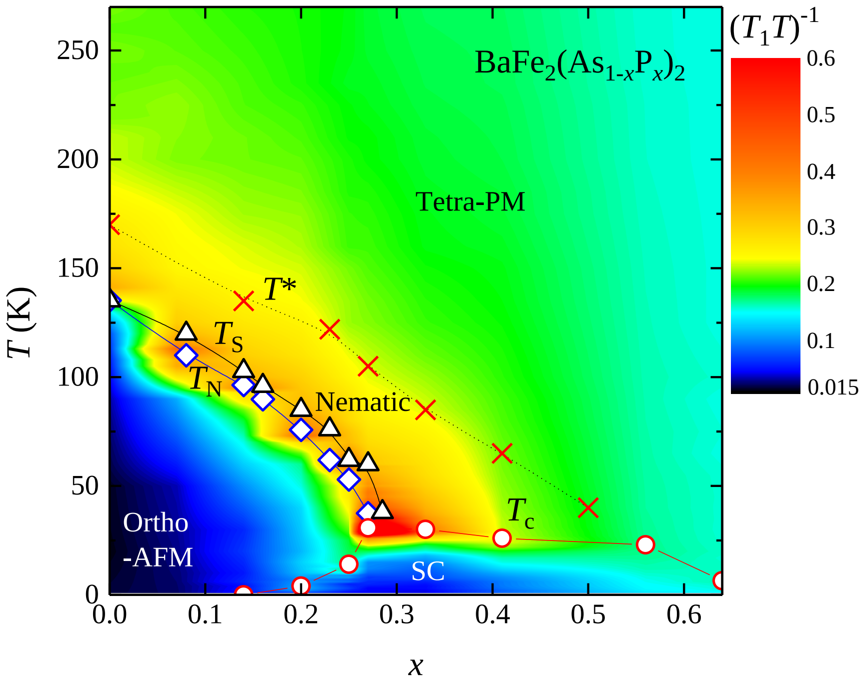

The nematicity enhances AFM fluctuations.

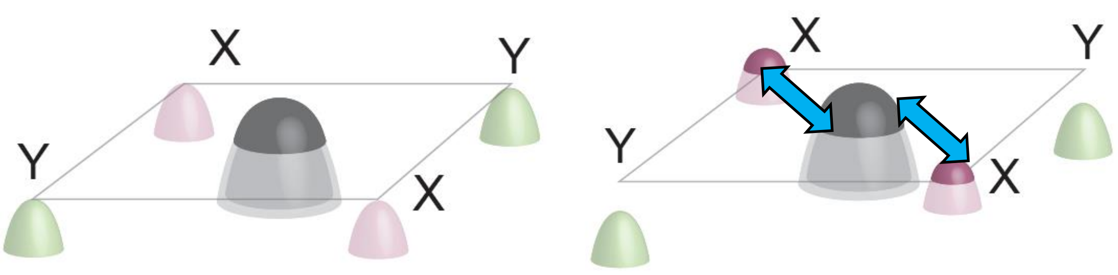

Coexistence of orbital degeneracy lifting and superconductivity

T. Sonobe *et al.*, unpublished

T=10 K (well below T_c)

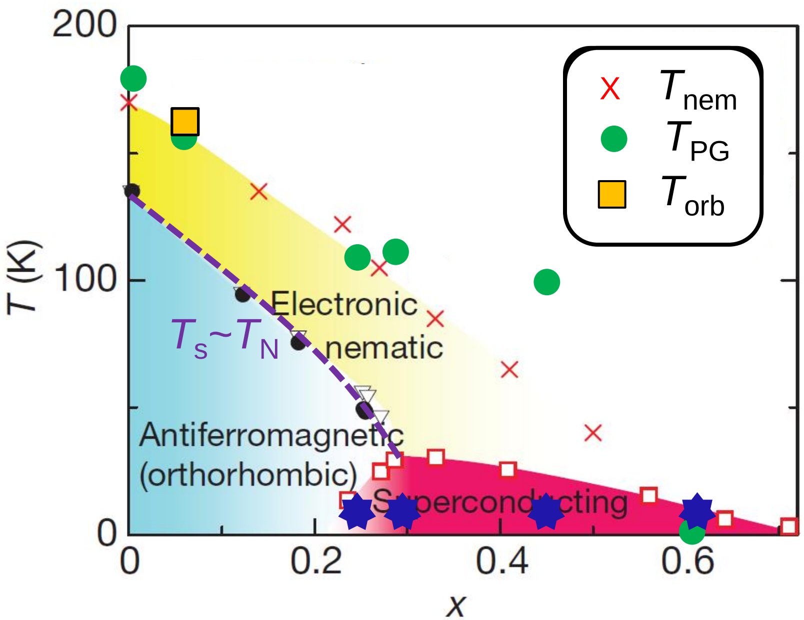

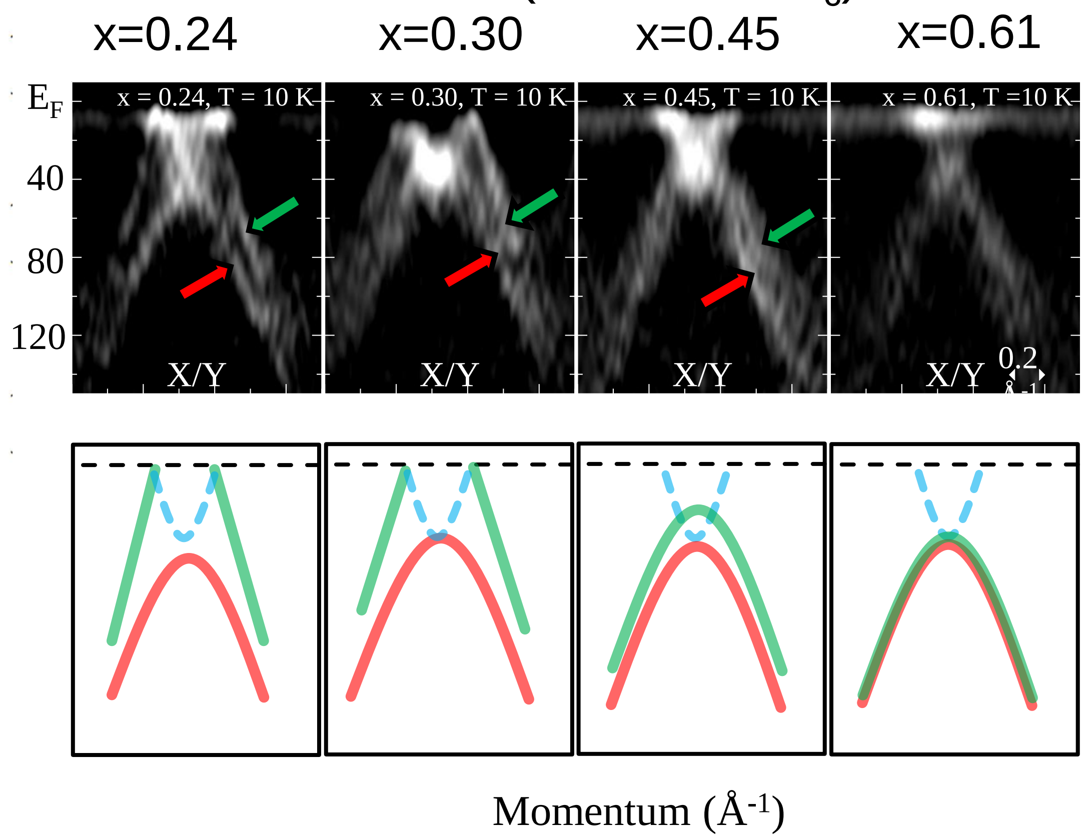

Nematic transition T_{nem}
Pseudogap formation T_{PG}
Orbital ordering T_{orb}

$T_{nem} \sim T_{PG} \sim T_{orb}$

Anisotropy in zx/yz orbitals persists in the SC dome

Relationship between nematicity and superconductivity

Coexistence of orbital degeneracy lifting and superconductivity

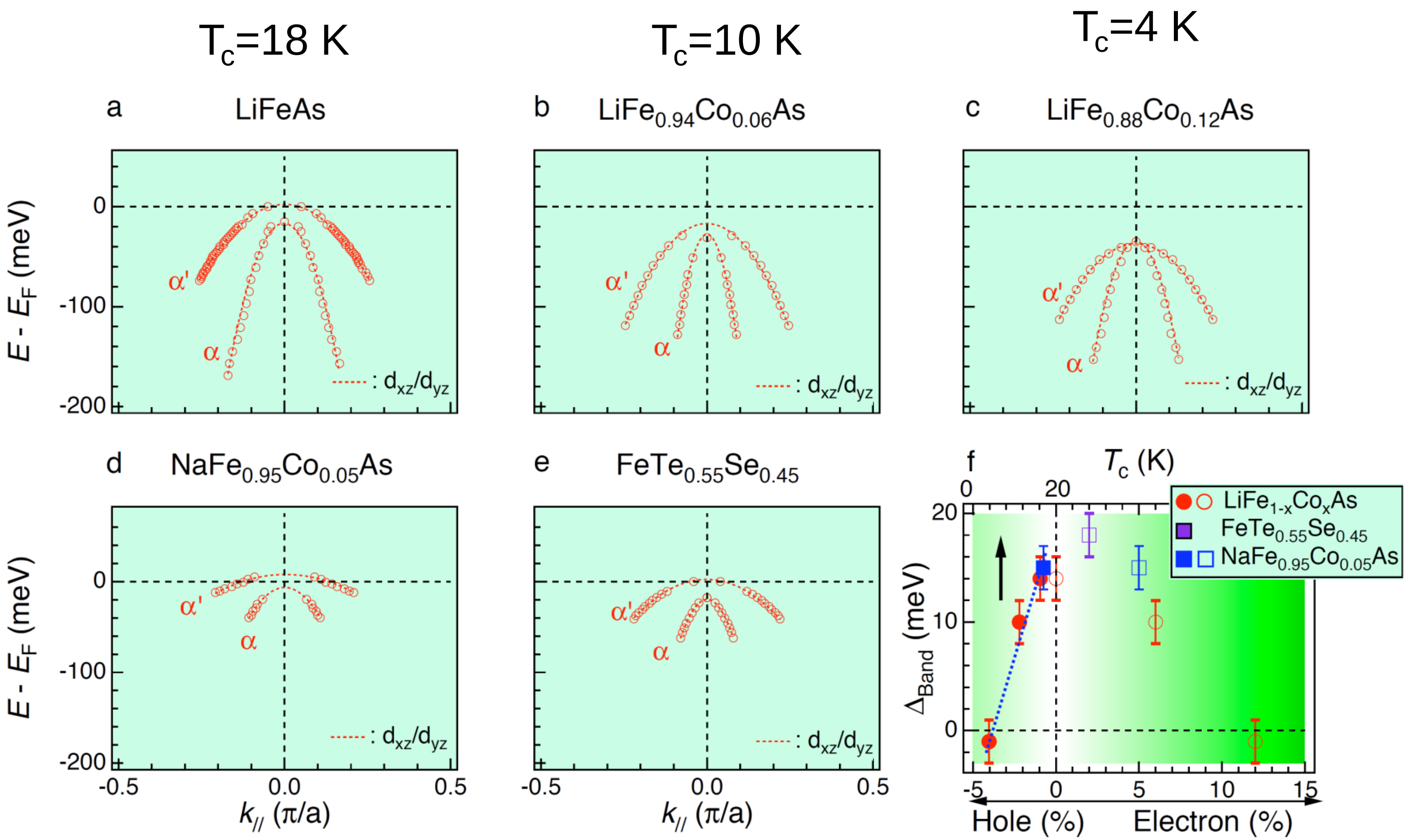

H. Miao *et al*. arXiv:1310.4601

Relationship between nematicity and superconductivity

Phase diagram

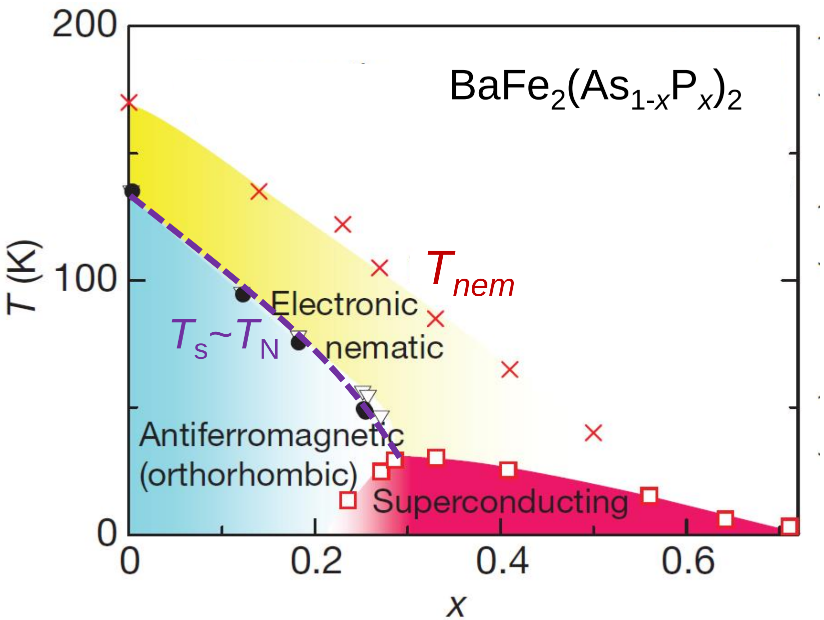

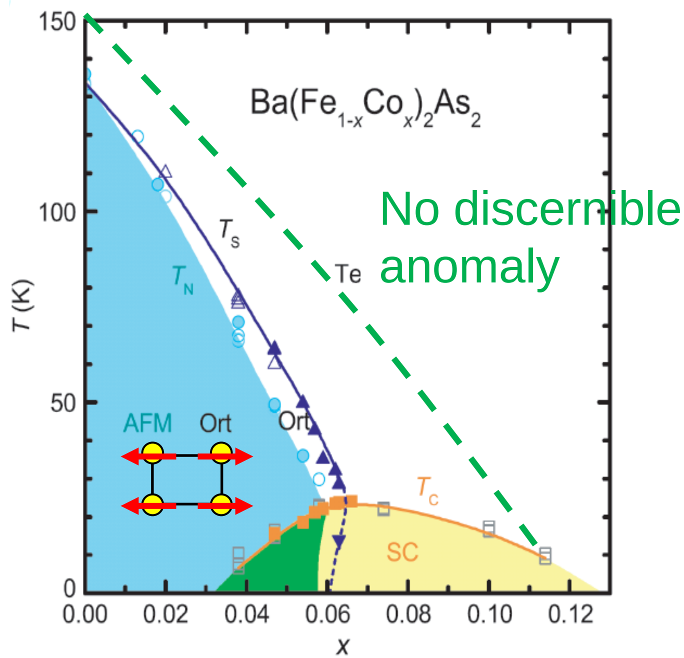

Elastic constant C_{66}

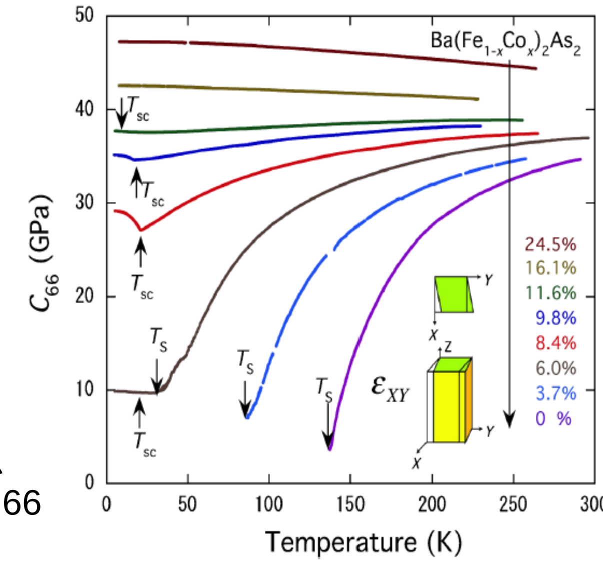

M. Yoshizawa *et al*., JPSJ (2012).

Phase diagram

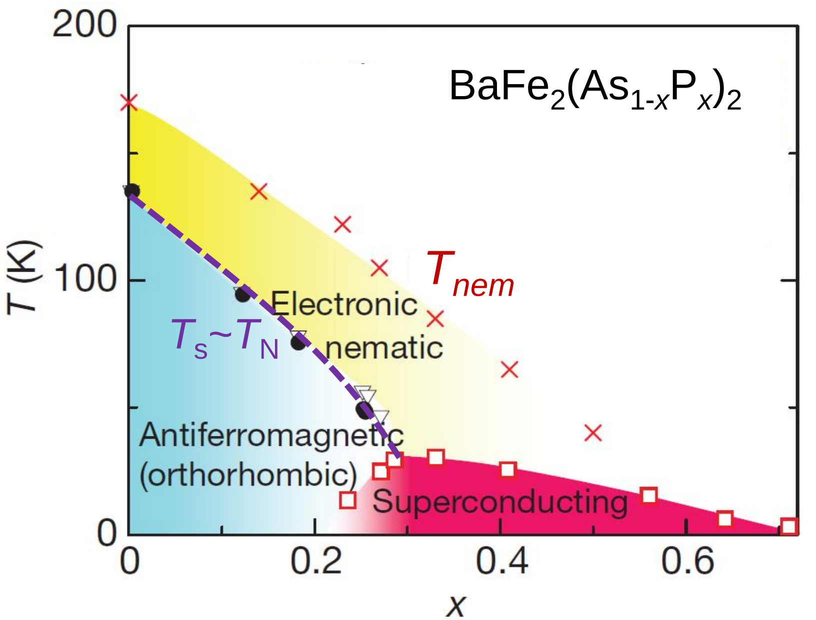

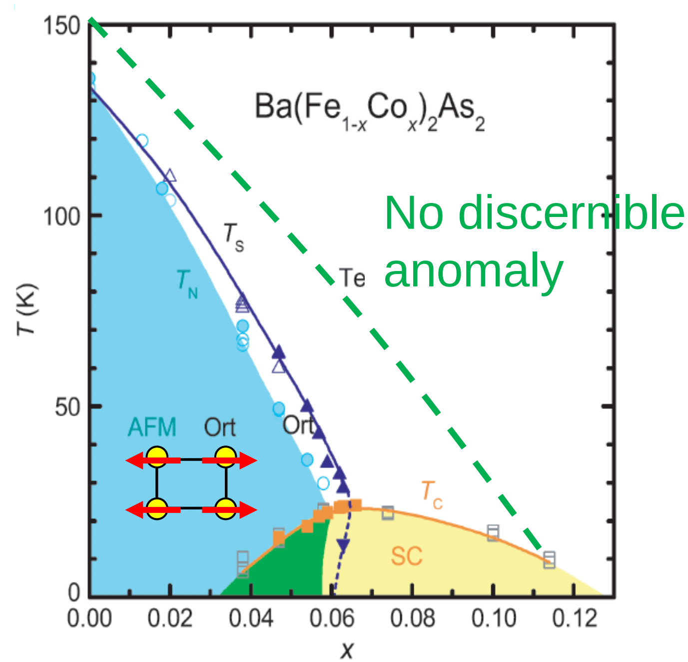

Antiferro type orbital ordering

(O_{xz} antiferro-quadrupole (AFQ) ordering)

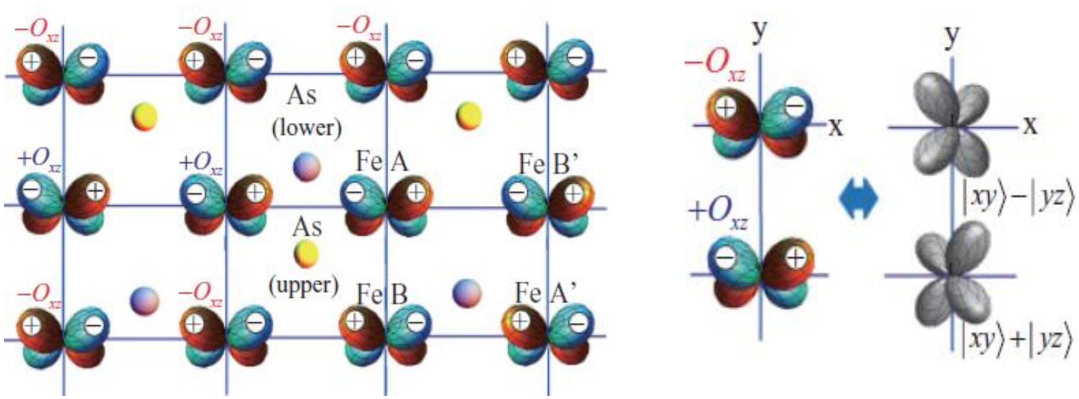

H. Kontani *et al*., Phys. Rev. B (2011).

q≠0 AF orbital ordering may be difficult to detect by long wave length (q=0) probes, such as elastic constant.

1. Quantum critical point lies beneath the SC dome

1. QCP is definitely important for the high-T_c superconductivity
2. The QCP is the origin of the non-Fermi liquid behavior.
3. Microscopic coexistence of superconductivity and SDW.

Magnetic QCP or orbital QCP?

2. BCS-BEC crossover in FeSe

A new highly spin-polarized phase

3. Nematicity in Iron pnictide

Nematic transition T_{nem}
Pseudogap formation T_{PG}
Orbital ordering T_{orb}

$T_{\mathrm{nem}} \sim T_{\mathrm{PG}} \sim T_{\mathrm{orb}}$

Is nematicity important for the superconductivity?
What is the origin of the nematicity, spin or orbital?